

Explorations in the Conformal Bootstrap

by

Dalimil Mazáč

A thesis
presented to the University of Waterloo
in fulfillment of the
thesis requirement for the degree of
Doctor of Philosophy
in
Physics

Waterloo, Ontario, Canada, 2017

© Dalimil Mazáč 2017

Examining Committee Membership

The following served on the Examining Committee for this thesis. The decision of the Examining Committee is by majority vote.

External Examiner	Xi Yin, Harvard University
Supervisors	Davide Gaiotto, Perimeter Institute Freddy Cachazo, Perimeter Institute
Internal Member	Roger Melko, University of Waterloo
Internal/External Member	Michael Rubinstein, University of Waterloo
Examiner	Rob Myers, Perimeter Institute

This thesis consists of material all of which I authored or co-authored: see Statement of Contributions included in the thesis. This is a true copy of the thesis, including any required final revisions, as accepted by my examiners.

I understand that my thesis may be made electronically available to the public.

Statement of Contributions

Chapter 2 of this thesis consists of material from the paper [1], co-authored with Davide Gaiotto and Miguel F. Paulos.

Chapter 3 of this thesis consists of material from the papers [2, 3], co-authored with Nikolay Bobev, Sheer El-Showk and Miguel F. Paulos.

Abstract

We investigate properties of various conformally invariant quantum systems, especially from the point of view of the conformal bootstrap.

First, we study twist line defects in three-dimensional conformal field theories. Numerical results from lattice simulations point to the existence of such conformal defect in the critical 3D Ising model. We show that this fact is supported by both epsilon expansion and the conformal bootstrap calculations. We find that our results are in a good agreement with the numerical data. We also make new predictions for operator dimensions and OPE coefficients from the bootstrap approach. In the process we derive universal bounds on one-dimensional conformal field theories and conformal line defects.

Second, we analyze the constraints imposed by the conformal bootstrap for theories with four supercharges in spacetime dimension $2 \leq d \leq 4$. We show how superconformal algebras with four Poincaré supercharges can be treated in a formalism applicable to any, in principle continuous, value of d and use this to construct the superconformal blocks for any $d \leq 4$. We then use numerical bootstrap techniques to derive upper bounds on the conformal dimension of the first unprotected operator appearing in the OPE of a chiral and an anti-chiral superconformal primary. We obtain an intriguing structure of three distinct kinks. We argue that one of the kinks smoothly interpolates between the $d = 2$, $\mathcal{N} = (2, 2)$ minimal model with central charge $c = 1$ and the theory of a free chiral multiplet in $d = 4$, passing through the critical Wess-Zumino model with cubic superpotential in intermediate dimensions.

Finally, we turn to the question of the analytic origin of the conformal bootstrap bounds. To this end, we introduce a new class of linear functionals acting on the conformal bootstrap equation. In 1D, we use the new basis to construct extremal functionals leading to the optimal upper bound on the gap above identity in the OPE of two identical primary operators of integer or half-integer scaling dimension. We also prove an upper bound on the twist gap in 2D theories with global conformal symmetry. When the external scaling dimensions are large, our functionals provide a direct point of contact between crossing in a 1D CFT and scattering of massive particles in large AdS_2 . In particular, CFT crossing can be shown to imply that appropriate OPE coefficients exhibit an exponential suppression characteristic of massive bound states, and that the 2D flat-space S-matrix should be analytic away from the real axis.

Acknowledgements

I would like to thank my advisor Davide Gaiotto for being a constant source of inspiration to keep improving my independent way of understanding physics. Through my interactions with Davide, I learned more than from anybody else how to ask the right questions, and to be bold in searching for the answers.

During my graduate years, I had the pleasure to closely collaborate with Nikolay Bobev and Miguel F. Paulos, from whom I learned both a great deal about physics and various aspects of life in academia. I am also grateful to my collaborators Sheer El-Showk, Edoardo Lauria and Emilio Trevisani for fun times spent figuring things out and their contributions to our work.

A special thanks goes to Marco Meineri, a great friend with whom I have shared numerous discussions that have helped me reach out of the comfort zone of my knowledge.

Next, I would like to thank Freddy Cachazo, Jaume Gomis and Pedro Vieira for helping to answer my questions about physics, and offering a far greater number of questions in return.

My life at the Perimeter Institute was vastly brightened up by the kindness, sense of humour and intellect of Shira Chapman, Lorenzo Di Pietro, and many others who have passed through Perimeter's corridors and offices over the years.

Finally, I am immensely grateful to my sister Kamila, grandmother Anna and parents Nataša and Milan for their unwavering love and support under all circumstances.

Table of Contents

List of Tables	xii
List of Figures	xiii
1 Introduction	1
1.1 The role of conformal field theories in physics	1
1.2 The conformal bootstrap	3
1.3 Overview of the thesis	5
2 The Twist Line Defect in the 3D Ising Model	7
2.1 Introduction	7
2.2 The \mathbb{Z}_2 Twist Defect	10
2.3 Epsilon Expansion	13
2.3.1 The two-point function in the free theory	14
2.3.2 The two-point function at one loop	15
2.3.3 Energy operator	17
2.3.4 The four-point function	19
2.3.5 The leading defect scalar and pseudoscalar	23
2.4 Bootstrapping the twist defect	24
2.4.1 The bootstrap equations	24
2.4.2 Constraints from the first crossing equation	28

2.4.3	Constraints from both crossing equations	30
2.5	Conclusions	32
2.A	Asymptotic evaluation of integrals	36
2.A.1	Half-integer spin operators	36
2.A.2	Energy operator	38
2.A.3	Dimensions of integer spin operators	39
2.A.4	$c_{\psi\psi\bar{D}}$ OPE coefficient	40
2.B	The four-point function without the defect	43
3	Superconformal Bootstrap with Four Supercharges	45
3.1	Introduction	45
3.2	Superconformal algebra in continuous dimension	48
3.2.1	General results	48
3.2.2	Realizations in integer $d \leq 4$	52
3.2.3	Unitarity bounds in general d	54
3.3	Superconformal blocks	58
3.3.1	Superconformal Casimir	58
3.3.2	Casimir equation and its solution	59
3.3.3	The relationship between conformal and superconformal blocks	63
3.3.4	Spectrum in a chiral OPE	64
3.4	Intermezzo: review of the Wess-Zumino model	67
3.5	Bootstrap setup	70
3.6	Bootstrap results	72
3.6.1	Scalar operator bounds	73
3.6.2	OPE and central charge	75
3.6.3	Two-dimensional $\mathcal{N} = 2$ minimal models	77
3.6.4	Bootstrapping the cWZ model in $2 \leq d \leq 4$	81
3.6.5	Additional kinks	85

3.7	Discussion	91
3.A	OPE derivation of 3d $\mathcal{N} = 2$ superconformal blocks	92
3.B	Decomposition of the generalized free chiral correlator	99
3.C	$\mathcal{N} = 2$ minimal models	100
4	Analytic Functionals for the Conformal Bootstrap	104
4.1	Introduction	104
4.2	Review	107
4.2.1	The conformal bootstrap and extremal functionals	107
4.2.2	The conformal bootstrap in one dimension	110
4.3	From derivative functionals towards the new basis	113
4.3.1	Inadequacy of the z -derivatives and the Zhukovsky variable	113
4.3.2	The new basis	117
4.4	Constructing extremal functionals	120
4.4.1	General properties of the new basis	120
4.4.2	The extremal functional for $\Delta_\psi = 1/2$	123
4.5	Higher values of Δ_ψ	130
4.5.1	Linear dependence of elementary functionals	130
4.5.2	Extremal functionals for $\Delta_\psi \in \mathbb{N}$	132
4.5.3	Fixing the remaining redundancy	135
4.5.4	Extremal functionals for $\Delta_\psi \in \mathbb{N} - \frac{1}{2}$	136
4.6	Emergence of AdS physics at large Δ_ψ	138
4.6.1	A review of massive scattering in large AdS_2	138
4.6.2	AdS_2 physics from crossing in a 1D CFT	142
4.7	An analytic bound in 2D	146
4.7.1	The new basis in 2D	146
4.7.2	Analytic bounds from factorized functionals	148
4.8	Future directions	150
4.A	Closed formulas for the integral kernel	151

List of Tables

2.1	A comparison of lattice data and the Wilson-Fisher fixed point at one loop.	18
2.2	A comparison of lattice data, the Wilson-Fisher fixed point at one loop, and bootstrap calculations.	33
2.3	Spectrum predictions from the bootstrap method.	33

List of Figures

2.1	The one-loop contribution to $\langle\phi(x_1)\phi(x_2)\rangle$	16
2.2	The diagrams contributing to $\psi_{s_1}\psi_{s_2}$ up to one loop.	21
2.3	Anomalous dimensions of the leading operators of spin s at one loop.	22
2.4	One-dimensional bounds derived from (2.60).	29
2.5	Single and two equation bound.	31
2.6	Spectra corresponding to the extremal solutions in figure 2.5.	32
2.7	One-dimensional bound, using two equations.	34
2.8	Spectra corresponding to the extremal solutions to crossing symmetry.	35
3.1	Upper bound on the lowest-dimension neutral scalar operator appearing in the $\Phi \times \bar{\Phi}$ OPE.	73
3.2	A close-up of the bounds in Figure 3.1.	74
3.3	The central charge, C_T , of the boundary solution.	76
3.4	A close-up of the curves in Figure 3.3.	77
3.5	An extended view of the upper bound on $\Delta_{[\Phi\bar{\Phi}]}$ in $d = 2$ (with $n_{max} = 9$).	78
3.6	Central charges and the OPE coefficient of $\Phi\bar{\Phi}$ in for $d = 2$	79
3.7	Predictions for the anomalous dimension of $\Phi\bar{\Phi}$ in the d -dimensional cWZ model.	82
3.8	Our prediction for the central charge, C_T , of the cWZ model in d dimensions normalized by the value for a free chiral superfield.	83
3.9	Bound plots for $\Phi\bar{\Phi}$ near $d = 4$ (left).	84

3.10	Properties of the second kink.	86
3.11	Properties of the third kink.	86
3.12	Properties of the third kink as a function of d	87
3.13	Scaling dimensions and OPE coefficients for the first three scalar operators in the the $\Phi \times \Phi$ OPE.	89
4.1	The action of a typical extremal functional for the bound on the scalar gap.	109
4.2	The numerical bootstrap bound in 1D.	112
4.3	The transformation (4.30) between the z and y coordinates.	115
4.4	The choice of integration contour leading to a well-defined action of ω . . .	120
4.5	The integral kernel $h(x)$ for $\Delta_\psi = 1/2$, given by equation (4.86).	125
4.6	The action of the extremal functional for $\Delta_\psi = 1/2$	126
4.7	The contour deformation in the y -coordinate used to find a closed formula for the coefficients b_j	127
4.8	Comparison of the analytical and numerical extremal functionals for $\Delta_\psi = 1/2$.	130
4.9	The action of the extremal functional for $\Delta_\psi = 2$	134
4.10	The analytic structure of the S-matrix on the first sheet.	139
4.11	The analytic extremal functional for $\Delta_\psi = 15$	143
4.12	Contour integrals describing the contributions of various states to the cross- ing equation (4.158) at the leading order as $\Delta_\psi \rightarrow \infty$	145

Chapter 1

Introduction

1.1 The role of conformal field theories in physics

It is the ultimate goal of science in general and theoretical physics in particular to derive the maximal amount of nontrivial predictions about the world we live in from the minimal set of assumptions concerning its fundamental laws. Indeed, the wonderful richness of physical phenomena compared to the relative simplicity of the laws they follow from has been a recurring theme in theoretical physics as well as its main driving force. Can we eventually identify the truly minimal set of assumptions that the laws of any consistent universe should satisfy? Is our universe the only solution of these constraints? While science has not yet advanced enough to provide definitive answers to these grand questions, or even to make them sufficiently well-defined, the same paradigm, commonly referred to as the *bootstrap*, has appeared in more concrete incarnations in various areas of theoretical physics. The main theme of this thesis is an exploration of the bootstrap program in the context of quantum field theories with conformal symmetry, where it is referred to as the *conformal bootstrap*. Before describing conformal bootstrap in more detail, we will review the role that conformal field theories play in physics.

Quantum field theory (QFT) sits at the heart of our current understanding of Nature. A wide variety of extended fluctuating systems, ranging from the propagation and interactions of particles in spacetime, through numerous condensed matter materials, to the large-scale structure of matter in our universe, are well described by various versions of QFT. As broad as the applicability of the framework of QFT is, our ability to extract predictions from specific models has been mostly limited to the regime where the constituents are only weakly interacting and perturbation theory is thus applicable. Since many relatively little-

understood phenomena, such as the low-energy dynamics of quantum chromodynamics or the high- T_c superconductivity, involve strongly-interacting quantum fields, it is of great interest to develop tools to analyze QFT outside of the regime of weak coupling. Conformal bootstrap is an example of such technique.

One of the main conceptual advances that QFT has brought into focus is the organization of physical phenomena into scales at which they occur. Indeed, the effective physics at long distances (IR) can be very different from the microscopic laws that define the model at short distances (UV). Naively, one might anticipate that the IR physics can depend on the UV parameters in an arbitrarily complicated manner, but this expectation turns out to be wrong. Instead, quantum field theory exhibits universality, with a wide variety of UV definitions exhibiting the same IR dynamics. This universality is a consequence of the existence of quantum field theories whose properties are independent of the length scale at which we probe the system. Typically, the invariance of these theories under scaling is enhanced to an invariance under all conformal transformations, and such models are referred to as conformal field theories (CFTs). A general scale-dependent QFT can then be understood as a deformation of a CFT by some of its scale-invariance breaking parameters. Although a general CFT has infinitely many possible deformations, only a small number of these influence the IR dynamics, which provides the explanation for universality. It should be noted that the properties of deformations of a CFT are in principle determined by data intrinsic to the undeformed theory. Although such description may not always be practical for answering various IR questions, it certainly adds to the significance of CFTs as the cornerstones in the landscape of QFTs.

In addition to their role in organizing the space of QFTs, CFTs have relevance for another fundamental problem in physics, namely that of quantum gravity. General relativity provides a good description of quantum gravity at long distance, where it is weakly coupled. The question of finding a consistent extension of general relativity valid up to an arbitrarily high energy turns out to be tightly constrained, with perturbative string theory providing the only solution found to date. Any insight into the dynamics of quantum gravity valid beyond perturbation theory is thus extremely valuable. Some progress can be made by placing a putative quantum gravity theory into a spacetime with the asymptotic geometry of the anti-de Sitter (AdS) space. The significance of the AdS space in this context stems from its following two properties. It has a timelike boundary, where a boundary condition must be chosen to produce well-defined physics in the bulk, and its isometry group coincides with the group of conformal transformations of the boundary. A more detailed analysis shows that this setup endows the boundary with the structure of a full-fledged CFT. In particular, the presence of dynamical gravity in the bulk implies the existence of a local stress tensor in the boundary CFT.

Compared to quantum gravity, our understanding of CFTs is on a much firmer footing. In particular, CFTs can be defined and studied fully non-perturbatively, as explained in the following section. The observations of the previous paragraph thus give us the opportunity to analyze non-perturbative quantum gravity in the language of conventional non-gravitational quantum field theory. Any quantum gravity theory that can be consistently placed in the AdS space defines a CFT in one less dimension. Conversely, the conditions under which a given CFT corresponds to a weakly-coupled quantum gravity in an AdS space are relatively well-understood.

In summary, conformal field theories are central to several defining questions in current theoretical physics. Moreover, their relatively rigid mathematical structure makes them amenable to exact methods not available in more general quantum field theories. Let us turn to describing this structure in more detail.

1.2 The conformal bootstrap

A conformal field theory is characterized by the properties of its allowed deformations. These deformations are called operators. They represent the allowed probes of the physical system and can come in a multitude of forms. The observables in a CFT are the correlation functions of operators. Writing \mathcal{O}_i , $i = 1, \dots, n$ for a collection of operators in a CFT, their correlation function is denoted as

$$\langle \prod_{i=1}^n \mathcal{O}_i \rangle. \tag{1.1}$$

It is a real number representing the expectation value of the result of an experiment where the collection of probes \mathcal{O}_i is inserted into our system. The most widely studied are local operators, corresponding to probes localized at a point, and denoted $\mathcal{O}(x)$. By virtue of the state-operator map, the local operators form a vector space endowed with a scalar product. In this thesis, we will be mostly concerned with unitary CFTs, where this scalar product is positive definite. The vector space is acted on by the conformal group and can be written as a direct sum of its irreducible representations, called conformal families. The irreducible representations appearing in physically sensible unitary theories are unitary highest-weight representations. The highest-weight states are called primary operators. The conformal family is specified by the quantum number of the primary states under dilatations, called the scaling dimension Δ , and the irreducible representation of $SO(d)$ rotations in which the primary states transform. The rest of the conformal family is spanned by so-called

descendants, which are derivatives of the primary operators. In summary, we can write the space of local operators \mathcal{A} as

$$\mathcal{A} = \bigoplus_{i \in \mathcal{P}} \mathcal{C}(\Delta_i, \rho_i), \quad (1.2)$$

where $\mathcal{C}(\Delta, \rho)$ stands for the conformal family with primary of scaling dimension Δ and $SO(d)$ irreducible representation ρ , and where the sum runs over all conformal families present in the CFT.

A key feature of CFTs is that the space of local operators carries a multiplicative structure. The so-called operator product expansion (OPE) allows us to expand the product of two local operators at different positions $\mathcal{O}_i(x)\mathcal{O}_j(y)$ in the basis \mathcal{A} of all local operators at a single location, such as

$$\mathcal{O}_i(x)\mathcal{O}_j(y) = \sum_{k \in \mathcal{A}} f_{ij}^k(x-y)\mathcal{O}_k(y). \quad (1.3)$$

The expansion coefficients $f_{ij}^k(x-y)$ are fixed by conformal invariance up to overall constants c_{ij}^k . Moreover, the contribution to the right-hand side coming from descendants is completely fixed by the contribution of their primary. The multiplicative structure is thus determined by the structure constants c_{ij}^k with labels i, j, k corresponding to primary operators. We can now use the OPE to reduce an arbitrary n -point function down to a sum over two-point functions, which are in turn determined in terms of Δ_i and ρ_i thanks to conformal invariance. Therefore, the collection of primary labels (Δ_i, ρ_i) together with the structure constants c_{ij}^k are in principle sufficient to reconstruct an arbitrary correlation function of local operators and for this reason are jointly referred to as the *CFT data*.

However, an arbitrary choice of the CFT data does not necessarily define a consistent theory. This is because the OPE in a sensible theory must be associative. The associativity imposed on a product of three primary operators is a constraint bilinear in the structure constants with a complicated dependence on the scaling dimensions and positions of the operators. The idea to use OPE associativity to constrain the CFT data is known as the conformal bootstrap, with the equations expressing associativity called conformal bootstrap equations. In its strongest form, conformal bootstrap states that physically sensible CFTs are in one to one correspondence with the sets of CFT data consistent with OPE associativity. Usually, additional requirements such as unitarity or the presence of a local stress tensor are added.

The conformal bootstrap equations constitute an infinite set of intricate constraints on the infinite amount of CFT data. Although a complete analytic understanding of the

consequences of these equations is currently not available, their constraining power has been demonstrated in a number of contexts. The applications range from constraints on CFTs relevant in condensed matter physics, through bounds on a possible conformal sector in particle physics beyond the Standard Model, to a more precise understanding of how quantum gravity in AdS emerges from a boundary CFT. Most prominently, a numerical implementation of the conformal bootstrap equations has led to a prediction of the critical exponents of the three-dimensional Ising model more precise than those obtained using any other method [4–8].

The conformal bootstrap has provided us with a new torchlight that brightens up the otherwise relatively dark and unexplored world of strongly-coupled quantum field theory. The remainder of this thesis will take us to several corners of this mysterious world and the conformal bootstrap will be our main companion on this journey. Let us turn to briefly describing the setting of the remaining chapters.

1.3 Overview of the thesis

Local operators do not exhaust the set of possible probes a given CFT may admit. Indeed, we can insert more general defects localized on submanifolds of various dimensions in the ambient space. For example, one-dimensional defects may represent infinitely massive particles propagating through our system, while codimension-one defects correspond to boundary conditions or domain walls etc. An especially interesting class of defects of a CFT are those that preserve the maximal possible subgroup of the conformal group, called *conformal defects*. Specifically, a d -dimensional conformal defect in a D -dimensional CFT should preserve the $SO(1, d) \times SO(D - d)$ subgroup of the (Euclidean) conformal group $SO(1, D)$.

Conformal defects at the same time enrich and constrain the dynamics of their ambient CFT. They come with their own spectrum of local operators, which are themselves subject to conformal bootstrap equations. Moreover, the CFT data of the bulk theory are intertwined with those of the defect via another set of bootstrap equations, thus allowing to constrain the bulk dynamics purely from the knowledge of the properties of the defect. These ideas are elaborated on in Chapter 2 based on [1], focusing on the example of the twist line defect in the 3D Ising model. We study the twist defect both using perturbation theory and non-perturbatively via the conformal bootstrap, arriving at a picture consistent with existing lattice simulations and making further predictions for additional defect CFT data.

Among various tools to analyze strongly-coupled quantum field theories, a privileged role is played by supersymmetry. Ensuring cancellations between bosonic and fermionic processes, it allows for a number of quantities to be computed exactly at any coupling. Supersymmetry and conformal bootstrap make for a powerful interplay, since supersymmetry fixes protected quantities, such as scaling dimensions of certain operators, which can then be used as an input of the conformal bootstrap equations to constrain unprotected observables. Chapter 3, based on [3], explores this idea in the context of superconformal theories with four supercharges. We first show how the superconformal bootstrap equations in these theories can be formulated in a unified manner across spacetime dimensions. Afterwards, we use these equations to derive universal bounds on the simplest unprotected quantities. The interacting IR fixed point of the theory of a single chiral superfield, known as the $\mathcal{N} = 2$ super-Ising model in three dimensions, is singled out by our analysis and we are able to make predictions for some of its CFT data which pass additional consistency checks.

The ability of the conformal bootstrap equations to place dramatic bounds on the CFT data pertaining to operators of small scaling dimension can be traced to the existence of certain linear functionals acting on the spaces of conformal blocks and having appropriate positivity properties. Most applications of the conformal bootstrap up to date have proceeded by numerically optimizing the linear functional to produce the most stringent bounds. It is clearly of great interest to construct the optimal functionals analytically since they can hold the key to an analytic solution of CFTs lying on the boundary of the space allowed by the conformal bootstrap equations. Chapter 4 of this thesis, based on [9], addresses this problem in one spacetime dimension. We construct analytically the optimal functional leading to an upper bound on the scaling dimension of the first non-trivial primary operator. The bound is saturated by the theory of free fermions. Although the extremal theory is rather simple, the construction of the functional is quite nontrivial and hopefully implies useful lessons about the nature of extremal functionals in higher dimensions and interacting theories. Furthermore, we use the optimal functional to show how several aspects of $\text{AdS}_2/\text{CFT}_1$ holography naturally emerge from the 1D conformal bootstrap equation.

Chapter 2

The Twist Line Defect in the 3D Ising Model

2.1 Introduction

As explained in more detail in Chapter 1, CFTs play an important role in many aspects of theoretical physics, from the concrete study of physical systems at criticality to abstract problems in mathematical physics. Although some CFTs can be given a weakly coupled description, the most interesting and commonly occurring CFTs are strongly coupled, and in three or more dimensions few analytic tools are available to study them. In supersymmetric or lower-dimensional examples, conformal invariant defects have played a useful role in probing the structure of CFTs. A conformal defect is a non-local observable, a modification of the theory which is localized on a lower-dimensional manifold and preserves an appropriate subgroup of the conformal group. It is natural to attempt to define and study defects in non-supersymmetric, commonly occurring CFTs. The 3d Ising model at criticality is a natural candidate: it is in a sense the simplest non-trivial 3d CFT and has been the subject of an intensive and rather successful analysis by a variety of theoretical and numerical tools [10] such as the ϵ -expansion and Monte Carlo simulations. More recently, interesting constraints on the Ising model [4–8] and other CFTs have been derived using the methods of the conformal bootstrap [11–56]

The simplest possible conformal defect in a CFT is a boundary condition. Boundary conditions in the 3d Ising model have been the subject of some theoretical [57, 58] and numerical study [59]. More recently, there have been attempts to “bootstrap” such boundary conditions [22], by looking at two-point functions of bulk operators in the presence of

the boundary. Another interesting example is a monodromy, or twist defect. The global Z_2 flavor symmetry of the Ising model allows for a natural definition of codimension two twist defects: under a rotation around the defect, local operators pick up a phase factor according to their Z_2 quantum numbers. Due to their topological nature, such defects are essentially guaranteed to flow to scale invariant defects in the IR and possibly to conformal defects.

The authors of reference [60] have used Monte Carlo simulations to provide numerical evidence for the existence of a twist defect in the 3d Ising model. In this chapter, we aim to present further evidence for this from different points of view. We shall take a two-pronged approach: direct analytic calculations using ϵ -expansion techniques; and the numerical methods of the conformal bootstrap. In both cases not only do we find excellent agreement with existent data, but we are also able to make new predictions that may be verified in the near future. As such, our work is a nice example of the interplay between theory, Monte Carlo simulations and the numerical bootstrap.

The ϵ -expansion, introduced by Wilson and Fisher [61], provides a framework to study the critical $O(N)$ models in a perturbative setting. A drawback of this method is its disregard of the conformal symmetry, and another is that high accuracy requires computations to high loop orders and Borel resummation due to the asymptotic nature of the perturbative expansion [62]. Nevertheless, the ϵ -expansion has been used to determine basic critical exponents in 3d rather precisely. The numerical bootstrap recently provided compelling evidence for the consistency of this method by identifying a family of solutions to crossing symmetry, interpolating between the 2d and 3d Ising model, and the 4d free scalar [63]. It is thus natural to use the ϵ -expansion as a source of data on the twist defect in the 3d Ising model. Concretely, we will start with the twist defect in the free theory, add a ϕ^4 coupling in the bulk and study correlation functions in the IR. The theory is expected to flow to the twist defect of the 3d Ising model. Performing one-loop computations, and setting $\epsilon = 1$, we find good agreement with the Monte Carlo data. The one-loop deviation from the 3d free theory is always in the right direction, and often surprisingly close to the measured value. Note that defect scaling dimensions have been studied for Wilson lines in 3d $U(1)$ gauge theory with matter in [64].

As was mentioned before, boundary conditions have been previously considered in the context of the conformal bootstrap. The main obstacle in such program is the lack of guaranteed positivity/unitarity constraints in the intermediate channel where the two bulk operators are fused together. Here we shall take a different approach, by considering directly correlators of defect operators. This guarantees positivity, but the price to pay is that it uses very little information about the bulk CFT itself, as the bulk operators do not appear in any fusion channel. The only properties of the bulk theory which affect directly

the four-point functions on the defect are its symmetries. The 3d Ising model should be a reasonable candidate for such an analysis, because it is strongly constrained by its symmetries: in a sense, it is the simplest 3d CFT with a Z_2 flavor symmetry. It would be interesting to investigate if such a strategy may be successful in the study of boundary conditions (codimension one defects). In this paper, we focus on the codimension two twist line defects, and thus consider the conformal bootstrap in the one-dimensional world volume of the defect.

The spectrum of operators on the defect contains operators of various $U(1)$ ‘spin’ (corresponding to rotations around the defect), which can be integer or half-integer according to the Z_2 charge of the operator. Further, the spectrum should contain a protected “displacement operator” D , of spin 1 and dimension 2. This is the operator one would add to the defect Lagrangian to deform the defect away from a straight line. We shall consider four-point functions of the simplest local operator ψ on the defect, the leading spin-1/2 operator, which occurs in the defect OPE of the Z_2 -odd bulk field σ (the Ising model spin field). However, in one dimension one must take care because a four-point function can be decomposed only into two crossing symmetry channels. There are therefore two crossing equations: in the four-point function $\langle \psi \bar{\psi} \psi \bar{\psi} \rangle$ both fusion channels have spin 0; but the correlator $\langle \psi \psi \bar{\psi} \bar{\psi} \rangle$ has both spin 0 and spin 1 fusion channels.

We shall explore the constraints following from the crossing equations, deriving universal bounds on one-dimension unitary CFTs. By forcing the spectrum to contain the displacement operator, we can derive a bound on the dimension of the leading parity-even spin-0 operator. In the extremal case where the bound is saturated, we can reconstruct a unique solution to crossing symmetry [23], and we find that for a certain value of the OPE coefficient of D the spectrum seems to match that of the defect, found both numerically and via ϵ -expansion. We also obtain a number of other operator dimensions and OPE coefficients which can be thought of as specific predictions for future numerical tests.

Here is a brief outline of this chapter. In section 2.2, we review the twist defect introduced in [60]. We work in the continuum limit, describing the expected symmetries, low-lying operators and the form of the operator product expansion. Section 2.3 is concerned with ϵ -expansion calculations. In section 2.4 we turn to the methods of the modern conformal bootstrap and conclude in Section 2.5 together with suggestions for further research.

2.2 The \mathbb{Z}_2 Twist Defect

Let us recall [60] that the twist line defect in the 3d Ising model can be constructed on the lattice by flipping the Ising coupling on a semi-infinite half-plane ending on a line of the dual lattice. Such semi-infinite surface is a topological defect, since physics is invariant under its arbitrary deformations fixing the boundary line, provided we also flip the spins in between the original and deformed surface. The boundary of such topological surface defect is precisely a twist line defect. In the continuum limit, correlation functions become discontinuous (antiperiodic) across the surface. Presumably the same twist line defect lies at the IR end of the renormalization group flow from the free theory with a \mathbb{Z}_2 twist defect generated by ϕ^4 coupling in the bulk.

The global spacetime symmetry group of a D -dimensional Euclidean parity-invariant CFT is $O^+(1, D+1)$, where parity or sphere inversion switches between the two connected components. A conformal \mathbb{Z}_2 twist line defect thus breaks the bulk symmetry $O^+(1, 4) \times \mathbb{Z}_2$ down to $O^+(1, 2) \times O'(2)$, where $O'(2)$ is a double cover of the group of rotations and reflections fixing the defect, such that the rotation by 2π is identified with the nonidentity element of \mathbb{Z}_2 . The dihedral symmetry D_8 of motions of the cubic lattice fixing the defect, discussed in [60], is a subgroup of $O'(2)$. $O^+(1, 2)$ is the spacetime symmetry group of the defect. At the level of Lie algebras, we have $so(1, 2) = sl(2, \mathbb{R})$, and the connected components of $O^+(1, 2)$ are switched by the reflection in a plane orthogonal to the defect or the sphere inversion centered on the defect. Following [60], we call the former the S -parity.

In this chapter, we will be concerned with local operators living on the twist defect. In the Ising model, these correspond to local modifications of the lattice model in close proximity of the defect line. Applying radial quantization centered at a point on the defect, the defect local operators are seen to correspond to the states of the CFT quantized on a two-punctured sphere, with each puncture inducing the \mathbb{Z}_2 action on the bulk fields. The local operators fall into representations of the group $O^+(1, 2) \times O'(2)$. The 1D conformal algebra $sl(2, \mathbb{R})$ is generated by operators P, D, K (respectively translations, dilations and special conformal transformations) satisfying the commutation relations

$$[D, P] = iP, \quad [D, K] = -iK, \quad [K, P] = -2iD. \quad (2.1)$$

Physically relevant irreps are the highest-weight representations labelled by the scale dimension $\Delta \geq 0$ of the primary $\mathcal{O}(x)$, i.e. $[K, \mathcal{O}(0)] = 0$, $[D, \mathcal{O}(0)] = i\Delta\mathcal{O}(0)$. $\Delta < 0$ would lead to correlation functions growing with distance and also violation of the unitarity bound by the first descendant.

The counterpart of unitarity in the Euclidean signature has been called ‘reflection-positivity’. In our setting, this property means that any correlation function of a configuration of real operators which is invariant under the S -parity is positive. Real operators in the Ising model are those appearing in the real operator algebra generated by the spin field. Reflection-positivity of the 3d Ising model is not spoiled by the defect line since the lattice transfer matrix in a plane perpendicular to the defect is unchanged with respect to the bulk theory. This leads us to define the (Euclidean) conjugate $C(\mathcal{O}(x)) \equiv \bar{\mathcal{O}}(x)$ as complex conjugate composed with S -parity, so that $\langle \bar{\mathcal{O}}(x)\mathcal{O}(y) \rangle \geq 0$. C is an antilinear map on the algebra of local operators which reverses the $O(2)$ spin and commutes with the other quantum numbers.

The commutativity properties of the symmetry algebra enable us to find a basis of defect primaries with well-defined S -parity, and $O(2)$ spin s , which is (half)integer for primaries even (odd) under the global Z_2 . Each $s = 0$ representation moreover carries $O(2)$ -parity, denoted B . We are free to choose the phase of the $s = 0$ primaries so that C acts on them as the identity. The basis of $|s| > 0$ primaries can be chosen so that $B(\mathcal{O}) = b_{\mathcal{O}}\bar{\mathcal{O}}$. From $BC = CB$ and $B^2 = 1$, we get $b_{\mathcal{O}} = e^{i\theta}$. Redefining $\mathcal{O} \rightarrow e^{-i\theta/2}\mathcal{O}$, we cancel the phase and get $B\mathcal{O} = \bar{\mathcal{O}}$, so that $|s| > 0$ do not carry any $O(2)$ -parity.

Exactly as in higher dimensions, conformal invariance fixes the form of two and three point functions. The difference in 1D is that the three point function coefficient $c_{\mathcal{O}_1\mathcal{O}_2\mathcal{O}_3}$ may depend on the cyclic order of the operators (signature of the permutation), since this order is invariant under the connected component of identity in the conformal group. In particular, note that for $x < y < z$

$$\langle \mathcal{O}_1(x)\mathcal{O}_2(y)\mathcal{O}_3(z) \rangle = (-1)^{S_1+S_2+S_3} \langle \mathcal{O}_3(-z)\mathcal{O}_2(-y)\mathcal{O}_1(-x) \rangle, \quad (2.2)$$

where $(-1)^{S_i}$ is the S -parity of \mathcal{O}_i . Hence

$$c_{\mathcal{O}_1\mathcal{O}_2\mathcal{O}_3} = (-1)^{S_1+S_2+S_3} c_{\mathcal{O}_2\mathcal{O}_1\mathcal{O}_3}. \quad (2.3)$$

Arbitrary cyclic permutations are generated by $P + K$. The sign in (2.3) will play an important role in one of our bootstrap equations.

Primary operators on the defect satisfy the usual operator product expansion

$$\mathcal{O}_1(x)\mathcal{O}_2(y) = \sum_{\mathcal{O}_3} \frac{c_{\mathcal{O}_1\mathcal{O}_2\bar{\mathcal{O}}_3}}{|x-y|^{\Delta_1+\Delta_2-\Delta_3}} \mathcal{D}_{\Delta_i}(x-y, \partial)\mathcal{O}_3(y), \quad (2.4)$$

where the sum runs over defect primaries and

$$\mathcal{D}_{\Delta_i}(x-y, \partial) = \sum_{n=0}^{\infty} \frac{(\Delta_1 + \Delta_3 - \Delta_2)_n}{n!(2\Delta_3)_n} (x-y)^n \partial^n \quad (2.5)$$

is fixed by conformal symmetry. Moreover, bulk operators can be expanded in terms of the defect operators in the so-called bulk-defect OPE [58, 65], which for a scalar primary in the bulk takes the form

$$\phi(x, z, \bar{z}) = \sum_{\mathcal{O}} C_{\mathcal{O}}^{\phi} \frac{\bar{z}^{s_{\mathcal{O}}}}{|z|^{\Delta_{\phi} - \Delta_{\mathcal{O}} + s_{\mathcal{O}}}} \mathcal{B}_{\Delta_{\mathcal{O}}}(|z|, \partial) \mathcal{O}(x), \quad (2.6)$$

where we use complex coordinates z, \bar{z} for the transverse directions, the sum is over defect primaries, and $s_{\mathcal{O}}$ denotes the $O(2)$ spin of \mathcal{O} . Conformal symmetry in the presence of the defect fixes $\langle \phi(x, z, \bar{z}) \bar{\mathcal{O}}(y) \rangle$ up to an overall constant $C_{\mathcal{O}}^{\phi}$, and consequently determines

$$\mathcal{B}_{\Delta}(|z|, \partial) = \sum_{n=0}^{\infty} \frac{(-1)^n (\Delta)_n}{n! (2\Delta)_{2n}} |z|^{2n} \partial^{2n}. \quad (2.7)$$

Notice that in particular, the boundary OPE coefficient $C_{\mathbb{1}}^{\phi}$ gives the expectation value of ϕ ,

$$\langle \phi(x, z, \bar{z}) \rangle = \frac{C_{\mathbb{1}}^{\phi}}{|z|^{\Delta_{\phi}}}. \quad (2.8)$$

Applying a 2π rotation to (2.6), we see that the defect expansion of a bulk operator ϕ even (odd) under the global Z_2 contains only defect primaries with integer (half-integer) spins. Typically, the bulk-defect OPE will contain an infinite tower of defect primaries at each allowed spin. An exception is the bulk free field, studied below, which only features one defect primary at each spin.

The defect spectrum always contains the displacement operator $D(x)$ which, when added to the Lagrangian, generates deformations of the defect. Its dimension and quantum numbers are fixed by the Ward identity expressing the breaking of transverse translational symmetry by the defect

$$\partial_a T^{ai}(x, z, \bar{z}) = D^i(x) \delta^2(z, \bar{z}), \quad (2.9)$$

where i label the transverse coordinates. Hence $\Delta_D = 2$, $s_D = 1$, and D is even under S -parity.

Let us illustrate the above in the simplest setting – the theory of the free massless real scalar ϕ in three dimensions, with twist defect for the global Z_2 . Applying the bulk equations of motion to the bulk-defect OPE of ϕ , we find that the scale dimension of the defect primary of (half-integer) spin s appearing in the OPE is $\Delta_s = |s| + 1/2$. We will denote this tower of operators by ψ_s . The field ϕ (and consequently each ψ_s) is even under S -parity. Reality of ϕ implies $\psi_{-s} = \bar{\psi}_s$. The lowest-lying non-identity defect primary is

$\psi \equiv \psi_{1/2}$ with scale dimension $\Delta_\psi = 1$. Since the scale dimension of the bulk spin field in the 3d Ising model is close to the free-field value, we expect the lowest-lying operator in the Ising defect spectrum to have dimension close to 1 and share the other quantum numbers with the free-theory ψ . Going back to the free theory, the $\bar{\psi}\psi$ OPE contains primary operators of schematic form $\mathcal{O}_n = \bar{\psi}\partial^n\psi$, $n \geq 0$. We have $\Delta_{\mathcal{O}_n} = n + 2$, $s_{\mathcal{O}_n} = 0$, and the S -parity, as well as $O(2)$ -parity of \mathcal{O}_n is $(-1)^n$. The $\psi\psi$ OPE features primaries with schematic form $\mathcal{S}_n = \psi\partial^{2n}\psi$ for $n \geq 0$. This time, we obtain $\Delta_{\mathcal{S}_n} = 2n + 2$, $s_{\mathcal{S}_n} = 1$, and the operators are even under S -parity. \mathcal{S}_0 is the only candidate for the displacement operator, since forming further OPEs will only create operators with dimensions greater than 2. In the next section, we will compute the first-order corrections to the scale dimensions of some of these operators, as well as their three point function constants at the Wilson-Fisher fixed point in $4 - \epsilon$ dimensions. In particular, we will check that $D \equiv \mathcal{S}_0$ is indeed protected at this order.

2.3 Epsilon Expansion

In order to study the properties of the twist defect at the Wilson-Fisher fixed point in $4 - \epsilon$ dimensions, we start with the $D = 2 - \epsilon$ dimensional twist defect in the free theory and add a bulk ϕ^4 interaction at the critical coupling. Since renormalization is a local property, the bulk flow is unaffected by the presence of the defect, and so the critical coupling is the usual $g = (4\pi)^2\epsilon/3 + O(\epsilon^2)$. Correlation functions of local bulk operators interpolate between two regimes – when the typical distances between the insertions are much smaller than the distance from the defect, the correlation functions become those of the Wilson-Fisher fixed point with no defect. In the opposite case, the correlation functions are controlled by the CFT data of the defect. In the latter regime, the distance from the defect acts as a UV cutoff.

In this section, we use bulk perturbation theory to study bulk correlation functions in the defect regime and thus determine the data associated to some important defect operators to the first order in ϵ . The reader uninterested in the details may skip directly to the results which are displayed in table 2.1.

2.3.1 The two-point function in the free theory

First, we will need the two-point function in the free theory alias the propagator. It is anti-periodic around the defect and satisfies

$$-\nabla^2 G_0(x_1, x_2) = \frac{4\pi^{D/2+1}}{\Gamma\left(\frac{D}{2}\right)} \delta^{D+2}(x_1 - x_2), \quad (2.10)$$

where we chose the normalization standard in CFT literature, resulting in the asymptotics

$$G_0(x_1, x_2) \stackrel{x_1 \rightarrow x_2}{\sim} \frac{1}{|x_1 - x_2|^d}. \quad (2.11)$$

Let x denote coordinates in the whole space and y those along the defect. The propagator can be easily found in momentum space

$$G_0(x_1, x_2) = \frac{2\pi^{D/2}}{\Gamma\left(\frac{D}{2}\right)} \sum_{s \in \mathbb{Z} + \frac{1}{2}} \int \frac{d^D k}{(2\pi)^D} e^{is(\theta_1 - \theta_2)} e^{ik \cdot (y_1 - y_2)} I_{|s|}(kr_-) K_{|s|}(kr_+), \quad (2.12)$$

where the Fourier transform is over the coordinates along the defect, θ is the angle around the defect, $r_- = \min(r_1, r_2)$, $r_+ = \max(r_1, r_2)$ and I_s, K_s are the modified Bessel functions. The contribution from spin s can be integrated to give

$$G_0(x_1, x_2, s) = \frac{1}{4^\Delta} \frac{\Gamma(\Delta)}{\Gamma\left(\frac{D}{2}\right) \Gamma\left(\Delta - \frac{D}{2} + 1\right)} \frac{e^{is(\theta_1 - \theta_2)}}{(r_1 r_2)^{\frac{D}{2}}} \xi^{-\Delta} \times \\ \times {}_2F_1\left(\Delta, \Delta - \frac{D}{2} + \frac{1}{2}; 2\Delta - D + 1; -\frac{1}{\xi}\right), \quad (2.13)$$

where $\Delta = |s| + D/2$ is the scaling dimension of the primary field ψ_s of spin s induced on the defect by ϕ in the bulk, and

$$\xi = \frac{(y_1 - y_2)^2 + (r_1 - r_2)^2}{4r_1 r_2} \quad (2.14)$$

is one of the two conformal cross-ratios, the other being the relative angle. The computation can be simplified by using conformal invariance – it is enough to evaluate the spin- s propagator at $r_1 = r_2$ since this fixes the dependence on ξ . $\xi \ll 1$, $\Delta\theta \ll 1$ is the regime controlled by the bulk CFT and $\xi \gg 1$ the regime controlled by the defect data. Defect channel scalar conformal blocks for equal external dimensions can be read off from (2.13),

since these depend only on the internal dimension Δ and space-time dimension. To compute the properties of ψ_s , we will need the spin- s two-point function in four dimensions, where (2.13) reduces to

$$G_0(x_1, x_2, s) \stackrel{D=2}{=} \frac{e^{is(\theta_1 - \theta_2)}}{4r_1 r_2} \frac{\xi^{-\frac{1}{2}}}{\sqrt{1 + \xi} (\sqrt{\xi} + \sqrt{1 + \xi})^{2|s|}}. \quad (2.15)$$

We can check that the infinite sum over spins produces the correct short distance singularity. Indeed, the full free two-point function can be resummed for $\theta_1 = \theta_2$

$$G_0(x_1, x_2) \stackrel{\theta_1 = \theta_2}{=} \frac{1}{|x_1 - x_2|^D} \frac{2\Gamma\left(\frac{D+1}{2}\right)}{\sqrt{\pi}\Gamma\left(\frac{D}{2}\right)} \xi^{-\frac{1}{2}} {}_2F_1\left(\frac{1}{2}, \frac{D+1}{2}; \frac{3}{2}; -\frac{1}{\xi}\right). \quad (2.16)$$

When $\xi \ll 1$, this reduces to the expected (2.11). For completeness, let us note that the full two-point function can be found explicitly in $D = 2$ by summing (2.15)

$$G_0(x_1, x_2) \stackrel{D=2}{=} \frac{1}{|x_1 - x_2|^2} \frac{\cos\left(\frac{\theta_1 - \theta_2}{2}\right)}{\sqrt{1 + \xi}}. \quad (2.17)$$

2.3.2 The two-point function at one loop

Leading defect operators of half-integer spin

In this subsection, we will compute the scaling dimensions of the operators ψ_s of spin $s = n + 1/2$, $n \in \mathbb{Z}_{\geq 0}$, induced by σ on the defect, as well as the bulk-defect OPE coefficient $C_{\psi_s}^\sigma$ to the first order in ϵ . If nothing too dramatic happens along the RG flow from the free massless scalar, these should be the leading operators of half-integer spin. We will consider the spin- s component of the bulk two-point function when the two insertions are taken close to the defect. Let us place both points at radius r and distance y along the defect, relative angle θ and denote $\lambda = r/y = 1/\sqrt{4\xi}$. From the bulk-defect OPE, we expect the spin- s component of the two-point function to have the following leading behaviour as $\lambda \rightarrow 0$

$$G(x_1, x_2, 1/2) = |C_{\psi_s}^\sigma|^2 \frac{e^{is\theta}}{r^{2\Delta_\sigma}} \lambda^{2\Delta_{\psi_s}} (1 + O(\lambda^2)). \quad (2.18)$$

The dependence of Δ_{ψ_s} and $C_{\psi_s}^\sigma$ on ϵ at one loop comes from two sources – the change of the free theory result with space-time dimension and the one-loop self-energy diagram (see figure 2.1). Using (2.13), one finds the free theory result

$$G_0(x_1, x_2, s) = \frac{\Gamma\left(s + \frac{D}{2}\right)}{\Gamma\left(\frac{D}{2}\right)\Gamma(s+1)} \frac{e^{is\theta}}{r^D} \lambda^{2s+D} (1 + O(\lambda^2)). \quad (2.19)$$

Expanding the Gamma functions, we obtain the free theory CFT data of ψ_s to the first order in ϵ

$$\Delta_{\psi_s} \stackrel{free}{=} s + 1 - \frac{\epsilon}{2} \quad (2.20)$$

$$|C_{\psi_s}^\sigma| \stackrel{free}{=} 1 + \frac{\psi(1) - \psi(s+1)}{4} \epsilon + O(\epsilon^2), \quad (2.21)$$

where $\psi(z) = (\log \Gamma(z))'$. The one-loop self-energy diagram should be evaluated in $D = 2$ since the coupling constant is itself proportional to ϵ . Taking care of the normalization and symmetry factor, the diagram's contribution is equal to

$$G_1(x_1, x_2, s) = -\frac{g}{32\pi^4} \int_{\mathbb{R}^4} d^4 x_0 G_0(x_1, x_0, s) G_0(x_0, x_0) G_0(x_0, x_2, s). \quad (2.22)$$

We need a regularized expression for the full free two-point function between coincident points $G_0(x_0, x_0)$ in $D = 2$. Starting either from (2.12) and evaluating the sum over spins for $D < 0$ (so in dimensional regularization), or taking the finite piece of (2.16), we find

$$G_0(x_0, x_0) = -\frac{\Gamma\left(\frac{D+1}{2}\right)}{2^{D-1} D \sqrt{\pi} \Gamma\left(\frac{D}{2}\right)} \frac{1}{r_0^D} \stackrel{D=2}{=} -\frac{1}{8} \frac{1}{r_0^2}. \quad (2.23)$$

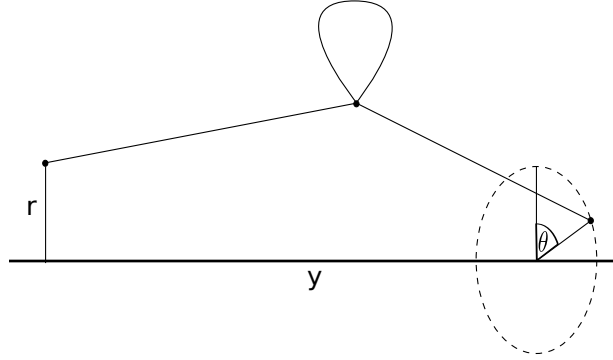


Figure 2.1: The one-loop contribution to $\langle \phi(x_1) \phi(x_2) \rangle$

Using $g = (4\pi)^2\epsilon/3$, and the free $D = 2$, spin- s propagator (2.15), and performing the trivial integration over the angle, the one-loop diagram becomes

$$G_1(x_1, x_2, s) = \frac{\epsilon}{24\pi} e^{is\theta} \int_{\mathbb{R}^2} dy_0 dz_0 \int_0^\infty \frac{dr_0}{r_0} \frac{(4r_0 r)^{2s}}{d_+ d_- e_+ e_- (d_+ + d_-)^{2s} (e_+ + e_-)^{2s}}, \quad (2.24)$$

where

$$d_\pm = \sqrt{\left(y_0 - \frac{y}{2}\right)^2 + z_0^2 + (r_0 \pm r)^2}$$

$$e_\pm = \sqrt{\left(y_0 + \frac{y}{2}\right)^2 + z_0^2 + (r_0 \pm r)^2}.$$

When $\lambda \rightarrow 0$, the integral is proportional to $\lambda^{2(s+1)} \log \lambda$, which is giving precisely the anomalous dimension of ψ_s . The asymptotic expansion (see Appendix 2.A.1) reveals that

$$G_1(x_1, x_2, s) = -\frac{\epsilon}{12s} \frac{e^{is\theta}}{r^2} \lambda^{2(s+1)} (\log \lambda + o(1)) \quad (2.25)$$

as $\lambda \rightarrow 0$. It follows that the one-loop contribution to Δ_{ψ_s} is $-\epsilon/24s$ and that to $|C_{\psi_s}^\sigma|$ vanishes. The CFT data at the Wilson-Fisher fixed point to the first order in ϵ are therefore

$$\Delta_{\psi_s} = s + 1 - \left(\frac{1}{2} + \frac{1}{24s}\right) \epsilon + O(\epsilon^2) \quad (2.26)$$

$$|C_{\psi_s}^\sigma| = 1 + \frac{\psi(1) - \psi(s+1)}{4} \epsilon + O(\epsilon^2). \quad (2.27)$$

The inverse power-law dependence of the anomalous dimension on spin is in agreement with the results of [66, 67]. The comparison to Monte Carlo data on $\psi = \psi_{1/2}$ and $\psi_{3/2}$ presented in [60] are reassuring, see table 2.1.

2.3.3 Energy operator

In this subsection, we will consider the two-point function in the bulk limit $\xi \ll 1$ in order to find the one-point function of the energy operator ϵ in the presence of the defect at one loop. Put the two insertions at the same θ , same radius r and distance y along the

quantity	3D free theory	Wilson-Fisher	Monte Carlo
Δ_ψ	1	0.917	0.9187(6)
$\Delta_{\psi_{3/2}}$	2	1.972	1.99(5)
Δ_D	2	2	2
Δ_s	2	2.167	2.27(1)
Δ_{p^0}	3	2.833	2.9(2)
Δ_{t_+}	3	3.111	3.1(5)
$ C_\psi^\sigma $	0.798	0.847	0.968(2)
$ C_{\psi_{3/2}}^\sigma $	0.651	0.680	0.61(9)
C_1^ϵ	-0.225	-0.141	-0.167(4)

Table 2.1: A comparison of lattice data and the Wilson-Fisher fixed point at one loop.

defect, so that $\lambda = r/y \gg 1$. Bulk OPE and conformal invariance of the one-point function dictates that

$$G(x_1, x_2) = \frac{1}{y^{2\Delta_\sigma}} [1 + c_{\sigma\sigma\epsilon} C_1^\epsilon \lambda^{-\Delta_\epsilon} (1 + o(1))], \quad (2.28)$$

where the o -notation now refers to the limit $\lambda \rightarrow \infty$. Expanding the free-theory result (2.16) around $\xi = \infty$ yields

$$G_0(x_1, x_2) = \frac{1}{y^D} \left[1 - \frac{2^{-D} \Gamma\left(\frac{D+1}{2}\right)}{\sqrt{\pi} \Gamma\left(\frac{D+2}{2}\right)} \lambda^{-D} (1 + O(\lambda^{-2})) \right], \quad (2.29)$$

which gives the following free-theory predictions for the CFT data associated to ϵ

$$\Delta_\epsilon \stackrel{free}{=} 2 - \epsilon \quad (2.30)$$

$$c_{\sigma\sigma\epsilon} C_1^\epsilon \stackrel{free}{=} -\frac{1}{8} \left[1 + \frac{2 \log 2 - \psi(3/2) + \psi(2)}{2} \epsilon \right] + O(\epsilon^2). \quad (2.31)$$

The one-loop self-energy can be evaluated using the full 4D propagator (2.17). Rather than starting directly from (2.17), it is more convenient to sum (2.24) over the spins, setting $\theta = 0$

$$G_1(x_1, x_2) = \frac{\epsilon}{3\pi} \int_{\mathbb{R}^2} dy_0 dz_0 \int_0^\infty dr_0 \frac{r}{d_+ d_- e_+ e_-} \frac{(d_+ + d_-)(e_+ + e_-)}{(d_+ + d_-)^2 (e_+ + e_-)^2 - (4rr_0)^2}. \quad (2.32)$$

Asymptotic expansion of this integral as $\lambda \rightarrow \infty$ shows (see Appendix 2.A.2)

$$G_1(x_1, x_2) = \frac{\epsilon}{y^2} \lambda^{-2} \left[\frac{1}{24} \log \lambda + \frac{\log 2}{12} + o(1) \right]. \quad (2.33)$$

We checked this result agrees with the computation which uses the full propagator (2.17). Combining the tree-level and one-loop result, we find the following properties of ϵ at one loop

$$\Delta_\epsilon = 2 - \frac{2}{3}\epsilon + O(\epsilon^2) \quad (2.34)$$

$$c_{\sigma\sigma\epsilon}C_1^\epsilon = -\frac{1}{8} \left[1 + \frac{2 \log 2 + 3\psi(2) - 3\psi(3/2)}{6} \epsilon \right] + O(\epsilon^2). \quad (2.35)$$

The formula for Δ_ϵ is in agreement with the standard result obtained using perturbation theory without the defect. We reproduce the computation in Appendix 2.B in order to find the OPE coefficient $c_{\sigma\sigma\epsilon} = \sqrt{2}(1 - \epsilon/6) + O(\epsilon^2)$. It follows that the one-point function coefficient of energy is

$$C_1^\epsilon = -\frac{1}{8\sqrt{2}} \left[1 + \frac{1 + 2 \log 2 + 3\psi(2) - 3\psi(3/2)}{6} \epsilon \right] + O(\epsilon^2). \quad (2.36)$$

As shown in table 2.1, the first order result is again in a good agreement with Monte Carlo data.

2.3.4 The four-point function

Leading defect operators of positive integer spin

Operators on the defect of integer spin can be found in the $\psi_{s_1}\psi_{s_2}$ OPEs. The most important of these is the displacement operator of spin one and protected dimension $D + 1 = 3 - \epsilon$. In the free theory, the normal ordered product $\psi_{s_1}\psi_{s_2}$ has scaling dimension $|s_1| + |s_2| + 2 - \epsilon$. Consequently, the space of lowest-lying operators of positive integer spin s is generated by all $\psi_{s_1}\psi_{s_2}$ with $s_1, s_2 > 0$ and $s_1 + s_2 = s$. After flowing to the Wilson-Fisher fixed point, this degeneracy is lifted. Let us denote $\mathcal{O}_{s,m} \equiv \psi_{m-\frac{1}{2}}\psi_{s-m+\frac{1}{2}}$ for $m = 1, \dots, \lfloor \frac{s+1}{2} \rfloor$, with the exception $\mathcal{O}_{2k-1,k} \equiv \psi_{k-\frac{1}{2}}\psi_{k-\frac{1}{2}}/\sqrt{2}$, so that $\mathcal{O}_{s,m}$ is normalized in the free theory. At the Wilson-Fisher fixed point, the matrix of two-point functions of $\mathcal{O}_{s,m}$ s is, to the first order in ϵ ,

$$\langle \mathcal{O}_{s,m}(y_1) \bar{\mathcal{O}}_{s,n}(y_2) \rangle = \frac{1}{y_{12}^{2s+4-2\epsilon}} [\delta_{mn} - 2\epsilon(\log y_{12})\Delta_{mn}^s], \quad (2.37)$$

where we ignored the possible corrections sub-leading in y_{12} . Denoting δ_s the minimal eigenvalue of Δ_{mn}^s , the lowest dimension at spin $s \in \mathbb{Z}_{>0}$ is, to the first order in ϵ

$$\Delta_s = s + 2 + \epsilon(\delta_s - 1). \quad (2.38)$$

In particular, if the displacement $D = \mathcal{O}_{1,1}$ is protected, we should have $\delta_1 = \Delta_{11}^1 = 0$.

In the following, we will find the matrix Δ_{mn}^s by studying the various spin components of the four-point function of ϕ when all four insertions are at the same radius r with $|y_{12}| = |y_{34}| = r/\lambda$ and $|y_{13}| = r/(\lambda\mu)$ such that $\lambda \ll 1$, $\mu \ll 1$. Using first the bulk-defect OPE, and then OPE on the defect, we find the leading piece of the four-point function for $s_1, s_2 > 0$, $s_3, s_4 < 0$ and $s_1 + s_2 = -s_3 - s_4 = s$

$$G(\{x_j, s_j\}_{j=1}^4) = \frac{\prod_{j=1}^4 \left(C_{\psi_{s_j}}^\sigma e^{is_j\theta_j} \lambda^{\Delta_{\psi_{s_j}}} \right)}{r^{4\Delta_\sigma}} \times \\ \times c_{\psi_{s_1}\psi_{s_2}\bar{\mathcal{O}}_{s,m}} c_{\psi_{s_3}\psi_{s_4}\mathcal{O}_{s,n}} \mu^{2s+4-2\epsilon} [\delta_{mn} + 2\epsilon(\log \mu)\Delta_{mn}^s], \quad (2.39)$$

where $\mathcal{O}_{s,m}$ is the normalized product $\psi_{s_1}\psi_{s_2}$ and $\bar{\mathcal{O}}_{s,n}$ is the normalized product $\psi_{s_3}\psi_{s_4}$. Recall that to $O(\epsilon^0)$, we have $C_{\psi_{s_j}}^\sigma = 1$ and from Wick's theorem

$$c_{\psi_{s_1}\psi_{s_2}\bar{\mathcal{O}}_{s,m}} = \begin{cases} 1 & \text{if } s_1 \neq s_2 \\ \sqrt{2} & \text{if } s_1 = s_2 \end{cases}. \quad (2.40)$$

In bulk perturbation theory, the contributions to the four-point function at the first order come from the diagrams with two disconnected loop-corrected propagators, and the contact four point interaction (see figure 2.2). The former give the leading contribution

$$G_{\text{disc.}}(\{x_j, s_j\}_{j=1}^4) = \frac{\prod_{j=1}^4 \left[e^{is_j\theta_j} (\lambda\mu)^{\Delta_{\psi_{s_j}}} \right]}{r^{4\Delta_\sigma}} (\delta_{s_1, -s_3} \delta_{s_2, -s_4} + \delta_{s_1, -s_4} \delta_{s_2, -s_3}), \quad (2.41)$$

while the contact interaction leads to the integral (following from (2.15))

$$G_{\text{con.}}(\{x_j, s_j\}_{j=1}^4) = -\frac{\epsilon}{2^7 3\pi} \int_{\mathbb{R}^2} dy_0 dz_0 \int_0^\infty \frac{dr_0}{r^4 r_0^3} \prod_{j=1}^4 \frac{e^{is_j\theta_j}}{\sqrt{\xi_j} \sqrt{1+\xi_j} (\sqrt{\xi_j} + \sqrt{1+\xi_j})^{2|s_j|}}, \quad (2.42)$$

where

$$\xi_j = \frac{(y_j - y_0)^2 + z_0^2 + (r - r_0)^2}{4rr_0}. \quad (2.43)$$

Asymptotic expansion gives the following leading piece (see Appendix 2.A.3)

$$G_{\text{con.}}(\{x_j, s_j\}_{j=1}^4) = \frac{4\epsilon}{3(s+1)} (\log \mu + O(1)) \frac{1}{r^4} \prod_{j=1}^4 [e^{is_j\theta_j} (\lambda\mu)^{|s_j|+1}], \quad (2.44)$$

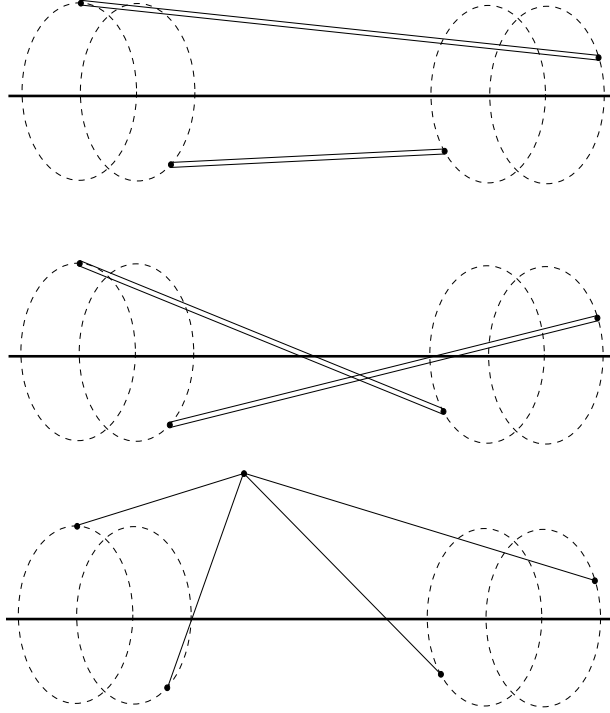


Figure 2.2: The diagrams contributing to the properties of $\psi_{s_1}\psi_{s_2}$ up to one loop. The double line denotes the one-loop-corrected propagator.

which is consistent with (2.39). Putting the disconnected and contact interaction diagrams together, we find the following values of the matrix of scaling dimensions Δ_{mn}^s

$$\Delta_{mn}^s = \begin{cases} \frac{2}{3(s+1)} & \text{if } m \neq n \\ \frac{2}{3(s+1)} - \frac{1}{12} \left(\frac{1}{2m-1} + \frac{1}{2s-2m+1} \right) & \text{if } m = n, 2m \neq s+1 \\ \frac{1}{3(s+1)} - \frac{1}{6s} & \text{if } m = n, 2m = s+1 \end{cases} \quad (2.45)$$

The first term comes from the contact interaction and the second from the disconnected diagrams (if present), where we need to use the one-loop-corrected $\Delta_{\psi_{s_j}}$ from (2.26). The first case occurs when $\{s_1, s_2\} \neq \{-s_3, -s_4\}$, when only the contact interaction contributes. The second case occurs when $\{s_1, s_2\} = \{-s_3, -s_4\}$ but $s_1 \neq s_2$. Finally, the third case occurs when $s_1 = s_2 = -s_3 = -s_4$.

The first thing to notice is that $\Delta_{11}^1 = 0$, so the displacement operator is indeed protected at the first order in ϵ . The next simplest case is $s = 2$, with a single operator $t_+ = \psi\psi_{\frac{3}{2}}$ of free-theory dimension $4 - \epsilon$ and anomalous dimension $\epsilon/9$. Numerical results

for the lowest eigenvalue of Δ_{mn}^s are shown in figure 2.3. The leading anomalous dimension converges to $-1/12$ as $s \rightarrow \infty$, which can be understood by noting that in this limit, $(e^j)_n = \delta_{nj}$ becomes an eigenvector of Δ_{mn}^s with eigenvalue

$$\lambda_j = -\frac{1}{12(2j-1)}. \quad (2.46)$$

It would be interesting to understand the asymptotic properties of the spectrum along the lines of [66, 67]. Unfortunately, the Monte Carlo data on higher-spin operators are not yet precise enough to provide a test of our results.

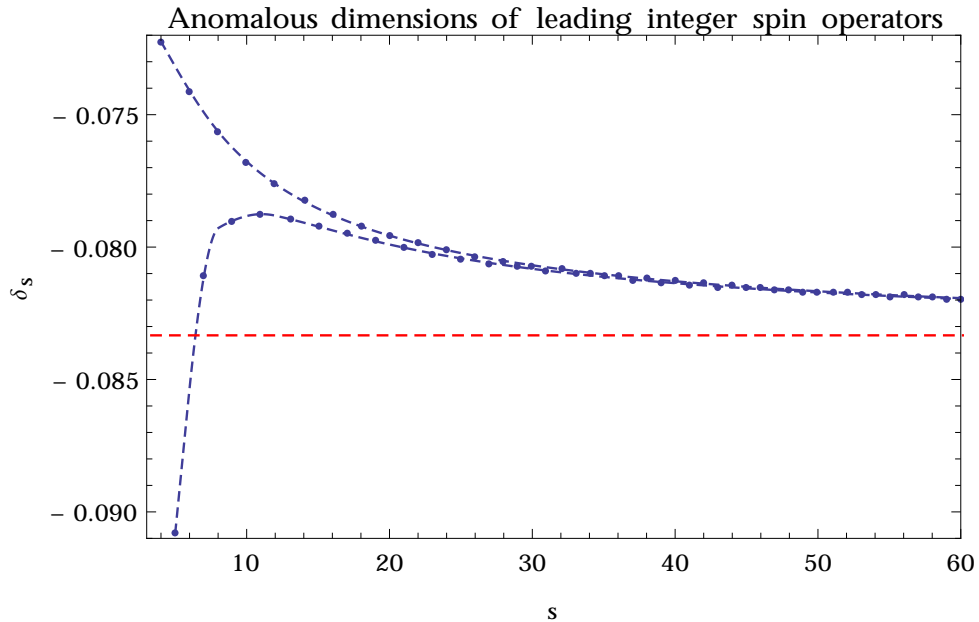


Figure 2.3: Anomalous dimensions of the leading operators of spin s at one loop. Dashed blue lines interpolate between the even and odd spins. They both asymptote to the dashed red line $\delta_s = -1/12$.

Computation of the next-to-leading order in μ of the contact interaction diagram (2.44) provides the first order correction to the OPE coefficients $c_{\psi_{s_1} \psi_{s_2} \mathcal{O}_{s,m}}$. The disconnected diagrams contribute only to $C_{\psi_{s_j}}^\sigma$. The computation is included in Appendix 2.A.4, the

result being

$$G_{\text{con.}} \left(x_1, \frac{1}{2}; x_2, \frac{1}{2}; x_3, -\frac{1}{2}; x_4, -\frac{1}{2} \right) = \epsilon \left(\frac{2}{3} \log \mu - \frac{8 \log 2 - 5}{6} + o(1) \right) \times \\ \times \frac{(\lambda\mu)^6}{r^4} e^{(\theta_1 + \theta_2 - \theta_3 - \theta_4)/2}, \quad (2.47)$$

from which it follows that

$$c_{\psi\psi\bar{D}} = \sqrt{2} \left(1 - \frac{8 \log 2 - 5}{24} \epsilon + O(\epsilon^2) \right). \quad (2.48)$$

2.3.5 The leading defect scalar and pseudoscalar

The above discussion was concerned only with operators of positive integer spin, but it is a simple matter to use the same method to find the dimension of the leading defect (non-identity) scalar. In the free theory, it is the operator $s = \bar{\psi}\psi$ of dimension $3 - \epsilon$. Now we can repeat the steps above with $s_1 = -s_2 = -s_3 = s_4 = 1/2$ and find that the computation is almost identical to that for the displacement operator, the only difference being in the free-theory OPE coefficients ($c_{\psi\psi\bar{D}} = \sqrt{2}$, $c_{\psi\bar{\psi}s} = 1$). In both cases, the contribution from the disconnected diagrams is $-\epsilon/6$ (twice the anomalous dimension of ψ). The contact interaction diagram contributes $\epsilon/6$ to the displacement, but $\epsilon/3$ to the scalar since in the former case, it is reduced by $|c_{\psi\psi\bar{D}}|^2=2$. Hence the dimension of s is

$$\Delta_s = 3 - \frac{5}{6} \epsilon + O(\epsilon^2). \quad (2.49)$$

Table 2.1 indicates that already the first order provides a considerable improvement towards the Monte Carlo results with respect to the free theory. We can also use the constant piece of (2.47) to conclude that

$$c_{\bar{\psi}\psi s} = 1 - \frac{8 \log 2 - 5}{12} \epsilon + O(\epsilon^2). \quad (2.50)$$

The leading free-theory defect operator with spin zero and negative S -parity is $p^0 = \bar{\psi} \overleftrightarrow{\partial} \psi / 2 = [(\partial\bar{\psi})\psi - \bar{\psi}(\partial\psi)]/2$. We wish to study it using the $\langle \phi(x_1) \overleftrightarrow{\partial} \phi(x_2) \phi(x_3) \overleftrightarrow{\partial} \phi(x_4) \rangle$ bulk correlator, where the derivatives act along the defect. We put all four points at the same distance from the defect and focus on the correct spin component of the four-point function. The contact interaction diagram for $\langle \phi(x_1) \phi(x_2) \phi(x_3) \phi(x_4) \rangle$ is completely

symmetric under any permutation of the four points. The antisymmetric derivative acting on x_3, x_4 thus makes the diagram vanish in the limit $x_3 \rightarrow x_4$. Hence the properties of p^0 to the first order are determined solely by the renormalization of ψ . We find

$$\Delta_{p^0} = 2\Delta_\psi + 1 + O(\epsilon^2) = 4 - \frac{7}{6}\epsilon + O(\epsilon^2). \quad (2.51)$$

The generalized free theory gives for the three point function constant

$$c_{\bar{\psi}\psi p^0} = \sqrt{\Delta_{p^0}} + O(\epsilon^2) = \sqrt{\frac{3}{2}} \left(1 - \frac{7}{36}\epsilon + O(\epsilon^2) \right). \quad (2.52)$$

We will be able to compare these predictions with data from conformal bootstrap in the following section.

2.4 Bootstrapping the twist defect

In this section we will apply the methods of the numerical conformal bootstrap to the one-dimensional defect directly. As outlined in the introduction, there are two distinct but related crossing equations which are relevant for our problem. Analysis of the first leads to an operator dimension bound in one dimension, similar to those derived between 2 and 4 dimensions in references [4, 13, 14, 63]. The bound appears to be saturated by the generalized free fermion. Adding an extra equation and demanding the existence of a displacement operator leads to more interesting bounds, and we are able to reconstruct the twist defect spectrum.

2.4.1 The bootstrap equations

The bootstrap equations that we use result from expanding four-point functions of $\psi, \bar{\psi}$ in different OPE channels. Four points on a line have only one invariant under the $SL(2, \mathbb{R})$ action. We take it to be

$$z = \frac{x_{12}x_{34}}{x_{13}x_{24}}. \quad (2.53)$$

We fix the order of the insertions to $x_1 < x_2 < x_3 < x_4$, which results in the constraint $0 < z < 1$. The four-point function of defect primaries \mathcal{O}_i of equal scale dimension d can be written as

$$\langle \mathcal{O}_1(x_1)\mathcal{O}_2(x_2)\mathcal{O}_3(x_3)\mathcal{O}_4(x_4) \rangle = \frac{1}{|x_{12}|^{2d}|x_{34}|^{2d}}g(z), \quad (2.54)$$

where $g(z)$ is an analytic function for $z \in (0, 1)$. Colliding x_1 and x_2 leads to the series expansion in conformal blocks

$$g(z) = \sum_{\mathcal{O}} c_{12\mathcal{O}} c_{34\bar{\mathcal{O}}} G_{\Delta_{\mathcal{O}}}(z), \quad (2.55)$$

where the sum runs over defect primaries, and $G_{\Delta}(z)$ is the 1D conformal block for equal external dimensions and internal dimension Δ . The conformal blocks are given by [68]

$$G_{\Delta}(z) = z^{\Delta} {}_2F_1(\Delta, \Delta; 2\Delta; z). \quad (2.56)$$

Colliding instead x_2 and x_3 and equating the two different representations of the four-point function leads to the crossing equation

$$\sum_{\mathcal{O}} c_{12\mathcal{O}} c_{34\bar{\mathcal{O}}} z^{-2d} G_{\Delta_{\mathcal{O}}}(z) = \sum_{\mathcal{O}} c_{23\mathcal{O}} c_{41\bar{\mathcal{O}}} (1-z)^{-2d} G_{\Delta_{\mathcal{O}}}(1-z) \quad (2.57)$$

valid for $z \in (0, 1)$.

$U(1)$ symmetry requires that a nonzero four-point function of ψ and $\bar{\psi}$ must contain two of each. There are two nonequivalent orders to consider: $\langle \bar{\psi}\psi\bar{\psi}\psi \rangle$ and $\langle \bar{\psi}\psi\psi\bar{\psi} \rangle$. Focusing on the first case, the exchanged operators come from the $\bar{\psi}\psi$ OPE, so they have $U(1)$ spin zero. Moreover, their S-parity equals the $O(2)$ parity since the two symmetries require in turn

$$\langle \bar{\psi}\psi\mathcal{O} \rangle = (-1)^{S(\mathcal{O})} \langle \psi\bar{\psi}\mathcal{O} \rangle = (-1)^{B(\mathcal{O})} \langle \psi\bar{\psi}\mathcal{O} \rangle. \quad (2.58)$$

We have seen this correlation between the parities in the $\bar{\psi}\psi$ OPE in the free theory example of section 2.2. Of course, the $\bar{\psi}\psi$ OPE starts with the identity. The coefficients of the conformal block expansion in the (12)(34) channel are $c_{\bar{\psi}\psi\mathcal{O}} c_{\bar{\mathcal{O}}\bar{\psi}\psi}$. Using the Hilbert space formalism, this equals

$$\langle \psi|\psi|\mathcal{O} \rangle \langle \mathcal{O}|\bar{\psi}|\psi \rangle = |\langle \psi|\psi|\mathcal{O} \rangle|^2 = |c_{\bar{\psi}\psi\mathcal{O}}|^2. \quad (2.59)$$

The (23)(41) contains the same set of spin-0 operators and the corresponding coefficients are $|c_{\psi\bar{\psi}\mathcal{O}}|^2$. But $c_{\psi\bar{\psi}\mathcal{O}} = \pm c_{\bar{\psi}\psi\mathcal{O}}$ thanks to the parity symmetries, so that the first bootstrap equation can be written as

$$\sum_{\mathcal{O}} |c_{\bar{\psi}\psi\mathcal{O}}|^2 [z^{-2d} G_{\Delta_{\mathcal{O}}}(z) - (1-z)^{-2d} G_{\Delta_{\mathcal{O}}}(1-z)] = 0. \quad (2.60)$$

We have thus obtained a conventional crossing equation with positive and equal coefficients on both sides, directly analogous to those used in higher dimensions [4, 63].

The equation resulting from the crossing symmetry of the $\langle\bar{\psi}\psi\psi\bar{\psi}\rangle$ correlation function is less standard. The (12)(34) channel still consists of primaries from the $\bar{\psi}\psi$ OPE, but this time, the coefficient is

$$c_{\bar{\psi}\psi\mathcal{O}}c_{\psi\bar{\psi}\bar{\mathcal{O}}} = (-1)^{S(\mathcal{O})}c_{\bar{\psi}\psi\mathcal{O}}c_{\bar{\psi}\psi\bar{\mathcal{O}}} = (-1)^{S(\mathcal{O})}|c_{\bar{\psi}\psi\mathcal{O}}|^2, \quad (2.61)$$

so that the conformal block expansion can distinguish between scalars and pseudoscalars at the cost of lost positivity. The (23)(41) channel comes from the $\psi\psi$ OPE, and so contains only spin-1 operators even under S-parity ($\langle\psi\psi\mathcal{S}\rangle = (-1)^{S(\mathcal{S})}\langle\psi\psi\mathcal{S}\rangle$). The coefficients are manifestly positive since

$$c_{\bar{\psi}\bar{\psi}\mathcal{S}}c_{\psi\psi\bar{\mathcal{S}}} = \langle\psi|\bar{\psi}|\mathcal{S}\rangle\langle\mathcal{S}|\psi|\psi\rangle = |c_{\psi\psi\bar{\mathcal{S}}}|^2. \quad (2.62)$$

The resulting bootstrap equation thus takes the form

$$\begin{aligned} \sum_{\mathcal{O}^+} |c_{\bar{\psi}\psi\mathcal{O}^+}|^2 z^{-2d} G_{\Delta_{\mathcal{O}^+}}(z) - \sum_{\mathcal{O}^-} |c_{\bar{\psi}\psi\mathcal{O}^-}|^2 z^{-2d} G_{\Delta_{\mathcal{O}^-}}(z) &= \\ &= \sum_{\mathcal{S}} |c_{\psi\psi\mathcal{S}}|^2 (1-z)^{-2d} G_{\Delta_{\mathcal{S}}}(1-z), \end{aligned} \quad (2.63)$$

where the first, second sum on the LHS runs over parity-even, odd scalars respectively, and the sum on the RHS runs over spin-1 primaries. We expect the lowest operator in the $\psi\psi$ OPE to be the displacement. Note that the difference in sign between the two bootstrap equations goes hand in hand with the fact that the crossed channel in (2.60) starts with the identity, while in (2.63), it starts at $\Delta > 0$. In the former case, the scalars and pseudoscalars together produce the strong singularity of the identity in the crossed channel, but in the later, their effect must cancel to leave a weaker singularity corresponding to the first spin-1 primary. Since the singularity in the crossed channel is produced by the tail of the set of primaries, it follows that there are infinitely many scalars as well as infinitely many pseudoscalars.

There is a family of simple solutions of the two bootstrap equations corresponding to a generalized free complex scalar in 1D. In this case, Wick's theorem implies ($x_1 < x_2 < x_3 < x_4$)

$$\langle\bar{\psi}(x_1)\psi(x_2)\bar{\psi}(x_3)\psi(x_4)\rangle = \frac{1}{|x_{12}|^{2d}|x_{34}|^{2d}} \left[1 + \left(\frac{z}{1-z}\right)^{2d} \right] \quad (2.64)$$

$$\langle\bar{\psi}(x_1)\psi(x_2)\psi(x_3)\bar{\psi}(x_4)\rangle = \frac{1}{|x_{12}|^{2d}|x_{34}|^{2d}} (1 + z^{2d}). \quad (2.65)$$

The first term in each bracket is the contribution of the identity, and the rest can be expanded in 1D conformal blocks as

$$\left(\frac{z}{1-z}\right)^{2d} = \sum_{n=0}^{\infty} \frac{(2d)_n^2}{n!(4d+n-1)_n} G_{2d+n}(z) \quad (2.66)$$

$$z^{2d} = \sum_{n=0}^{\infty} \frac{(-1)^n (2d)_n^2}{n!(4d+n-1)_n} G_{2d+n}(z), \quad (2.67)$$

so that the $\bar{\psi}\psi$ OPE contains scalars of dimensions $2d + 2n$, $n \geq 0$, and pseudoscalars of dimensions $2d + 2n + 1$, $n \geq 0$. (2.65) in the crossed channel becomes

$$\langle \psi(x_1)\psi(x_2)\bar{\psi}(x_3)\bar{\psi}(x_4) \rangle = \frac{1}{|x_{12}|^{2d}|x_{34}|^{2d}} \left[z^{2d} + \left(\frac{z}{1-z}\right)^{2d} \right] \quad (2.68)$$

with conformal block expansion

$$z^{2d} + \left(\frac{z}{1-z}\right)^{2d} = \sum_{m=0}^{\infty} \frac{2(2d)_{2m}^2}{(2m)!(4d+2m-1)_{2m}} G_{2d+2m}(z), \quad (2.69)$$

so that the spin-1 sector consists of dimensions $2d + 2m$, $m \geq 0$.

Unless we put constraints on the spin-1 spectrum, any solution of (2.60) can be extended to a solution of both (2.60) and (2.63). Indeed, let

$$\sum_i |\lambda_i|^2 [z^{-2d} G_{\Delta_i}(z) - (1-z)^{-2d} G_{\Delta_i}(1-z)] = 0 \quad (2.70)$$

be a solution of the first equation and take the $\Delta > 0$ spectrum in the even and odd scalar sectors identical, with $|c_{\bar{\psi}\psi\mathcal{O}_i^+}|^2 = |c_{\bar{\psi}\psi\mathcal{O}_i^-}|^2 = |\lambda_i|^2/2$. (2.60) is automatically satisfied and in (2.63), the nonidentity scalars and pseudoscalars cancel out. Moreover, (2.66) guarantees that we can use a tower of spin-1 operators of dimensions $2d + n$, $n \geq 0$ to cancel the contribution of the identity.

Let us comment on the domain of applicability of our bootstrap equations. (2.60) by itself does not know in any way about the bulk theory and merely expresses the constraints of crossing and unitarity for a 1D CFT. It is (2.63) together with the assumption that the $\psi\psi$ OPE starts with the displacement that identifies the line as a codimension two object. Indeed, the structure of the OPE suggests a displacement operator which carries charge 1 under a transverse $SO(2)$ rotation symmetry, and a bosonic operator ψ of half-integral rotation quantum number¹.

¹Of course, the bounds derived from the bootstrap equations may apply to other situations which

2.4.2 Constraints from the first crossing equation

As a warm-up, let us consider first the constraints that follow from the first bootstrap equation (2.60). This kind of equation has been previously analyzed in the literature, though not in one dimension. The major difference is that here there are no spin- L representations other than $L = 0$. Operators are labeled only by their conformal dimensions, along with discrete quantum numbers. The method for deriving constraints from equation (2.60) has been explained in detail elsewhere, so here we will content ourselves with a brief summary. We first expand it in derivatives around $z = 1/2$ up to some finite order. By setting each individual Taylor coefficient to zero, we are left with a system of linear equations with constraints, namely that the OPE coefficients should be positive and that at least one of them (that of the identity operator) is strictly non-zero. This is a linear programming problem, which can be solved with standard algorithms, such as the simplex method. Alternatively, we can try to disprove that such an equation can hold, by finding a linear functional which is non-negative on all possible vectors (namely, for any Δ). We will follow the former route, using our own numerical implementation of the simplex algorithm. This has the advantage that the output is automatically a solution to the crossing symmetry constraints – a spectrum, made up of operator dimensions and OPE coefficients, which solve the crossing equations – as opposed to the linear functional method, where a spectrum has to be extracted by examining the zeros of the functional [23].

Our approach is to fix d , the dimension of $\psi, \bar{\psi}$ and ask for the maximum allowed dimension of the first scalar appearing in the $\psi\bar{\psi}$ OPE. We do this by excluding from the sum rule (2.60) all vectors with dimension below some value Δ_s (apart from the identity). We then increase this gap until no solution can be found. The result is shown in figure 2.4.

The result is a relatively boring straight line, which seems to very nearly coincide with the curve corresponding to the 1d generalized free fermion. This amounts to the four-point function

$$\langle \psi(x_1)\psi(x_2)\psi(x_3)\psi(x_4) \rangle = \frac{1}{|x_{12}|^{2d}|x_{34}|^{2d}} \left[1 + \left(\frac{z}{1-z} \right)^{2d} - z^{2d} \right] \quad (2.71)$$

with conformal block expansion

$$1 + \left(\frac{z}{1-z} \right)^{2d} - z^{2d} = 1 + \sum_{j=0}^{\infty} \frac{2(2d)_{2j+1}^2}{(2j+1)!(4d+2j)_{2j+1}} G_{2d+2j+1}(z), \quad (2.72)$$

include operators with similar quantum numbers. For example, a codimension 3 defect has an $SO(3)$ rotation symmetry, and may have an operator of spin 1/2 under that $SO(3)$. One could focus on a single component ψ of that doublet and on the $SO(2)$ Cartan subgroup of the full rotation group, using our analysis for a sub-optimal bound.

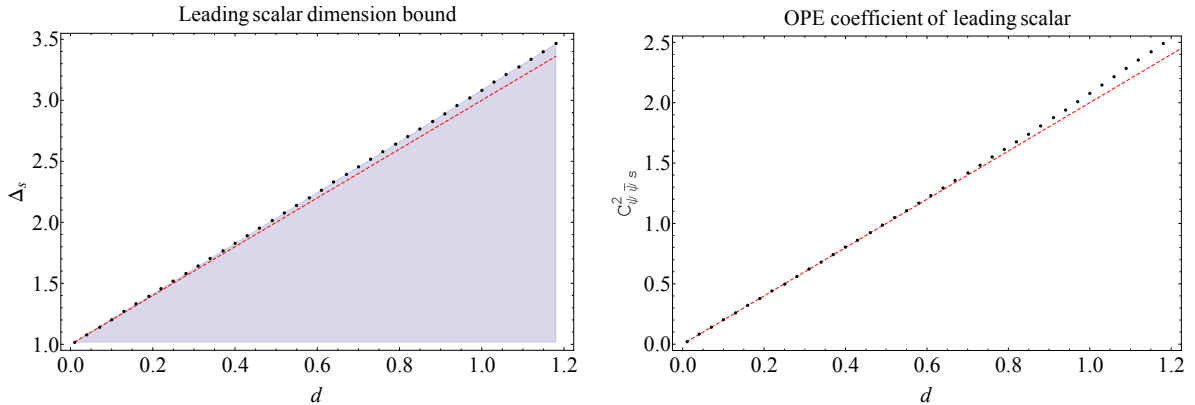


Figure 2.4: One-dimensional bounds derived from (2.60). In red the curves corresponding to the generalized free fermion solution. Left: bound on scalar dimension. Right: OPE coefficient of the leading scalar, in the solution to crossing corresponding to the dots on the top plot.

so that the minimal exchanged primary above the identity has $\Delta_s = 2d + 1$. We can find solutions to crossing at any point below our bound curve. In the extremal case where we sit directly on the bound itself, the solution is generically unique [23]. In this case we expect this solution to closely match the generalized free fermion. On the same figure on the right-hand side we compare the OPE coefficient of the leading scalar obtained with the bootstrap with that of the generalized free fermion – namely $|c_{\psi\bar{\psi}\mathcal{O}}|^2 = 2d$. Overall the agreement is quite good for small d and gradually gets worse as d increases. As we increase the accuracy in our numerical procedure, by augmenting the total number of derivatives (here we have used 50), the agreement gets better and better for larger and larger values of d . As for the twist defect CFT, it lies well inside the bound, and as such, through bounds alone we cannot reach it, at least not with a single equation. This is unlike the situation described in [63], where the Ising model lies on an interesting point (a kink) in the dimension bound. Here we are not as lucky and must work a bit harder to obtain an interesting result.

2.4.3 Constraints from both crossing equations

We now turn to deriving constraints by using both crossing equations. We use the conformal dimension to label operators, and define

$$F_{\Delta}(z) = G_{\Delta}(z) - \left(\frac{z}{1-z}\right)^{2d} G_{\Delta}(1-z), \quad (2.73)$$

$$S_{\Delta}(z) = G_{\Delta}(z), \quad (2.74)$$

$$T_{\Delta}(z) = -\left(\frac{z}{1-z}\right)^{2d} G_{\Delta}(1-z) \quad (2.75)$$

With this notation, it follows that we can write (2.60) and (2.63) in vector form.

$$\sum_{\mathcal{O}^+} a_{\Delta}^+ \begin{pmatrix} F_{\Delta}(z) \\ S_{\Delta}(z) \end{pmatrix} + \sum_{\mathcal{O}^-} a_{\Delta}^- \begin{pmatrix} F_{\Delta}(z) \\ -S_{\Delta}(z) \end{pmatrix} + \sum_{\mathcal{S}} b_{\Delta} \begin{pmatrix} 0 \\ T_{\Delta}(z) \end{pmatrix} = 0 \quad (2.76)$$

where all coefficients appearing in the above are explicitly positive. The procedure now is the same as in the single equation case. We evaluate the sum rule and its derivatives at $z = 1/2$ (up to 40) and attempt to find a solution imposing various constraints. Since the spectrum is now split into three different sectors, we have more freedom in setting up the problem. Since we are looking for the twist defect, we are interested in solutions to crossing where the first spin-1 operator is the displacement, which has dimension 2. Therefore we shall impose a gap, by disallowing any spin-1 operators with dimension below 2 in the sum rule above. Figure 2.5 shows the bound derived by scanning over the dimension d of ψ while imposing the same gap on the dimension of the parity odd and parity even scalars. The bound is clearly more restrictive up to some value of d , beyond which it returns to the original single equation result. This can be understood by recalling that a solution of the first equation can be extended to a solution of both as long as the gap imposed in the spin-1 sector does not exceed $2d$. We can see this directly by examining the spectra of the solutions to crossing living at the boundary of the bound. In figure 2.6 we show the odd and even scalar spectra corresponding to these solutions. It is clear that for high enough d the spectra become identical in these two channels, as we expect. A detailed examination of the OPE coefficients shows that this occurs precisely at $d = 1$.

As it is clear, this approach is unfortunately still not sufficient to find the twist defect. From table 2.1 we expect there to be a parity even scalar of dimension about 2.27 when $d \simeq 0.9187$, which is allowed, but not saturated by our bound. Hence we consider a different strategy. Since we know that the defect must contain a spin-1 operator with dimension 2 in its spectrum, we shall impose this directly on the sum rule. More concretely, we fix

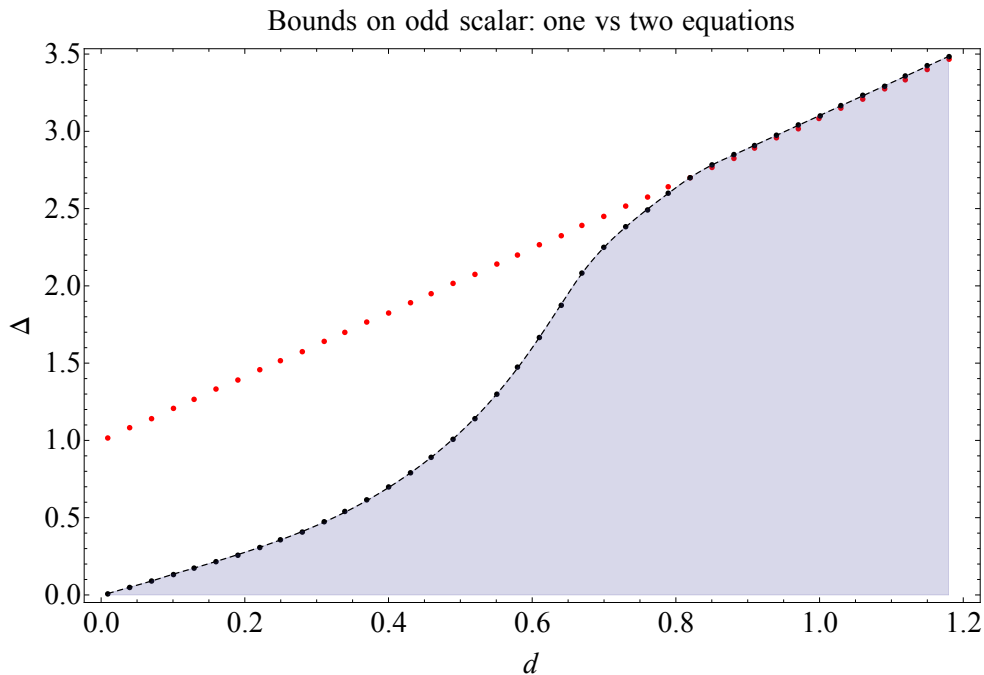


Figure 2.5: Single equation bound in red and two equation bound in black. In the latter, the leading scalar is parity odd, up to about $d = 1$, where the parity even and odd scalars have identical spectra.

the OPE coefficient of the D operator in the sum rule to some value, and we determine the maximum gap in the parity even sector consistent with crossing symmetry. We can do this for various values of d , but we will be interested in the experimentally relevant $d = 0.9187$. Figure 2.7 shows the resulting bound. We see that the bound is saturated by a solution to crossing including a parity even scalar of dimension 2.27 for an OPE squared value of about 1.8. Notice that this is consistent with the results of the ϵ -expansion, which indicate that the OPE coefficient square should be $\simeq 1.9$. We can determine the spectrum of this solution, and this is shown in figure 2.8. Remarkably, we find a parity odd scalar of dimension $\simeq 2.9$ in the solution, signaling that this is indeed the twist defect. We summarize our spectrum results in table 2.2. Besides the spectrum data present on the table, the bootstrap also predicts other operators and their OPE coefficients. The accuracy of these depends on the number of derivatives. We can estimate the error by repeating the calculations at different numbers of derivatives and seeing how the results change. Doing this we further predict the existence of the operators shown in table 2.3, with an estimated error of 5% or less.

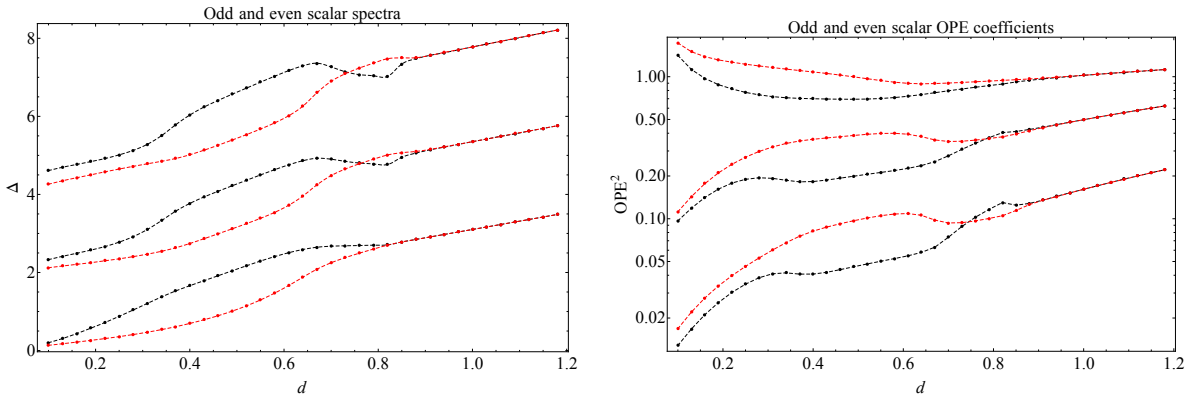


Figure 2.6: Spectra corresponding to the extremal solutions in figure 2.5. In black (red) the parity even (odd) scalars. On the left the operator dimensions, and their OPE coefficients on the right. The correspondence between both is reversed: larger OPE coefficients correspond to lower dimension operators.

To summarize, we have used as input the dimension of ψ ; the dimension of the first even scalar s ; and the existence of a spin 1 operator D of dimension 2. Using this information, and assuming the defect spectrum lies on the bound of figure 2.7, we have been able to determine the OPE coefficient of D in the $\psi\psi$ operator product. Further, we have checked the existence of an odd scalar of dimension $\simeq 2.9$ and its OPE coefficient, and predict a further six operator dimensions and OPE coefficients. We could have gone further by doing more intensive calculations, but we are limited by the relatively large error in the dimension of s determined from the lattice. As it stands, our confidence that we are finding the correct solution to crossing hinges on obtaining the correct operator dimension for p° and an OPE coefficient for the displacement operator consistent with the ϵ -expansion. It would be very interesting to further test this by extending the *epsilon*-expansion calculations or doing further lattice simulations.

2.5 Conclusions

We have offered new points of view on the twist line defect in the 3d Ising model – the ϵ -expansion and the conformal bootstrap of the defect four-point functions. While the ϵ -

quantity	Bootstrap	ϵ -expansion	Monte Carlo
Δ_ψ	<i>0.9187</i>	0.917	0.9187(6)
Δ_D	<i>2</i>	2	2
Δ_s	<i>2.27</i>	2.167	2.27(1)
Δ_{p^o}	<i>2.92</i>	2.833	2.9(2)
$c_{\psi\psi s}$	<i>0.95</i>	0.955	???
$c_{\psi\psi\bar{D}}$	<i>1.345</i>	1.382	???
$c_{\psi\bar{\psi}p^o}$	<i>0.988</i>	0.987	???

Table 2.2: A comparison of lattice data, the Wilson-Fisher fixed point at one loop, and bootstrap calculations. We have italicized numbers which are used as inputs to the bootstrap method.

Type	Dimension	OPE ²
0 ⁺	4.12	0.66
0 ⁺	6.29	0.26
0 ⁻	5.11	0.45
0 ⁻	7.42	0.15
1	3.98	0.99
1	6.20	0.38

Table 2.3: Spectrum predictions from the bootstrap method.

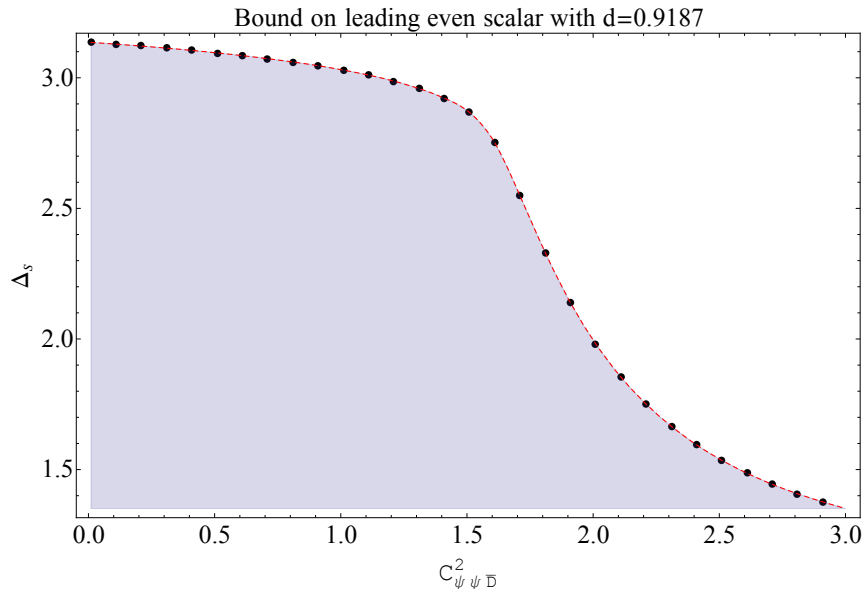


Figure 2.7: One-dimensional bound, using two equations.

expansion at one loop leads to a surprisingly good agreement with the Monte Carlo results, the identification of the defect spectrum from conformal bootstrap is not as straightforward as in the case of the bulk theory [4]. In spite of this, we believe we have successfully found the 1D defect theory by forcing the inclusion of the displacement operator in the spectrum, at the cost of using more data, namely the dimensions of the leading parity even scalar s and of ψ as determined from the lattice. The pay-off is that we determine a number of other quantities, namely operator dimensions and their OPE coefficients, which match well with results of the ϵ -expansion. It is quite interesting that the inclusion of the second equation in the bootstrap set-up results in significant improvement of the bound, despite the lack of positivity in the spin-0 channel.

Several extensions of our work offer themselves. The $O(N)$ models allow twist line defects for arbitrary $R \in O(N)$, and it should be straightforward to generalize the ϵ -expansion calculation at least in the case when $R = -I$. Although our bootstrap bounds apply to this defect for any N by taking ψ to be a fixed component of a spin-1/2 $O(N)$ vector, it may be worth repeating the analysis for $\langle \bar{\psi}_i \psi_j \bar{\psi}_k \psi_l \rangle$, $\langle \bar{\psi}_i \psi_j \psi_k \bar{\psi}_l \rangle$ while separating the exchanged primaries according to their $O(N)$ representations, as in [25]. Large- N computations for the defect should also be possible. Note that $O(N)$ can also be interpreted as the spacetime symmetry of the transverse directions, so that conformal bootstrap on the line can be used to constrain higher-dimensional CFTs. It may also be interesting to

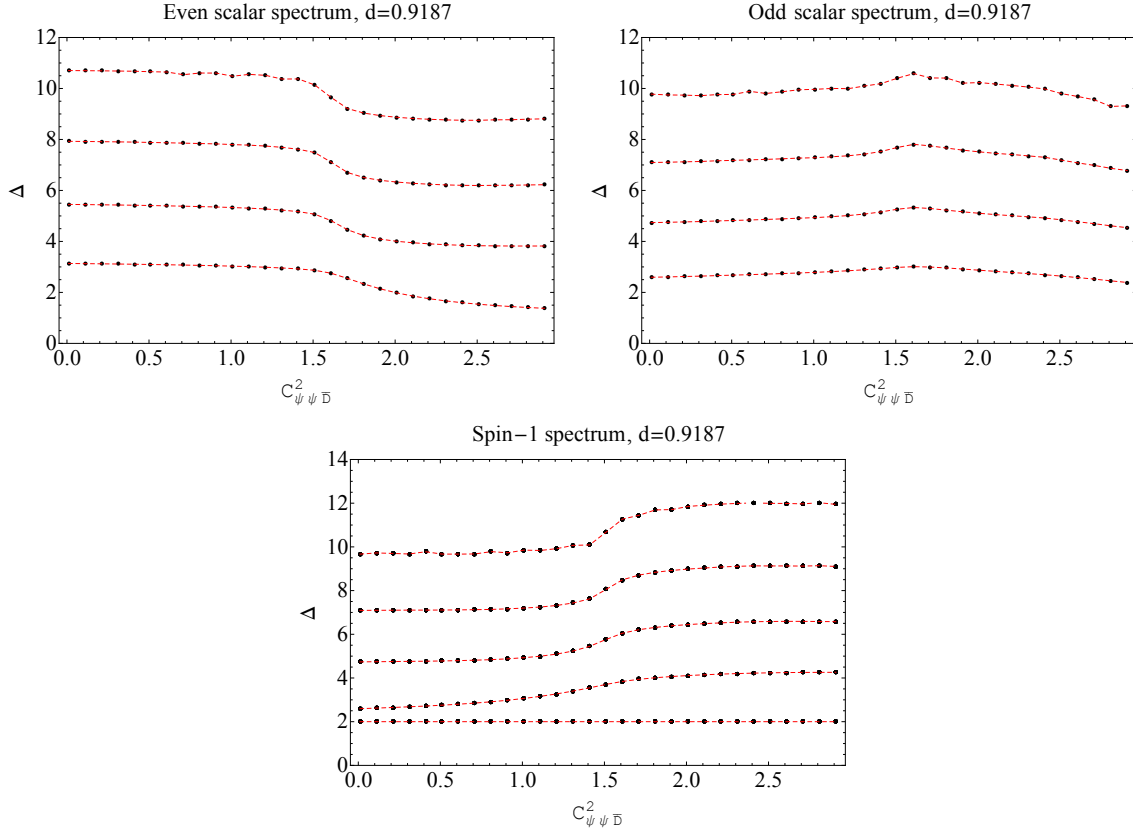


Figure 2.8: Spectra corresponding to the extremal solutions to crossing symmetry - the unique solutions at the boundary of our bounds.

see how the bootstrap bound evolves for the $2 - \epsilon$ dimensional defect in the Wilson-Fisher CFT.

1D CFTs can also serve as simple test cases for analytical understanding of the conformal bootstrap. In particular, the coincidence of the single equation bound with the generalized free fermion begs for an analytical explanation. Note that the techniques of [66] and [67] are not directly applicable since they require the presence of two cross-ratios. Also for this reason, the study of crossing of the bulk two-point function in the presence of a defect may be a fruitful direction of research.

2.A Asymptotic evaluation of integrals

2.A.1 Half-integer spin operators

The one-loop properties of ψ_s are encoded in the asymptotic properties of the integral (2.24) as $\lambda \rightarrow 0$. To find these asymptotics, we start by the substitution $y_0 = ya$, $z_0 = yb$, $r_0 = yc$, which leads to

$$G_1(x_1, x_2, s) = \epsilon \frac{2^{4(s-1)}}{3\pi} \frac{e^{is\theta}}{r^2} \lambda^{2(s+1)} \int_{\mathbb{R}^3} dadbdc \frac{c^{2s-1}}{d_+ d_- e_+ e_- (d_+ + d_-)^{2s} (e_+ + e_-)^{2s}}, \quad (2.77)$$

where

$$d_{\pm} = \sqrt{\left(a - \frac{1}{2}\right)^2 + b^2 + (c \pm \lambda)^2}$$

$$e_{\pm} = \sqrt{\left(a + \frac{1}{2}\right)^2 + b^2 + (c \pm \lambda)^2},$$

and where we extended the domain of integration to the full \mathbb{R}^3 , which is admissible since $2s - 1$ is even. Let us denote

$$I(\lambda) = \frac{2^{4(s-1)}}{3\pi} \int_{\mathbb{R}^3} dadbdc \frac{c^{2s-1}}{d_+ d_- e_+ e_- (d_+ + d_-)^{2s} (e_+ + e_-)^{2s}}. \quad (2.78)$$

As $\lambda \rightarrow 0$, the integral is logarithmically divergent around $(a, b, c) = (\pm 1/2, 0, 0)$, with λ acting as a point-splitting regulator. We expect $I(\lambda) = \alpha \log \lambda + \beta + o(1)$ and our goal is to determine α and β . Our general strategy will be to introduce an auxiliary parameter N and split the integration domain into two parts. In this case, denote $I_1(\lambda, N)$ the integral above restricted to the union of the two spheres of radii λN surrounding the two singularities, and denote $I_2(\lambda, N)$ the integral over the rest of \mathbb{R}^3 so that $I(\lambda) = I_1(\lambda, N) + I_2(\lambda, N)$. $I_{1,2}(\lambda, N)$ simplify in the limit $N \rightarrow \infty$, $N\lambda \rightarrow 0$ if we do not care about terms which vanish as $\lambda \rightarrow 0$. Working first with $I_1(\lambda, N)$, and focusing on the sphere surrounding $(a, b, c) = (1/2, 0, 0)$, note that in the limit $\lambda N \rightarrow 0$, we can replace $e_{\pm} = 1$. Making further the substitution $a = 1/2 + \lambda x$, $b = \lambda y$, $c = \lambda z$, we find that λ -dependence disappears

$$I_1(\lambda, N) = \frac{2^{2s-3}}{3\pi} \int_{x^2 + y^2 + z^2 \leq N^2} dx dy dz \frac{z^{2s-1}}{f_+ f_- (f_+ + f_-)^{2s}} + o(1), \quad (2.79)$$

where

$$f_{\pm} = \sqrt{x^2 + y^2 + (z \pm 1)^2}. \quad (2.80)$$

The integrals over x and y can be done explicitly, leaving us with

$$I_1(\lambda, N) = \frac{2^{2s}}{12s} \int_0^N dz \left[\frac{(z^{2s} + 1) - |z^{2s} - 1|}{2^{2s+1}z} - \frac{z^{2s-1}}{(\sqrt{N^2 + 2z + 1} + \sqrt{N^2 - 2z + 1})^{2s}} \right] + o(1). \quad (2.81)$$

It is now a matter of a simple calculation to show that

$$I_1(\lambda, N) = \frac{1}{12s} \log N + o(1). \quad (2.82)$$

Let us consider $I_2(\lambda, N)$, denoting $D = \{(a, b, c) \in \mathbb{R}^3 | (a \pm 1/2)^2 + b^2 + c^2 \geq (\lambda N)^2\}$ the domain of integration. As $N \rightarrow \infty$, we can write $d_+ = d_-$, $e_+ = e_-$ up to terms of $O(N^{-1})$, so that

$$I_2(\lambda, N) = \frac{1}{48\pi} \int_D dadbdc \frac{c^{2s-1}}{(r_+ r_-)^{2(s+1)}} + o(1), \quad (2.83)$$

where

$$r_{\pm} = \sqrt{\left(a \pm \frac{1}{2}\right)^2 + b^2 + c^2}. \quad (2.84)$$

Let us perform the inversion around $(1/2, 0, 0)$, so that D is mapped to the region D' between the sphere of radius $\lambda N + O((\lambda N)^2)$ centered around $(-1/2, 0, 0)$ and sphere of radius $1/(\lambda N)$ centered around $(1/2, 0, 0)$. The integral simplifies considerably

$$I_2(\lambda, N) = \frac{1}{48\pi} \int_{D'} dadbdc \frac{c^{2s-1}}{r_+^{2(s+1)}} + o(1). \quad (2.85)$$

Working up to terms vanishing as $\lambda N \rightarrow 0$, we can modify D' by making the inner sphere have radius exactly λN , and shifting the outer sphere so that it is also centered around $(-1/2, 0, 0)$. After these modifications, the integral becomes almost trivial, the result being

$$I_2(\lambda, N) = -\frac{1}{12s} \log(\lambda N) + o(1). \quad (2.86)$$

Combining I_1 and I_2 , the dependence on N drops out as expected and we find

$$I(\lambda) = -\frac{1}{12s} \log \lambda + o(1), \quad (2.87)$$

so that $\alpha = -1/(12s)$ and $\beta = 0$.

2.A.2 Energy operator

In order to find the asymptotic behaviour of the integral (2.32) as $\lambda \rightarrow \infty$, which gives the one-loop properties of the energy operator, let us start by making the substitution $y_0 = ra$, $z_0 = rb$, $r_0 = rc$, after which we obtain

$$G_1(x_1, x_2) = \frac{\epsilon}{6\pi} \frac{1}{r^2} \int_{\mathbb{R}^3} dadbdc \frac{1}{d_+ d_- e_+ e_-} \frac{(d_+ + d_-)(e_+ + e_-)}{(d_+ + d_-)^2 (e_+ + e_-)^2 - (4c)^2}, \quad (2.88)$$

where

$$d_{\pm} = \sqrt{\left(a - \frac{\mu}{2}\right)^2 + b^2 + (c \pm 1)^2}$$

$$e_{\pm} = \sqrt{\left(a + \frac{\mu}{2}\right)^2 + b^2 + (c \pm 1)^2},$$

and where we extended the domain of integration to the whole \mathbb{R}^3 and write $\mu = 1/\lambda$. Let us denote $J(\mu) = r^2 G_1(x_1, x_2)/\epsilon$. Analogously to the previous computation, μ acts as a point-splitting regulator for the logarithmic singularities at $(0, 0, \pm 1)$. We proceed along the same lines, splitting the domain into the union of the spheres of radii $N\mu$ centered at $(0, 0, \pm 1)$, and the rest of \mathbb{R}^3 , and considering the limit $N \rightarrow \infty$, $N\mu \rightarrow 0$. We start analyzing the integral $J_1(\mu, N)$ over the spheres. Concentrating on the sphere centered at $(0, 0, 1)$, and making the substitution $a = \mu x$, $b = \mu y$, $c = 1 + \mu z$, we find

$$d_+ = e_+ = 2 + \mu z + O(\mu^2)$$

$$d_- = \mu \sqrt{\left(x - \frac{1}{2}\right)^2 + y^2 + z^2 + O(\mu^2)}$$

$$e_- = \mu \sqrt{\left(x + \frac{1}{2}\right)^2 + y^2 + z^2 + O(\mu^2)},$$

so that the integral becomes

$$J_1(\mu, N) = \frac{1}{48\pi} \int_{x^2 + y^2 + z^2 \leq N^2} dx dy dz \frac{1}{f_+ f_- (f_+ + f_-)} + o(1), \quad (2.89)$$

where

$$f_{\pm} = \sqrt{\left(x \pm \frac{1}{2}\right)^2 + y^2 + z^2}. \quad (2.90)$$

Notice that after scaling the variables by $1/2$, the integral is equivalent to $I_1(\lambda, 2N)/4$ from (2.79) with $s = 1/2$, so that we immediately obtain

$$J_1(\mu, N) = \frac{1}{4}I_1(\mu, 2N, s = 1/2) + o(1) = \frac{1}{24}(\log N + \log 2) + o(1). \quad (2.91)$$

Shifting to $J_2(\mu, N)$, we can use $d_{\pm} = e_{\pm}$, so that

$$J_2(\mu, N) = \frac{1}{6\pi} \int_D dadbdc \frac{1}{(d_+d_-)^2} \frac{(d_+ + d_-)^2}{(d_+ + d_-)^4 - (4c)^2} + o(1), \quad (2.92)$$

where the domain is $D = \{(a, b, c) \in \mathbb{R}^3 | a^2 + b^2 + (c \pm 1)^2 \geq (\mu N)^2\}$. Scaling the variables by 2 and applying inversion centered at $(0, 0, 1)$, the integral simplifies greatly

$$J_2(\mu, N) = \frac{1}{192\pi} \int_{D'} dadbdc \frac{1}{\left[a^2 + b^2 + \left(c + \frac{1}{2}\right)^2\right]^{\frac{3}{2}}} + o(1), \quad (2.93)$$

where $D' = \{(a, b, c) \in \mathbb{R}^3 | a^2 + b^2 + (c \pm 1/2)^2 \geq (\mu N/2)^{\pm 1}\}$. Modifying the integration domain as in the previous section, to make it into the region between two concentric spheres of mutually inverse radii, we easily find the result

$$J_2(\mu, N) = -\frac{1}{24} \log \left(\frac{\mu N}{2} \right) + o(1), \quad (2.94)$$

so that indeed the N dependence cancels in the final result and we obtain

$$J(\mu) = -\frac{1}{24} \log \mu + \frac{1}{12} \log 2 + o(1), \quad (2.95)$$

so that

$$G_1(x_1, x_2) = \frac{\epsilon}{r^2} \left[\frac{1}{24} \log \lambda + \frac{\log 2}{12} + o(1) \right] \quad (2.96)$$

as $\lambda \rightarrow \infty$.

2.A.3 Dimensions of integer spin operators

We start the analysis of the integral (2.42) by making the substitution $x_0 = ar/(\lambda\mu)$, $y_0 = br/(\lambda\mu)$, $z_0 = cr/(\lambda\mu)$, after which the integral becomes

$$G_{\text{con.}}(\{x_j, s_j\}_{j=1}^4) = \epsilon \frac{e^{i \sum_j s_j \theta_j}}{r^4} (\lambda\mu)^{2(s+2)} K(\mu, \lambda), \quad (2.97)$$

where

$$K(\mu, \lambda) = -\frac{2}{3\pi} \int_{\mathbb{R}^2} dadb \int_0^\infty dcc \prod_{j=1}^4 \frac{(4c)^{|s_j|}}{d_j e_j (d_j + e_j)^{2|s_j|}}, \quad (2.98)$$

where

$$d_j = \sqrt{(a - a_j)^2 + b^2 + (c - \lambda\mu)^2}$$

$$e_j = \sqrt{(a - a_j)^2 + b^2 + (c + \lambda\mu)^2},$$

where $a_1 = -1/2 - \mu/2$, $a_2 = -1/2 + \mu/2$, $a_3 = 1/2 - \mu/2$, $a_4 = 1/2 + \mu/2$. We want to study the asymptotic behaviour as $\lambda, \mu \rightarrow \infty$. Note that for fixed $\mu > 0$, the integral is non-singular in the limit $\lambda \rightarrow \infty$, so we may set $\lambda = 0$, and use $d_j = e_j$. Writing $K(\mu) = K(\mu, 0)$, we thus have

$$K(\mu) = -\frac{2}{3\pi} \int_{\mathbb{R}^2} dadb \int_0^\infty dc \frac{c^{2s+1}}{\prod_{j=1}^4 d_j^{2|s_j|+2}}, \quad (2.99)$$

where

$$d_j = \sqrt{(a - a_j)^2 + b^2 + c^2}. \quad (2.100)$$

As $\mu \rightarrow \infty$, the singularities collide pairwise around $(\pm 1/2, 0, 0)$, inducing logarithmic singularities, so again, we expect $K(\mu) = \gamma \log \mu + O(1)$. The constant γ , which is related to the anomalous dimension, can be found by changing the role of μ from a point-splitting regulator, to a hard regulator, i.e. setting $\mu = 0$ in the integrand, but omitting the half-spheres of radii μ centered around $(\pm 1/2, 0, 0)$ from the integration domain. The arguments from the previous subsections make this statement rigorous. Near $(1/2, 0, 0)$, we can replace $d_1 = d_2 = 1$, $d_3 = d_4$, so that the near-singularity behavior of the integral is

$$K(\mu) = -\frac{8}{3} \int_{\mu} \frac{dr}{r} \int_0^{\frac{\pi}{2}} d\theta \sin \theta (\cos \theta)^{2s+1} + O(1) = \frac{4}{3(s+1)} + O(1). \quad (2.101)$$

Hence equation (2.44) follows.

2.A.4 $c_{\psi\psi\bar{D}}$ OPE coefficient

In order to find the one-loop-corrected OPE coefficients $c_{\psi_{s_1}\psi_{s_2}\mathcal{O}_s}$, we would need to work much harder, repeating the analysis involving the auxiliary parameter N on the complicated integral (2.98), and finding the eigenvectors of the first-order dilatation operator.

Here we content ourselves with the analysis in the one-dimensional case $s_1 = s_2 = 1/2$, which gives the correction to the OPE coefficient $c_{\psi\psi\bar{D}}$. Our goal is thus to find the constant piece of (2.99) when $|s_j| = 1/2$, $s = 1$

$$K(\mu) = -\frac{2}{3\pi} \int_{\mathbb{R}^2} dadb \int_0^\infty dc \frac{c^3}{\prod_{j=1}^4 d_j^3}. \quad (2.102)$$

As in the previous sections, we introduce parameter N , and split the integration domain into the union of the two half-spheres of radii μN centered at $(\pm 1/2, 0, 0)$ and the rest of the 3D half-space, denoting the two resulting integrals $K_1(\mu, N)$, $K_2(\mu, N)$ respectively. $K_2(\mu, N)$ can be dealt with easily by applying the previously used methods. As $\mu N \rightarrow 0$, we can write $d_1 = d_2 = \sqrt{(a - 1/2)^2 + b^2 + c^2}$, $d_3 = d_4 = \sqrt{(a + 1/2)^2 + b^2 + c^2}$. Then, applying inversion centered at $(1/2, 0, 0)$ and shifting the outer half-sphere to become concentric with the inner one, we arrive at the simple integral

$$K_2(\mu, N) = -\frac{2}{3\pi} \int_{\mu N}^{(\mu N)^{-1}} \frac{dr}{r} \int d\Omega_{S_+^2} (\cos \theta)^3 + o(1), \quad (2.103)$$

where S_+^2 denotes the upper half of S^2 , i.e. $\theta \in [0, \pi/2]$. It follows that K_2 does not contribute to the constant term

$$K_2(\mu, N) = \frac{2}{3} \log(\mu N) + o(1). \quad (2.104)$$

Moving on to $K_1(\mu, N)$, let us focus on the half-sphere centered at $(1/2, 0, 0)$ and write $a = 1/2 + \mu x$, $b = \mu y$, $c = \mu z$, so that

$$K_1(\mu, N) = -\frac{4}{3\pi} \int_D dx dy dz \frac{z^3}{[(x - \frac{1}{2})^2 + y^2 + z^2]^{\frac{3}{2}} [(x + \frac{1}{2})^2 + y^2 + z^2]^{\frac{3}{2}}} + o(1), \quad (2.105)$$

where $D = \{(x, y, z) \in \mathbb{R}^3 | z \geq 0, x^2 + y^2 + z^2 \leq N^2\}$. The integral over z can be done with the result (dropping sub-leading terms)

$$K_1(\mu, N) = \frac{4}{3\pi} \int_{x^2 + y^2 < N^2} dx dy \left[\frac{1}{N^2} - \left(\frac{1 + \frac{x^2 + y^2}{N^2}}{r_+ + r_-} \right)^2 \right] + o(1), \quad (2.106)$$

where

$$r_{\pm} = \sqrt{\left(x \pm \frac{1}{2}\right)^2 + y^2}. \quad (2.107)$$

The first term of (2.106) trivially integrates to $4/3$, and we will denote the remaining integral $L(N)$. Scaling the variables by N , we find

$$L(N) = -\frac{4}{3\pi} \int_{x^2+y^2 < 1} dx dy \left(\frac{1+x^2+y^2}{\sqrt{\left(x + \frac{1}{2N}\right)^2 + y^2} + \sqrt{\left(x - \frac{1}{2N}\right)^2 + y^2}} \right)^2. \quad (2.108)$$

We can simplify the integral by repeating our trick of splitting the integration domain into the disc of radius M/N and the remaining annulus and consider the limit $M \rightarrow \infty$, $M/N \rightarrow 0$. Denote the disc integral by $L_1(M, N)$ and the annulus integral by $L_2(M, N)$. When evaluating L_2 , we can set $1/N = 0$ in the integrand and arrive at

$$L_2(M, N) = -\frac{2}{3} \int_{\frac{M}{N}}^1 dr r \frac{(1+r^2)^2}{r^2} + o(1) = \frac{2}{3} \log \left(\frac{M}{N} \right) - \frac{5}{6} + o(1), \quad (2.109)$$

so that L_2 contributes $-5/6$ to the constant term. It remains to find the constant term in $L_1(M, N)$. Scaling the variables by N , the integral becomes

$$L_1(M, N) = -\frac{4}{3\pi} \int_{x^2+y^2 < M} dx dy \frac{1}{\left(\sqrt{\left(x + \frac{1}{2}\right)^2 + y^2} + \sqrt{\left(x - \frac{1}{2}\right)^2 + y^2} \right)^2} + o(1). \quad (2.110)$$

The angular integration can be done in terms of elliptic integrals or hypergeometric functions, and the radial integral can then be expanded as $M \rightarrow \infty$

$$L_1(M, N) = -\frac{2}{3} \log M + \frac{1 - 4 \log 2}{3} + o(1). \quad (2.111)$$

Hence, putting all the constants together

$$K_1(\mu, N) = -\frac{2}{3} \log N - \frac{8 \log 2 - 5}{6} + o(1), \quad (2.112)$$

and so

$$K(\mu) = \frac{2}{3} \log \mu - \frac{8 \log 2 - 5}{6} + o(1) \quad (2.113)$$

as $\mu \rightarrow 0$.

2.B The four-point function without the defect

In this appendix, we will compute the one-loop correction to the four-point function of ϕ in the ϕ^4 theory without the defect in order to find properties of ϵ at one loop. Placing the four insertions on a line, with distances $|x_{12}| = |x_{34}| = r$, $|x_{13}| = |x_{24}| = r/\mu$, $\mu \ll 1$, the OPE predicts

$$G(x_1, x_2, x_3, x_4) = \frac{1}{r^{4\Delta_\sigma}} [1 + c_{\sigma\sigma\epsilon}^2 \mu^{2\Delta_\epsilon} (1 + o(1))]. \quad (2.114)$$

The free-theory values are $\Delta_\sigma = 1 - \epsilon/2$, $\Delta_\epsilon = 2 - \epsilon$, $c_{\sigma\sigma\epsilon} = \sqrt{2}$, where the first result holds also at the Wilson-Fisher fixed point up to corrections of $O(\epsilon^2)$. The one-loop self-energy vanishes in the massless ϕ^4 theory, so the only contribution comes from the contact four point interaction

$$G_1 = -(2\pi)^4 g \int d^4 x_0 G(x_1, x_0) G(x_2, x_0) G(x_3, x_0) G(x_4, x_0) = -\frac{\epsilon}{3\pi^2} \int d^4 x_0 \frac{1}{x_{01}^2 x_{02}^2 x_{03}^2 x_{04}^2}. \quad (2.115)$$

After scaling the integration variables as $x_0 = ry/\mu$, the integral becomes

$$G_1 = \frac{\epsilon}{r^4} \mu^4 H(\mu), \quad (2.116)$$

where

$$H(\mu) = -\frac{1}{3\pi^2} \int d^4 y \frac{1}{(y - \frac{1+\mu}{2}\hat{n})^2 (y - \frac{1-\mu}{2}\hat{n})^2 (y + \frac{1-\mu}{2}\hat{n})^2 (y + \frac{1+\mu}{2}\hat{n})^2}, \quad (2.117)$$

where \hat{n} is a unit vector in a fixed direction. As $\mu \rightarrow 0$, the integral develops logarithmic singularities at $y = \pm\hat{n}/2$. We can compute the logarithmic and constant piece exactly as before, splitting $H(\mu) = H_1(\mu, N) + H_2(\mu, N)$, where $H_1(\mu, N)$ is the integral over the union of the two spheres of radii μN , centered at $\pm\hat{n}/2$, and $H_2(\mu, N)$ over their complement in \mathbb{R}^4 . Again, we work in the limit $N \rightarrow \infty$, $\mu N \rightarrow 0$. Working with H_1 and focusing on the sphere centered at $\hat{n}/2$, we can set the distances to the far singularities equal to one, and upon rescaling the variables by μ , we obtain

$$H_1(\mu, N) = -\frac{2}{3\pi^2} \int_{R^2 < N^2} dy^4 \frac{1}{(y - \frac{1}{2}\hat{n})^2 (y + \frac{1}{2}\hat{n})^2} + o(1). \quad (2.118)$$

The integral can be evaluated exactly

$$\frac{1}{\pi^2} \int_{R^2 < N^2} dy^4 \frac{1}{(y - \frac{1}{2}\hat{n})^2 (y + \frac{1}{2}\hat{n})^2} \stackrel{N > \frac{1}{2}}{=} \log(4N^2 + 1) + 1, \quad (2.119)$$

giving the following asymptotics

$$H_1(\mu, N) = -\frac{4}{3} \log N - \frac{2}{3} + o(1). \quad (2.120)$$

Moving on to $H_2(\mu, N)$, we can set $\mu = 0$ in the integrand, and use our usual trick of doing the inversion centered at $\hat{n}/2$, after which the integration domain becomes the region between the sphere of radius $\mu N + O((\mu N)^2)$ centered at $-\hat{n}/2$ and the sphere of radius $1/(\mu N)$ centered at $\hat{n}/2$. Ignoring terms vanishing as $\mu N \rightarrow 0$, we can make the former radius exactly μN and make the spheres concentric, so that

$$H_2(\mu, N) = -\frac{1}{3\pi^2} \int_{\mu N < R < (\mu N)^{-1}} \frac{d^4 y}{R^4} + o(1) = \frac{4}{3} \log(\mu N) + o(1). \quad (2.121)$$

Hence

$$H(\mu) = \frac{4}{3} \log \mu - \frac{2}{3} + o(1). \quad (2.122)$$

Comparing with the expansion (2.114), this gives the following properties of the energy operator

$$\Delta_\epsilon = 2 - \frac{2}{3}\epsilon + O(\epsilon^2) \quad (2.123)$$

$$c_{\sigma\sigma\epsilon} = \sqrt{2} \left(1 - \frac{\epsilon}{6}\right) + O(\epsilon^2). \quad (2.124)$$

Chapter 3

Superconformal Bootstrap with Four Supercharges

3.1 Introduction

The ingredients for the bootstrap program are minimal, namely conformal symmetry, unitarity, and crossing symmetry of the four-point function. Strikingly, this is sufficient to derive highly non-trivial, non-perturbative constraints on the space of generic conformal field theories. Beginning with [17, 18], it has been shown that, as it is natural to expect, imposing additional symmetries on the CFT allows one to obtain even stronger constraints. A particularly interesting possibility is to consider supersymmetry. Supersymmetry leads to exact results for specific quantities such as the dimensions of chiral operators. This is a nice complement to the conformal bootstrap approach, which, although very powerful – it can determine and bound unprotected quantities – is a somewhat blunt instrument, since it addresses general properties for the space of *all* consistent conformal field theories. When supersymmetry is combined with the conformal bootstrap we expect an interesting interplay where exact information is used to restrict bootstrap searches to specific theories or classes of theories whereupon one can obtain accurate information about the unprotected part of the spectrum.

Bootstrap methods have been previously applied to theories with various amounts of supersymmetry. Theories with maximal supersymmetry are very constrained and thus particularly suited for analysis using bootstrap technology. This has been explored in four [26, 69–71] and three [30] dimensions where various bounds on the spectrum of conformal dimensions and OPE coefficients were found. It turns out that theories with at least sixteen

superconformal charges in various dimensions admit a remarkable algebraic structure which leads to the closure of the crossing equations on the space of certain protected operators. This was uncovered in [72] where it was shown that in four-dimensional CFTs with $\mathcal{N} = 2$ supersymmetry one can solve analytically for correlation functions of some protected operators by exploiting an underlying chiral algebra. This feature was further explored to great efficacy in six [73], four [74, 75] and three dimensions [76]. These analytic results can then be used as input to perform a numerical bootstrap analysis and obtain bounds on the spectrum of unprotected operators in these highly symmetric theories [35, 76].

While theories with eight or more Poincaré supercharges are quite rigid and possess deep mathematical properties, their dynamics is highly constrained. Thus it is worthwhile to explore theories with less supersymmetry, which are harder to control, but perhaps of greater phenomenological interest. This motivates our study in this chapter of CFTs with four Poincaré supercharges (eight superconformal charges). Some of the first papers on the modern incarnation of the bootstrap program studied $\mathcal{N} = 1$ SCFTs in $d = 4$ [17, 20, 27]. Very little has been done in two and three dimensions, a notable exception being the work in [77] which studied SCFTs with four superconformal charges in $d = 3$, i.e. CFTs with $\mathcal{N} = 1$ supersymmetry.

In this chapter, we aim to fill this gap by applying bootstrap methods to SCFTs with four Poincaré supercharges in any dimension in the range $2 \leq d \leq 4$. This corresponds to $\mathcal{N} = (2, 2)$ and $\mathcal{N} = 2$ theories in $d = 2$ and $d = 3$, respectively, and to $\mathcal{N} = 1$ SCFTs in $d = 4$. Moreover, one of the advantages of bootstrap methods is that they allow for a straightforward analytic continuation into fractional values of the spacetime dimension. This has been explored before in [63], where the numerical bootstrap results were successfully compared with analytic calculations for the Wilson-Fisher fixed point in $d < 4$. Here we follow a similar approach, tracking the four-supercharge version of the Wilson-Fisher fixed point from four to two dimensions. This CFT is simply the critical Wess-Zumino (cWZ) model, i.e. the theory of a single chiral superfield with cubic superpotential at its infrared fixed point. As compared to the non-supersymmetric case, we have a lot less room for error here, since the conformal dimension of the “spin” field is protected and equal to $(d - 1)/3$ in any spacetime dimension d . Remarkably, we show that bounds on the dimension of the leading scalar operator in a chiral-antichiral OPE exhibit “kinks” (as in *e.g.* [4, 14]) at precisely this point for all $2 \leq d < 4$. They range from the $(2, 2)$ $c = 1$ supersymmetric minimal model in $d = 2$, where the numerical bootstrap agrees with various exact results, all the way to the free theory in $d = 4$. In $d = 3$, we find a kink at conformal dimension $2/3$, and are able to read off the dimension of the leading unprotected scalar, which is approximately 1.9098. Also in $d = 3$, our bootstrap prediction for the two-point function of the stress-tensor is in close agreement with the exact localization calculation

of [78]. Furthermore, for $d \lesssim 4$ our results for the dimension of the leading unprotected scalar agree with those of the one-loop ϵ -expansion [79]. This strongly suggests that in 3d our kink does indeed describe the super-Ising model. This theory is of some interest in condensed matter physics [80–83].

Part of the difficulty in bootstrapping supersymmetric theories lies in determining the form of the superconformal blocks. Supersymmetry organizes conformal into superconformal multiplets, and accordingly conformal blocks of primaries with different dimensions and spins also become grouped. The calculation of superconformal blocks for general external operators can be a cumbersome technical problem. In this chapter, we find the superconformal blocks in theories with four supercharges for external scalar superconformal primary operators with arbitrary scaling dimensions. A crucial ingredient is that at least two of these operators should be chiral primaries. Our approach is facilitated by the existence of a formal dimensional continuation of the superconformal algebra with four supercharges to arbitrary dimension $d \leq 4$. The commutation relations for the ordinary conformal algebra formally make sense when we let the spacetime vector indices run from 1 to d , since Jacobi identities can be verified without specializing to a fixed integer d . Here we show that this picture can be extended to include fermionic generators, namely four Poincaré supercharges and four conformal supercharges. We are able to write down (anti)commutation relations among all generators without specializing to a fixed d and demonstrate the validity of all super-Jacobi identities in an essentially dimension-independent way. The superconformal blocks can then be found in general d using the fact that they are eigenfunctions of the quadratic Casimir operator of this superconformal algebra. This method is similar to the way in which non-supersymmetric conformal blocks were found in [84]. Our general results reduce to previously studied cases, namely $d = 2$ and $d = 4$ [17, 85, 86]. Remarkably, we find that for any dimension, the superconformal blocks take the same functional form as ordinary, non-supersymmetric, blocks where the dimensions of external and propagating operators are shifted. This fact was also observed for $d = 2, 4$ in [86].

We begin our exploration in the next section, where we describe a construction of the superconformal algebras in $d \leq 4$ in a unified framework. This is necessary in order to properly define the Casimir operator of the algebra and its action on local operators, which is used in Section 3.3 to find the superconformal blocks. In Section 3.4, we provide a short review of the properties of the critical Wess-Zumino model in general dimension. Section 3.5 describes the set of crossing equations that we utilize in the numerical bootstrap procedure, the results of which are presented and discussed in Section 3.6. We finish with a discussion in Section 3.7. Several appendices complement the main text with technical results.

3.2 Superconformal algebra in continuous dimension

3.2.1 General results

We begin by presenting what we would like to call the dimensional continuation of the superconformal algebra with four Poincaré supercharges to an arbitrary spacetime dimension $d \leq 4$. The superconformal algebras in the traditional sense exist only for integer values of d . We will show however that some insight can be gained by considering a set of (anti)commutation relations which formally make sense for any real $0 \leq d \leq 4$, such that we obtain the corresponding superconformal algebras for integer d . We believe that this language is useful because it allows us to

- cast the $d = 4$ $\mathcal{N} = 1$, $d = 3$ $\mathcal{N} = 2$, $d = 2$ $\mathcal{N} = (2, 2)$ and $d = 1$ $\mathcal{N} = 4$ superconformal algebras in a unified way, where d enters only as a real parameter in the (anti)commutation relations (besides defining the range for the spacetime vector index),
- derive unitarity bounds on highest-weight representations for the whole d -dependent family in a unified manner, and verify they reduce to the correct results for the algebras in integer d ,
- find the superconformal blocks as analytic functions of d .

It is a well-known fact that the $d = 3$, $\mathcal{N} = 2$, and $d = 2$, $\mathcal{N} = (2, 2)$ Poincaré supersymmetry algebras are dimensional reductions of the $\mathcal{N} = 1$ algebra in $d = 4$, with the extra $U(1)$ R-symmetry in $d = 2$ coming from rotations in the two “transverse” dimensions. Here, we generalize this dimensional reduction to the full superconformal algebra. Imposing the Jacobi identities in a superconformal algebra leads to non-trivial polynomial relations for the generators of the Clifford algebra, this being the essential reason for the scarcity of superconformal algebras [87]. Consistency of our approach requires a continuous version of these identities valid in any $d \leq 4$. The identities can be checked for any $d = 0, 1, \dots, 4$ and at the level of traces even for continuous d . The superconformal algebra thus exists in continuous dimension in the same sense as the ordinary conformal algebra, where Jacobi identities can be checked formally without fixing spacetime dimension. Moreover, we show in Section 3.3 that superconformal blocks can be derived as analytic functions of d exactly as in the non-supersymmetric case [84, 88].

We work in Euclidean signature, with reality conditions equivalent to those imposed by unitarity in Lorentzian signature.¹ The unhatted Latin indices will run over the unreduced spacetime directions $i = 1, \dots, d$, while the hatted indices over the reduced ones $\hat{i} = d + 1, \dots, 4$. The bosonic generators include the usual momenta P_i , special conformal K_i , dilation D , and rotation M_{ij} generators, with $i, j = 1, \dots, d$, the $U(1)$ R-symmetry R , and finally the rotations in the reduced dimensions $M_{\hat{i}\hat{j}}$. Because of our formal approach, it is important to keep the reduced rotations $M_{\hat{i}\hat{j}}$ for any d , although there are no physical generators for $d > 2$. In our conventions, the bosonic commutation relations are

$$\begin{aligned}
[M_{ij}, M_{kl}] &= -i(\delta_{il}M_{jk} + \delta_{jk}M_{il} - \delta_{ik}M_{jl} - \delta_{jl}M_{ik}), \\
[M_{\hat{i}\hat{j}}, M_{\hat{k}\hat{l}}] &= -i(\delta_{\hat{i}\hat{l}}M_{\hat{j}\hat{k}} + \delta_{\hat{j}\hat{k}}M_{\hat{i}\hat{l}} - \delta_{\hat{i}\hat{k}}M_{\hat{j}\hat{l}} - \delta_{\hat{j}\hat{l}}M_{\hat{i}\hat{k}}), \\
[M_{ij}, P_k] &= -i(\delta_{jk}P_i - \delta_{ik}P_j), \\
[M_{ij}, K_k] &= -i(\delta_{jk}K_i - \delta_{ik}K_j), \\
[D, P_i] &= -iP_i, \\
[D, K_i] &= iK_i, \\
[P_i, K_j] &= -2i(\delta_{ij}D + M_{ij}),
\end{aligned} \tag{3.1}$$

with all other commutators vanishing. The Hermitian conjugation rules are

$$D^\dagger = -D, \quad R^\dagger = R, \quad M_{ij}^\dagger = M_{ij}, \quad M_{\hat{i}\hat{j}}^\dagger = M_{\hat{i}\hat{j}}, \quad P_i^\dagger = K_i. \tag{3.2}$$

We note that in our conventions, the action of the dilation generator D on an operator \mathcal{O} is $[D, \mathcal{O}] = -i\Delta\mathcal{O}$, where Δ is the conformal dimension of \mathcal{O} .

The fermionic generators include four Poincaré supercharges, Q , and four conformal supercharges, S . The former will be denoted Q_α^+ , $Q_{\dot{\alpha}}^-$, with $\alpha, \dot{\alpha} = 1, 2$, where the upper index denotes the R-charge eigenvalue, ± 1 , and the lower index transforms under the $SO(d) \times SO(4-d)$ rotations. As indicated by the dot, the supercharges with different R-charge are allowed to transform non-equivalently under rotations, as is the case for $\mathcal{N} = 1$ in $d = 4$. The conformal supercharges are Hermitian conjugates of the Poincaré supercharges

$$S^{\alpha-} = (Q_\alpha^+)^\dagger, \quad S^{\dot{\alpha}+} = (Q_{\dot{\alpha}}^-)^\dagger. \tag{3.3}$$

With this convention for placement of indices, contraction of an upper and a lower index of the same kind is an invariant operation since any representation of the compact group

¹The four-dimensional Euclidean superconformal algebra with four Poincaré supercharges does not admit unitary representations. This is not important for us since we insist on unitarity in Lorentzian signature. We thank Toine Van Proeyen for emphasizing this point.

$SO(d) \times SO(4-d)$ is unitary. Let us now sketch how the structure of the superconformal algebra, with the generators above, follows from the Jacobi identities. With the exception of the anticommutator of Poincaré and conformal supercharges, we simply reproduce the $d = 4$, $\mathcal{N} = 1$ superconformal algebra, but we think it is worthwhile to show how the structure emerges in a d -independent language.

Jacobi identities involving D or R imply that both sides of an (anti)commutation relation must have the same scaling dimension and R-charge, and we always impose these constraints in what follows. Furthermore repeated indices always imply a summation. The basic building block is the anticommutator of Poincaré supercharges, which takes the form

$$\{Q_\alpha^+, Q_{\dot{\alpha}}^-\} = \Sigma_{\alpha\dot{\alpha}}^i P_i, \quad (3.4)$$

where $\Sigma_{\alpha\dot{\alpha}}^i$ is an, as yet, unspecified tensor. Using the conjugation rules (3.2), (3.3) one finds

$$\{S^{\dot{\alpha}+}, S^{\alpha-}\} = \bar{\Sigma}_i^{\dot{\alpha}\alpha} K_i, \quad (3.5)$$

with $\bar{\Sigma}_i^{\dot{\alpha}\alpha} = (\Sigma_{\alpha\dot{\alpha}}^i)^*$. The only generators that can appear in the anticommutator of a Poincaré and a conformal supercharge are D , R , M_{ij} and $M_{\dot{i}\dot{j}}$. Rotation invariance dictates that D comes multiplied with one of the invariant tensors δ_{β}^{α} , $\delta_{\dot{\beta}}^{\dot{\alpha}}$. Let us normalize our supercharges so that

$$\begin{aligned} \{S^{\alpha-}, Q_{\beta}^+\} &= i\delta_{\beta}^{\alpha} D + \dots, \\ \{S^{\dot{\alpha}+}, Q_{\dot{\beta}}^-\} &= i\delta_{\dot{\beta}}^{\dot{\alpha}} D + \dots, \end{aligned} \quad (3.6)$$

where the dots stand for the contribution of other generators. The Jacobi identities coming from the triplets $[Q_\alpha^+, Q_{\dot{\alpha}}^-, K_i]$ and $[S^{\dot{\alpha}+}, S^{\alpha-}, P_i]$ then determine the following commutators

$$\begin{aligned} [K_i, Q_\alpha^+] &= \Sigma_{\alpha\dot{\alpha}}^i S^{\dot{\alpha}+}, \\ [K_i, Q_{\dot{\alpha}}^-] &= \Sigma_{\alpha\dot{\alpha}}^i S^{\alpha-}, \\ [P_i, S^{\dot{\alpha}+}] &= -\bar{\Sigma}_i^{\dot{\alpha}\alpha} Q_\alpha^+, \\ [P_i, S^{\alpha-}] &= -\bar{\Sigma}_i^{\dot{\alpha}\alpha} Q_{\dot{\alpha}}^-. \end{aligned} \quad (3.7)$$

We denote the representation matrices of rotations on the supercharges as m_{ij} , \tilde{m}_{ij} , i.e.

$$\begin{aligned} [M_{ij}, Q_\alpha^+] &= (m_{ij})_\alpha^\beta Q_\beta^+, \\ [M_{ij}, Q_{\dot{\alpha}}^-] &= (\tilde{m}_{ij})_{\dot{\alpha}}^{\dot{\beta}} Q_{\dot{\beta}}^-, \\ [M_{ij}, S^{\dot{\alpha}+}] &= -(\tilde{m}_{ij})_{\dot{\beta}}^{\dot{\alpha}} S^{\dot{\beta}+}, \\ [M_{ij}, S^{\alpha-}] &= -(m_{ij})_\beta^\alpha S^{\beta-}, \end{aligned} \quad (3.8)$$

where the latter two follow from the former two using the conjugation rules in (3.2) and (3.3). Note that the matrices m_{ij} , \tilde{m}_{ij} are necessarily antisymmetric in the space-time indices. The Jacobi identities for the triplets $[P_i, K_j, Q_\alpha^+]$ and $[P_i, K_j, Q_\alpha^-]$ imply

$$\begin{aligned}\Sigma_j \bar{\Sigma}_i &= \delta_{ij} + 2im_{ij}, \\ \bar{\Sigma}_i \Sigma_j &= \delta_{ij} + 2i\tilde{m}_{ij}.\end{aligned}\tag{3.9}$$

Taking the symmetric parts implies that the Σ_i tensors satisfy the Clifford algebra

$$\begin{aligned}\Sigma_i \bar{\Sigma}_j + \Sigma_j \bar{\Sigma}_i &= 2\delta_{ij}, \\ \bar{\Sigma}_i \Sigma_j + \bar{\Sigma}_j \Sigma_i &= 2\delta_{ij},\end{aligned}\tag{3.10}$$

while taking the antisymmetric parts leads to explicit formulas for the rotation generators in terms of Σ_i

$$\begin{aligned}m_{ij} &= -\frac{i}{4}(\Sigma_j \bar{\Sigma}_i - \Sigma_i \bar{\Sigma}_j), \\ \tilde{m}_{ij} &= -\frac{i}{4}(\bar{\Sigma}_i \Sigma_j - \bar{\Sigma}_j \Sigma_i).\end{aligned}\tag{3.11}$$

Since we would like our algebras to be related by the dimensional reduction, we will take (3.8), (3.10), and (3.11) to hold also for the hatted indices $\hat{i}, \hat{j} = d+1, \dots, 4$, thus defining the action of the extra R-symmetry. It remains to determine the anticommutators between Poincaré and conformal supercharges, i.e. $\{S^{\alpha-}, Q_\beta^+\}$ and $\{S^{\hat{\alpha}+}, Q_{\hat{\beta}}^-\}$. It follows from the $[S^{\alpha-}, Q_\beta^+, P_i]$, $[S^{\hat{\alpha}+}, Q_{\hat{\beta}}^-, P_i]$ Jacobi identities that M_{ij} appears contracted with the corresponding tensor m_{ij} or \tilde{m}_{ij} with unit coefficient. The most general form of the anticommutators which can be checked, using only (3.10), to be consistent with all Jacobi identities except for those involving three fermionic generators, is

$$\begin{aligned}\{S^{\alpha-}, Q_\beta^+\} &= \delta_\beta^\alpha (iD - aR) + (m_{ij})_\beta^\alpha M_{ij} + b(m_{\hat{i}\hat{j}})_\beta^\alpha M_{\hat{i}\hat{j}}, \\ \{S^{\hat{\alpha}+}, Q_{\hat{\beta}}^-\} &= \delta_{\hat{\beta}}^{\hat{\alpha}} (iD + aR) + (\tilde{m}_{ij})_{\hat{\beta}}^{\hat{\alpha}} M_{ij} + b(\tilde{m}_{\hat{i}\hat{j}})_{\hat{\beta}}^{\hat{\alpha}} M_{\hat{i}\hat{j}},\end{aligned}\tag{3.12}$$

for some real constants a, b . It remains to check whether the Jacobi identities involving three fermionic generators are satisfied. The Jacobi identity coming from the triplet $[Q_\alpha^+, Q_{\hat{\alpha}}^-, S^{\beta-}]$ leads to

$$\bar{\Sigma}_i^{\hat{\alpha}\alpha} \Sigma_{\beta\hat{\beta}}^i = \frac{2a+1}{2} \delta_\beta^\alpha \delta_{\hat{\beta}}^{\hat{\alpha}} + (m_{ij})_\beta^\alpha (\tilde{m}_{ij})_{\hat{\beta}}^{\hat{\alpha}} + b(m_{\hat{i}\hat{j}})_\beta^\alpha (\tilde{m}_{\hat{i}\hat{j}})_{\hat{\beta}}^{\hat{\alpha}}.\tag{3.13}$$

The rotation generators are traceless in the spinor indices, so taking the trace of this equation with respect to both pairs of indices and noting that (3.10) implies

$$\text{tr}(\Sigma^i \bar{\Sigma}_i) = 2d,\tag{3.14}$$

we find

$$a = \frac{d-1}{2}. \quad (3.15)$$

To fix b , we consider the Jacobi identity of the triplet $[Q_\alpha^+, Q_\beta^+, S^{\gamma-}]$, which leads to

$$\frac{d-2}{2} \delta_\beta^\alpha \delta_\delta^\gamma + (\alpha \leftrightarrow \gamma) = (m_{ij})_\beta^\alpha (m_{ij})_\delta^\gamma + b (m_{\hat{i}\hat{j}})_\beta^\alpha (m_{\hat{i}\hat{j}})_\delta^\gamma + (\alpha \leftrightarrow \gamma). \quad (3.16)$$

There is an analogous identity with dotted indices. Contracting all spinor indices and using that (3.10) and (3.11) imply

$$(m_{ij})_\beta^\alpha (m_{ij})_\alpha^\beta = \frac{d(d-1)}{2}, \quad (m_{\hat{i}\hat{j}})_\beta^\alpha (m_{\hat{i}\hat{j}})_\alpha^\beta = \frac{(4-d)(3-d)}{2}, \quad (3.17)$$

so we find

$$3(d-2) = \frac{d(d-1)}{2} + b \frac{(4-d)(3-d)}{2}, \quad (3.18)$$

which holds in continuous d for $b = -1$. The final form of the sought anticommutators is thus

$$\begin{aligned} \{S^{\alpha-}, Q_\beta^+\} &= \delta_\beta^\alpha \left(iD - \frac{d-1}{2} R \right) + (m_{ij})_\beta^\alpha M_{ij} - (m_{\hat{i}\hat{j}})_\beta^\alpha M_{\hat{i}\hat{j}}, \\ \{S^{\dot{\alpha}+}, Q_{\dot{\beta}}^-\} &= \delta_{\dot{\beta}}^{\dot{\alpha}} \left(iD + \frac{d-1}{2} R \right) + (\tilde{m}_{ij})_{\dot{\beta}}^{\dot{\alpha}} M_{ij} - (\tilde{m}_{\hat{i}\hat{j}})_{\dot{\beta}}^{\dot{\alpha}} M_{\hat{i}\hat{j}}. \end{aligned} \quad (3.19)$$

We have demonstrated that identities (3.13), (3.16) are satisfied in any d after contracting the spinor indices. We do not know of a d -independent way to argue for their validity in their uncontracted form. However, one can make an explicit choice of the 4d Σ matrices satisfying (3.10), and check the identities for all dimensions of interest. Indeed, they are satisfied for any consistent choice of Σ matrices for any $d = 0, 1, \dots, 4$. This exhausts all the constraints imposed by Jacobi identities, thus showing that our algebra is consistent in any $d \leq 4$.

3.2.2 Realizations in integer $d \leq 4$

In this section, we illustrate that our interpolation reduces to the expected algebras in integer number of dimensions. This is of course necessary since they are the unique superconformal algebras with four Poincaré supercharges and a $U(1)$ R-symmetry in the respective number of spacetime dimensions.

For $d = 4$, our algebra is manifestly the $\mathcal{N} = 1$ superconformal algebra with complexification $sl(4|1)$, with two pairs of Poincaré supercharges, with opposite R-charge,

transforming in the two inequivalent Weyl representations. The value $a = (d - 1)/2 = 3/2$ leads to the well-known chirality condition on scalar superconformal primaries, $\Delta = 3q/2$, with Δ the dimension and q the R-charge.

For $d = 3$, we reproduce the $\mathcal{N} = 2$ superconformal algebra, whose complexification is $osp(2|4)$. Choosing $\Sigma_{\alpha\dot{\alpha}}^i = (\sigma_i)^{\dot{\alpha}}_{\alpha}$ for $i = 1, 2, 3$, where σ_i are the usual Pauli matrices, we find that $Q_{\dot{\alpha}}^-$ transforms as a complex conjugate of Q_{α}^+ , so that a lower (upper) dotted index is equivalent to an upper (lower) undotted index, and all indices can be raised and lowered using $\epsilon^{\alpha\beta}$, $\epsilon_{\alpha\beta}$. The complete algebra is presented in Appendix 3.A.

The relevant superconformal algebra in two dimensions is the global part of the $\mathcal{N} = (2, 2)$ superconformal algebra in the NS-NS sector. The complexified Lie superalgebra is $sl(2|1)_l \oplus sl(2|1)_r$. Working on the holomorphic (left-moving) side, we have the usual bosonic generators L_n , $n = -1, 0, 1$, R-symmetry Ω , and fermionic generators $G_{\pm 1/2}^{\pm}$. They satisfy the following (anti)commutation relations

$$\begin{aligned} [L_m, L_n] &= (m - n) L_{m+n}, \\ [L_m, G_r^{\pm}] &= \left(\frac{m}{2} - r\right) G_{m+r}^{\pm}, \\ [\Omega, G_r^{\pm}] &= \pm G_r^{\pm}, \\ \{G_r^+, G_s^-\} &= 2L_{r+s} + (r - s)\Omega, \end{aligned} \tag{3.20}$$

with all other (anti)commutators vanishing. The anti-holomorphic generators, which we denote with a bar, satisfy exactly the same algebra. Making the traditional choice $\Sigma_{\alpha\dot{\alpha}}^i = (\sigma_i)^{\alpha}_{\dot{\alpha}}$ for $i = 1, 2, 3$ and $\Sigma_{\alpha\dot{\alpha}}^4 = i\delta_{\alpha\dot{\alpha}}$, our interpolating algebra from Section 3.2.1 reproduces (3.20) after the following identification for the bosonic generators

$$\begin{aligned} P_1 &= -i(L_{-1} + \bar{L}_{-1}), & P_2 &= L_{-1} - \bar{L}_{-1}, \\ K_1 &= i(L_1 + \bar{L}_1), & K_2 &= L_1 - \bar{L}_1, \\ D &= -i(L_0 + \bar{L}_0), & M_{12} &= -L_0 + \bar{L}_0, \\ R &= \Omega + \bar{\Omega}, & M_{34} &= \frac{\Omega - \bar{\Omega}}{2}, \end{aligned} \tag{3.21}$$

and the following for the fermionic generators

$$\begin{aligned} Q_1^+ &= G_{-1/2}^+, & Q_2^+ &= \bar{G}_{-1/2}^+, \\ Q_1^- &= \bar{G}_{-1/2}^-, & Q_2^- &= G_{-1/2}^-, \\ S^{1+} &= \bar{G}_{1/2}^-, & S^{2+} &= G_{1/2}^+, \\ S^{1-} &= G_{1/2}^-, & S^{2-} &= \bar{G}_{1/2}^-. \end{aligned} \tag{3.22}$$

Finally consider the case $d = 1$. In this dimension, the generator R drops out from equations (3.19), and indeed from the expression for the conformal Casimir as shown in Section 3.3.1. Hence, it may be safely dropped from the algebra. Since $4 = 1 + 3$, the situation is quite similar to the $d = 3$ case detailed above and in appendix 3.A. In particular, the rotation generators in the directions 2, 3, 4 describe an $su(2)$ algebra acting as an R-symmetry on the supercharges. Analogously to $d = 3$, we make the choice $\Sigma_{\alpha\dot{\beta}}^{\hat{i}} = (\sigma_{\hat{i}-1})^{\dot{\beta}}_{\alpha}$ for $\hat{i} = 2, 3, 4$, where σ_a are the usual Pauli matrices and $\Sigma_{\alpha\dot{\beta}}^1 = i\delta_{\alpha}^{\dot{\beta}}$. A lower dotted index has the same transformation under the R-symmetry as an upper undotted index and vice versa, so that we can write

$$Q^{\alpha-} \equiv Q_{\dot{\alpha}}^-, \quad S_{\alpha}^+ \equiv S^{\alpha+}. \quad (3.23)$$

Spinor indices can be raised and lowered using $\epsilon^{\alpha\beta}$, $\epsilon_{\alpha\beta}$. We also define

$$H \equiv P_1, \quad K \equiv K_1, \quad R_{\hat{i}-1} \equiv \frac{1}{2}\epsilon_{\hat{i}-1, \hat{j}-1, \hat{k}-1} M_{\hat{j}\hat{k}}, \quad (3.24)$$

and find that the algebra becomes $psu(1, 1|2)$, described by the non-zero commutators:

$$\begin{aligned} [H, K] &= -2iD, & [D, H] &= -iH, & [D, K] &= iK, \\ \{Q_{\alpha}^+, Q^{\beta-}\} &= i\delta_{\alpha}^{\beta} H, & [D, Q_{\alpha}^+] &= -\frac{i}{2}Q_{\alpha}^+, & [D, Q^{\alpha-}] &= -\frac{i}{2}Q^{\alpha-}, \\ \{S_{\alpha}^+, S^{\beta-}\} &= -i\delta_{\alpha}^{\beta} K, & [D, S_{\alpha}^+] &= \frac{i}{2}S_{\alpha}^+, & [D, S^{\alpha-}] &= \frac{i}{2}S^{\alpha-}, \\ \{S^{\alpha-}, Q_{\beta}^+\} &= iD\delta_{\beta}^{\alpha} - (\sigma_i)_{\beta}^{\alpha} R_i, & [K, Q_{\alpha}^+] &= iS_{\alpha}^+, & [K, Q^{\alpha-}] &= iS^{\alpha-}, \\ \{S_{\alpha}^+, Q^{\beta-}\} &= iD\delta_{\alpha}^{\beta} - (\sigma_i)_{\alpha}^{\beta} R_i, & [H, S_{\alpha}^+] &= iQ_{\alpha}^+, & [H, S^{\alpha-}] &= iQ^{\alpha-}, \\ [R_i, R_j] &= i\epsilon_{ijk} R_k, & [R_i, X_{\alpha}^+] &= \frac{1}{2}(\sigma_i)_{\alpha}^{\beta} X_{\beta}^+, & [R_i, X^{\alpha-}] &= \frac{1}{2}(\sigma_i)_{\beta}^{\alpha} X^{\beta-}, \end{aligned} \quad (3.25)$$

where in the last line X stands for either Q or S .

3.2.3 Unitarity bounds in general d

It will be useful for Section 3.3.4 to work out the unitarity bounds, in general dimension, for the symmetric traceless representation and the representation in the tensor product of the symmetric traceless and the spinors. The unitary representations in integer d were found in [89, 90] but our goal here is to offer a derivation that formally makes sense in general d . It was noted in [91] that the free scalar CFT in non-integer d contains negative-norm

states. This casts doubt on whether one can have unitary CFTs in fractional dimensions. Here, we will be modest and will derive necessary conditions for unitarity in general d , by focusing on the lowest levels, assuming that superconformal primaries have positive norm.

Suppose $|\mathcal{O}_A\rangle$ is a superconformal primary of dimension Δ , R-charge q , transforming in a representation R of $SO(d) \times SO(4-d)$. Using a standard argument, [89, 92–94], it follows from (3.19) that the Q_α^+ descendants of $|\mathcal{O}_A\rangle$ have non-negative norm when

$$\Delta \geq \frac{d-1}{2}q + a_R + a_r - \min_{R' \subset R \otimes r} (a_{R'}) , \quad (3.26)$$

where a_R denotes the eigenvalue of representation R under the following Casimir

$$\frac{1}{2}M_{ij}M_{ij} - \frac{1}{2}M_{\hat{i}\hat{j}}M_{\hat{i}\hat{j}} , \quad (3.27)$$

and r denotes the spinor representation in which Q_α^+ transforms, with a_r its eigenvalue under (3.27). Similarly, the $Q_{\dot{\alpha}}^-$ descendants of $|\mathcal{O}_A\rangle$ have non-negative norm whenever

$$\Delta \geq -\frac{d-1}{2}q + a_R + a_{\bar{r}} - \min_{R' \subset R \otimes \bar{r}} (a_{R'}) , \quad (3.28)$$

where \bar{r} is the representation in which $Q_{\dot{\alpha}}^-$ transforms. In Euclidean signature, the bar operation on $SO(d) \times SO(4-d)$ representations corresponds to parity, rather than complex conjugation, but we will refer to it as conjugation for simplicity. It remains to evaluate a_R on the representations of interest. Suppose $R = S_s$ is the symmetric traceless tensor of spin s . Since it has no indices in the reduced dimensions, we find just the $SO(d)$ eigenvalue

$$a_{S_s} = s(s+d-2) . \quad (3.29)$$

Consider now the spinor representations r, \bar{r} . It follows from (3.10) that their eigenvalue under $\frac{1}{2}M_{ij}M_{ij}$ is $\frac{d(d-1)}{8}$, which matches the expected values $\frac{1}{4}, \frac{3}{4}, \frac{3}{2}$ in $d = 2, 3, 4$, respectively. The spinor indices $\alpha, \dot{\alpha}$ necessarily transform also under the reduced rotations $M_{\hat{i}\hat{j}}$, and indeed, the eigenvalue under $\frac{1}{2}M_{\hat{i}\hat{j}}M_{\hat{i}\hat{j}}$ is related to the eigenvalue under $\frac{1}{2}M_{ij}M_{ij}$ by replacing $d \mapsto 4-d$. Hence the eigenvalue under (3.27) is

$$a_r = a_{\bar{r}} = \frac{d(d-1)}{8} - \frac{(4-d)(3-d)}{8} = \frac{3(d-2)}{4} . \quad (3.30)$$

Let us move on to the representation $|\mathcal{O}_{\alpha i_1 \dots i_s}\rangle$, symmetric and traceless in the s vector indices, and satisfying the irreducibility criterion $\bar{\Sigma}_{i_1}^{\dot{\alpha}\alpha} |\mathcal{O}_{\alpha i_1 \dots i_s}\rangle = 0$. We denote this representation as P_s . The action of the $SO(d)$ Casimir can be evaluated in general d using the

dimensional continuation of the superconformal algebra from the previous sections with the result

$$\frac{1}{2}M_{jk}M_{jk}|\mathcal{O}_{\alpha i_1 \dots i_s}\rangle = \left[\frac{d(d-1)}{8} + s(s+d-1) \right] |\mathcal{O}_{\alpha i_1 \dots i_s}\rangle. \quad (3.31)$$

This expression reduces to the expected $(s + \frac{1}{2})^2$ in $d = 2$; $j(j+1)$, with $j = s + \frac{1}{2}$, in $d = 3$; and $2[j_1(j_1+1) + j_2(j_2+1)]$, with $j_1 = \frac{s+1}{2}$, $j_2 = \frac{s}{2}$, in $d = 4$. We have already seen that

$$\frac{1}{2}M_{\hat{j}\hat{k}}M_{\hat{j}\hat{k}}|\mathcal{O}_{\alpha i_1 \dots i_s}\rangle = \frac{(4-d)(3-d)}{8} |\mathcal{O}_{\alpha i_1 \dots i_s}\rangle, \quad (3.32)$$

leading to

$$a_{P_s} = s(s+d-1) + \frac{3(d-2)}{4}. \quad (3.33)$$

The same formula is valid for the conjugate representation $|\mathcal{O}_{\dot{\alpha} i_1 \dots i_s}\rangle$.

Finally, we will need the Casimir for the representation $|\mathcal{O}_{\alpha\beta i_1 \dots i_s}\rangle$, symmetric in $\alpha\beta$, symmetric and traceless in the vector indices, and satisfying $\bar{\Sigma}_{i_1}^{\dot{\alpha}\alpha} |\mathcal{O}_{\alpha\beta i_1 \dots i_s}\rangle = 0$. We denote this representation by Q_s . The superconformal algebra is not sufficient to find the individual eigenvalues of the $SO(d)$ and $SO(4-d)$ Casimir operators because of the cross-term occurring when the two rotation generators each act on one spinor index. Fortunately, the identity in (3.16) is precisely what is needed to evaluate this cross-term in the difference of the two Casimirs. The final result is

$$a_{Q_s} = s(s+d) + 2(d-2). \quad (3.34)$$

This result is in harmony with the results in $d = 3, 4$, where the contribution of the $SO(4-d)$ Casimir must vanish. Indeed, in $d = 3$, $a_{Q_s} = (s+1)(s+2)$, corresponding to the $j = s+1$ representation, and in $d = 4$, $a_{Q_s} = (s+2)^2$, corresponding to the $j_1 = \frac{s}{2}+1$, $j_2 = \frac{s}{2}$ representation. Formula (3.34) applies also to the conjugate representation $|\mathcal{O}_{\dot{\alpha}\dot{\beta} i_1 \dots i_s}\rangle$.

We are now in a position to derive the unitarity bounds at level one for the S_s and P_s representations. Due to the covariance of the $\bar{\Sigma}$ tensor, we have the decompositions $S_s \otimes r = \bar{P}_{s-1} \oplus P_{s+1}$, $S_s \otimes \bar{r} = P_{s-1} \oplus \bar{P}_{s+1}$, valid for $s > 0$. The first direct summand has a smaller value of a , leading to the unitarity bound for the symmetric traceless representation

$$\Delta_{S_s} \geq \frac{d-1}{2}|q| + s + d - 2, \quad s > 0. \quad (3.35)$$

This formula reduces to the well-known results in integer d . For the special case $s = 0$, unitarity at the first level implies only $\Delta \geq \frac{d-1}{2}|q|$. However, this condition is not sufficient

for unitarity, since the level-two state $|\mathcal{P}\rangle = \epsilon^{\alpha\beta} Q_\alpha^+ Q_\beta^+ |\mathcal{O}_A\rangle$ has norm

$$\langle \mathcal{P} | \mathcal{P} \rangle = 4 \left(\Delta - \frac{d-1}{2} q \right) \left(\Delta - \frac{d-1}{2} q - d + 2 \right). \quad (3.36)$$

An analogous result holds for $|\tilde{\mathcal{P}}\rangle = \epsilon^{\dot{\alpha}\dot{\beta}} Q_{\dot{\alpha}}^- Q_{\dot{\beta}}^- |\mathcal{O}_A\rangle$, leading to the unitary representations

$$\begin{aligned} \Delta_{S_0} &= \frac{d-1}{2} |q|, \\ \Delta_{S_0} &\geq \frac{d-1}{2} |q| + d - 2. \end{aligned} \quad (3.37)$$

Consider now the representation P_s . We have $P_s \otimes r = S_s \oplus Q_s$, $P_s \otimes \bar{r} = Q_{s-1} \oplus S_{s+1}$, with the first direct summand having the smaller value of a_R . Equations (3.26), (3.28) thus lead to the bound

$$\Delta_{P_s} \geq \left| \frac{d-1}{2} (q+1) - 1 \right| + s + d - \frac{3}{2}. \quad (3.38)$$

In $d = 3$, this reduces to the expected $\Delta \geq |q| + s + \frac{3}{2} = |q| + j + 1$, with $j = s + \frac{1}{2}$. In $d = 4$, it becomes $\Delta \geq \left| \frac{3}{2} q + \frac{1}{2} \right| + s + \frac{5}{2} = \left| \frac{3}{2} q + j_1 - j_2 \right| + j_1 + j_2 + 2$, with $j_1 = \frac{s+1}{2}$, $j_2 = \frac{s}{2}$, in perfect agreement with [89, 90]. The unitarity bound for the conjugate representation \bar{P}_s is obtained simply by flipping the sign of q in (3.38)

$$\Delta_{\bar{P}_s} \geq \left| \frac{d-1}{2} (q-1) + 1 \right| + s + d - \frac{3}{2}. \quad (3.39)$$

The notions of short and semi-short representations are useful because operators in these representations often have dimensions protected from quantum corrections. A superconformal chiral scalar operator belongs to a short multiplet and obeys the first equation in (3.37) with $q > 0$, an anti-chiral operator obeys the same equation with $q < 0$. For the symmetric traceless representation of spin s , the semi-short multiplets are those for which the superconformal primary saturates (3.35), which for $s = 0$ is the same as saturating the second equation in (3.37).

Necessary conditions for unitary representations of the nonsupersymmetric conformal algebra in general dimension are presented in Section 6 of [90] (see also [95]) and they are generally weaker than the ones for the superconformal algebra discussed here. It is also useful to recall that a free scalar field in d dimensions necessarily has

$$\Delta_{\text{free}} = \frac{d-2}{2}, \quad (3.40)$$

and a conserved current of spin s in any CFT obeys

$$\Delta_{\text{cc}} = s + d - 2. \quad (3.41)$$

3.3 Superconformal blocks

A standard method for finding conformal and superconformal blocks is by utilizing the Casimir equation [84, 86]. Having formulated a dimensional continuation of the superconformal algebra with four Poincaré supercharges, we are in a position to find the Casimir equation and its solution for a large class of superconformal blocks in general d . This is done in Sections 3.3.1, 3.3.2. Remarkably, as was already noticed in [86], superconformal blocks are closely related to non-supersymmetric conformal blocks with shifted scaling dimensions and we provide an interpretation of this fact in Section 3.3.3. In section 3.3.4 we deal with an important case not captured by the Casimir approach, namely that of superconformal blocks in the chiral channel.

3.3.1 Superconformal Casimir

In this section, we find the quadratic Casimir of the relevant superconformal algebra in general dimension. The quadratic Casimir must be a linear combination of the quadratic Casimir C_b of the bosonic conformal subalgebra $so(d+1,1)$, the Casimir of the reduced rotations, $so(4-d)$, R^2 , and terms quadratic in the fermionic generators. Invariance under D , R , M_{ij} , and $M_{\hat{i}\hat{j}}$ reduces the possibilities to

$$C = C_b + c_1 S^{\alpha+} Q_{\alpha}^{-} + c_2 Q_{\alpha}^{-} S^{\alpha+} + c_3 S^{\alpha-} Q_{\alpha}^{+} + c_4 Q_{\alpha}^{+} S^{\alpha-} + c_5 R^2 + c_6 M_{\hat{i}\hat{j}} M_{\hat{i}\hat{j}}, \quad (3.42)$$

with c_i so far undetermined constants. Note that

$$C_b = -D^2 - \frac{1}{2}(P_i K_i + K_i P_i) + \frac{1}{2} M_{ij} M_{ij}. \quad (3.43)$$

The coefficients c_i can be determined by requiring $[C, Q_{\alpha}^{+}] = [C, Q_{\alpha}^{-}] = 0$. Using (3.19) and looking at the coefficients of DQ_{α}^{+} , DQ_{α}^{-} , $Q_{\alpha}^{+}D$ and $Q_{\alpha}^{-}D$ leads to $c_1 = c_3 = -c_2 = -c_4 = 1/2$. Similarly, the coefficient of RQ_{α}^{+} determines $c_5 = -(d-1)/4$. Finally, the coefficient of $M_{\hat{i}\hat{j}}Q_{\alpha}^{+}$ fixes $c_6 = -1/2$, leading to the final result

$$C = -D^2 - \frac{1}{2}(P_i K_i + K_i P_i) + \frac{1}{2} M_{ij} M_{ij} - \frac{1}{2} M_{\hat{i}\hat{j}} M_{\hat{i}\hat{j}} - \frac{d-1}{4} R^2 + \frac{1}{2} ([S^{\alpha+}, Q_{\alpha}^{-}] + [S^{\alpha-}, Q_{\alpha}^{+}]). \quad (3.44)$$

It is instructive to study the contribution of the R-symmetries in $d=2$, where, after using (3.21), one finds

$$\frac{1}{2} M_{\hat{i}\hat{j}} M_{\hat{i}\hat{j}} + \frac{d-1}{4} R^2 = \frac{1}{4} [(\Omega - \bar{\Omega})^2 + (\Omega + \bar{\Omega})^2] = \frac{1}{2} (\Omega^2 + \bar{\Omega}^2). \quad (3.45)$$

The contribution is a sum of a holomorphic and an antiholomorphic part as expected. The eigenvalue of C when acting on a superconformal family, where the superconformal primary has dimension Δ , R-charge q , and transforms as a symmetric traceless tensor of spin s under M_{ij} and as a singlet under $M_{\hat{i}\hat{j}}$, is

$$\lambda_C = \Delta(\Delta - d + 2) + s(s + d - 2) - \frac{d-1}{4}q^2. \quad (3.46)$$

To find this, we have used the eigenvalue of the usual conformal Casimir operator C_b when acting on a conformal primary [84]

$$\lambda_{C_b} = \Delta(\Delta - d) + s(s + d - 2). \quad (3.47)$$

3.3.2 Casimir equation and its solution

Here, we derive a formula for the superconformal blocks in theories invariant under the superconformal algebra in Section 3.2, for the four-point function $\langle \phi_1 \phi_2 \phi_3 \phi_4 \rangle$, where ϕ_i are scalar superconformal primaries with dimensions Δ_i and R-charges q_i . In addition, we assume that ϕ_1 and ϕ_3 are chiral, i.e. $Q_\alpha^+ \phi_{1,3} = 0$, or equivalently

$$\Delta_{1,3} = \frac{d-1}{2}q_{1,3}. \quad (3.48)$$

A superconformal block corresponds to the contribution of a single superconformal family produced in the OPE of ϕ_1 and ϕ_2 . It is therefore an eigenfunction of the superconformal Casimir (3.44) applied to the first two operators. Due to the appearance of supercharges, the resulting equation will relate the superconformal block of $\langle \phi_1 \phi_2 \phi_3 \phi_4 \rangle$ to the one of $\langle \psi_1^{\dot{\alpha}} \psi_2^\alpha \phi_3 \phi_4 \rangle$, where $\psi_{1,2}$ is a supersymmetric descendant of $\phi_{1,2}$. In the limit $|x_4| \rightarrow \infty$, we can use a supersymmetric Ward identity to reduce the latter correlator to a differential operator acting on $\langle \phi_1 \phi_2 \phi_3 \phi_4 \rangle$ and thus derive a differential equation for the original superconformal block. Consider the action of the fermionic part of the superconformal Casimir on the product $\phi_1(x_1)\phi_2(x_2)$. Using the chirality of ϕ_1 and the superconformal algebra, one can show that

$$\begin{aligned} & \frac{1}{2} ([S^{\dot{\alpha}+}, Q_{\dot{\alpha}}^-] + [S^{\alpha-}, Q_\alpha^+]) (\phi_1(x_1)\phi_2(x_2)) |0\rangle = \\ & = [(S^{\alpha-} \phi_1(x_1))(Q_\alpha^+ \phi_2(x_2)) - (Q_{\dot{\alpha}}^- \phi_1(x_1))(S^{\dot{\alpha}+} \phi_2(x_2)) + 2(\Delta_1 + \Delta_2)\phi_1(x_1)\phi_2(x_2)] |0\rangle, \end{aligned} \quad (3.49)$$

where the action of conserved charges on local operators is the usual one via the commutator. From

$$\phi(x) = e^{ix \cdot P} \phi(0) e^{-ix \cdot P}, \quad (3.50)$$

and using (3.7), it follows that

$$(S^{\alpha-} \phi_1(x_1)) = i x_1^i \bar{\Sigma}_i^{\dot{\alpha}\alpha} (Q_{\dot{\alpha}}^- \phi_1(x_1)), \quad (S^{\dot{\alpha}+} \phi_2(x_2)) = i x_2^i \bar{\Sigma}_i^{\dot{\alpha}\alpha} (Q_{\alpha}^+ \phi_2(x_2)). \quad (3.51)$$

It remains to relate the correlator

$$\langle (Q_{\dot{\alpha}}^- \phi_1(x_1)) (Q_{\alpha}^+ \phi_2(x_2)) \phi_3(x_3) \phi_4(x_4) \rangle, \quad (3.52)$$

to $\langle \phi_1(x_1) \phi_2(x_2) \phi_3(x_3) \phi_4(x_4) \rangle$. Starting from the Ward identity

$$\langle [Q_{\alpha}^+, (Q_{\dot{\alpha}}^- \phi_1(x_1)) \phi_2(x_2) \phi_3(x_3) \phi_4(x_4)] \rangle = 0, \quad (3.53)$$

and using the anticommutator of Poincaré supercharges, (3.4), and the chirality of ϕ_3 , we find

$$\begin{aligned} & \langle (Q_{\dot{\alpha}}^- \phi_1(x_1)) (Q_{\alpha}^+ \phi_2(x_2)) \phi_3(x_3) \phi_4(x_4) \rangle + \langle (Q_{\dot{\alpha}}^- \phi_1(x_1)) \phi_2(x_2) \phi_3(x_3) (Q_{\alpha}^+ \phi_4(x_4)) \rangle = \\ & = -i \Sigma_{\alpha\dot{\alpha}}^i \partial_i^{x_1} \langle \phi_1(x_1) \phi_2(x_2) \phi_3(x_3) \phi_4(x_4) \rangle. \end{aligned} \quad (3.54)$$

Conformal invariance ensures that no information is lost if we take the limit $x_4 \rightarrow \infty$. The leading behavior of a correlation function containing a primary $\mathcal{O}(x)$ of dimension Δ and arbitrary Lorentz quantum numbers as $|x| \rightarrow \infty$ is $|x|^{-2\Delta}$. Thus the second term on the left-hand side of (3.54) is subleading in the limit $|x_4| \rightarrow \infty$, since Q_{α}^+ increases the dimension of ϕ_4 by 1/2. In the derivation of the differential equation, we can then replace

$$\langle (Q_{\dot{\alpha}}^- \phi_1(x_1)) (Q_{\alpha}^+ \phi_2(x_2)) \phi_3(x_3) \phi_4(x_4) \rangle, \quad (3.55)$$

with

$$-i \Sigma_{\alpha\dot{\alpha}}^i \partial_i^{x_1} \langle \phi_1(x_1) \phi_2(x_2) \phi_3(x_3) \phi_4(x_4) \rangle, \quad (3.56)$$

while remembering that we must send $|x_4|$ to infinity at the end of the calculation. Combining this with (3.51), and using

$$\text{tr}(\Sigma^i \bar{\Sigma}_j) = 2\delta^i_j, \quad (3.57)$$

which follows from the Clifford algebra, we find the action of the fermionic part of the superconformal Casimir on the four-point function to be

$$\begin{aligned} & \left\langle \frac{1}{2} ([S^{\dot{\alpha}+}, Q_{\dot{\alpha}}^-] + [S^{\alpha-}, Q_{\alpha}^+]) (\phi_1(x_1) \phi_2(x_2)) \phi_3(x_3) \phi_4(x_4) \right\rangle \sim \\ & \sim 2(x_{12} \cdot \partial_{x_1} + \Delta_1 + \Delta_2) \langle \phi_1(x_1) \phi_2(x_2) \phi_3(x_3) \phi_4(x_4) \rangle, \end{aligned} \quad (3.58)$$

where $x_{ij} \equiv x_i - x_j$, and the \sim symbol means equality up to terms subleading as $|x_4| \rightarrow \infty$.

The contribution of a single superconformal family of the superconformal primary \mathcal{O} to the four-point function takes the form

$$\langle \phi_1(x_1)\phi_2(x_2)\phi_3(x_3)\phi_4(x_4) \rangle|_{\mathcal{O}} = \frac{c_{\phi_1\phi_2}^{\mathcal{O}} c_{\phi_3\phi_4}^{\mathcal{O}}}{|x_{12}|^{\Delta_1+\Delta_2} |x_{34}|^{\Delta_3+\Delta_4}} \frac{|x_{24}|^{\Delta_{12}} |x_{14}|^{\Delta_{34}}}{|x_{14}|^{\Delta_{12}} |x_{13}|^{\Delta_{34}}} \mathcal{G}_{\Delta_{\mathcal{O}},s}^{\Delta_{12},\Delta_{34}}(z, \bar{z}), \quad (3.59)$$

where $\mathcal{G}_{\Delta,s}^{\Delta_{12},\Delta_{34}}(z, \bar{z})$ is the superconformal block and $\Delta_{ij} \equiv \Delta_i - \Delta_j$. Here z and \bar{z} are related to the usual conformally invariant cross-ratios u, v as

$$u \equiv \frac{x_{12}^2 x_{34}^2}{x_{13}^2 x_{24}^2} = z\bar{z}, \quad v \equiv \frac{x_{14}^2 x_{23}^2}{x_{13}^2 x_{24}^2} = (1-z)(1-\bar{z}). \quad (3.60)$$

The operator (3.58) translates into the following action on the superconformal block

$$2[z(1-z)\partial + \bar{z}(1-\bar{z})\bar{\partial}] \mathcal{G}_{\Delta,s}^{\Delta_{12},\Delta_{34}}(z, \bar{z}) - \Delta_{34}(z+\bar{z}) \mathcal{G}_{\Delta,s}^{\Delta_{12},\Delta_{34}}(z, \bar{z}), \quad (3.61)$$

where $\partial \equiv \partial_z$ and $\bar{\partial} \equiv \partial_{\bar{z}}$. The action of the R-symmetry cancels on the two sides of the superconformal Casimir equation, and using the result for the conformal Casimir [84], the differential equation for the superconformal block becomes

$$\mathcal{D} \mathcal{G}_{\Delta,s}^{\Delta_{12},\Delta_{34}}(z, \bar{z}) = [\Delta(\Delta - d + 2) + s(s + d - 2)] \mathcal{G}_{\Delta,s}^{\Delta_{12},\Delta_{34}}(z, \bar{z}), \quad (3.62)$$

where the differential operator \mathcal{D} is given by

$$\begin{aligned} \mathcal{D} \equiv & 2z^2(1-z)\partial^2 + 2\bar{z}^2(1-\bar{z})\bar{\partial}^2 + (\Delta_{12} - \Delta_{34} - 4)(z^2\partial + \bar{z}^2\bar{\partial}) + 2(z\partial + \bar{z}\bar{\partial}) + \\ & + \frac{1}{2}(\Delta_{12} - 2)\Delta_{34}(z + \bar{z}) + 2(d-2)\frac{z\bar{z}}{z-\bar{z}} [(1-z)\partial - (1-\bar{z})\bar{\partial}]. \end{aligned} \quad (3.63)$$

It turns out that this equation has a simple solution in terms of the ordinary non-supersymmetric conformal blocks. This has also been pointed out for $d=4$ and $\phi_1 = \phi_3 = \bar{\phi}_2 = \bar{\phi}_4$ in [86]. Indeed, the solution with the correct $z, \bar{z} \rightarrow 0$ behavior is

$$\mathcal{G}_{\Delta,s}^{\Delta_{12},\Delta_{34}}(u, v) = u^{-1/2} G_{\Delta+1,s}^{\Delta_{12}-1,\Delta_{34}-1}(u, v), \quad (3.64)$$

where $G_{\Delta,s}^{\Delta_{12},\Delta_{34}}(u, v)$ is the non-supersymmetric conformal block and we switched to the usual cross-ratios u, v . We comment on the relationship between conformal and superconformal blocks in the next section. It is also possible to decompose the superconformal block into conformal blocks using a relation found in [68]. Using the convention where the $u \rightarrow 0, v \rightarrow 1$ behavior of the conformal blocks is

$$G_{\Delta,s}^{\Delta_{12},\Delta_{34}}(u, v) \sim \frac{(-1)^s}{2^s} u^{\frac{\Delta-s}{2}} (1-v)^s, \quad (3.65)$$

the decomposition reads

$$\mathcal{G}_{\Delta,s}^{\Delta_{12},\Delta_{34}} = G_{\Delta,s}^{\Delta_{12},\Delta_{34}} + a_1 G_{\Delta+1,s+1}^{\Delta_{12},\Delta_{34}} + a_2 G_{\Delta+1,s-1}^{\Delta_{12},\Delta_{34}} + a_3 G_{\Delta+2,s}^{\Delta_{12},\Delta_{34}}, \quad (3.66)$$

where

$$\begin{aligned} a_1 &\equiv -\frac{(\Delta + \Delta_{12} + s)(\Delta + \Delta_{34} + s)}{2(\Delta + s)(\Delta + s + 1)}, \\ a_2 &\equiv -\frac{s(s + d - 3)(\Delta + \Delta_{12} - s - d + 2)(\Delta + \Delta_{34} - s - d + 2)}{2(2s + d - 4)(2s + d - 2)(\Delta - s - d + 2)(\Delta - s - d + 3)}, \\ a_3 &\equiv \frac{\Delta(\Delta - d + 3)(\Delta + \Delta_{12} + s)(\Delta + \Delta_{34} + s)(\Delta + \Delta_{12} - s - d + 2)(\Delta + \Delta_{34} - s - d + 2)}{4(2\Delta - d + 4)(2\Delta - d + 2)(\Delta + s)(\Delta + s + 1)(\Delta - s - d + 2)(\Delta - s - d + 3)}. \end{aligned} \quad (3.67)$$

It follows that whenever a superconformal family contributes to a given four-point function, as in (3.59), it is through the superconformal primary, \mathcal{O} , and three other conformal primaries (and all their conformal descendants). The three conformal primaries are supersymmetric descendants of \mathcal{O} , with dimensions and spins that can be read off from (3.66).

A few comments are in order. Notice that for $\Delta_{12} = \Delta_{34} = 0$ the coefficients do not have poles for dimension and spin consistent with the unitarity bounds, and furthermore their sign is consistent with unitarity. For Δ_{12} and Δ_{34} different from zero, there can be poles, for Δ, s saturating the unitarity bound, but this is expected since the leading block itself diverges. This is related to the fact that conserved currents can only couple to scalars with identical dimensions.

It is useful to pause for a moment and compare our solution for $\mathcal{G}_{\Delta,s}^{\Delta_{12},\Delta_{34}}(u, v)$ to previous results in integer dimensions. For the special case of the $d = 4, \mathcal{N} = 1$ superconformal blocks studied in [17, 86], our solution is in agreement with their result since conformal blocks are invariant under $\Delta_{12} \leftrightarrow -\Delta_{34}$. For $d = 2$, the explicit form of the solution is (up to an overall constant)

$$\mathcal{G}_{\Delta,s}^{\Delta_{12},\Delta_{34}}(z, \bar{z}) = j_{\frac{\Delta+s}{2}}(z)j_{\frac{\Delta-s}{2}}(\bar{z}) + z \leftrightarrow \bar{z}, \quad (3.68)$$

where

$$j_h(z) \equiv z^h {}_2F_1\left(h - \frac{\Delta_{12}}{2} + 1, h + \frac{\Delta_{34}}{2}; 2h + 1; z\right). \quad (3.69)$$

This also agrees with the result found in [86], up to the transformation $z \leftrightarrow z/(z - 1)$, or equivalently $x_1 \leftrightarrow x_2$, and after taking into account the following identity

$$z^h {}_2F_1(h + 1, h, 2h + 1; z) = \left(\frac{z}{1 - z}\right)^h {}_2F_1\left(h, h, 2h + 1; \frac{z}{z - 1}\right). \quad (3.70)$$

As a cross-check on the Casimir approach, appendix 3.A contains a derivation of the coefficients in (3.67) for $d = 3$, using the constraints of superconformal symmetry and chirality of $\phi_{1,3}$ on the OPE. It is conceivable that this type of OPE derivation of the superconformal blocks can be carried out in general d using the superconformal algebra of Section 3.2.

Finally, we would like to point out some curious relations between the coefficients in (3.67). For $d = 2$ and $d = 4$ one has $a_3 = a_1 a_2$. This identity is not true in general dimension. However, if one considers a_i as a formal function $a_i(\Delta, s, d, \Delta_{12}, \Delta_{34})$ one finds

$$a_3(\Delta, s, d, \Delta_{12}, \Delta_{34}) = a_1(\Delta, s, d, \Delta_{12}, \Delta_{34}) a_2(-s, -\Delta, d, \Delta_{12}, \Delta_{34}). \quad (3.71)$$

3.3.3 The relationship between conformal and superconformal blocks

The relation in (3.64) between superconformal and ordinary conformal blocks can be given a simple interpretation. Consider the contribution of the superconformal family of the superconformal primary \mathcal{O} to the correlator $\langle \phi_1 \phi_2 \phi_3 \phi_4 \rangle$ as in (3.59). It can be rewritten, via (3.64), as

$$\begin{aligned} & \langle \phi_1(x_1) \phi_2(x_2) \phi_3(x_3) \phi_4(x_4) \rangle |_{\mathcal{O}} = \\ & = |x_{24}|^2 \frac{c_{\phi_1 \phi_2}^{\mathcal{O}} c_{\phi_3 \phi_4}^{\mathcal{O}}}{|x_{12}|^{\Delta_1 + \Delta_2 + 1} |x_{34}|^{\Delta_3 + \Delta_4 + 1}} \left(\frac{|x_{24}|}{|x_{14}|} \right)^{\Delta_{12} - 1} \left(\frac{|x_{14}|}{|x_{13}|} \right)^{\Delta_{34} - 1} G_{\Delta_{\mathcal{O}} + 1, s_{\mathcal{O}}}^{\Delta_{12} - 1, \Delta_{34} - 1}(u, v). \end{aligned} \quad (3.72)$$

Up to the $|x_{24}|^2$ prefactor, this has the form of the contribution of the *conformal* family of a *conformal* primary $\tilde{\mathcal{O}}$ to the four-point function of some new fields $\tilde{\phi}_i$

$$\langle \phi_1(x_1) \phi_2(x_2) \phi_3(x_3) \phi_4(x_4) \rangle |_{\mathcal{O}} = |x_{24}|^2 \langle \tilde{\phi}_1(x_1) \tilde{\phi}_2(x_2) \tilde{\phi}_3(x_3) \tilde{\phi}_4(x_4) \rangle |_{\tilde{\mathcal{O}}}, \quad (3.73)$$

where the quantum numbers of operators with a tilde are related to the original ones as

$$\begin{aligned} \Delta_{\tilde{\phi}_1} &= \Delta_{\phi_1}, \\ \Delta_{\tilde{\phi}_2} &= \Delta_{\phi_2} + 1, \\ \Delta_{\tilde{\phi}_3} &= \Delta_{\phi_3}, \\ \Delta_{\tilde{\phi}_4} &= \Delta_{\phi_4} + 1, \\ \Delta_{\tilde{\mathcal{O}}} &= \Delta_{\mathcal{O}} + 1, \quad s_{\tilde{\mathcal{O}}} = s_{\mathcal{O}}. \end{aligned} \quad (3.74)$$

Hence, the terms in the *superconformal* block expansion of $\langle \phi_1(x_1)\phi_2(x_2)\phi_3(x_3)\phi_4(x_4) \rangle$ are in one-to-one correspondence with the terms of the *conformal* block expansion of

$$\langle \tilde{\phi}_1(x_1)\tilde{\phi}_2(x_2)\tilde{\phi}_3(x_3)\tilde{\phi}_4(x_4) \rangle = \frac{1}{|x_{24}|^2} \langle \phi_1(x_1)\phi_2(x_2)\phi_3(x_3)\phi_4(x_4) \rangle . \quad (3.75)$$

Moreover, since the only difference between the four-point functions $\langle \phi_1\phi_2\phi_3\phi_4 \rangle$ and $\langle \tilde{\phi}_1\tilde{\phi}_2\tilde{\phi}_3\tilde{\phi}_4 \rangle$ is the factor $|x_{24}|^2$, we can mimic their relationship by writing

$$\begin{aligned} \tilde{\phi}_{1,3} &= \phi_{1,3} , \\ \tilde{\phi}_{2,4} &= \sigma\phi_{2,4} , \end{aligned} \quad (3.76)$$

where σ is a real scalar conformal primary field of scaling dimension $\Delta_\sigma = 1$ not interacting with any of the ϕ_i . Therefore, there is no regularization needed in defining the composite operators $\sigma\phi_{2,4}$, and the correlation function factorizes as

$$\langle \phi_1(x_1)(\sigma\phi_2)(x_2)\phi_3(x_3)(\sigma\phi_4)(x_4) \rangle = \langle \sigma(x_2)\sigma(x_4) \rangle \langle \phi_1(x_1)\phi_2(x_2)\phi_3(x_3)\phi_4(x_4) \rangle . \quad (3.77)$$

It may sound surprising that the conformal block expansion of $\langle \phi_1(\sigma\phi_2)\phi_3(\sigma\phi_4) \rangle$ is the same as the superconformal block expansion of $\langle \phi_1\phi_2\phi_3\phi_4 \rangle$. Each superconformal primary $\mathcal{O}^{(0)}$ in the $\phi_1 \times \phi_2$ OPE gives rise to four conformal primaries $\mathcal{O}^{(j)}$, $j = 0, \dots, 3$, and each of these gives rise to infinitely many conformal primaries in the $\phi_1 \times \sigma\phi_2$ OPE, of the schematic form $\sigma\partial^n\mathcal{O}^{(j)}$, $n = 0, 1, \dots$. For the proposed relationship between the two expansions to hold, there must occur numerous cancellations among the various conformal primaries, leaving only the contribution of the lowest one $\sigma\mathcal{O}^{(0)}$. Indeed, denoting the conformal descendant of $\mathcal{O}^{(0)}$ with dimension $\Delta_{\mathcal{O}} + 1$ and spin $s_{\mathcal{O}} + 1$ as $\mathcal{O}^{(1)}$, the contribution of the conformal primary $\sigma\mathcal{O}^{(1)}$ is cancelled by the contribution of $\sigma\overset{\leftrightarrow}{\partial}\mathcal{O}^{(0)}$, which has the same dimension and spin. Remarkably, this cancellation continues to hold for all the higher-lying conformal primaries, leaving only $\sigma\mathcal{O}^{(0)}$.

It will be curious to study whether the relation in (3.73) between correlation functions in a superconformal field theory and those in a non-supersymmetric conformal field theory can ever be realized for some theories of physical interest.

3.3.4 Spectrum in a chiral OPE

When considering conformal bootstrap for the correlator $\langle \phi_1\phi_2\phi_3\phi_4 \rangle$ with $\phi_{1,3}$ chiral primaries and $\phi_{2,4}$ superconformal primaries, there is another possibility for an OPE expansion, namely fusing ϕ_1 and ϕ_3 . Chirality implies that all conformal primaries appearing

in this OPE must be annihilated by Q_α^+ and it is the goal of this section to derive which components of superconformal multiplets have this property.

Suppose that \mathcal{P} is a conformal primary of dimension $\Delta_{\mathcal{P}}$ and R-charge $q_{\mathcal{P}}$ in the symmetric traceless representation of spin s , satisfying $[Q_\alpha^+, \mathcal{P}] = 0$. Further, assume that \mathcal{P} is a supersymmetric descendant of the superconformal primary \mathcal{O} , where \mathcal{O} has dimension Δ and R-charge q . The $SO(d) \times SO(4-d)$ representation R in which \mathcal{O} transforms depends on the precise way \mathcal{P} is obtained from \mathcal{O} through the action of supercharges. The relationship between \mathcal{O} and \mathcal{P} is constrained by observing that the superconformal Casimir (3.44) must have the same eigenvalue on \mathcal{O} and \mathcal{P} . Since \mathcal{P} is annihilated by both K_i and Q_α^+ , it is also annihilated by their anticommutator $S^{\dot{\alpha}+}$. One can then use the superconformal algebra to evaluate the action of C on \mathcal{P} purely in terms of its quantum numbers, with the resulting eigenvalue

$$\lambda_1 = \Delta_{\mathcal{P}}(\Delta_{\mathcal{P}} - d) + s(s + d - 2) - \frac{d-1}{4}q_{\mathcal{P}}^2 + (d-1)q_{\mathcal{P}}, \quad (3.78)$$

where the last term arises from the fermionic generators. Similarly, one can evaluate the eigenvalue of C on \mathcal{O} using the fact that it is a superconformal primary, the result being

$$\lambda_2 = \Delta(\Delta - d + 2) + a_R - \frac{d-1}{4}q^2, \quad (3.79)$$

where a_R is the $SO(d) \times SO(4-d)$ Casimir familiar from Section 3.2.3. Moreover, for each conformal primary in the superconformal multiplet, there are relations of the form $\Delta_{\mathcal{P}} = \Delta + \frac{m}{2}$, $m = 0, \dots, 4$, $q_{\mathcal{P}} = q + n$, $n = -2, \dots, 2$, and we can proceed case by case and determine whether $\lambda_1 = \lambda_2$ is consistent. We label each case by $(q_{\mathcal{P}}, R)$ and use the notation of Section 3.2.3 for the $SO(d) \times SO(4-d)$ representations.

- At level zero, we have the single case $(q_{\mathcal{P}} = q, R = S_s)$, and $\lambda_1 = \lambda_2$ implies

$$\Delta = \frac{d-1}{2}q, \quad (3.80)$$

which corresponds to a unitary representation only if $s = 0$, i.e. \mathcal{P} must be a chiral primary. In other words, the chiral superconformal primaries must have $s = 0$.

- There are four cases to consider at level one: $(q+1, \bar{P}_{s-1})$, $(q+1, P_s)$, $(q-1, P_{s-1})$, $(q-1, \bar{P}_s)$, corresponding to $\mathcal{P}_{i_1 \dots i_s} = \bar{\Sigma}_{i_1}^{\dot{\alpha}\alpha} Q_\alpha^+ \mathcal{O}_{\dot{\alpha}i_2 \dots i_s}$, $\mathcal{P}_{i_1 \dots i_s} = \epsilon^{\alpha\beta} Q_\alpha^+ \mathcal{O}_{\beta i_1 \dots i_s}$, $\mathcal{P}_{i_1 \dots i_s} = \bar{\Sigma}_{i_1}^{\dot{\alpha}\alpha} Q_\alpha^- \mathcal{O}_{\alpha i_2 \dots i_s}$, $\mathcal{P}_{i_1 \dots i_s} = \epsilon^{\dot{\alpha}\dot{\beta}} Q_{\dot{\alpha}}^- \mathcal{O}_{\dot{\beta} i_1 \dots i_s}$ respectively, where in the first and third case

we also need to symmetrize with respect to the extra vector index. For the first case, $\lambda_1 = \lambda_2$ implies

$$\Delta = \frac{d-1}{2}q + s - 1 + \frac{d}{2}, \quad (3.81)$$

which is precisely the unitarity bound (3.39) for \bar{P}_{s-1} . The first case is therefore allowed only if the superconformal multiplet of \mathcal{O} contains the non-trivial null states $Q_\alpha^+ \mathcal{P}$. We call a null state trivial if it can be seen to vanish without resorting to the computation of its norm. For example, $Q_1^+ Q_1^+ \mathcal{O}$ is a trivial null state. The shortening condition (3.81) translates into

$$\Delta_{\mathcal{P}} = \frac{d-1}{2}q_{\mathcal{P}} + s, \quad s > 0, \quad (3.82)$$

and thus can be thought of as a natural extension of (3.80) to $s > 0$. The remaining three cases all lead to non-trivial linear relations between Δ , q and s , but none of these relations corresponds to the appearance of a non-trivial null-state. Therefore, they all lead to a contradiction since we know that $Q_\alpha^+ \mathcal{P}$ must be non-trivial null states, since if they were trivial null-states, the condition $\lambda_1 = \lambda_2$ would itself be trivial.

- We simply state the results for level two. The only case not leading to the type of contradiction we saw for the three disallowed cases at level one is $(q+2, S_s)$, i.e. $\mathcal{P}_{i_1 \dots i_s} = \epsilon^{\alpha\beta} Q_\alpha^+ Q_\beta^+ \mathcal{O}_{i_1 \dots i_s}$, which can be easily seen to always satisfy $Q_\alpha^+ \mathcal{P} = 0$ without the need for a shortening condition on \mathcal{O} . There are then two allowed types of unitary representations. Either \mathcal{O} is antichiral, i.e. $s = 0$ and $\Delta = -\frac{d-1}{2}q$, leading to

$$\Delta_{\mathcal{P}} = -\frac{d-1}{2}q_{\mathcal{P}} + d, \quad (3.83)$$

or \mathcal{O} is generic, satisfying (3.35) (including $s = 0$), which leads to

$$\Delta_{\mathcal{P}} \geq \left| \frac{d-1}{2}q_{\mathcal{P}} - d + 1 \right| + s + d - 1. \quad (3.84)$$

We must also remember that for $s = 0$, the superconformal primary must satisfy the unitarity bound $\Delta \geq \frac{d-2}{2}$.

- Of the four cases at level three, the condition $\lambda_1 = \lambda_2$ does not lead to an immediate contradiction only for $(q+1, \bar{P}_{s-1})$. Similarly to what happens at level one, $\lambda_1 = \lambda_2$ in this case implies a consistent shortening condition. The novelty here is that this shortening also kills the state \mathcal{P} , and thus there are no consistent possibilities at level three.

- There is only one conformal primary at level four, but $\lambda_1 = \lambda_2$ does not lead to a consistent shortening condition on \mathcal{O} , so the primary at level four can not appear in the chiral OPE.

Essentially identical results were derived in [20, 96] for $d = 4$, $\mathcal{N} = 1$ in the context of the OPE of a chiral operator Φ with itself. The new feature of the generalization to $d < 4$ is the appearance of the level-two descendant of an antichiral primary (3.83). From R-charge conservation we have $\frac{d-1}{2}q_{\mathcal{P}} = 2\Delta_{\Phi}$ which, combined with the unitarity bound $\Delta \geq \frac{d-2}{2}$ for the operator \mathcal{O} , implies that the antichiral case can only be included if

$$\Delta_{\Phi} \leq \frac{d}{4}. \quad (3.85)$$

Thus in $d = 4$, the antichiral case can only appear when Φ is the scalar component of a free chiral superfield, where we know it does not appear since there is no coupling between Φ and any other fields. However, in $d < 4$, there is a finite window for Δ_{Φ} where the level-two descendant of an antichiral primary can make a contribution, and we will see it plays a crucial role in the Wess-Zumino model, since its appearance corresponds to the Yukawa coupling.

It follows from the above discussion that only one kind of allowed conformal primary \mathcal{P} from the same superconformal multiplet can appear in the $\phi_1 \times \phi_3$ OPE, and therefore the superconformal blocks coincide with the usual conformal blocks. Supersymmetry plays a role in this channel only through constraints on the spectrum of conformal primaries that can appear in the OPE.

3.4 Intermezzo: review of the Wess-Zumino model

In this section, we remind the reader of some basic facts about the massless Wess-Zumino model in $d \leq 4$ [97]. A nice review on the subject can be found in [98]. The model consists of the theory of a single chiral superfield Υ with cubic superpotential $W(\Upsilon) = \frac{1}{3}\lambda\Upsilon^3$. Equivalently, this is a theory of a complex boson and fermion with the Lagrangian

$$\mathcal{L}_{\text{WZ}} = \partial_{\mu}\bar{\phi}\partial^{\mu}\phi + i\bar{\psi}\gamma^{\mu}\partial_{\mu}\psi + |\lambda|^2|\phi|^4 + (\lambda\phi\psi_{\alpha}\epsilon^{\alpha\beta}\psi_{\beta} + c.c.). \quad (3.86)$$

The classical dimension of the coupling λ is $\frac{\epsilon}{2}$, with $\epsilon \equiv 4 - d$, and it is convenient to define the dimensionless coupling $\tilde{\lambda} = \mu^{-\epsilon/2}\lambda$, where μ is the renormalization scale.

Supersymmetry implies that the superpotential is not renormalized. Therefore the β -function of $\tilde{\lambda}$ is determined by the anomalous dimension of the chiral field Φ , which is the lowest component of the superfield Υ

$$\beta_{\tilde{\lambda}} = \tilde{\lambda} \left[-\frac{\epsilon}{2} + 3\gamma_{\Phi}(\tilde{\lambda}) \right], \quad (3.87)$$

where $\gamma_{\Phi} = -\frac{1}{2} \frac{d \log Z}{d \log \mu}$ and the factor of 3 comes from the fact that $W(\Upsilon)$ is cubic. Since we know from perturbation theory and unitarity that $\gamma_{\Phi}(\tilde{\lambda}) > 0$ for $\tilde{\lambda} \ll 1$, we expect that for sufficiently small ϵ , the theory has an interacting IR fixed point with unbroken supersymmetry at a coupling $\tilde{\lambda}^* > 0$. This CFT is what we refer to as the critical WZ model (cWZ). The exact relation (3.87) implies that at the fixed point the anomalous dimension is

$$\gamma_{\Phi}(\tilde{\lambda}^*) = \frac{4-d}{6}, \quad (3.88)$$

and hence

$$\Delta_{\Phi} = \frac{d-2}{2} + \gamma_{\Phi}(\tilde{\lambda}^*) = \frac{d-1}{3}. \quad (3.89)$$

This formula can also be deduced from the exact superconformal relationship between scaling dimension and R-charge of a chiral field $\Delta = \frac{d-1}{2}q$, since the R-charge of the superpotential is $q_W = 2$ and thus $q_{\Phi} = 2/3$.

An equivalent way to state the result in (3.89) is that the ϵ -expansion of the critical exponent $\eta \equiv 2\Delta_{\Phi} - (d-2)$ is exact at the leading order

$$\eta = 2\gamma_{\Phi}(\tilde{y}^*) = \frac{\epsilon}{3}. \quad (3.90)$$

The critical exponent ν , characterizing the divergence of the correlation length as the temperature approaches the critical temperature, is related to the scaling dimension of the lowest uncharged scalar, $[\bar{\Phi}\Phi]$, as follows

$$\nu^{-1} = d - \Delta_{[\bar{\Phi}\Phi]}. \quad (3.91)$$

It is not protected by supersymmetry and has been computed at one loop in the ϵ -expansion [79, 80]

$$\nu = \frac{1}{2} + \frac{\epsilon}{4} + \mathcal{O}(\epsilon^2), \quad (3.92)$$

leading to

$$\Delta_{[\bar{\Phi}\Phi]} = 2 + \mathcal{O}(\epsilon^2). \quad (3.93)$$

The critical exponent ω , characterizing the approach to scaling, is related to the scaling dimension of the lowest irrelevant scalar operator, \mathcal{O} , as

$$\omega = \Delta_{\mathcal{O}} - d. \quad (3.94)$$

It is reasonable to expect that \mathcal{O} is the supersymmetric descendant of $[\bar{\Phi}\Phi]$ obtained by acting on $[\bar{\Phi}\Phi]$ with four Q supercharges. This leads to $\Delta_{\mathcal{O}} = \Delta_{[\bar{\Phi}\Phi]} + 2$, implying the exact relation

$$\omega = 2 - \nu^{-1}. \quad (3.95)$$

Finally, let us note that the equation of motion for Υ can be written in superspace language as

$$D_{\alpha}D^{\alpha}\bar{\Upsilon} = \partial_{\Upsilon}W(\Upsilon), \quad (3.96)$$

where D_{α} is the superspace derivative corresponding to the action of the supercharge Q_{α}^{+} that annihilates the chiral superfield Υ . This implies that the chiral ring of the fixed-point theory has the relation

$$\Phi^2 = 0. \quad (3.97)$$

In the language of the CFT data, this means that the OPE $\Phi \times \Phi$ does not contain a chiral primary. From the results of Section 3.3.4 we can conclude that all operators that appear in the OPE are then exact under Q_{α}^{+} .

There is another piece of data available about the cWZ model in $d = 3$ that we will seek to match with the bootstrap results, namely the coefficient of the two-point function of the stress tensor, denoted by C_T . In SCFTs with four supercharges, the two-point function of the stress tensor is proportional to the two-point function of the R-current τ_{RR} . In [99], it was shown how τ_{RR} can be computed for $d = 3$, $\mathcal{N} = 2$ SCFTs from the squashed-sphere partition function $F(b)$

$$\tau_{RR} = \frac{2}{\pi^2} \text{Re} \left. \frac{\partial^2 F(b)}{\partial b^2} \right|_{b=1}, \quad (3.98)$$

where b is the squashing parameter, $b = 1$ corresponding to the round sphere. A formula for the squashed-sphere partition function of $d = 3$, $\mathcal{N} = 2$ theories was found using localization in [100]. Denoting by $\tau_{RR}^{(\text{free})}$ the two-point function of the R-current in the theory of a single free chiral multiplet, it was found in [78] that²

$$\frac{C_T}{C_T^{(\text{free})}} = \frac{\tau_{RR}}{\tau_{RR}^{(\text{free})}} \simeq 0.7268. \quad (3.99)$$

We will comment further on this ratio in Section 3.6.

²We are grateful to Simone Giombi, Igor Klebanov, and Silviu Pufu for bringing this result to our attention.

3.5 Bootstrap setup

In this section, we review the derivation of a set of crossing symmetry equations which we later solve numerically. The results of the previous sections suggest that the structure of these “bootstrap equations” should be very similar to those that were studied in the case of $d = 4$, $\mathcal{N} = 1$ SCFTs in [18–20, 96], and indeed this is what we find.

We are interested in the crossing symmetry constraints for the four-point function $\langle \Phi \bar{\Phi} \Phi \bar{\Phi} \rangle$, where Φ is a chiral operator with dimension Δ_Φ and $\bar{\Phi}$ is its charge conjugate. The chirality condition imposes that the R-charge is given by $q_\Phi = \frac{2}{d-1} \Delta_\Phi = \frac{2}{d-1} \Delta_{\bar{\Phi}} = -q_{\bar{\Phi}}$. Conformal symmetry fixes the four point function to take the form

$$\langle \Phi(x_1) \bar{\Phi}(x_2) \Phi(x_3) \bar{\Phi}(x_4) \rangle \equiv \frac{g(u, v)}{|x_{12}|^{2\Delta_\Phi} |x_{34}|^{2\Delta_\Phi}}, \quad (3.100)$$

where the cross-ratios u, v are defined in (3.60). Let us ignore supersymmetry for the moment but still insist on the presence of a $U(1)$ global symmetry under which Φ and $\bar{\Phi}$ have opposite charges. The OPE leads to a decomposition of $g(u, v)$ in terms of conformal blocks $G_{\Delta, s}(u, v)$. For instance, in the (12) channel we take $x_1 \rightarrow x_2$, and get

$$g(u, v) = \sum_{\mathcal{O}} (-1)^s |c_{\Phi \bar{\Phi}}^{\mathcal{O}}|^2 G_{\Delta, s}(u, v). \quad (3.101)$$

Recall that we are using the normalization (3.65). Equality of the OPEs in the three channels leads to the constraints

$$v^{\Delta_\Phi} \sum_{\mathcal{O}} (-1)^s |c_{\Phi \bar{\Phi}}^{\mathcal{O}}|^2 G_{\Delta, s}(u, v) = u^{\Delta_\Phi} \sum_{\mathcal{O}} (-1)^s |c_{\Phi \bar{\Phi}}^{\mathcal{O}}|^2 G_{\Delta, s}(v, u), \quad (12) = (14), \quad (3.102)$$

$$v^{\Delta_\Phi} \sum_{\mathcal{O}} |c_{\Phi \bar{\Phi}}^{\mathcal{O}}|^2 G_{\Delta, s}(u, v) = u^{\Delta_\Phi} \sum_{\mathcal{P}} |c_{\Phi \Phi}^{\mathcal{P}}|^2 G_{\Delta, s}(v, u), \quad (12) = (13), \quad (3.103)$$

where \mathcal{O}, \mathcal{P} are conformal primaries appearing in the $\Phi \times \bar{\Phi}$, and $\Phi \times \Phi$ OPE, respectively. Symmetrizing and antisymmetrizing equation (3.103) with respect to $u \leftrightarrow v$ allows us to write the equations in (3.102), (3.103) as the system

$$\sum_{\mathcal{O}^+} |c_{\Phi \bar{\Phi}}^{\mathcal{O}^+}|^2 \begin{pmatrix} F_{\Delta, s}^{\Delta_\Phi} \\ F_{\Delta, s}^{\Delta_\Phi} \\ H_{\Delta, s}^{\Delta_\Phi} \end{pmatrix} + \sum_{\mathcal{O}^-} |c_{\Phi \bar{\Phi}}^{\mathcal{O}^-}|^2 \begin{pmatrix} F_{\Delta, s}^{\Delta_\Phi} \\ -F_{\Delta, s}^{\Delta_\Phi} \\ -H_{\Delta, s}^{\Delta_\Phi} \end{pmatrix} + \sum_{\mathcal{P}} |c_{\Phi \Phi}^{\mathcal{P}}|^2 \begin{pmatrix} 0 \\ F_{\Delta, s}^{\Delta_\Phi} \\ -H_{\Delta, s}^{\Delta_\Phi} \end{pmatrix} = 0. \quad (3.104)$$

The first/second sum in (3.104) runs over uncharged conformal primaries with even/odd spin respectively. The third term in (3.104) is a sum over conformal primaries of charge $2q_\Phi$ and contains even spins only. The functions F, H in (3.104) are defined as

$$\begin{aligned} F_{\Delta,s}^{\Delta_\Phi} &\equiv (-1)^s [v^{\Delta_\Phi} G_{\Delta,s}(u, v) - u^{\Delta_\Phi} G_{\Delta,s}(v, u)] , \\ H_{\Delta,s}^{\Delta_\Phi} &\equiv (-1)^s [v^{\Delta_\Phi} G_{\Delta,s}(u, v) + u^{\Delta_\Phi} G_{\Delta,s}(v, u)] . \end{aligned} \quad (3.105)$$

Including the effects of supersymmetry simply means replacing conformal blocks by the superconformal blocks appropriate for each channel, and taking into account superconformal unitarity bounds. As we showed in Section 3.3, the superconformal blocks in the $\Phi\bar{\Phi}$ channel are linear combinations of four non-supersymmetric conformal blocks, while in the $\Phi\Phi$ channel, at most one conformal primary from a superconformal multiplet can appear, meaning that superconformal blocks are equal to non-supersymmetric conformal blocks. Equations (3.66), (3.67) with $\Delta_{12} = \Delta_{34} = 0$, lead us to define

$$\begin{aligned} \mathcal{F}_{\Delta,s}^{\Delta_\Phi} &\equiv F_{\Delta,s}^{\Delta_\Phi} + c_1 F_{\Delta+1,s+1}^{\Delta_\Phi} + c_2 F_{\Delta+1,s-1}^{\Delta_\Phi} + c_3 F_{\Delta+2,s}^{\Delta_\Phi} , \\ \tilde{\mathcal{F}}_{\Delta,s}^{\Delta_\Phi} &\equiv (-1)^s (F_{\Delta,s}^{\Delta_\Phi} - c_1 F_{\Delta+1,s+1}^{\Delta_\Phi} - c_2 F_{\Delta+1,s-1}^{\Delta_\Phi} + c_3 F_{\Delta+2,s}^{\Delta_\Phi}) , \\ \tilde{\mathcal{H}}_{\Delta,s}^{\Delta_\Phi} &\equiv (-1)^s (H_{\Delta,s}^{\Delta_\Phi} - c_1 H_{\Delta+1,s+1}^{\Delta_\Phi} - c_2 H_{\Delta+1,s-1}^{\Delta_\Phi} + c_3 H_{\Delta+2,s}^{\Delta_\Phi}) , \end{aligned} \quad (3.106)$$

where

$$c_1 \equiv -a_1|_{\Delta_{12}=\Delta_{34}=0}, \quad c_2 \equiv -a_2|_{\Delta_{12}=\Delta_{34}=0}, \quad c_3 \equiv a_3|_{\Delta_{12}=\Delta_{34}=0}, \quad (3.107)$$

and the a_i were defined in (3.67). The supersymmetric version of equation (3.104) then reads

$$\sum_{\mathcal{O}^+} |c_{\Phi\bar{\Phi}}^{\mathcal{O}^+}|^2 \begin{pmatrix} \mathcal{F}_{\Delta,s}^{\Delta_\Phi} \\ \tilde{\mathcal{F}}_{\Delta,s}^{\Delta_\Phi} \\ \tilde{\mathcal{H}}_{\Delta,s}^{\Delta_\Phi} \end{pmatrix} + \sum_{\mathcal{O}^-} |c_{\Phi\bar{\Phi}}^{\mathcal{O}^-}|^2 \begin{pmatrix} \mathcal{F}_{\Delta,s}^{\Delta_\Phi} \\ \tilde{\mathcal{F}}_{\Delta,s}^{\Delta_\Phi} \\ \tilde{\mathcal{H}}_{\Delta,s}^{\Delta_\Phi} \end{pmatrix} + \sum_{\mathcal{P}} |c_{\Phi\Phi}^{\mathcal{P}}|^2 \begin{pmatrix} 0 \\ F_{\Delta,s}^{\Delta_\Phi} \\ -H_{\Delta,s}^{\Delta_\Phi} \end{pmatrix} = 0, \quad (3.108)$$

The first two sums run over superconformal primaries of vanishing R-charge and even/odd spin respectively, while the third sum runs over conformal primaries of R-charge $q_{\mathcal{P}} = 2q_\Phi = \frac{4}{d-1}\Delta_\Phi$. All terms in the sums are constrained by superconformal unitarity bounds, and the third sum also by $[Q_\alpha^+, \mathcal{P}] = 0$, as analyzed in Section 3.3.4. We can summarize the constraints on the spectrum as follows

$$\mathcal{O}^+ : \quad \Delta = 0, \Delta \geq s + d - 2, \quad s = 0, 2, 4, \dots, \quad (3.109a)$$

$$\mathcal{O}^- : \quad \Delta \geq s + d - 2, \quad s = 1, 3, 5, \dots, \quad (3.109b)$$

$$\mathcal{P} : \quad \begin{cases} \Delta = 2\Delta_\Phi + s, & s = 0, 2, \dots, \\ \Delta = d - 2\Delta_\Phi, & s = 0, \quad \Delta_\Phi \leq d/4, \\ \Delta \geq |2\Delta_\Phi - (d-1)| + s + (d-1), & s = 0, 2, \dots \end{cases} \quad (3.109c)$$

Equations (3.108), together with the spectrum specifications (3.109), constitute a *linear program* for the various OPE coefficients squared. Solving this kind of problem is the basis of the numerical (conformal) bootstrap program, and the procedure has by now been described extensively in the literature. Here, we shall provide a very brief description of how such a problem can be solved, and refer the reader to [5, 33] for further details.

The first step is to reduce the continuously infinite functional equations to some finite set of constraints. The usual bootstrap procedure is to Taylor expand to some given order in the two cross-ratios u and v (or an alternative coordinate system). The number of derivative components is most conveniently labeled by a parameter n_{\max} , in terms of which the total number of constraints is $\frac{1}{2}(n_{\max} + 1)(n_{\max} + 2)$. Standard algorithms, such as Dantzig's simplex method, can then be used to try to obtain a set of OPE coefficients which solve the equations. This may or may not be possible, depending on the set of operators that we allow in the crossing equations. In particular, to derive bounds, one imposes constraints on the sets of operators allowed in the sum rule (3.108) until a solution can no longer be found. Typically, this constraint is a gap in the set of uncharged scalar operators, so that if a solution cannot be found for a given n_{\max} , then it is ruled out definitively. Increasing the parameter n_{\max} can then only lead to tighter bounds. In this work, our calculations were done using a modification of a Python-based arbitrary precision³ simplex method solver for semi-infinite linear programs [5]. The package [33] was also used as a cross-check on some results.

3.6 Bootstrap results

Having developed the technology to analyze crossing symmetry for SCFTs with four Poincaré supercharges in various dimensions, we now apply it to study and constrain the space of allowed theories. Theories with only four Poincaré supercharges do not exist in $d > 4$ and, while the status of SCFTs (and CFTs) in $d < 2$ is certainly an interesting question, for this study, we choose to restrict ourselves to $2 \leq d \leq 4$.

Since we made no use of parity invariance in our derivation of superconformal blocks and crossing relations, our bounds also apply to unitary theories which do not preserve parity, such as $\mathcal{N} = 2$ superconformal Chern-Simons-matter theories in $d = 3$.

Unless otherwise specified, all the plots shown in this section were made using $n_{\max} = 6$

³In the implementation used in this chapter arbitrary-precision arithmetic was used only for matrix inversion as lower precision generation of conformal blocks proved sufficient at the values of n_{\max} presented here.

which gives 84 constraints (28 terms in the Taylor expansion of the three-vector identity in (3.108)).

3.6.1 Scalar operator bounds

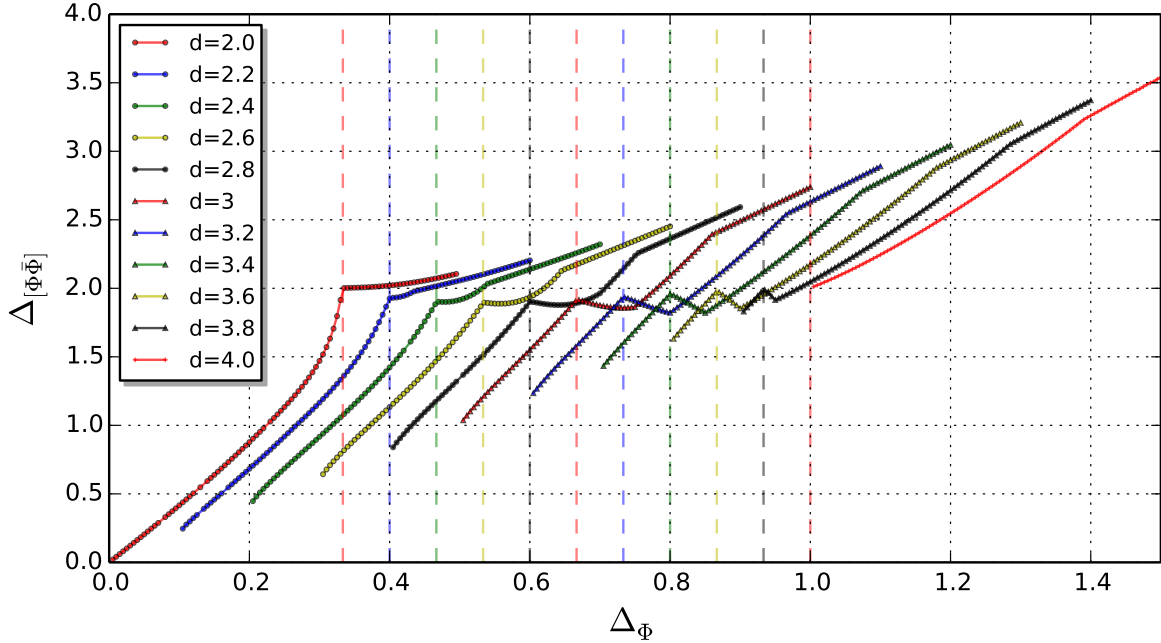


Figure 3.1: Upper bound on the lowest-dimension neutral scalar operator, $[\Phi\bar{\Phi}]$, appearing in the $\Phi \times \bar{\Phi}$ OPE. The dashed vertical lines correspond to $\Delta_\Phi = \frac{d-1}{3}$, the protected dimension of Φ in the cWZ model in dimension d . The value of d associated to a line is indicated by its color, which matches the corresponding bound plot.

We begin our numerical exploration by determining bounds on the scaling dimension of the first scalar operator in the $\Phi \times \bar{\Phi}$ OPE as a function of Δ_Φ . This corresponds to the lowest dimension scalar in the \mathcal{O}^+ channel in equation (3.108). Throughout this section, we will refer to this operator schematically as $[\Phi\bar{\Phi}]$, following the weak-coupling intuition of it being the composite operator of Φ and $\bar{\Phi}$. Bounds in various dimensions, $d = 2, \dots, 4$,

are shown in Figures 3.1 and 3.2 for a range of conformal dimensions $\Delta_0 \leq \Delta_\Phi \leq \Delta_0 + \frac{1}{2}$ (with $\Delta_0 = \frac{d-2}{2}$ the conformal dimension of a free scalar in dimension d).

Figures 3.1 and 3.2 exhibit a variety of interesting features.

1. A clear kink at $\Delta_\Phi = \frac{d-1}{3}$ where we conjecture that the bound is saturated by the d -dimensional critical Wess-Zumino model with a cubic superpotential.
2. A second kink located at $\Delta_\Phi = \frac{d}{4}$ that is very sharp for $3 \leq d \leq 4$, but seems to soften, and may no longer exist, for $d < 3$.
3. A third kink at some value of $\Delta_\Phi > \frac{d}{4}$. In $d = 3$ the value is $\Delta_\Phi \approx 0.86$. In $d = 4$ this feature appears at $\Delta_\Phi \approx 1.38$ and is likely the same feature first observed in [20].

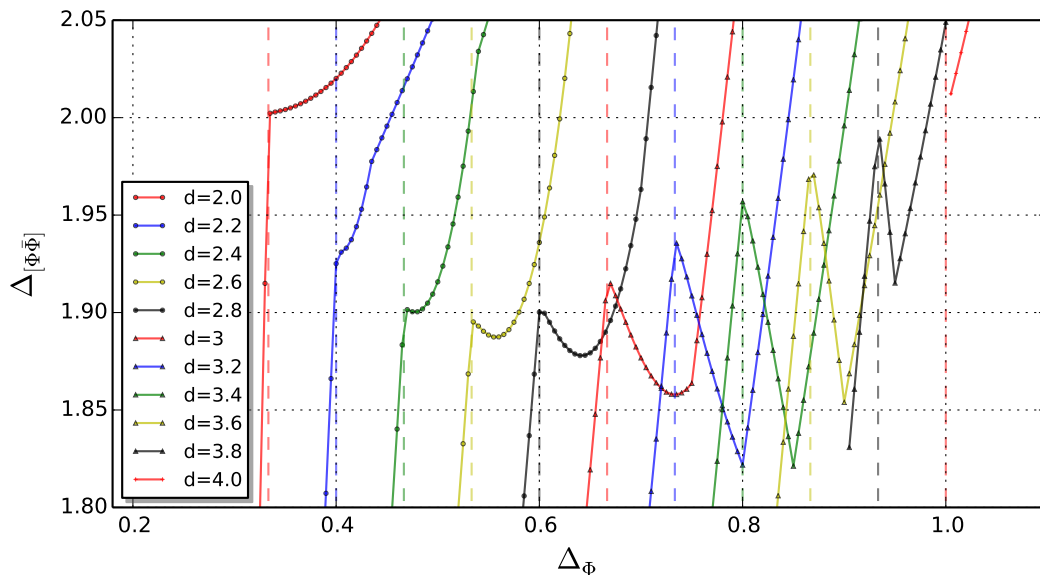


Figure 3.2: A close-up of the bounds in Figure 3.1. Note that the first kink in every dimension corresponds to $\Delta_\Phi = \frac{d-1}{3}$ (the locations of the vertical lines).

The location of the second feature described above, $\Delta_\Phi = \frac{d}{4}$, coincides with a kinematically special point. This is the value of Δ_Φ where the scalar operator \mathcal{P} in the $\Phi \times \Phi$ OPE with dimension $d - 2\Delta_\Phi$ is a superdescendant of a superconformal primary which hits the unitarity bound (see (3.109) and the discussion around (3.85)). The third kink, however, does not seem to correspond to any kinematically special point. We will discuss these two features in more detail in Section 3.6.5.

3.6.2 OPE and central charge

In addition to placing bounds on operator dimensions, the numerical bootstrap allows us to extract the spectrum and OPE coefficients associated with the “extremal” solution that saturates these bounds [23]. In particular, we can use this procedure to deduce $|c_{\Phi\bar{\Phi}T}|^2$, the squared OPE coefficient of the stress-tensor in the $\Phi \times \bar{\Phi}$ OPE, from which we can compute C_T (the canonical normalization of the stress-tensor two-point function) associated with the solutions lying along the bounding curves in Figure 3.1. In two dimensions, C_T reduces to $2c$, where c is the central charge of the left/right Virasoro algebra. In general dimension, C_T is not always related to a conformal anomaly, but we still refer to it as the central charge. In terms of the OPE coefficient in our normalization, equation (3.65), the central charge⁴ is

$$C_T = \frac{\Delta_\Phi^2}{|c_{\Phi\bar{\Phi}T}|^2} \left(\frac{d}{d-1} \right)^2. \quad (3.110)$$

In theories with four Poincaré supercharges, the stress-tensor is not a superconformal primary, but rather lies in the supermultiplet of the R-current, so what we actually read off with our approach is $|c_{\Phi\bar{\Phi}J}|^2$ with J a conserved spin-one superconformal primary (of dimension $\Delta_J = d-1$). From this, we extract the OPE coefficient of the spin-two descendant using (3.107). Note also that unlike in [63], here we are not maximizing the stress-tensor (or R-current) OPE coefficient, but rather simply extracting it from a particular solution, characterized by having a maximal allowed dimension of $[\Phi\bar{\Phi}]$.

In the normalization given above, a free boson has $C_T^{(b)} = \frac{d}{d-1}$ while a free Dirac fermion has $C_T^{(f)} = d$, so for a free chiral multiplet we have

$$C_T^{(\text{free})} = 2C_T^{(b)} + C_T^{(f)} = \frac{d(d+1)}{d-1}. \quad (3.111)$$

The values of $C_T^{(\text{free})}$ for $d = 2, \dots, 4$ are shown in Figures 3.3 and 3.4 as large crosses which, as expected, sit at the limiting value of C_T as Δ_Φ approaches the unitarity bound in dimension d .

The C_T plots share a lot of the structure of the $\Delta_{[\Phi\bar{\Phi}]}$ plots. We find local minima (that are global minima within the range of the plot) at $\Delta_\Phi = \frac{d-1}{3}$ corresponding to the exact dimension of the chiral field in the d -dimensional cWZ model. Moreover, a sharp spike

⁴We follow the normalization of [88], in particular equation (4.2) in that reference.

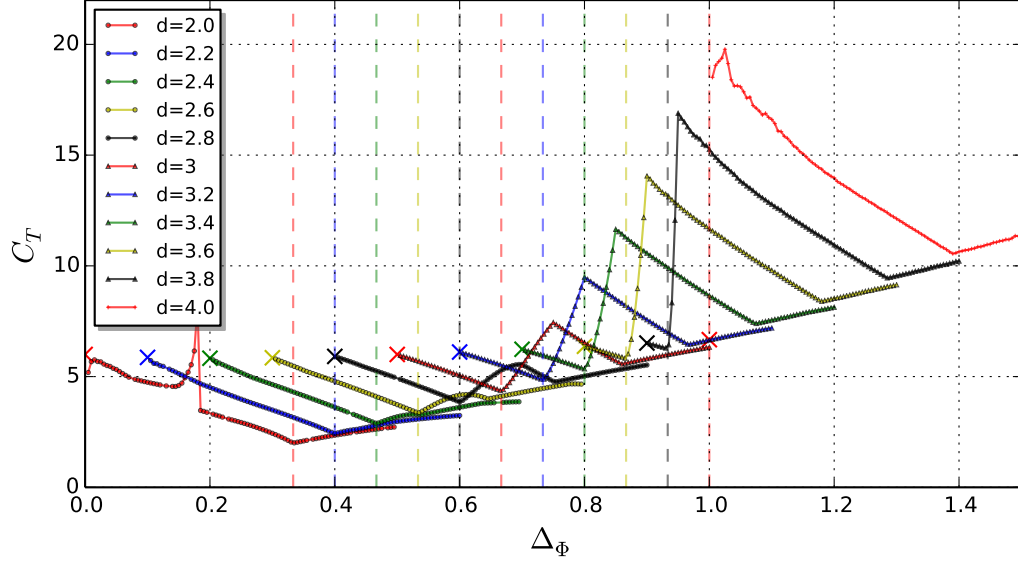


Figure 3.3: The central charge, C_T , of the boundary solution, i.e. when $\Delta_{[\Phi\bar{\Phi}]}$ saturates the bounds given in Figure 3.1. The crosses denote the value of C_T for a free chiral multiplet in dimension d . The dashed vertical lines lie at $\Delta_\Phi = \frac{d-1}{3}$, corresponding to the chiral primary field of the cWZ model in dimension d .

appears for $3 \leq d \leq 4$ at $\Delta_\Phi = \frac{d}{4}$. This spike is a local maximum of the C_T curve rather than a minimum. Once more, it is not clear if this last feature persists for $d < 3$. There is also a third feature: another local minimum at the value of Δ_Φ corresponding to the third kink in the bounds plot. This also implies a local C_T minimum in $d = 4$ for the kink at $\Delta_\Phi \approx 1.4$, as first observed in [20].

It is important to emphasize that the curves depicted in Figures 3.3 and 3.4 are *not* the result of maximizing the stress-tensor OPE and hence are not, in any strict sense, lower bounds on C_T . However, a preliminary comparison of $\Delta_{[\Phi\bar{\Phi}]}$ maximization and C_T minimization (analogous to the analysis in [63]) suggests that these two are equivalent, at least in the region $\Delta_\Phi \lesssim \frac{d-1}{3}$. A more thorough investigation of this question is left to future studies.

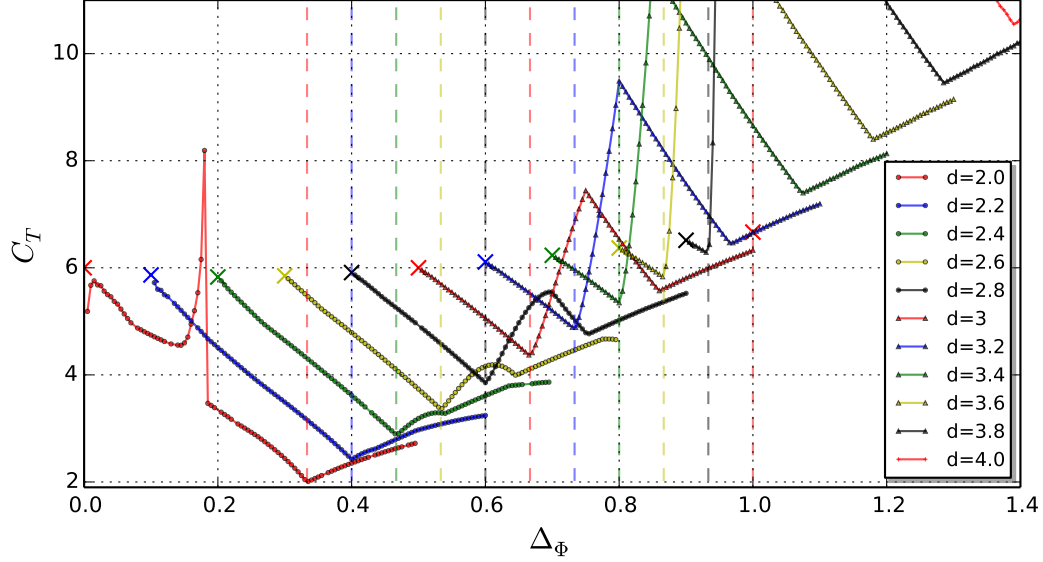


Figure 3.4: A close-up of the curves in Figure 3.3. The minimum in every dimension exactly corresponds to $\Delta_\Phi = \frac{d-1}{3}$ (the locations of the vertical lines). Note that C_T in $d = 2$ lies precisely at 2, corresponding to the known value $c = \bar{c} = 1$ of the lowest $\mathcal{N} = 2$ minimal model (see Section 3.6.3).

3.6.3 Two-dimensional $\mathcal{N} = 2$ minimal models

As there is a great deal known about two-dimensional superconformal minimal models, we can use them as a benchmark to compare various exactly known quantities with our numerical estimates. In Appendix 3.C, we summarize some of the salient features of these theories.

The $\mathcal{N} = 2$ minimal models are labeled by a positive integer k , which determines their central charge via

$$c = \frac{3k}{k+2}. \quad (3.112)$$

Superconformal primaries in these models are labeled by two integers $n = 0, \dots, k$ and $m = -n, -n+2, \dots, n$ with (holomorphic) dimension h and R-charge Ω

$$h_{n,m} = \frac{n(n+2) - m^2}{4(k+2)}, \quad \Omega = \frac{m}{(k+2)}. \quad (3.113)$$

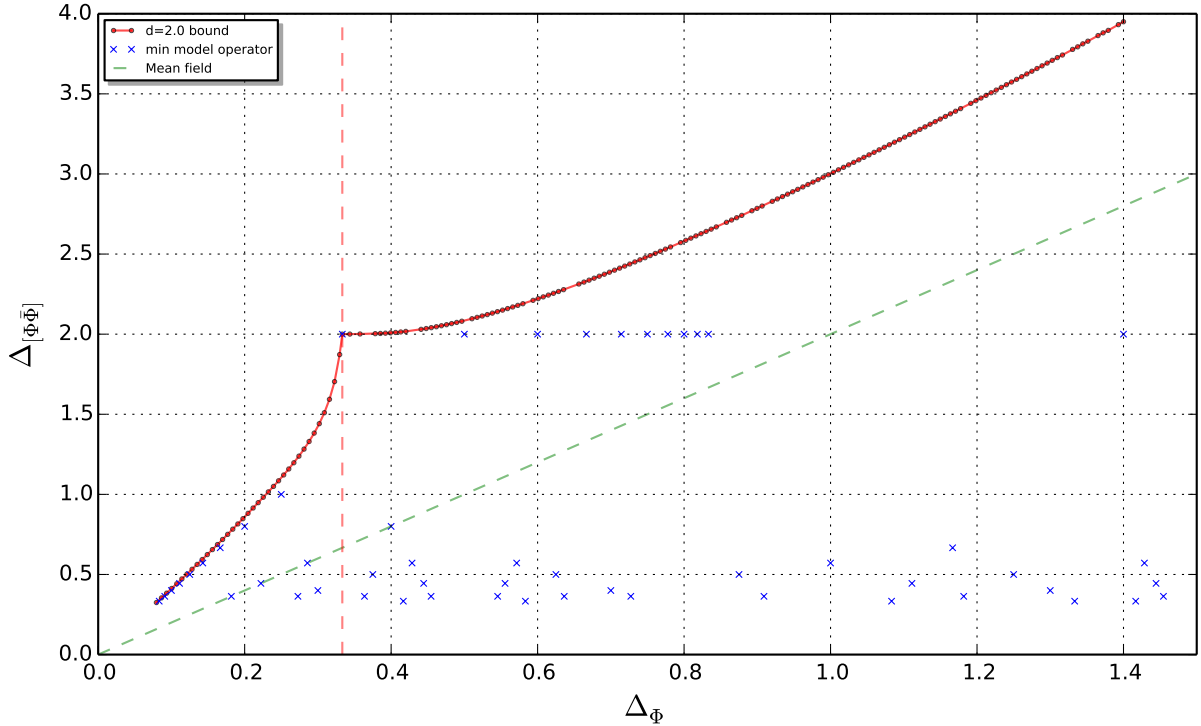


Figure 3.5: An extended view of the upper bound on $\Delta_{[\Phi\bar{\Phi}]}$ in $d = 2$ (with $n_{max} = 9$). The blue crosses mark the exact dimensions of operators from various superconformal minimal models. The cross at $(\frac{1}{3}, 2)$ corresponds to the super-Ising model (i.e. the $k = 1$ super-Virasoro minimal model). The dashed green line corresponds to $\Delta_{[\Phi\bar{\Phi}]} = 2\Delta_{\Phi}$, the expected value in mean field theory.

The chiral (antichiral) primaries have $m = \pm n$, respectively. In principle, one can apply the superconformal bootstrap to two-dimensional conformal theories with generic spectrum and only $(0, 2)$ supersymmetry. However, in our analysis, we have restricted to theories with $(2, 2)$ supersymmetry and a diagonal spectrum. Our conventions imply that $C_T = 2c$.

The model with $k = 1$ has $C_T = 2$ and two super-Virasoro primary operators of dimension $\Delta_{1,\pm 1} = \frac{1}{3}$ and R-charge $q = \pm \frac{2}{3}$ (and of course the identity $\Delta_{0,0} = 0$). The $\Phi_{1,1} \times \Phi_{1,-1}$ OPE contains only the super-Virasoro family of the identity, so that the first primary of the global superconformal algebra appearing after the identity is $\Omega_{-1}\bar{\Omega}_{-1}|0\rangle$, which has $\Delta = 2$. Indeed, this operator must appear in the OPE of any chiral primary and its conjugate in any local two-dimensional $\mathcal{N} = 2$ SCFT. This immediately allows us

to determine that all hypothetical CFTs saturating our bounds for $\Delta_\Phi \gtrsim 1/3$ cannot be local theories. It is possible that adding more constraints (i.e. derivatives in the crossing symmetry relations) will bring the bound down, but we know that at best, it can asymptote to the line $\Delta_{[\Phi\bar{\Phi}]} = 2\Delta_\Phi$, corresponding to a supersymmetric version of mean field theory (also known as generalized free field theory). Note that the latter indeed does not have a local stress tensor and hence does not benefit from the standard enhancement to the infinite conformal symmetry in $d = 2$.

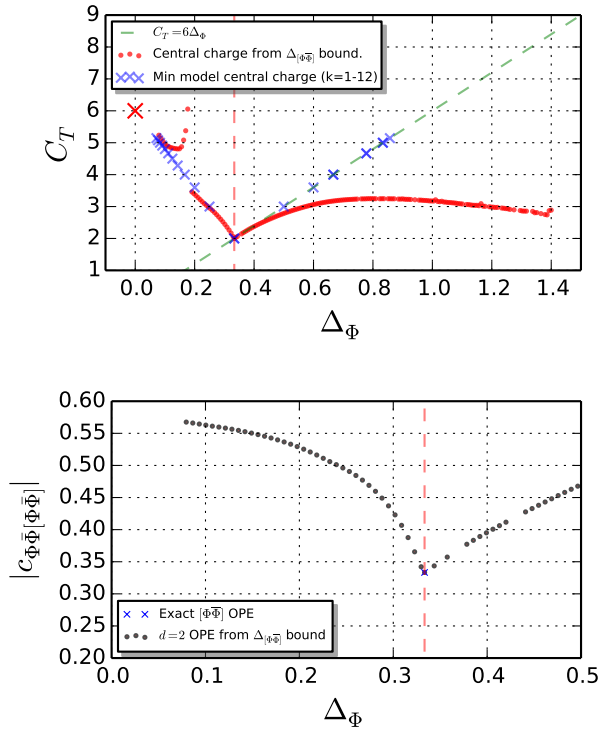


Figure 3.6: Central charges (*left*), and the OPE coefficient of $[\Phi\bar{\Phi}]$ (*right*), for $d = 2$, extracted from the boundary solution in Figure 3.5 . The blue crosses give the expected values of C_T for the first few super minimal-models ($k = 1, \dots, 11$). The dashed green line, $C_T = 6\Delta_\Phi$, is the unitarity bound discussed in Appendix 3.C. Both figures were made with $n_{max} = 9$.

In Figure 3.5, we focus our attention on the $d = 2$ bound and superimpose the dimensions of known minimal model operators. At $\Delta_\Phi = \frac{1}{3}$, we find that the bound is very close

to 2, suggesting that the $k = 1$ minimal model saturates our bound. This observation is further confirmed in the left panel of Figure 3.6, where we show that $C_T \approx 2$ at this point as expected. As a further check we plot, in the right panel of Figure 3.6, the absolute value⁵ of the OPE coefficient $|c_{\Phi\bar{\Phi}[\Phi\bar{\Phi}]}|$. There is clearly a cusp at $\Delta_\Phi = \frac{1}{3}$, $|c_{\Phi\bar{\Phi}[\Phi\bar{\Phi}]}| \approx \frac{1}{3}$, which is indeed the expected value for this OPE coefficient in the $k = 1$ model (see Appendix 3.C for a derivation). Let us emphasize once more that the OPE coefficients appearing in our figures are not computed by maximizing any OPE coefficient but rather are extracted from the solutions saturating the $\Delta_{[\Phi\bar{\Phi}]}$ bound (see [23]).

As mentioned above, $\Delta_\Phi = \frac{d-1}{3}$ is the expected dimension of the protected operator Φ of the cWZ model, which can be thought of as a super-symmetric generalization of the Ising model. The $k = 1$ model fits naturally into this role, being the simplest super-Virasoro minimal model. Moreover, it was shown in [101, 102] that precisely the minimal model with $k = 1$ arises from an $\mathcal{N} = 2$ Ginzburg-Landau theory with a cubic superpotential, i.e. the two-dimensional incarnation of the Wess-Zumino model.

To the left of $\Delta_\Phi = 1/3$, we see that the upper bound on $\Delta_{[\Phi\bar{\Phi}]}$ is very nearly saturated at points corresponding to $\Phi = \Phi_{1,1}$, $\bar{\Phi} = \Phi_{1,-1}$, $[\Phi\bar{\Phi}] = \Phi_{2,0}$ in the minimal models with $k \geq 2$, which lie at

$$\Delta_\Phi = \frac{1}{(k+2)}, \quad \Delta_{[\Phi\bar{\Phi}]} = \frac{4}{(k+2)}, \quad k \geq 2. \quad (3.114)$$

From the left panel in Figure 3.6 it seems, however, that for $\Delta_\Phi < 1/3$, the central charges extracted from the boundary solutions do not precisely match those of the $k > 1$ minimal models. This suggests that the latter do not exactly saturate our bound⁶ at the given constraint level, a phenomenon which has also been observed for the higher minimal models in the non-supersymmetric case. It may be that imposing further constraints, i.e. higher values of n_{max} , will improve the situation but, as this is not our focus here, we leave this question for future explorations.

The blue crosses in Figure 3.5 to the right of the super-Ising point $(1/3, 2)$ correspond to the fusion of $\Phi_{k,k}$, i.e. the chiral primary with the highest conformal dimension in the k -th minimal model, with its conjugate $\Phi_{k,-k}$. As noted above, in this case, $[\Phi\bar{\Phi}] = \Omega_{-1}\bar{\Omega}_{-1}|0\rangle$, and thus $\Delta_{[\Phi\bar{\Phi}]} = 2$. Our numerical bound does show a short plateau with $\Delta_{[\Phi\bar{\Phi}]} = 2$ just

⁵Since OPE coefficients only appear squared in the crossing symmetry relations we consider, we only have access to their magnitude, not their sign.

⁶The “extremal functional method” advocated in [23] requires a very precise determination of the maximal scalar gap in order to yield (generically) a unique solution. Moreover, if this maximal value is sufficiently far from the expected value of $\Delta_{[\Phi\bar{\Phi}]}$ in a particular theory, then the resulting spectrum might be quite different.

to the right of the super-Ising kink. These boundary solutions are ruled out however in a full-fledged $\mathcal{N} = 2$ SCFT with super-Virasoro symmetry. This can be seen by the virtue of the unitarity bound $C_T \geq 6\Delta_{\Phi_{\max}}$ (see Appendix 3.C), which is shown in the left panel of Figure 3.6 as the green dashed line. However, it is reassuring that C_T corresponding to the numerical solution of the crossing on the boundary asymptotes to $C_T = 6\Delta_{\Phi}$, and hence to the correct value in the minimal models.

3.6.4 Bootstrapping the cWZ model in $2 \leq d \leq 4$

In this section, we analyse in more detail the numerical bootstrap results at $\Delta_{\Phi} = \frac{d-1}{3}$ for $2 \leq d \leq 4$. As previously noted, this value of Δ_{Φ} is significant as it corresponds to the protected dimension of a chiral primary operator in the d -dimensional cWZ model. As the bounds for every $2 \leq d \leq 4$ in Figure 3.1 have a kink precisely at this value of Δ_{Φ} , we conjecture that the bounds are saturated by the operator $[\Phi\bar{\Phi}]$ in the d -dimensional cWZ theory.

As argued in [91], it is likely that theories in fractional dimension are non-unitary and may even suffer further pathologies. Nonetheless, they provide a useful interpolation between theories in integer dimension, allowing us to track critical exponents and other features as a function of the dimensions. This idea is similar in spirit to the ϵ -expansion. The literature on the cWZ model is rather sparse and very few critical exponents have been computed and only to leading order, see [79, 80, 83].

As discussed in Section 3.4, the dimension of $[\Phi\bar{\Phi}]$ in this theory has only been computed to the first order in the ϵ -expansion

$$\Delta_{[\Phi\bar{\Phi}]} = 2 - \epsilon + \frac{1}{\nu} = 2 + \mathcal{O}(\epsilon^2), \quad (3.115)$$

so we do not have precise estimates to compare with. Our numerical results for the maximal value of $\Delta_{[\Phi\bar{\Phi}]}$ at $\Delta_{\Phi} = (d-1)/3$ are presented in Figure 3.7. To give a better sense for this quantity, we plot both the anomalous dimension $\Delta_{[\Phi\bar{\Phi}]} - (d-2)$ against the anomalous dimension $\Delta_{\Phi} - \frac{d-2}{2}$, and the difference $\Delta_{[\Phi\bar{\Phi}]} - 2$ as a function of ϵ . The latter gives an estimate for the form of the unknown $\mathcal{O}(\epsilon^2)$ corrections in (3.115). We also plot, in Figure 3.8, the values of C_T at $\Delta_{\Phi} = (d-1)/3$, normalized with respect to C_T for a free chiral field. Recall, from Figure 3.4, that these correspond to local minima of C_T which we conjecture to correspond to the d -dimensional cWZ model.

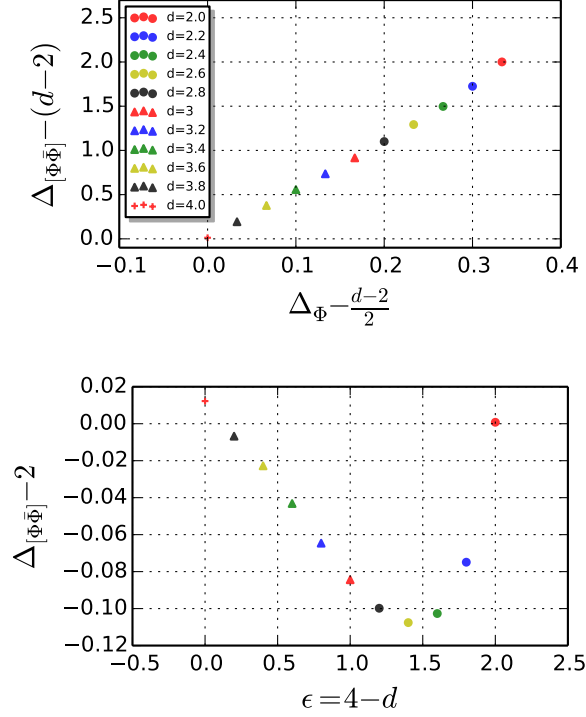


Figure 3.7: Predictions for the anomalous dimension of $[\Phi\bar{\Phi}]$ in the d -dimensional cWZ model. The ϵ -expansion for this operator dimension is known to linear order and gives $\Delta_{[\Phi\bar{\Phi}]} = 2 + \mathcal{O}(\epsilon^2)$ so on the RHS we show $\Delta_{[\Phi\bar{\Phi}]} - 2$ as a function of ϵ .

The location of the kink and the fact that it corresponds to the exact result, $\Delta_{[\Phi\bar{\Phi}]} = 2$, in $d = 2$ supports our claim that we are indeed studying the cWZ theory. Moreover, equation (3.115) is consistent with what we observe in Figure 3.2; namely that $\Delta_{[\Phi\bar{\Phi}]} \approx 2$ for $2 \leq d \leq 4$.

The strongest evidence for our conjecture comes, however, not from a critical exponent, but from the computation of C_T . As discussed in Section 3.4, it is possible to determine this quantity, in $d = 3$, by taking derivatives of the squashed-sphere partition function, a quantity that is exactly computable via localization. This computation yields $C_T/C_T^{(\text{free})} \simeq 0.7268$ while our best numerical estimate (in [3]) gives $0.72652(33)$, putting the exact value

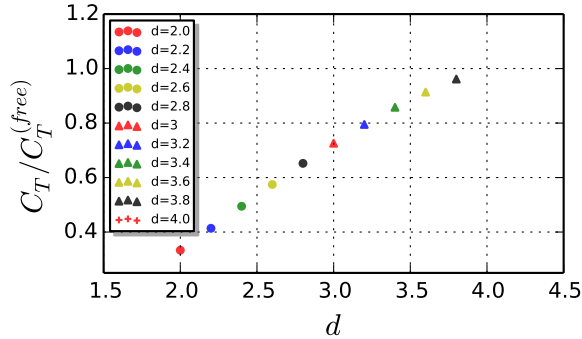


Figure 3.8: Our prediction for the central charge, C_T , of the cWZ model in d dimensions normalized by the value for a free chiral superfield, $C_T^{\text{free}} = \frac{d(d+1)}{d-1}$. This data is extracted from the solution which saturates the bounds given in Figure 3.1 at $\Delta_\Phi = \frac{d-1}{3}$. The exact value in $d = 3$ can be computed via localization to be $\simeq 0.7268$ while in this figure ($n_{max} = 6$) we find ~ 0.7260 (see [3] for a more precise determination).

just within our error bars. As noted in Section 3.6.2, we have checked (in $d = 3$) that for $\Delta_\Phi \lesssim 2/3$, the value of C_T extracted from the OPE coefficients of the solution maximizing $\Delta_{[\Phi\bar{\Phi}]}$ does, indeed, correspond to what one would get using C_T -minimization in the sense of [5] (i.e. it is the *minimal* value of C_T , as a function of Δ_Φ , consistent with unitarity and crossing symmetry under the very mild additional assumption of not having additional scalars of very low dimension). Since the exact value of C_T is close to saturating this lower bound (which will only increase as we increase n_{max}) one could conceivably turn this into a *proof* that the theory under consideration is necessarily the cWZ model.

Near $d = 4$, we expect that the ϵ -expansion should yield good numerical estimates so, as an additional test of our results, we would like to check the vanishing of the $\mathcal{O}(\epsilon)$ term in (3.115) by studying our bounds for small ϵ . In Figure 3.9, we show the $\Delta_{[\Phi\bar{\Phi}]}$ bounds, now computed for $d = 3.95 - 3.99$ in steps of 0.01. We expect that the low-order ϵ -expansion should yield reasonable results for these small values of $\epsilon \sim 0.01 - 0.05$. The first thing to note about the bounds is that we see (at this resolution) that the kink does not exactly coincide with $\Delta_\Phi = \frac{d-1}{3}$ but rather is very slightly to the right of that value. Although we know that the cWZ theory has an operator exactly at $\Delta_\Phi = \frac{d-1}{3}$, we also know our bounds are not optimal (as we are using a relatively small number of Taylor coefficients corresponding to $n_{max} = 6$), and the bound curve will move down as we increase the

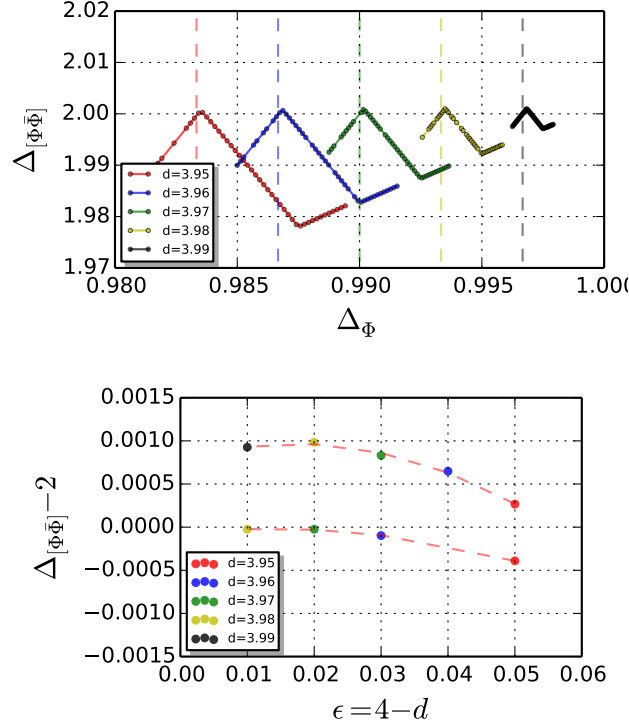


Figure 3.9: Bound plots for $[\Phi\bar{\Phi}]$ near $d = 4$ (left). On closer inspection, the kink in the bound plot is slightly to the right of $\Delta_\Phi = \frac{d-1}{3}$ (shown as dashed vertical lines). As explained in the text, we read off and plot (right) $\Delta_{[\Phi\bar{\Phi}]}$ at the bound both at the local maximum (top curve) and the value $\Delta_\Phi = \frac{d-1}{3}$ (bottom curve).

number of constraints. In fact, in [3] we show that, for $d = 3$, the minimum of the C_T curve does indeed correspond much more closely to $\Delta_\Phi = \frac{d-1}{3}$, and that as we add more derivatives, the kink in the $\Delta_{[\Phi\bar{\Phi}]}$ bound moves left towards $\Delta_\Phi = \frac{d-1}{3}$ and towards the minimum of the C_T plots.

We will nonetheless be conservative here and estimate the value of $\Delta_{[\Phi\bar{\Phi}]}$ using two different procedures and show that our results are relatively robust. In the first approach, we simply extract the value of the bound at $\Delta_\Phi = \frac{d-1}{3}$. The second approach is to read off the value of $\Delta_{[\Phi\bar{\Phi}]}$ at the local maximum in the left plot of Figure 3.9. In both cases, we find a quadratic fit for $\Delta_{[\Phi\bar{\Phi}]} - 2$ as a function of ϵ and read off the subleading terms in equation (3.115). The two fits are shown in the right plot in Figure 3.9 with the lower curve corresponding to the values at $\Delta_\Phi = \frac{d-1}{3}$.

The results for the two fits are:

$$\Delta_{[\Phi\bar{\Phi}]} - 2 = -0.283 \epsilon^2 + 7.76 \times 10^{-3} \epsilon + 7.17 \times 10^{-5}, \quad \Delta_{[\Phi\bar{\Phi}]} \text{ at } \Delta_{\Phi} = \frac{d-1}{3}, \quad (3.116)$$

$$\Delta_{[\Phi\bar{\Phi}]} - 2 = -0.648 \epsilon^2 + 22.3 \times 10^{-3} \epsilon + 77.4 \times 10^{-5}, \quad \Delta_{[\Phi\bar{\Phi}]} \text{ at local max}, \quad (3.117)$$

It is clear that the quadratic coefficient depends on how we choose to extract $\Delta_{[\Phi\bar{\Phi}]}$, meaning that our bounds have not converged sufficiently. What does seem rather robust however, is that the constant and linear pieces are orders of magnitude smaller than the quadratic piece, consistent with the ϵ -expansion prediction in equation (3.115).

3.6.5 Additional kinks

In every dimension in the range $2 \leq d \leq 4$, we clearly observe a kink at $\Delta_{\Phi} = \frac{d-1}{3}$ which, as explained above, very likely corresponds to the cWZ model. For $3 \leq d \leq 4$, there is also a very clear kink at $\Delta_{\phi} = \frac{d}{4}$, but it stops being sharp below $d = 3$. Moreover, for $2 \leq d \leq 4$, there is yet one more kink at some $\Delta_{\Phi} > \frac{d}{4}$ that is an extension of the $d = 4$ kink first observed in [20]. In this section, we initiate a very brief exploration of these two structures. We will refer to them as the second and third kink even though the former may not exist for $d < 3$, rendering the name “third kink” somewhat incorrect in those dimensions. Thus by “third kink”, we will always mean the feature located at $\Delta_{\Phi} > \frac{d}{4}$.

In Figure 3.10, we plot the dimension bound for $\Delta_{[\Phi\bar{\Phi}]}$ and the central charge extracted from Figure 3.1 at $\Delta_{\Phi} = \frac{d}{4}$. This kink is distinct from the first and third kink, and from various other crossing symmetry kinks that have appeared in the literature [5, 63], in two important ways. First, as is clear from Figure 3.3, it corresponds to a local *maximum* of the central charge rather than a minimum. This statement is not entirely accurate as Figure 3.3 is not a central charge bound plot, in the sense of [5], but rather the central charge corresponding to the saturating solution, which, *a priori*, may not minimize the central charge. Second, this kink occurs at a kinematically special point in terms of the constraints imposed by supersymmetry. Precisely at $\Delta_{\Phi} = \frac{d}{4}$, the two additional scalar operators allowed in the R-charged channel at dimensions $\Delta = d - 2\Delta_{\Phi}$ and $\Delta = 2\Delta_{\Phi}$ have equal dimensions, see (3.109). For this reason, one might suspect that the second kink is a kinematical feature of the boundary solution that may not correspond to any

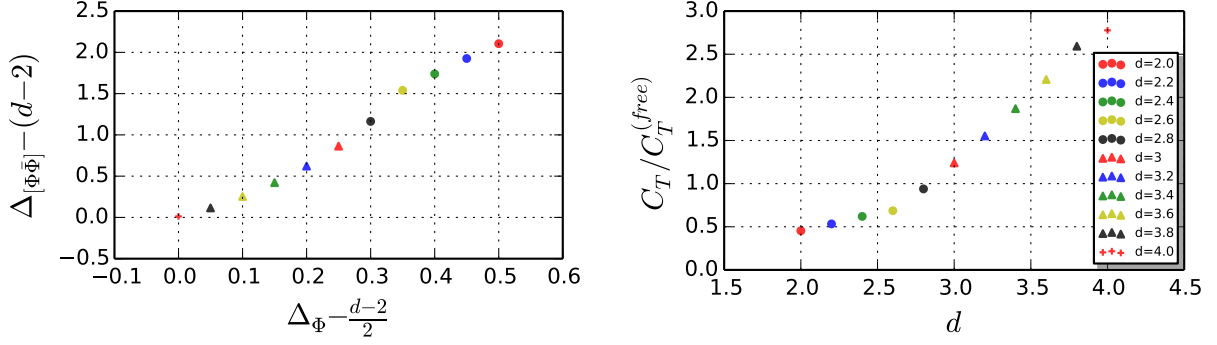


Figure 3.10: Second kink: the anomalous dimension of $\Delta_{[\Phi\bar{\Phi}]}$ vs that of Δ_Φ at $\Delta_\Phi = \frac{d}{4}$ for $2 \leq d \leq 4$ (left). The central charge, normalized by that of a free chiral superfield, at $\Delta_\Phi = \frac{d}{4}$ (right).

physically interesting theory. The fact that this structure does not continue below $d = 3$, whereas the coincidence of the two operator dimensions persists, might, however, suggest otherwise. Motivated by this possibility, in Section 3.6.5, we discuss some initial attempts to guess a physical theory corresponding to the second kink, and provide some guidance for others who would try their hand at this task.

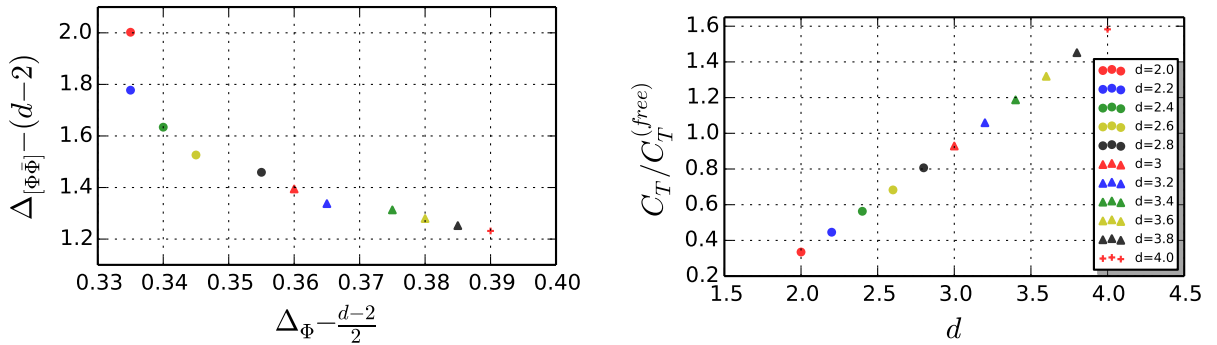


Figure 3.11: Third kink: the anomalous dimension of $\Delta_{[\Phi\bar{\Phi}]}$ vs that of Δ_Φ for the third kink (left); the central charge, normalized by that of a free chiral superfield, for the third kink (right).

The third kink is much more “traditional”, since it locally minimizes C_T and also appears at values of Δ_Φ which do not enjoy any known significance. As mentioned before, these kinks seem to be a continuation of the one first observed at $d = 4$ in [20]. The third kink merges with the first in $d = 2$, and thus becomes the $\mathcal{N} = 2$ minimal model with $k = 1$.

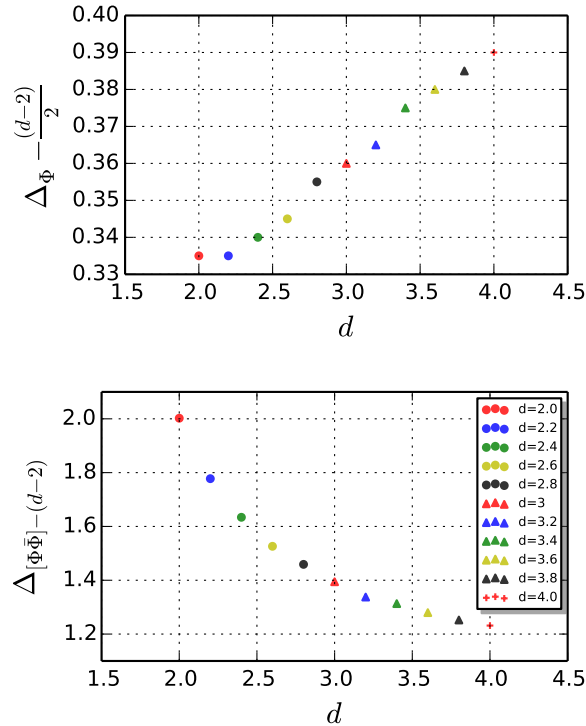


Figure 3.12: Third kink: the anomalous dimension of Δ_Φ as a function of d for the third kink (*left*); the anomalous dimension of $\Delta_{[\Phi\bar{\Phi}]}$ as a function of d for the third kink (*right*).

In Figure 3.11, we display the anomalous dimension of $\Delta_{[\Phi\bar{\Phi}]}$ as a function of the anomalous dimension of Δ_Φ , as well as the ratio C_T/C_T^{free} as a function of d , for the third kink. We determine the location of the kink by choosing the minimum of C_T (or equivalently the location of the kink in the $\Delta_{[\Phi\bar{\Phi}]}$ bound) up to the resolution of Figure 3.3, which is⁷ ~ 0.005 . For $d = 2$, we do not see any distinct kink and since already at $d = 2.2$, the

⁷As we have not conducted any systematic convergence estimate for our bounds, we do not make any claim that this resolution bounds the error in any way.

location of the kinks seems to be merging, we assume that for $d = 2$ the first and third kink coincide. To exhibit the structure of the third kink in more detail we also provide, in Figure 3.12, plots of the anomalous dimensions of Δ_Φ and $\Delta_{[\Phi\bar{\Phi}]}$ at the kink as a function of d .

Some speculations

In this section, we would like to offer some speculations about the nature of the second and third kinks.

The second kink is kinematically special, since here the two candidate scalar conformal primaries in the $\Phi \times \Phi$ OPE (Φ^2 , with dimension $2\Delta_\Phi$, and $Q^2\bar{\Psi}$, with dimension $d - 2\Delta_\Phi$) have equal dimensions, see (3.109). Between $\Delta_\Phi = (d - 1)/3$ and this point, the bound on $[\Phi\bar{\Phi}]$ is linearly decreasing, and an analysis of the $\Phi \times \Phi$ OPE coefficients shows that all along this line, the Φ^2 operator is not present, see Figure 3.13. At $\Delta_\Phi = d/4$, the chiral scalar field Ψ becomes a free field, and so it should decouple from the spectrum. At this precise point, the Φ^2 operator reappears, and it is this transition that marks the appearance of the second kink. It is interesting to note that the kink persists all the way to $d = 4$, where it seems to lead to a very abrupt change in the central charge. Although our numerics present problems close to the free theory point in $d = 4$, it seems then that the second kink describes free theory with more than one chiral superfields. A natural guess is three chiral superfields, since this gives⁸ $C_T = 20$, which seems to be very close to the asymptotic value in Figure 3.3.

We are then led to guess that the second kink describes a theory with three chiral superfields, X, Y, Z . Furthermore, we expect a superpotential term X^2Y , which implies that if Y becomes free at the fixed point, then one has $\Delta_X = d/4$ as required. In $d = 3$, we can use F-maximization to find the scaling dimensions of the chiral fields [103]. We have found two superpotentials which seem to have the right properties, namely $W = X^2Y + XZ$, and $W = X^2Y + Y^2Z^2$. In the first case, the fixed-point conformal dimensions (which are equal to the R-charges in $d = 3$), as fixed by F -maximization, come out to be $\Delta_X = 3/4$, $\Delta_Y = 1/2$, and $\Delta_Z = 5/4$. In the second case, one finds that the dimension of Z at the fixed point is naively below the unitarity bound. This signals the emergence of accidental flavor symmetries which mix with the R -symmetry, modifying the F -maximization procedure.

⁸ At precisely the free point, there are extra spin-1 and spin-2 currents which mix with the stress-tensor. Our numerics cannot disentangle these, hence the discontinuous jump to the single-field value of C_T at the free point.

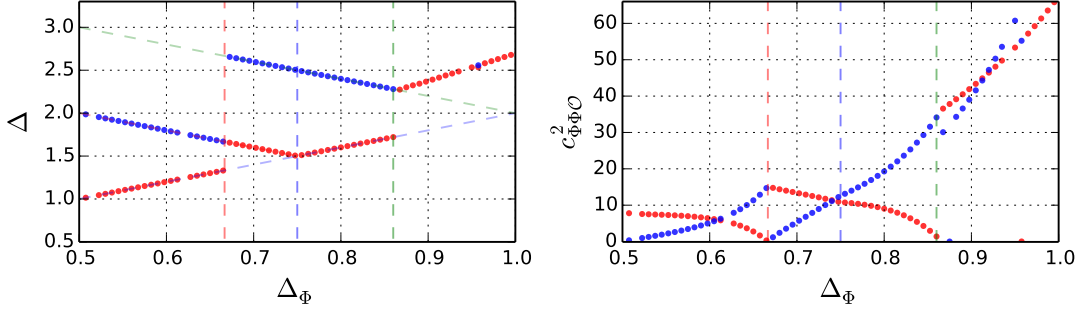


Figure 3.13: Scaling dimensions (*left*) and OPE coefficients (*right*) for the first three scalar operators in the the $\Phi \times \Phi$ OPE, extracted from the saturating solution, for $d = 3$ with $n_{max} = 9$. Operators appear in both plots with the same color (chosen according to ordering in the scaling dimension plot). Note the decoupling of Φ^2 at $\Delta_\Phi = 2/3$, corresponding to the cWZ model, as well as at the location of the third kink at $\Delta_\Phi \sim 0.86$.

This accidental flavor symmetry is accounted for by noting that the field Z becomes free and thus $\Delta_Z = 1/2$. This then leads to $\Delta_Y = 1/2$ and $\Delta_X = 3/4$.

To distinguish between the two guesses above, we need another observable. A convenient choice is the central charge C_T . As mentioned above, by computing the partition function on a squashed sphere, it is possible to determine $\tau_{RR}/\tau_{RR}^{\text{free}} = C_T/C_T^{\text{free}}$, with τ_{RR} the R-current two-point function coefficient. For the two superpotentials above we find

$$\frac{\tau_{RR}(3/4) + \tau_{RR}(1/2) + \tau_{RR}(5/4)}{\tau_{RR}(1/2)} = 1, \quad W = X^2Y + XZ, \quad (3.118)$$

$$\frac{\tau_{RR}(3/4) + 2\tau_{RR}(1/2)}{\tau_{RR}(1/2)} \simeq 2.5603, \quad W = X^2Y + Y^2Z^2. \quad (3.119)$$

This should be compared with the ratio $C_T/C_T^{\text{free}} \simeq 1.24$ that we obtain from Figure 3.10 (to avoid any confusion in the formulas above, we are normalizing by dividing by the values for a single free chiral field). Indeed, it appears we would need $\Delta_Z \simeq 1.14$, which seems hard to obtain from a polynomial superpotential with three chiral superfields.

To finish the discussion on the second kink, we should mention the intriguing possibility that the corresponding theory is in fact non-unitary. Violations of unitarity are not necessarily excluded by our bootstrap methods, as long as squares of OPE coefficients remain. This exotic suggestion is motivated by the observation that

$$\frac{4\tau_{RR}(3/4) - \tau_{RR}(1/2)}{\tau_{RR}(1/2)} \simeq 1.2413. \quad (3.120)$$

This suggests that the field theory actually contains five chiral superfields, but one of them has the wrong sign kinetic term, so that in terms of C_T , they effectively appear as three chiral superfields. Considering the superpotential $W = (X^2 + Z^2 + W^2 + V^2)Y$, F -maximization leads to $\Delta_Y < 1/2$, which is below the unitarity bound, and signals that the field Y is actually free, i.e. $\Delta_Y = 1/2$. After taking this into account, we find $\Delta_X = \Delta_Z = \Delta_W = \Delta_V = 3/4$. Hence, it appears that this theory has all the right properties to match our second kink.

The attentive reader may have noticed a small sleight of hand here. When a chiral field becomes free, it decouples from the rest of the theory and hence stops contributing to the OPE coefficient of the conserved spin-2 current. Therefore, C_T derived from numerical bootstrap measures the two-point function of the stress-tensor of the interacting part of the CFT only, and we should leave out the free contributions in (3.118), (3.119), (3.120). However, we expect that the extra field is free only precisely at the kink and not in its immediate neighbourhood, and thus we should include its contribution by continuity. We would then also expect that another spin-one superconformal primary approaches the unitarity bound as we approach the kink, providing the extra $U(1)$ symmetry of the free chiral. Unfortunately, preliminary numerical studies suggest that this is not so.

Let us focus now on the line of theories for $(d-1)/3 < \Delta_\Phi < d/4$. The decoupling of Φ^2 suggests a chiral ring relation $\Phi^2 = 0$. One particular such theory is the Wess-Zumino model with two chiral superfields Υ, Λ and a cubic superpotential of the form $W = \lambda\Upsilon^2\Lambda$. Denoting the lowest components of the superfields by Φ and Ψ respectively, this model yields the correct OPE $\Phi \times \Phi = Q^2\bar{\Psi}$, i.e. the operator Φ^2 is absent. In addition, we have the relation $\Delta_\Psi = (d-1) - 2\Delta_\Phi$, which follows from chirality and R-charge conservation. The exact dimensions in this model can be determined in $d = 3$ by F -maximization, as shown in [78], giving $\Delta_\Phi \simeq 0.708$. Could it be that our bound is saturated by this theory? Unfortunately this is not so. In the same reference, the authors compute $\tau_{\text{RR}} \simeq 0.380$, whence it follows that

$$\frac{C_T}{C_T^{\text{free}}} = \frac{\tau_{\text{RR}}}{\tau_{\text{RR}}(1/2)} \approx 1.52. \quad (3.121)$$

On the other hand, from Figure 3.4, we read off that at $\Delta_\Phi \simeq 0.708$, $C_T \simeq 6$, and hence $C_T/C_T^{\text{free}} \simeq 1$, very different from what we obtain above.

Consider now the third kink, which was first observed in $d = 4$ [20]. Our analysis adds a few more pieces of information about a putative theory sitting there. First, the kink continues to exist all the way to $d = 2$, where it apparently merges with the $C_T = 2c = 2$, $\mathcal{N} = 2$ minimal model. Second, the chiral field Φ^2 disappears from the spectrum also at this kink, as witnessed by Figure 3.13. In $d = 2$, this corresponds to the non-existence of

a dimension-2/3 Virasoro primary in the $c = 1$ model. This is a strong hint that the chiral ring of the theory at the kink has a relation $\Phi^2 = 0$. Since the kink does not merge with the free theory in $d = 4$, we do not expect it can be described by a Lagrangian for a collection of chiral superfields. It is conceivable it arises as an IR fixed point of a non-abelian gauge theory in $d = 4$, or even an abelian gauge theory in $d = 3$. Note that the central charge C_T in $d = 4$ is rather low – about 1.6 times that of the free chiral multiplet and only about a half of a single free vector multiplet.

3.7 Discussion

In this chapter, we have investigated the constraints of the conformal bootstrap on superconformal field theories with four Poincaré supercharges in $d \leq 4$. The cases $d = 2$ and $d = 3$ have not been analyzed before and thus we provide new universal bounds on unitary SCFTs with $\mathcal{N} = 2$ supersymmetry in these dimensions. We have also shown that the bounds display three interesting features (kinks), one of which we have conjecturally identified as the infrared fixed point of the single-field Wess-Zumino model with cubic superpotential. This conjecture is supported by the matching of the protected dimension of the chiral field, comparison of the value of C_T with an exact calculation by supersymmetric localization in $d = 3$, the structure of the OPE in the chiral sector, ϵ -expansion computations, and the agreement with exact results in $d = 2$. In [3], we take this conjecture at face value to provide a detailed study of the theory for $d = 3$.

It is clearly of great interest to elucidate the remaining two kinks. We expect that at least the third kink corresponds to a physical theory, since it shares many features with the better-understood Ising-like kinks. Perhaps a good candidate theory can be found with the correct value of C_T , and a gauge-invariant chiral operator Φ with the right dimension and chiral ring relation $\Phi^2 = 0$. It could also be interesting to see if C_T can be derived using localization in continuous d , in the spirit of [104], and matched with our results for the cWZ model or used as a tool to probe the other kinks.

The crucial ingredient in this work was to formulate a dimension-independent approach to superconformal algebras with four Poincaré supercharges in $d \leq 4$. This allowed us, among other things, to write down the action of the superconformal Casimir on a four-point function as a differential equation, whose solutions in turn gave us the superconformal blocks relevant for the bootstrap analysis. This approach can be extended to superconformal theories with eight Poincaré supercharges in general dimension, the parent algebra being the $(1, 0)$ superconformal algebra in six dimensions. Theories with this amount of

supersymmetry are particularly suited for bootstrap analysis since, apart from the case $d = 2, 4$, they do not admit marginal deformations. Work on this is currently in progress.

It is intriguing that the supersymmetric conformal blocks can be recast as non-supersymmetric ones with shifted external dimensions. In this chapter, we have extended this observation, previously noted in [86] for $d = 2, 4$, to any dimension and more general external operators. In the same reference, the authors showed that certain $\mathcal{N} = 2$ superblocks in four dimensions are given by a similar expression, this time with a shift by two units. It would be interesting to see if there is any deep reason for this connection and if the latter result also extends to other spacetime dimensions.

We have only briefly touched upon the extension of our analysis to $d < 2$. While the superconformal blocks we derived should be valid in any $d \leq 4$, it is not clear whether one can use the numerical bootstrap techniques to extract interesting information in $d = 1$ [105]. This certainly deserves further study since superconformal quantum-mechanical models are ubiquitous and should be dual to the AdS_2 near horizon regions of some extremal black holes.

Another interesting avenue for future exploration is to combine the constraints from superconformal symmetry studied here with the simplifications that occur in large N CFTs, i.e. when correlation functions factorize. This was explored to some extent with $\mathcal{N} = 4$ supersymmetry in $d = 4$ in [71] but much remains to be understood. The interest in this problem stems in part from the AdS/CFT correspondence and the fact that string theory leads to a vast landscape of holographic duals to SCFTs with four supercharges.

3.A OPE derivation of 3d $\mathcal{N} = 2$ superconformal blocks

In this Appendix, we provide further evidence for the formulae (3.66), (3.67) by explicitly determining the coefficients a_i from constraints imposed by $d = 3$, $\mathcal{N} = 2$ superconformal invariance on the OPE.⁹ As a first order of business let us present the explicit realization of the $d = 3$, $\mathcal{N} = 2$ algebra. The bosonic generators are just the conformal generators and the R-charge $\{R, M_{ij}, D, P_i, K_i\}$. They satisfy the commutation relations already presented in (3.1). A realization of these commutation relations in terms of differential operators is

⁹It is quite possible that these results can be derived also using techniques from superspace similar to the ones in [106].

given by

$$\begin{aligned}
M_{jk} &= -i(x_j \partial_k - x_k \partial_j) , \\
K_j &= -i(x_k x^k \partial_j - 2x_j x^k \partial_k) , \\
P_j &= -i \partial_j , \quad D = i x^k \partial_k , \quad R = r .
\end{aligned} \tag{3.122}$$

Note that the action of the conformal generators on operators in the CFT picks up a minus sign relative to (3.122). See the discussion around equations (2.28)-(2.31) in [90].

The fermionic generators are $Q_\alpha^\pm, S^{\alpha\pm}$, where $\alpha = 1, 2$ is the Dirac index. The Dirac representation is self-dual, with the isomorphism with the dual representation provided by the antisymmetric tensor $\epsilon^{12} = -\epsilon^{21} = \epsilon_{21} = -\epsilon_{12} = 1$. Thus in $d = 3$ there is no real distinction between the α and $\dot{\alpha}$ index used in Section 3.2 and we will omit the dots in this Appendix. Hermitian conjugation acts as $(Q_\alpha^\pm)^\dagger = S^{\alpha\mp}$. Let $(\sigma_i)^\alpha_\beta$ be the usual Pauli matrices

$$\sigma_1 \equiv \begin{pmatrix} 0 & 1 \\ 1 & 0 \end{pmatrix} , \quad \sigma_2 \equiv \begin{pmatrix} 0 & -i \\ i & 0 \end{pmatrix} , \quad \sigma_3 \equiv \begin{pmatrix} 1 & 0 \\ 0 & -1 \end{pmatrix} , \tag{3.123}$$

and further define

$$(\sigma_i)_{\alpha\beta} = \epsilon_{\alpha\gamma} (\sigma_i)^\gamma_\beta , \quad (\sigma_i)^{\alpha\beta} = (\sigma_i)^\alpha_\gamma \epsilon^{\gamma\beta} , \quad (\sigma_i)_\alpha^\beta = \epsilon_{\alpha\gamma} (\sigma_i)^\gamma_\delta \epsilon^{\delta\beta} . \tag{3.124}$$

The action of the bosonic generators on the fermionic ones is then

$$\begin{aligned}
[R, Q_\alpha^\pm] &= \pm Q_\alpha^\pm , & [R, S^{\alpha\pm}] &= \pm S^{\alpha\pm} , \\
[M_{ij}, Q_\alpha^\pm] &= \frac{1}{2} \epsilon_{ijk} (\sigma_k)^\beta_\alpha Q_\beta^\pm , & [M_{ij}, S^{\alpha\pm}] &= \frac{1}{2} \epsilon_{ijk} (\sigma_k)_\beta^\alpha S^{\beta\pm} , \\
[D, Q_\alpha^\pm] &= -\frac{i}{2} Q_\alpha^\pm , & [D, S^{\alpha\pm}] &= \frac{i}{2} S^{\alpha\pm} , \\
[P_i, S^{\alpha\pm}] &= -(\sigma_i)^{\beta\alpha} Q_{\beta\pm} , & [K_i, Q_\alpha^\pm] &= (\sigma_i)_{\beta\alpha} S^{\beta\pm} ,
\end{aligned} \tag{3.125}$$

with all other commutators vanishing. Note that ϵ_{ijk} is the completely antisymmetric tensor in three dimensions. Finally, the anticommutation relations among the fermionic generators are

$$\begin{aligned}
\{Q_\alpha^+, Q_\beta^-\} &= P_i (\sigma_i)_{\alpha\beta} , & \{S^{\alpha+}, S^{\beta-}\} &= K_i (\sigma_i)^{\alpha\beta} , \\
\{S^{\alpha-}, Q_\beta^+\} &= (iD - R) \delta^\alpha_\beta + \frac{1}{2} \epsilon_{ijk} M_{ij} (\sigma_k)^\alpha_\beta , \\
\{S^{\alpha+}, Q_\beta^-\} &= (iD + R) \delta^\alpha_\beta + \frac{1}{2} \epsilon_{ijk} M_{ij} (\sigma_k)^\alpha_\beta ,
\end{aligned} \tag{3.126}$$

with all other anticommutators vanishing. This algebra is of course in harmony with the general presentation in Section 3.2 of the superconformal algebras in $d \leq 4$.

Generalities

Let us first consider a CFT without supersymmetry and review how a conformal multiplet, with primary $\mathcal{P}_{i_1\dots i_s}$ of dimension Δ in the symmetric traceless representation of spin s , contributes to the four-point function, $\langle\phi_1\phi_2\phi_3\phi_4\rangle$, of scalar primaries ϕ_i of dimensions Δ_i . Define the OPE coefficient, $c_{\phi_1\phi_2}^{\mathcal{P}}$, by writing the contribution of the conformal family of \mathcal{P} to the $\phi_1 \times \phi_2$ OPE as¹⁰

$$\phi_1(x)|\phi_2\rangle = \dots + c_{\phi_1\phi_2}^{\mathcal{P}}|x|^{-\Delta_1-\Delta_2+\Delta-s}x^{i_1}\dots x^{i_s} [|\mathcal{P}_{i_1\dots i_s}\rangle + \text{desc.}] + \dots \quad (3.127)$$

The contribution of level-one descendants in the square bracket is

$$\text{desc.} = \alpha(x \cdot P)|\mathcal{P}_{i_1\dots i_s}\rangle + \beta x_{i_1}P^j|\mathcal{P}_{ji_2\dots i_s}\rangle + \dots, \quad (3.128)$$

where

$$\begin{aligned} \alpha &= -\frac{i}{2} \frac{\Delta + \Delta_{12} + s}{\Delta + s}, \\ \beta &= -\frac{i}{2} \frac{s\Delta_{12}}{(\Delta + s)(\Delta - s - 1)}. \end{aligned} \quad (3.129)$$

The two-point function of \mathcal{P} and its conjugate $\bar{\mathcal{P}}$ takes the form

$$\langle\mathcal{P}_{i_1\dots i_s}(x)\bar{\mathcal{P}}_{j_1\dots j_s}(y)\rangle = \frac{f_{\mathcal{P}\bar{\mathcal{P}}}}{|x-y|^{2\Delta}} \left[\frac{1}{s!} \sum_{\sigma \in S_s} \prod_{n=1}^s I_{i_n j_{\sigma(n)}}(x-y) - \text{traces} \right], \quad (3.130)$$

where S_s is the permutation group on s elements and

$$I_{ij}(x) = \delta_{ij} - 2 \frac{x_i x_j}{|x|^2}. \quad (3.131)$$

It is useful to note that the coefficient $f_{\mathcal{P}\bar{\mathcal{P}}}$ also appears in the scalar product

$$\langle\mathcal{P}_{i_1\dots i_s}|\mathcal{P}_{j_1\dots j_s}\rangle = f_{\mathcal{P}\bar{\mathcal{P}}} \left(\frac{1}{s!} \sum_{\sigma \in S_s} \prod_{n=1}^s \delta_{i_n j_{\sigma(n)}} - \text{traces} \right). \quad (3.132)$$

With these normalizations, the contribution of the conformal family to the four-point function is

$$\langle\phi_1(x_1)\phi_2(x_2)\phi_3(x_3)\phi_4(x_4)\rangle|_{\mathcal{P}} = \frac{f_{\mathcal{P}\bar{\mathcal{P}}} c_{\phi_1\phi_2}^{\mathcal{P}} c_{\phi_3\phi_4}^{\bar{\mathcal{P}}}}{|x_{12}|^{\Delta_1+\Delta_2}|x_{34}|^{\Delta_3+\Delta_4}} \frac{|x_{24}|^{\Delta_{12}}|x_{14}|^{\Delta_{34}}}{|x_{14}|^{\Delta_{12}}|x_{13}|^{\Delta_{34}}} G_{\Delta,s}^{\Delta_{12},\Delta_{34}}(u,v), \quad (3.133)$$

¹⁰In this appendix we freely use the operator-state correspondence, which is valid in any CFT in Euclidean signature. The state corresponding to an operator $\phi(x)$ will be denoted by $|\phi\rangle$.

where $G_{\Delta,s}^{\Delta_{12},\Delta_{34}}(u,v)$ is the conformal block whose normalization is determined as in (3.65). The following derivation of the superconformal blocks relies on the observation that when ϕ_i are superconformal primaries and $\phi_{1,3}$ chiral primaries, superconformal symmetry fixes the OPE coefficients and two-point functions of all contributing conformal primaries from the same superconformal multiplet in terms of those of the superconformal primary.

Consider now the correlator $\langle\phi_1\phi_2\phi_3\phi_4\rangle$ in a 3d, $\mathcal{N} = 2$ SCFT, where ϕ_i are scalar superconformal primaries, with $\phi_{1,3}$ chiral, i.e. $[Q_\alpha^+, \phi_{1,3}] = 0$. We wish to determine which conformal primaries in the superconformal family of a superconformal primary \mathcal{P} can appear in both the OPE of $\phi_1 \times \phi_2$ and the OPE of $\bar{\phi}_3 \times \bar{\phi}_4$. Only those conformal primaries can contribute to the above four-point function. Consider the OPE $\phi_1(x)|\phi_2\rangle$. It follows from the chirality of ϕ_1 and the superconformal algebra that $[S^{\alpha+}, \phi_1(x)] = 0$. Hence

$$S^{\alpha+}\phi_1(x)|\phi_2\rangle = 0, \quad (3.134)$$

since ϕ_2 is a superconformal primary. Similarly,

$$S^{\alpha-}\bar{\phi}_3(x)|\bar{\phi}_4\rangle = 0. \quad (3.135)$$

Consequently, the conformal primary with the lowest dimension from a given superconformal family that contributes to both OPEs must be annihilated by $S^{\alpha\pm}$, and thus this operator is necessarily the superconformal primary. It follows that the superconformal primary has integer spin and its R-charge is given by $q = q_1 + q_2 = -q_3 - q_4$. Let us denote this operator with $\mathcal{P}_{i_1\dots i_s}^{(0)}$, and its dimension and spin with Δ and s , respectively. All other contributing conformal primaries from the same supermultiplet must have integer spin and R-charge q . The conformal primaries in the multiplet have dimensions $\Delta + n/2$, with $n = 0, \dots, 4$ labelling the number of Q supercharges acting on $\mathcal{P}_{i_1\dots i_s}^{(0)}$. These operators have integer spin only when n is even. For $s > 0$ and generic $\Delta - |q|$, there are four candidate conformal primaries with dimension $\Delta + 1$. $\mathcal{P}^{(1)}$ with spin $s + 1$, $\mathcal{P}^{(2)}$ with spin $s - 1$, and \mathcal{P}^{+-} , \mathcal{P}^{-+} , both with spin s . All four can be obtained by acting with linear combinations of the products $Q_\alpha^\pm Q_\beta^\mp$ on $\mathcal{P}^{(0)}$. Consider the action of spacetime parity $x^i \mapsto -x^i$. A proper tensor of spin s transforms as $(-1)^s$, while a pseudotensor as $(-1)^{s+1}$. The supercharges Q_a^\pm “square to the momentum”, and thus must transform such that any product transforms as $Q_\alpha^\pm Q_\beta^\mp \mapsto -Q_\alpha^\pm Q_\beta^\mp$. It follows that $\mathcal{P}^{(1)}$, $\mathcal{P}^{(2)}$ have the same parity as $\mathcal{P}^{(0)}$, while \mathcal{P}^{+-} , \mathcal{P}^{-+} have the opposite. In theories invariant under parity, this gives an argument why only $\mathcal{P}^{(1)}$ and $\mathcal{P}^{(2)}$ can contribute. However, the Casimir approach from the main text does not require parity invariance and thus shows that our formula for superconformal blocks is valid in general. Finally, there is a conformal primary $\mathcal{P}^{(3)}$ with dimension $\Delta + 2$, spin s and R-charge q , obtained from $\mathcal{P}^{(0)}$ by acting with a linear

combination of products of four Q 's, which can also contribute to the four-point function. In the following subsections, we show how the constraints (3.134) and (3.135) fix the OPE coefficients of $\mathcal{P}^{(1)}$, $\mathcal{P}^{(2)}$, and $\mathcal{P}^{(3)}$ in terms of those of $\mathcal{P}^{(0)}$ and also compute the two-point functions $f_{\mathcal{P}^{(i)}\bar{\mathcal{P}}^{(i)}}$ for $i = 1, 2, 3$ in terms of $f_{\mathcal{P}^{(0)}\bar{\mathcal{P}}^{(0)}}$. We find that

$$a_i = \frac{f_{\mathcal{P}^{(i)}\bar{\mathcal{P}}^{(i)}}}{f_{\mathcal{P}^{(0)}\bar{\mathcal{P}}^{(0)}}} \frac{c_{\phi_1\phi_2}^{\mathcal{P}^{(i)}} c_{\phi_3\phi_4}^{\bar{\mathcal{P}}^{(i)}}}{c_{\phi_1\phi_2}^{\mathcal{P}^{(0)}} c_{\phi_3\phi_4}^{\bar{\mathcal{P}}^{(0)}}}, \quad (3.136)$$

reproduce the results in (3.67) for $d = 3$.

The contribution of $\mathcal{P}^{(1)}$

It is useful to define the operator

$$T_j(x, y) \equiv (\sigma_j)^{\alpha\beta} [(x - y)Q_\alpha^+ Q_\beta^- - (x + y)Q_\alpha^- Q_\beta^+]. \quad (3.137)$$

An explicit expression for $\mathcal{P}^{(1)}$ is then given by

$$|\mathcal{P}_{i_1 \dots i_{s+1}}^{(1)}\rangle = \frac{1}{s+1} \sum_{n=1}^{s+1} T_{i_n}(\Delta + s, q) |\mathcal{P}_{i_1 \dots \hat{i}_n \dots i_{s+1}}^{(0)}\rangle - \text{traces}, \quad (3.138)$$

where the notation $i_1 \dots \hat{i}_n \dots i_{s+1}$ means that the index i_n is omitted from the string of indices, and the traces are subtracted to make the resulting state traceless. Applying S_α^+ to the OPE $\phi_1(x)|\phi_2\rangle$ mixes the contribution of level-one conformal descendants of $\mathcal{P}^{(0)}$, (3.128), with that of the conformal primary $\mathcal{P}^{(1)}$. Requiring that the result vanishes and looking at the coefficient of the highest power of $\bar{z} = x_1 - ix_2$ leads to

$$c_{\phi_1\phi_2}^{\mathcal{P}^{(1)}} = -\frac{i(\Delta + \Delta_{12} + s)}{4(\Delta + s)(\Delta + s + 1)(\Delta + s + q)} c_{\phi_1\phi_2}^{\mathcal{P}^{(0)}}, \quad (3.139)$$

and hence also

$$c_{\phi_3\phi_4}^{\bar{\mathcal{P}}^{(1)}} = -\frac{i(\Delta + \Delta_{34} + s)}{4(\Delta + s)(\Delta + s + 1)(\Delta + s - q)} c_{\phi_3\phi_4}^{\bar{\mathcal{P}}^{(0)}}. \quad (3.140)$$

Note the opposite sign of the R-charge in the denominators of (3.139), (3.140) resulting from the presence of the conjugate operator. The two-point function can be found by using the superconformal algebra

$$f_{\mathcal{P}^{(1)}\bar{\mathcal{P}}^{(1)}} = 8(\Delta + s)(\Delta + s + 1)(\Delta + s + q)(\Delta + s - q) f_{\mathcal{P}^{(0)}\bar{\mathcal{P}}^{(0)}}. \quad (3.141)$$

Putting the pieces together, we find

$$a_1 = \frac{f_{\mathcal{P}^{(1)}\bar{\mathcal{P}}^{(1)}}}{f_{\mathcal{P}^{(0)}\bar{\mathcal{P}}^{(0)}}} \frac{c_{\phi_1\phi_2}^{\mathcal{P}^{(1)}} c_{\phi_3\phi_4}^{\bar{\mathcal{P}}^{(1)}}}{c_{\phi_1\phi_2}^{\mathcal{P}^{(0)}} c_{\phi_3\phi_4}^{\bar{\mathcal{P}}^{(0)}}} = -\frac{(\Delta + \Delta_{12} + s)(\Delta + \Delta_{34} + s)}{2(\Delta + s)(\Delta + s + 1)}, \quad (3.142)$$

in agreement with (3.67).

The contribution of $\mathcal{P}^{(2)}$

The conformal primary $\mathcal{P}^{(2)}$ is given by the contraction

$$|\mathcal{P}_{i_1\dots i_{s-1}}^{(2)}\rangle = T_j(\Delta - s - 1, q)|\mathcal{P}_{j i_1\dots i_{s-1}}^{(0)}\rangle, \quad (3.143)$$

so that the resulting state is automatically symmetric and traceless. Using again (3.134), and this time looking at the next-to-leading power of $\bar{z} = x_1 - ix_2$ fixes

$$c_{\phi_1\phi_2}^{\mathcal{P}^{(2)}} = -\frac{is(\Delta + \Delta_{12} - s - 1)}{4(2s + 1)(\Delta - s)(\Delta - s - 1)(\Delta - s - 1 + q)} c_{\phi_1\phi_2}^{\mathcal{P}^{(0)}}, \quad (3.144)$$

and similarly

$$c_{\phi_3\phi_4}^{\bar{\mathcal{P}}^{(2)}} = -\frac{is(\Delta + \Delta_{34} - s - 1)}{4(2s + 1)(\Delta - s)(\Delta - s - 1)(\Delta - s - 1 - q)} c_{\phi_3\phi_4}^{\bar{\mathcal{P}}^{(0)}}. \quad (3.145)$$

The norm of $|\mathcal{P}^{(2)}\rangle$ is

$$f_{\mathcal{P}^{(2)}\bar{\mathcal{P}}^{(2)}} = 8 \frac{(2s + 1)}{(2s - 1)} (\Delta - s)(\Delta - s - 1)(\Delta - s - 1 + q)(\Delta - s - 1 - q) f_{\mathcal{P}^{(0)}\bar{\mathcal{P}}^{(0)}}, \quad (3.146)$$

leading to

$$a_2 = \frac{f_{\mathcal{P}^{(2)}\bar{\mathcal{P}}^{(2)}}}{f_{\mathcal{P}^{(0)}\bar{\mathcal{P}}^{(0)}}} \frac{c_{\phi_1\phi_2}^{\mathcal{P}^{(2)}} c_{\phi_3\phi_4}^{\bar{\mathcal{P}}^{(2)}}}{c_{\phi_1\phi_2}^{\mathcal{P}^{(0)}} c_{\phi_3\phi_4}^{\bar{\mathcal{P}}^{(0)}}} = -\frac{s^2(\Delta + \Delta_{12} - s - 1)(\Delta + \Delta_{34} - s - 1)}{2(4s^2 - 1)(\Delta - s)(\Delta - s - 1)}, \quad (3.147)$$

in harmony with (3.67) for $d = 3$.

The contribution of $\mathcal{P}^{(3)}$

In order to be able to write a relatively compact expression for $\mathcal{P}^{(3)}$ it is convenient to define the following operator, which takes symmetric traceless tensors of spin s and dimension Δ , into symmetric traceless tensors of spin s , dimension $\Delta + 1$, and opposite parity

$$U_\eta^{ab} : |\psi_{i_1 \dots i_s}\rangle \mapsto \eta \epsilon^{\alpha\beta} Q_\alpha^a Q_\beta^b |\psi_{i_1 \dots i_s}\rangle + i \sum_{n=1}^s \varepsilon_{j i_n k} (\sigma_j)^{\alpha\beta} Q_\alpha^a Q_\beta^b |\psi_{k i_1 \dots \hat{i}_n \dots i_s}\rangle, \quad (3.148)$$

where $a, b = \pm$ are R-charge indices, $\eta \in \mathbb{C}$, and ε_{ijk} is the standard antisymmetric tensor with $\varepsilon_{123} = 1$. This operator is useful also to write down the other four conformal primaries with dimension $\Delta + 1$. We find that

$$\begin{aligned} |\mathcal{P}^{+-}\rangle &= U_{\Delta-1+q}^{+-} |\mathcal{P}^{(0)}\rangle, \\ |\mathcal{P}^{-+}\rangle &= U_{\Delta-1-q}^{-+} |\mathcal{P}^{(0)}\rangle, \\ |\mathcal{P}^{++}\rangle &= U_\eta^{++} |\mathcal{P}^{(0)}\rangle, \\ |\mathcal{P}^{--}\rangle &= U_\eta^{--} |\mathcal{P}^{(0)}\rangle, \end{aligned} \quad (3.149)$$

are conformal primaries, the first two of which have been discussed below (3.135). The parameter η is arbitrary for the last two cases since the second part of (3.148) drops out by the symmetry of $(\sigma_j)^{\alpha\beta}$, and the anticommutativity of supercharges of the same R-charge. We must remember that U_η^{ab} acts not only on the Hilbert space, but also on the vector indices. The conformal primary of dimension $\Delta + 2$ and spin s can then be written as

$$\begin{aligned} |\mathcal{P}^{(3)}\rangle &= (\Delta + s - q)(\Delta - s - 1 - q) (U_\Delta^{++} U_\Delta^{--} - U_{\Delta+q}^{+-} U_{\Delta-1+q}^{+-} - U_{\Delta-q}^{-+} U_{\Delta-1+q}^{-+}) |\mathcal{P}^{(0)}\rangle + \\ &+ (\Delta + s + q)(\Delta - s - 1 + q) (U_\Delta^{--} U_\Delta^{++} - U_{\Delta-q}^{-+} U_{\Delta-1-q}^{-+} - U_{\Delta+q}^{+-} U_{\Delta-1-q}^{+-}) |\mathcal{P}^{(0)}\rangle. \end{aligned} \quad (3.150)$$

Note that the second line is obtained from the first by flipping all R-charge indices and the sign of the R-charge. Using once again (3.134), and looking at the leading power of \bar{z} for the lowest scaling dimension where $|\mathcal{P}^{(3)}\rangle$ contributes, one can show that

$$c_{\phi_1 \phi_2}^{\mathcal{P}^{(3)}} = - \frac{(\Delta + \Delta_{12} + s)(\Delta + \Delta_{12} - s - 1) c_{\phi_1 \phi_2}^{\mathcal{P}^{(0)}}}{16(4\Delta^2 - 1)(\Delta^2 - s^2)(\Delta^2 - (s+1)^2)(\Delta + s + q)(\Delta - s - 1 + q)}, \quad (3.151)$$

and so

$$c_{\phi_3 \phi_4}^{\bar{\mathcal{P}}^{(3)}} = - \frac{(\Delta + \Delta_{34} + s)(\Delta + \Delta_{34} - s - 1) c_{\phi_3 \phi_4}^{\bar{\mathcal{P}}^{(0)}}}{16(4\Delta^2 - 1)(\Delta^2 - s^2)(\Delta^2 - (s+1)^2)(\Delta + s - q)(\Delta - s - 1 - q)}. \quad (3.152)$$

The norm is

$$f_{\mathcal{P}^{(3)}\bar{\mathcal{P}}^{(3)}} = 64\Delta^2(4\Delta^2 - 1)(\Delta^2 - s^2)(\Delta^2 - (s+1)^2)((\Delta + s)^2 - q^2)((\Delta - s - 1)^2 - q^2)f_{\mathcal{P}^{(0)}\bar{\mathcal{P}}^{(0)}}, \quad (3.153)$$

so that

$$a_3 = \frac{f_{\mathcal{P}^{(3)}\bar{\mathcal{P}}^{(3)}} c_{\phi_1\phi_2}^{\mathcal{P}^{(3)}} c_{\phi_3\phi_4}^{\bar{\mathcal{P}}^{(3)}}}{f_{\mathcal{P}^{(0)}\bar{\mathcal{P}}^{(0)}} c_{\phi_1\phi_2}^{\mathcal{P}^{(0)}} c_{\phi_3\phi_4}^{\bar{\mathcal{P}}^{(0)}}} = \frac{\Delta^2(\Delta + \Delta_{12} + s)(\Delta + \Delta_{12} - s - 1)(\Delta + \Delta_{34} + s)(\Delta + \Delta_{34} - s - 1)}{4(4\Delta^2 - 1)(\Delta^2 - s^2)(\Delta^2 - (s+1)^2)}, \quad (3.154)$$

in complete agreement with (3.67) for $d = 3$.

3.B Decomposition of the generalized free chiral correlator

A natural solution to the crossing equation using the conformal blocks in (3.64) in both channels corresponds to the supersymmetric analogue of the generalized free field. The elementary fields of this theory are a chiral scalar primary $\phi(x)$ of dimension Δ_ϕ , its supersymmetric descendants – a fermion $\psi_a(x) = (Q_a^- \phi(x))$, and the auxiliary field $F(x) = \epsilon^{ab} Q_a^- Q_b^- \phi(x)$, as well as their conjugates. The correlators are computed using Wick's theorem, where each field only couples to its conjugate. The decomposition of the correlator $\langle \phi \bar{\phi} \phi \bar{\phi} \rangle$ into ordinary conformal blocks was given in [107]. We can use this decomposition together with (3.66) to find the decomposition into superconformal blocks

$$\begin{aligned} \langle \phi(x_1) \bar{\phi}(x_2) \phi(x_3) \bar{\phi}(x_4) \rangle &= \frac{1}{|x_{12}|^{2\Delta_\phi} |x_{34}|^{2\Delta_\phi}} \left[1 + \left(\frac{u}{v} \right)^{\Delta_\phi} \right] = \\ &= \frac{1}{|x_{12}|^{2\Delta_\phi} |x_{34}|^{2\Delta_\phi}} \left[\mathcal{G}_{0,0}^{0,0}(u, v) + \sum_{n,s \geq 0} p_{n,s} \mathcal{G}_{2\Delta_\phi + 2n + s, s}^{0,0}(u, v) \right], \end{aligned} \quad (3.155)$$

where

$$p_{n,s} = \frac{(-2)^s (\Delta_\phi)_{n+s}^2 (\Delta_\phi - \frac{d}{2} + 1)_n^2}{n! s! (2\Delta_\phi + 2n + s)_s (s + \frac{d}{2})_n (2\Delta_\phi + n - d + 2)_n (2\Delta_\phi + n + s - \frac{d}{2} + 1)_n}, \quad (3.156)$$

and $(x)_n \equiv \Gamma(x+n)/\Gamma(x)$ is the Pochhammer symbol. This decomposition serves as a further test of the validity of the superconformal blocks in (3.64). The result in (3.155), (3.156) strongly resembles the decomposition of the four-point function of non-supersymmetric

generalized free fields into ordinary conformal blocks given in equation (43) of [107]. In fact the two results are identical to each other (up to an overall normalization) if one fixes $\Delta_1 = \Delta_2 = \Delta_\phi$ in equation (43) of [107], and performs the shift $2\Delta_\phi \mapsto 2\Delta_\phi - 1$ in the denominator of (3.156). This is reminiscent of the observations in Section 3.3.3.

3.C $\mathcal{N} = 2$ minimal models

Generalities

Here we collect some well-known facts about $\mathcal{N} = 2$ minimal models in two dimensions, see for example [108]. For a discussion on $\mathcal{N} = 1$ minimal models see [109]. The (holomorphic) infinite-dimensional $\mathcal{N} = 2$ superconformal algebra in two dimensions is:

$$\begin{aligned}
[L_m, L_n] &= \frac{c}{12} (m^3 - m) \delta_{m+n,0} + (m - n) L_{m+n}, & \{G_r^+, G_s^+\} &= \{G_r^-, G_s^-\} = 0, \\
[L_m, G_r^\pm] &= \left(\frac{m}{2} - r\right) G_{m+r}^\pm, & [\Omega_n, G_r^\pm] &= \pm G_{r+n}^\pm, \\
[L_m, \Omega_n] &= -n \Omega_{m+n}, & [\Omega_m, \Omega_n] &= \frac{c}{3} m \delta_{m+n,0}. \\
\{G_r^+, G_s^-\} &= \frac{c}{3} \left(r^2 - \frac{1}{4}\right) \delta_{r+s,0} + 2L_{r+s} + (r - s)\Omega_{r+s}, & &
\end{aligned} \tag{3.157}$$

Here m and n are integers and in the NS sector r and s are half-integers. The modes of the energy momentum tensor are L_m , those of the superconformal R-symmetry are Ω_n and the two supercharges have modes G_r^\pm . The real number c is the (left or right moving) central charge and it is related to the conformal anomaly of the CFT.

The finite, $sl(2|1)$, subalgebra of the superconformal algebra, given in (3.20), is obtained from (3.157) by restricting to the generators $\{L_{-1,0,1}, \Omega \equiv \Omega_0, G_{\pm 1/2}^\pm\}$. Unitary representations of the infinite-dimensional $\mathcal{N} = 2$ superconformal algebra exist for any real $c \geq 3$ and for the discrete values

$$c = \frac{3k}{k+2}, \quad k = 0, 1, 2, \dots \tag{3.158}$$

This discrete series is usually referred to as the $\mathcal{N} = 2$ minimal models. The dimensions and R-charges of the superconformal primary operators in the NS sector of the k -th minimal model are labeled by two integers m and n

$$h = \frac{n(n+2) - m^2}{4(k+2)}, \quad \Omega = \frac{m}{k+2}, \quad 0 \leq n \leq k, \quad -n \leq m \leq n, \quad m+n = \text{even}. \tag{3.159}$$

The fusion rules for $\mathcal{N} = 2$ minimal models are derived in [110, 111] (see also [112]).¹¹ The superconformal primaries in the k -th minimal model will be denoted by $\phi_{n,m}$. The fusion rules are then

$$\phi_{n_1, m_1} \times \phi_{n_2, m_2} = \sum_{n=\frac{m_2-n_2}{2}}^{\frac{m_2+n_2}{2}} \phi_{n_1-m_2+2n, m_1+m_2} . \quad (3.160)$$

The k -th $\mathcal{N} = 2$ minimal model has a \mathbb{Z}_{k+2} symmetry generated by some of the primaries in the Ramond sector, see [110]. Chiral, antichiral primaries are superconformal primaries also annihilated by $G_{-1/2}^+$, $G_{-1/2}^-$, respectively, which is equivalent to $\Omega = \pm 2h$. In the minimal models, these are operators with $m = \pm n$, respectively.

One can derive a universal bound for the central charge of a two-dimensional $\mathcal{N} = 2$ SCFT using the infinite-dimensional superconformal algebra, see for example [113]. Using unitarity and the algebra in (3.157) one finds

$$0 \leq \langle \phi | \{G_{-3/2}^+, G_{3/2}^-\} | \phi \rangle = \langle \phi | \left(2L_0 - 3\Omega + \frac{2c}{3} \right) | \phi \rangle , \quad (3.161)$$

for any superconformal primary $|\phi\rangle$. Thus we arrive at the following constraint for the dimension and R-charge of any superconformal primary

$$2h - 3\Omega + \frac{2c}{3} \geq 0 , \quad (3.162)$$

which becomes $h \leq c/6$ for a chiral primary. The bound is saturated only if the state $G_{-3/2}^+ |\phi\rangle$ is null. The highest-dimension chiral primary in every minimal model has $m = n = k$ and saturates the bound. If we have a unitary $(2, 2)$ SCFT with a diagonal spectrum, i.e. $\bar{h} = h = \Delta/2$, we arrive at the following lower bound on the central charge

$$C_T \geq 6\Delta_{\max} , \quad (3.163)$$

where Δ_{\max} is the highest dimension of a superconformal primary in the theory. One can repeat the same analysis with the state $G_{-(2p+1)/2}^+ |\phi\rangle$ with $p = 1, 2, 3, \dots$ and find the bound

$$C_T \geq \frac{12}{p+1} \Delta_{\max} , \quad (3.164)$$

Clearly the strongest bound is obtained for $p = 1$ as in (3.163).

¹¹Notice that there is a factor of $1/2$ difference between our conventions for the R-charge and the ones in [110, 111].

In Section 3.6.3 we claimed that in every unitary CFT with $\mathcal{N} = (2, 2)$ supersymmetry there is always an operator (or state) of dimension $\Delta = 2$ which is a superdescendant of the identity. This state is given by

$$\Omega_{-1}\bar{\Omega}_{-1}|0\rangle, \quad (3.165)$$

where $|0\rangle$ is the NS vacuum and Ω_{-1} is defined in (3.157). This state clearly has dimension $\Delta = h + \bar{h} = 2$ and R-charge $q = \Omega + \bar{\Omega} = 0$. Moreover its norm is given by

$$\langle 0|\Omega_1\bar{\Omega}_1\Omega_{-1}\bar{\Omega}_{-1}|0\rangle = \frac{c^2}{9}. \quad (3.166)$$

Therefore in a unitary theory the state is never null since $c > 0$.

Super-Ising in $d = 2$

The theory with $c = 1$ can be realized in terms of a single compact boson, φ , at a specific radius $R = \sqrt{3}$ [112, 114]. There are three superconformal primary operators

$$\phi_{1,\pm 1} =: e^{\pm \frac{i}{\sqrt{3}}\varphi} :, \quad \phi_{0,0} = 1. \quad (3.167)$$

The operator $\phi_{1,1}$ is chiral with $\Delta = q/2 = \frac{1}{3}$, and is identified with the (holomorphic part of the) operator Φ in Section 3.6.3. Similarly the operator $\phi_{1,-1}$ is antichiral with $\Delta = -q/2 = \frac{1}{3}$, and is identified with the operator $\bar{\Phi}$. One can now use the formula

$$: e^{ia\varphi(z_1)} :: e^{ib\varphi(z_2)} := (z_1 - z_2)^{ab} : e^{ia\varphi(z_1)+ib\varphi(z_2)} :, \quad (3.168)$$

where a and b are some constants, to find the OPE

$$\phi_{1,1}(z_1)\phi_{1,-1}(z_2) \sim \frac{1}{(z_1 - z_2)^{1/3}} + \frac{i}{\sqrt{3}}\partial_{z_2}\varphi(z_2)(z_1 - z_2)^{2/3} + \dots \quad (3.169)$$

We normalize all two point functions in the theory to have coefficients 1 and define the operator $\mathcal{O}_\epsilon(z) \equiv i\partial_z\varphi(z)$, which has dimension $h = 1$. The operator of dimension $\Delta = 2$, which should be identified with $[\Phi\bar{\Phi}]$ from Section 3.6.3, is obtained by taking $\mathcal{O}_\epsilon(z)\bar{\mathcal{O}}_\epsilon(\bar{z}) = \partial_z\varphi(z)\partial_{\bar{z}}\bar{\varphi}(\bar{z})$. Another useful OPE is given by

$$i\partial_{z_1}\varphi(z_1) : e^{ia\varphi(z_2)} : \sim a \frac{: e^{ia\varphi(z_2)} :}{z_1 - z_2} + \dots \quad (3.170)$$

With these OPEs at hand one finds the following three point function

$$\langle \phi_{1,1}(z_1)\phi_{1,-1}(z_2)\mathcal{O}_\epsilon(z_3) \rangle = \frac{1}{\sqrt{3}} \frac{1}{(z_1 - z_2)^{-2/3}(z_2 - z_3)(z_1 - z_3)} . \quad (3.171)$$

Combining the left and right-moving sectors one finds the three-point function

$$\langle \Phi(z_1, \bar{z}_1)\bar{\Phi}(z_2, \bar{z}_2)[\Phi\bar{\Phi}](z_3, \bar{z}_3) \rangle = \frac{1}{3} \frac{1}{|z_1 - z_2|^{-4/3}|z_2 - z_3|^2|z_1 - z_3|^2} . \quad (3.172)$$

Thus we find that the OPE coefficient denoted by $c_{\Phi\bar{\Phi}[\Phi\bar{\Phi}]}$ is given by

$$c_{\Phi\bar{\Phi}[\Phi\bar{\Phi}]} = \frac{1}{3} . \quad (3.173)$$

This matches nicely with the numerical value at the kink in the right panel of Figure 3.6.

A comment on two supercharges

Finally, let us mention a tangential observation about bootstrap of $(1, 1)$ SCFTs in $d = 2$, complementing the results of [77] with $\mathcal{N} = 1$ supersymmetry in $d = 3$. Analogously to that study, also with $(1, 1)$ supersymmetry in $d = 2$, the superconformal blocks are equal to the conformal blocks, so that there are no additional constraints from crossing symmetry besides the numerical bounds obtained in [4, 13]. However, it may happen that the leading scalar appearing in the $\sigma \times \sigma$ OPE is the superdescendant of σ itself. In this case, we have the extra constraint $\Delta_{[\sigma\sigma]} = \Delta_\sigma + 1$. The result is that the two lines intersect at $\Delta_\sigma \approx 1/5$ and $\Delta_\epsilon \approx 6/5$ for $d = 2$. These dimensions correspond to the Virasoro minimal model with central charge $c = 7/10$, i.e. the tricritical Ising model. This is in fact the first $\mathcal{N} = 1$ minimal model [109], in harmony with the analogous results of [77] in $d = 3$.

Chapter 4

Analytic Functionals for the Conformal Bootstrap

4.1 Introduction

As exemplified in the previous chapters, unitarity and associativity of the operator product expansion have proven very powerful in constraining the dynamics of CFTs in various dimensions. Focusing on the analytic results, these principles can be used for example to derive universal behaviour of CFTs at large spin [66, 67], the emergence of local physics in the AdS dual [115], Hofman-Maldacena bounds [116] or causality [117].

Some of the most exciting consequences of the conformal bootstrap equations are constraints on the low-lying spectrum of operators. Most prominently, there is a strong numerical evidence that the 3D Ising model at criticality is the unique 3D CFT with a \mathbb{Z}_2 symmetry and precisely one relevant scalar primary operator of each \mathbb{Z}_2 charge [4–6]. In spite of a substantial progress on the numerical front, little has been learnt about the analytic origin of these constraints. The main aim of this chapter is to take some steps towards such analytic understanding.

A standard example of an equation arising in the conformal bootstrap expresses the crossing symmetry of the four-point function of identical scalar primary operators $\phi(x)$ and takes the form

$$\sum_{\mathcal{O} \in \phi \times \phi} (c_{\phi\phi\mathcal{O}})^2 F_{\mathcal{O}}(z, \bar{z}) = 0, \quad (4.1)$$

where the sum runs over primary operators present in the $\phi \times \phi$ OPE, $c_{\phi\phi\mathcal{O}}$ is the corresponding OPE coefficient, and $F_{\mathcal{O}}(z, \bar{z})$ are functions related to conformal blocks and

completely fixed by conformal symmetry in terms of the quantum numbers of ϕ and \mathcal{O} and the dimension of spacetime. Unitarity implies $(c_{\phi\phi\mathcal{O}})^2 > 0$.

(4.1) can be looked upon as a vector equation in the infinite-dimensional vector space of functions of two complex variables z and \bar{z} . It is mostly due to the infinite-dimensional nature of the problem that an extraction of physical consequences from (4.1) is not a simple task. The challenge is to identify a direction in this vector space along which the bootstrap equation is the most revealing. Speaking more formally, any linear functional acting on the space of functions $F_{\mathcal{O}}(z, \bar{z})$ can be applied to (4.1), leading to a single constraint on the CFT data. Some functionals lead to stronger constraints than others. The functionals leading to optimal constraints have been called extremal functionals [23]. The extremal functional depends on the precise question we are asking but can be expected to carry valuable physical information about conformal field theories. An analytic construction of various extremal functionals is therefore a promising strategy for understanding the bootstrap bounds.

One example of a constraint that (4.1) implies for the CFT data is an upper bound on the gap in the spectrum of scalar \mathcal{O} above identity. This bound exhibits a kink at the critical Ising model both in two and three dimensions, and the two are continuously connected across dimensions [63]. An analytic derivation of the shape of this bound already in 2D with global conformal symmetry is therefore a very important problem.

In the present chapter, we take a step in this direction by finding the optimal upper bound on the gap in one-dimensional theories with global conformal symmetry. Such theories are interesting in their own right since they describe conformal line defects in higher-dimensional CFTs [1, 60], models of (super)conformal quantum mechanics, as well as field theories placed in AdS_2 [118]. The conformal bootstrap equations in 1D are relatively simple since the conformal blocks are hypergeometric functions of a single cross-ratio z . Moreover, the global conformal blocks in 2D are products of two copies of 1D conformal blocks so one can hope to lift bootstrap results from 1D to 2D.

In chapter 2, we presented numerical evidence that in unitary 1D CFTs, the optimal upper bound on the scaling dimension of the lowest primary operator above identity in the OPE of two identical primary operators $\psi(x)$ is

$$\tilde{\Delta} = 2\Delta_{\psi} + 1 \tag{4.2}$$

for any $\Delta_{\psi} > 0$. In fact, the bound can not be any lower since this value is saturated by the boundary correlators of a free massive Majorana fermion in AdS_2 . Indeed, the primary operators in the $\psi \times \psi$ OPE are the two-particle states $\psi \overleftrightarrow{\partial}^{2j+1} \psi$, $j \geq 0$, the lowest scaling dimension being $2\Delta_{\psi} + 1$.

We will prove that $2\Delta_\psi + 1$ is the optimal bound for Δ_ψ positive integer or half-integer by analytically constructing the corresponding extremal functionals. Traditional numerical bootstrap relies on functionals in the form of linear combinations of derivatives in z evaluated at the crossing-symmetric point $z = 1/2$. We will demonstrate that the correct extremal functionals do not lie in the space spanned by this set. Instead, we will introduce a new class of functionals taking the form of integrals of the discontinuity of the conformal blocks on the branch cut $z \in (1, \infty)$ against a suitable integral kernel. The integral kernel corresponding to the extremal functional can be fixed analytically. We checked that the derivative functionals coming from the numerics converge to our analytic functional when expressed in the new basis as we approach the optimal bound.

Thanks to its distinguished nature, the analytic extremal functional ω_{Δ_ψ} can be expected to imply important consequences for any 1D CFT. Acting with ω_{Δ_ψ} on the equation (4.1), we obtain

$$\sum_{\mathcal{O} \in \psi \times \psi} (c_{\psi\psi\mathcal{O}})^2 \omega_{\Delta_\psi}(F_{\mathcal{O}}(z)) = 0. \quad (4.3)$$

The free fermion theory trivially satisfies this equation since ω_{Δ_ψ} vanishes on the spectrum of the extremal solution. However, (4.3) represents a universal constraint satisfied by any consistent four-point function. This constraint is particularly revealing for $\Delta_\psi \gg 1$. We will show that a family of unitary solutions of (4.3) where the dimensions of all primary operators scale linearly with Δ_ψ as $\Delta_\psi \rightarrow \infty$ has many features of a boundary four-point function corresponding to scattering in a massive QFT placed in large AdS_2 . Specifically, we will recover the precise exponential suppression of OPE coefficients of operators corresponding to bound states seen in [118–120] and universal behaviour of OPE coefficients corresponding to two-particle states derived in [118]. The validity of equation (4.3) will then be seen to require analyticity of the flat-space S-matrix in the upper-half plane, together with a sum rule for the OPE coefficients of two-particle states at rest.

Finally, we can use the relationship between 1D conformal blocks and 2D global conformal blocks to lift the 1D extremal functionals to closely related functionals acting on the 2D crossing equation. These functionals then imply that the OPE of two identical scalar primaries $\phi(x)$ must contain a non-identity global conformal primary with twist τ satisfying

$$\tau \leq 2\Delta_\phi + 2. \quad (4.4)$$

This bound is valid without assuming Virasoro symmetry, so also for 2D conformal boundaries and surface defects. Theories with Virasoro symmetry automatically satisfy it thanks to the existence of zero-twist operators other than identity. However, when $0 < \Delta_\phi < 1$, we can show that the bound must be satisfied by a primary with strictly positive twist, thereby getting a nontrivial prediction also in the presence of Virasoro symmetry.

The rest of this chapter is organized as follows. Section 4.2 is a review of ideas useful in the remaining parts, namely extremal functionals and the conformal bootstrap in 1D. We use section 4.3 to motivate and introduce a new class of 1D bootstrap functionals. In section 4.4, we explain the virtues of the new basis and analytically construct the extremal functional for $\Delta_\psi = 1/2$. We extend the construction to other integer and half-integer values of Δ_ψ in section 4.5. We explain how applying the new functionals at large Δ_ψ naturally leads to the physics of massive (1+1)D QFTs in large AdS₂ in section 4.6 and prove an upper bound on the minimal twist in 2D in section 4.7. Future directions are outlined in section 4.8.

4.2 Review

4.2.1 The conformal bootstrap and extremal functionals

The simplest example of constraints that the conformal bootstrap imposes on the low-lying spectrum of primary operators comes from considering the four-point function of a neutral scalar primary operator $\phi(x)$. Thanks to the conformal symmetry, the four-point function takes the form

$$\langle \phi(x_1)\phi(x_2)\phi(x_3)\phi(x_4) \rangle = \frac{1}{|x_{12}|^{2\Delta_\phi}|x_{34}|^{2\Delta_\phi}} A(z, \bar{z}), \quad (4.5)$$

with $A(z, \bar{z})$ unconstrained by conformal symmetry alone, and where z and \bar{z} are defined by their relation to the conformal cross-ratios

$$z\bar{z} = \frac{x_{12}^2 x_{34}^3}{x_{13}^2 x_{24}^2}, \quad (1-z)(1-\bar{z}) = \frac{x_{14}^2 x_{23}^3}{x_{13}^2 x_{24}^2}, \quad (4.6)$$

with $x_{ij} = x_i - x_j$. Applying the operator product expansion (OPE) to $\phi(x_1)\phi(x_2)$ leads to the following expansion of $A(z, \bar{z})$

$$A(z, \bar{z}) = \sum_{\mathcal{O} \in \phi \times \phi} (c_{\phi\phi\mathcal{O}})^2 G_{\Delta_{\mathcal{O}}, s_{\mathcal{O}}}(z, \bar{z}), \quad (4.7)$$

where the sum ranges through primary operators appearing in the $\phi \times \phi$ OPE, which are characterized by their scaling dimension $\Delta_{\mathcal{O}}$ and spin $s_{\mathcal{O}}$. The conformal blocks $G_{\Delta, s}(z, \bar{z})$ are fixed by conformal symmetry in terms of Δ , s and the dimension of spacetime d . In unitary theories, $(c_{\phi\phi\mathcal{O}})^2$ has the following interpretation in terms of the scalar product $\langle \cdot | \cdot \rangle$ in the Hilbert space of the theory on $S^{d-1} \times \mathbb{R}$

$$(c_{\phi\phi\mathcal{O}})^2 = \frac{\langle \phi | \phi(0) | \mathcal{O} \rangle \langle \mathcal{O} | \phi(0) | \phi \rangle}{\langle \mathcal{O} | \mathcal{O} \rangle} = \frac{|\langle \mathcal{O} | \phi(0) | \phi \rangle|^2}{\langle \mathcal{O} | \mathcal{O} \rangle} \quad (4.8)$$

and thus is positive. We can assume the identity operator appears in the $\phi \times \phi$ OPE. Crucially, we can also apply the OPE to $\phi(x_1)\phi(x_4)$, leading to the expansion

$$A(z, \bar{z}) = \left[\frac{z\bar{z}}{(1-z)(1-\bar{z})} \right]^{\Delta_\phi} \sum_{\mathcal{O} \in \phi \times \phi} (c_{\phi\phi\mathcal{O}})^2 G_{\Delta_\mathcal{O}, s_\mathcal{O}}(1-z, 1-\bar{z}). \quad (4.9)$$

The consistency of the expansions (4.7), (4.9) can be written more succinctly as

$$\sum_{\mathcal{O} \in \phi \times \phi} (c_{\phi\phi\mathcal{O}})^2 F_{\Delta_\mathcal{O}, s_\mathcal{O}}(z, \bar{z}) = 0, \quad (4.10)$$

where

$$F_{\Delta, s}(z, \bar{z}) = (z\bar{z})^{-\Delta_\phi} G_{\Delta, s}(z, \bar{z}) - (z \leftrightarrow 1-z, \bar{z} \leftrightarrow 1-\bar{z}). \quad (4.11)$$

Equation (4.10) imposes constraints on the spectrum of primary operators in the $\phi \times \phi$ OPE. Only for certain choices of the spectrum will there exist positive coefficients $(c_{\phi\phi\mathcal{O}})^2$ satisfying (4.10). $F_{\Delta, s}(z, \bar{z})$ should be thought of as a holomorphic function of two independent complex variables z, \bar{z} . In each of the variables, it has branch points at $z, \bar{z} = 0, 1, \infty$, where the branch cuts can be chosen to run from $-\infty$ to 0 and from 1 to ∞ . Equation (4.10) holds everywhere away from these branch cuts. Either of the two OPE expansions stops converging on some of the branch cuts, and consequently it is not legal to analytically continue the equation through the branch cuts. However, the equation holds arbitrarily close to the branch cuts, provided we stay on the first sheet.

The mechanism through which equation (4.10) constrains the spectrum in the $\phi \times \phi$ OPE can be usefully cast in the language of linear functionals ω acting on the functions $F_{\Delta, s}(z, \bar{z})$. Indeed, suppose we have such functional

$$\omega : F_{\Delta, s} \mapsto \omega(\Delta, s) \in \mathbb{R} \quad (4.12)$$

and suppose that ω is non-negative on a candidate spectrum \mathcal{S} of primary operators appearing in the $\phi \times \phi$ OPE

$$\forall (\Delta, s) \in \mathcal{S} : \quad \omega(\Delta, s) \geq 0. \quad (4.13)$$

Applying ω to (4.10) we find that \mathcal{S} can be a consistent spectrum only if ω vanishes on all of \mathcal{S} . Moreover, the converse also holds, namely whenever we have a spectrum \mathcal{S} for which no solution of (4.10) can be found, there is always a functional non-negative on all of \mathcal{S} and strictly positive on at least one operator $(\Delta, s) \in \mathcal{S}$.

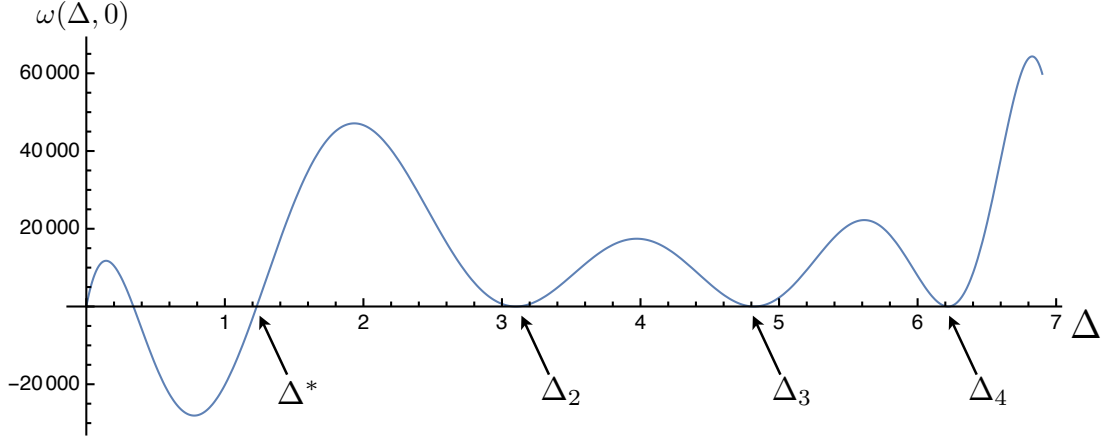


Figure 4.1: The action of a typical extremal functional for the bound on the scalar gap on $F_{\Delta,0}$. The leading non-identity operator appears at a first-order zero with a positive slope, while higher operators lie at second-order zeros.

In order to search for an upper bound on the gap in the scalar sector above identity without reference to the rest of the spectrum, we should focus on nonzero functionals such that¹

$$\begin{aligned}
 \omega(0,0) &\geq 0 \\
 \omega(\Delta,0) &\geq 0 \quad \text{for } \Delta \geq \Delta^* \\
 \omega(\Delta,s) &\geq 0 \quad \text{for } \Delta \geq d+s-2 \text{ and } s \geq 2.
 \end{aligned} \tag{4.14}$$

The minimal Δ^* for which such ω exists coincides with the upper bound on the scalar gap. We denote this upper bound as $\tilde{\Delta}$. Consider a unitary solution to crossing with gap $\tilde{\Delta}$. As pointed out in [23], all operators in the solution must correspond to zeros of any functional ω for which $\Delta^* = \tilde{\Delta}$. Functionals for which $\Delta^* = \tilde{\Delta}$ are called extremal functionals. Figure 4.1 illustrates how a typical extremal functional corresponding to the upper bound on the scalar gap acts on $F_{\Delta,0}$. It vanishes at $\Delta = 0$ and has a first-order zero and positive slope at the lowest non-identity operator with dimension Δ^* . The functional must be negative immediately to the left of Δ^* since otherwise it would not exclude solutions with gap smaller than Δ^* . Higher-lying scalar operators in the spectrum sit at second-order zeros since the functional must vanish there without ever becoming negative for $\Delta > \Delta^*$.

Generically, we expect both the extremal functional and the corresponding extremal

¹In numerical implementations, the first condition is usually replaced by $\omega(0,0) = 1$ in order to avoid the identically zero functional. Such functionals can only become extremal asymptotically, when $\omega(\Delta,s)/\omega(0,0) \rightarrow \infty$ for a generic (Δ,s) outside of the spectrum.

solution of (4.10) to be unique up to an overall positive rescaling. One counterexample is the free theory point in 4D, i.e. $\Delta_\phi = 1$, where an infinite class of extremal functionals leads to the unique free theory solution. The extremal functionals for the 1D bound studied in this chapter will be unique up to an overall rescaling. There is no reason for all the zeros of the extremal functional to correspond to operators appearing in the solution to crossing with nonzero OPE coefficient. A typical example is the first first-order zero in Figure 4.1 with negative slope, but sometimes even spurious second-order zeros can occur above Δ^* . We will find that the extremal functionals for 1D bootstrap do not contain such subtleties.

One should view the extremal functional as the optimal lens with which to study the bootstrap equation. It is the functional that projects the infinite-dimensional bootstrap equation on a one-dimensional space in the most revealing manner. It is likely that understanding the mechanism through which the conformal bootstrap leads to bounds on the gap, features in these bounds as well as islands in multi-correlator bootstrap amounts to understanding the precise nature of the extremal functionals. In this chapter, we will also see that extremal functionals carry valuable physical information about solutions to crossing distinct from the extremal solution. Indeed, the extremal functionals for the 1D bootstrap bound will be shown to naturally lead to the physics of QFT in AdS_2 of large radius when the external scaling dimensions are large.

4.2.2 The conformal bootstrap in one dimension

There are good reasons to start an analytic study of the constraining power of the bootstrap equations in one spacetime dimension. The kinematics is very simple, and explicit formulas exist for arbitrary conformal blocks. Moreover, one can hope to lift the 1D results to 2D, where the conformal blocks are linear combinations of products of the 1D blocks. Finally, as we saw in chapter 2, an explicit formula likely exists for the optimal 1D bootstrap bound, begging for an analytic explanation. Numerous interesting systems exhibit the global conformal symmetry in one dimension, including conformal boundaries in 2D CFTs, line defects in general CFTs [1, 60], and various examples of $\text{AdS}_2/\text{CFT}_1$ holography.

Here and in the rest of the chapter, by conformal symmetry we always mean the global conformal symmetry. In one dimension, the conformal group is $SL(2)$, with generators D, P, K satisfying commutation relations

$$[D, P] = P, \quad [D, K] = -K, \quad [K, P] = 2D. \quad (4.15)$$

Unitary highest-weight representations, corresponding to primary fields, are labelled by the scaling dimension Δ . There are no rotations and therefore no spin. Two- and three-point

functions are completely fixed in terms of Δ_i and structure constants c_{ijk} .² Four points on a line give rise to a single cross-ratio

$$z = \frac{x_{12}x_{34}}{x_{13}x_{24}}. \quad (4.16)$$

We can focus on the kinematic region where $x_1 < x_2 < x_3 < x_4$ and use the three conformal generators to set $x_1 = 0$, $x_3 = 1$, $x_4 = \infty$, so that $x_2 = z \in (0, 1)$. The four-point function of identical primary fields $\psi(x)$ takes the form

$$\langle \psi(x_1)\psi(x_2)\psi(x_3)\psi(x_4) \rangle = \frac{1}{|x_{12}|^{2\Delta_\psi}|x_{34}|^{2\Delta_\psi}} A(z), \quad (4.17)$$

where $A(z)$ can be expanded in conformal blocks

$$A(z) = \sum_{\mathcal{O} \in \psi \times \psi} (c_{\psi\psi\mathcal{O}})^2 G_{\Delta_{\mathcal{O}}}(z). \quad (4.18)$$

The 1D conformal block is just the chiral half of the 2D global conformal block [88]

$$G_\Delta(z) = z^\Delta {}_2F_1(\Delta, \Delta; 2\Delta; z). \quad (4.19)$$

Assuming $\psi(x)$ is a real field, the conformal block expansion starts with the identity operator with $\Delta = 0$. The crossing equation reads

$$\sum_{\mathcal{O} \in \psi \times \psi} (c_{\psi\psi\mathcal{O}})^2 F_{\Delta_{\mathcal{O}}}(z) = 0, \quad (4.20)$$

where

$$F_\Delta(z) = z^{-2\Delta_\psi} G_\Delta(z) - (1-z)^{-2\Delta_\psi} G_\Delta(1-z). \quad (4.21)$$

As we saw in section 2.4, standard numerical bootstrap applied to (4.20) using derivatives at the crossing-symmetric point $z = 1/2$ leads to an upper bound on the scaling dimension of the first non-identity operator in the $\psi \times \psi$ OPE. The bound seems to converge to

$$\tilde{\Delta} = 2\Delta_\psi + 1 \quad (4.22)$$

as the number of derivatives is increased. Figure 4.2, which we repeat here for reader's convenience from chapter 2, shows a comparison of the numerical bound using 50 derivatives and the exact line (4.22). The matching seems to deteriorate for higher Δ_ψ . It is a well-known feature of numerical bootstrap using derivatives that convergence slows down

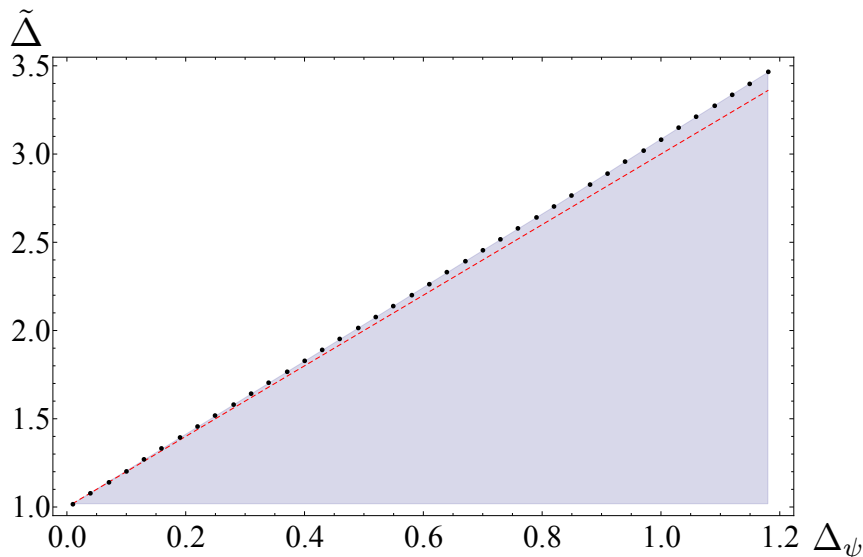


Figure 4.2: Black dots: Numerical bootstrap bound on the gap above identity following from (4.20), using 50 derivatives. Red dashed line: $\tilde{\Delta} = 2\Delta_\psi + 1$.

dramatically as the external scaling dimension is increased, so one should not take this mismatch too seriously.

In fact, the bound can never be lower than $2\Delta_\psi + 1$ because this value is saturated by the unitary solution to crossing corresponding to the generalized free real fermion in 1D, which also arises as the boundary dual of the free massive Majorana fermion in AdS_2 . The four-point function takes the form

$$\langle \psi(x_1)\psi(x_2)\psi(x_3)\psi(x_4) \rangle = \frac{1}{|x_{12}|^{2\Delta_\psi}|x_{34}|^{2\Delta_\psi}} - \frac{1}{|x_{13}|^{2\Delta_\psi}|x_{24}|^{2\Delta_\psi}} + \frac{1}{|x_{14}|^{2\Delta_\psi}|x_{23}|^{2\Delta_\psi}}, \quad (4.23)$$

where Δ_ψ can take an arbitrary positive value. In other words

$$A(z) = 1 + \left(\frac{z}{1-z} \right)^{2\Delta_\psi} - z^{2\Delta_\psi}. \quad (4.24)$$

$A(z)$ can be decomposed in conformal blocks with positive coefficients, the spectrum being

$$\Delta_j = 2\Delta_\psi + 2j + 1, \quad j \in \mathbb{Z}_{\geq 0}. \quad (4.25)$$

²Note that unlike in higher dimensions, $c_{ijk} \neq c_{jik}$ in general because two operators can not be continuously swapped in 1D. However, we still expect $c_{ijk} = c_{jki}$ since a line is conformally equivalent to a circle.

The primary operators appearing in this OPE are $\psi \overleftrightarrow{\partial}^{2j+1} \psi$, corresponding to two-particle states in AdS_2 . The gap is indeed $2\Delta_\psi + 1$. The existence of this solution together with evidence from the numerics suggests $2\Delta_\psi + 1$ is the optimal bootstrap bound. As explained in the previous subsection, proving this claim amounts to constructing (for each $\Delta_\psi > 0$) a nonzero functional ω_{Δ_ψ} acting on functions $F_\Delta(z)$ defined in (4.21)

$$\omega_{\Delta_\psi} : F_\Delta(z) \mapsto \omega_{\Delta_\psi}(\Delta) \in \mathbb{R} \quad (4.26)$$

such that

$$\begin{aligned} \omega_{\Delta_\psi}(0) &= 0 \\ \omega_{\Delta_\psi}(\Delta) &= 0 \quad \text{for } \Delta = 2\Delta_\psi + 2j + 1, \quad j \in \mathbb{Z}_{\geq 0} \\ \omega_{\Delta_\psi}(\Delta) &\geq 0 \quad \text{for } \Delta \geq 2\Delta_\psi + 1 \end{aligned} \quad (4.27)$$

One of the main results of this chapter is to construct such ω_{Δ_ψ} explicitly when Δ_ψ is a positive integer or half-integer, and thus find the optimal bootstrap bound for these values.

4.3 From derivative functionals towards the new basis

4.3.1 Inadequacy of the z -derivatives and the Zhukovsky variable

We will now discuss what the numerics have to say about the nature of the extremal functionals and introduce a new class of functionals that we use to construct the extremal functionals analytically in later sections. The discussion is framed in the context of 1D bootstrap but we expect analogous comments to apply in higher dimensions too.

Numerical searches for functionals excluding candidate spectra have used the basis consisting of derivatives of functions $F_\Delta(z)$ defined through (4.21), evaluated at the crossing-symmetric point $z = 1/2$. In practice, one truncates the space to derivatives of maximal degree $2N - 1$. Let $\omega^{(N)}$ be the extremal functional in this truncated space and write

$$\omega^{(N)} = \sum_{j=1}^N \frac{a_j^{(N)}}{(2j-1)!} \left. \frac{d^{2j-1}}{dz^{2j-1}} \right|_{z=1/2} \quad (4.28)$$

with $a_j^{(N)} \in \mathbb{R}$. It is natural to wonder whether the extremal functional corresponding to the optimal bootstrap bound lies in the basis of derivatives, in other words whether $\omega^{(N)}$ converges in this basis as $N \rightarrow \infty$. At least for the 1D bootstrap problem at hand, the numerics indicate that this is not the case, and we expect the same happens in higher

dimensions too. Since the functional is defined only up to an overall positive rescaling, let us normalize the leading coefficient as $|a_1^{(N)}| = 1$. It turns out that (for any Δ_ψ) as N is increased, higher coefficients diverge as increasing powers of N

$$a_j^{(N)} \stackrel{N \rightarrow \infty}{\sim} \beta_j N^{j-1}. \quad (4.29)$$

Hence the optimal extremal functional can not be a linear combination of derivatives at $z = 1/2$. The result (4.29) resembles the evaluation of functions $F_\Delta(z)$ at a point that moves to infinity in the z -plane as N increases. There is another instructive way to look at this divergence as follows. Equation (4.20) holds everywhere in the complex z -plane away from the branch cuts located at $z \in (-\infty, 0)$ and $z \in (1, \infty)$. However, derivatives at $z = 1/2$ have access to information about $F_\Delta(z)$ only within the radius of convergence of $F_\Delta(z)$ around this point, i.e. only in $|z - 1/2| < 1/2$, see Figure 4.3. The result (4.29) is thus telling us that the existence of the optimal bootstrap bound crucially relies on complex analytic behaviour of the functions $F_\Delta(z)$ outside of this disc.

There is a simple way to keep using derivatives at $z = 1/2$ while getting access to the whole complex plane. We can map the complex plane without the two branch cuts to the interior of the unit disc via a version of the Zhukovsky transformation

$$z(y) = \frac{(1+y)^2}{2(1+y^2)}, \quad (4.30)$$

illustrated in Figure 4.3.

The points $z = 0, 1/2, 1$ correspond to $y = -1, 0, 1$ respectively, while $z = \infty$ corresponds to the pair $y = \pm i$. The pair of branch cuts in the z -plane gets mapped to the unit circle. Crossing symmetry $z \leftrightarrow 1 - z$ gets mapped to $y \leftrightarrow -y$ and the Taylor expansion of $F_\Delta(z(y))$ around $y = 0$ converges in the whole interior of the unit disc.

We can wonder whether the optimal extremal functional can be written as a linear combination of derivatives with respect to y evaluated at $y = 0$. For any finite N , the space of functionals generated by $\{\partial_z^{2j-1}|_{z=1/2}, 1 \leq j \leq N\}$ and by $\{\partial_y^{2j-1}|_{y=0}, 1 \leq j \leq N\}$ coincide. However, when we express the extremal functional for any finite N in terms of the y -derivatives as

$$\omega^{(N)} = \sum_{j=1}^N \frac{b_j^{(N)}}{(2j-1)!} \left. \frac{d^{2j-1}}{dy^{2j-1}} \right|_{y=0} \quad (4.31)$$

and normalize $|b_1^{(N)}| = 1$, we find the other coefficients converge

$$b_j \equiv \lim_{N \rightarrow \infty} b_j^{(N)}, \quad (4.32)$$

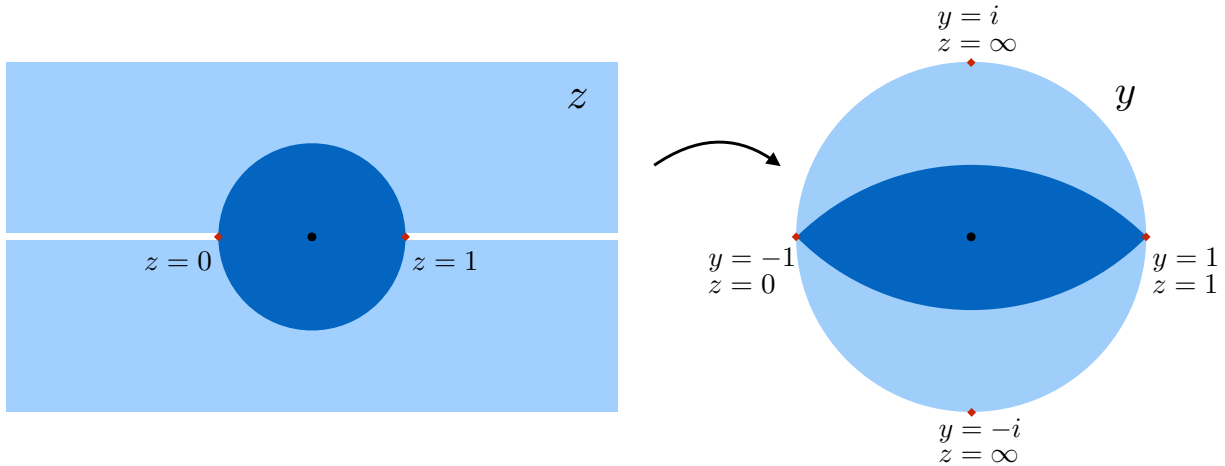


Figure 4.3: The transformation (4.30) between the z and y coordinates. z -derivatives evaluated at $z = 1/2$ can reconstruct the values of $F_{\Delta}(z)$ only in the dark-blue region, while y -derivatives at $y = 0$ can reconstruct the values everywhere away from the branch cuts.

in other words, the optimal extremal functional can be written as

$$\omega = \sum_{j=1}^{\infty} \frac{b_j}{(2j-1)!} \left. \frac{d^{2j-1}}{dy^{2j-1}} \right|_{y=0} \quad (4.33)$$

for some $b_j \in \mathbb{R}$. One could now try to fix coefficients b_j leading to a functional with the desired properties (4.27). However, it will turn out there is another representation of ω better suited for this task. This representation takes the form of an integral of the discontinuity of $F_{\Delta}(z)$ across the branch cut $z \in (1, \infty)$ against suitable integral kernels. To go from y -derivatives to such integrals, notice first that any derivative at $y = 0$ of a function $f(y)$ holomorphic inside the unit disc can be written as a contour integral

$$f^{(k)}(0) = \frac{k!}{2\pi i} \oint_{\Gamma} \frac{dy}{y} y^{-k} f(y), \quad (4.34)$$

where the contour Γ winds once around the origin and lies inside the unit disc. If $k \geq 1$, nothing changes with the insertion of an extra holomorphic term

$$f^{(k)}(0) = \frac{k!}{2\pi i} \oint_{\Gamma} \frac{dy}{y} (y^{-k} - y^k) f(y). \quad (4.35)$$

Taking Γ to be the unit circle,³ parametrized as $y = e^{i\theta}$, the integral becomes

$$f^{(k)}(0) = \frac{k!}{i\pi} \int_0^{2\pi} d\theta \sin(k\theta) f(e^{i\theta}) . \quad (4.36)$$

Since we will be taking $f(y) = F_\Delta(z(y))$, we can assume $f(\bar{y}) = f(y)$. Consequently, the last integral is only sensitive to the imaginary part of $f(y)$ on the unit circle. A general odd derivative functional can now be written as

$$\omega(f) = \sum_{j=1}^{\infty} \frac{b_j}{(2j-1)!} f^{(2j-1)}(0) = \frac{1}{\pi} \int_0^{2\pi} d\theta g(\theta) \text{Im}[f(e^{i\theta})] , \quad (4.37)$$

where

$$g(\theta) = \sum_{j=1}^{\infty} b_j \sin[(2j-1)\theta] . \quad (4.38)$$

We can use symmetries of $F_\Delta(z)$ to simplify the result to

$$\omega(F_\Delta) = \frac{4}{\pi} \int_0^{\pi/2} d\theta g(\theta) \text{Im}[F_\Delta(z(e^{i\theta}))] \quad (4.39)$$

with $z(y)$ given by (4.30). Since the unit circle in the y -coordinate corresponds to the pair of branch cuts of F_Δ in the z -coordinate, we see that we can write the functional as an integral of the imaginary part, or in other words discontinuity, of $F_\Delta(z)$ on the branch cut $z \in (1, \infty)$ against an appropriate integral kernel.⁴ The coefficients b_j are simply the Fourier coefficients of this kernel when the latter is written in the θ coordinate. However, there is a basis of functions on the branch cut which is more natural than the sines for the problem at hand. Namely the complete set of eigenfunctions of the conformal Casimir regular at the endpoints of the branch cut. In 1D, these eigenfunctions are simply Legendre polynomials of an appropriate coordinate. We are going to show soon how to fix the coefficients of the extremal functionals analytically in this basis. We can then always use the representation (4.38) and (4.39) to go back to the derivative basis.

³The contour can be taken all the way to the unit circle only in the absence of singularities of $f(y)$ on $|y| = 1$. If these are present, we need to avoid them along infinitesimal arcs in the interior of the unit circle.

⁴We thank Miguel Paulos for suggesting to look at functionals involving the discontinuity of the conformal block.

4.3.2 The new basis

As explained in the previous section, we want to write the extremal functionals as integral kernels applied to the imaginary part of F_Δ defined in (4.21) on the branch cut $z \in (1, \infty)$. Let us write

$$F_\Delta(z) = g_\Delta(z) - g_\Delta(1 - z), \quad (4.40)$$

where

$$g_\Delta(z) = z^{\Delta-2\Delta_\psi} {}_2F_1(\Delta, \Delta; 2\Delta; z). \quad (4.41)$$

It is convenient to map the branch cut to the unit interval $x \in (0, 1)$ via

$$x = \frac{z-1}{z}. \quad (4.42)$$

Let us denote

$$\begin{aligned} f_\Delta^+(x) &= \lim_{\epsilon \rightarrow 0^+} \frac{1}{\pi} \text{Im} [g_\Delta(z(x) + i\epsilon)] \\ f_\Delta^-(x) &= \lim_{\epsilon \rightarrow 0^+} \frac{1}{\pi} \text{Im} [g_\Delta(1 - z(x) - i\epsilon)] \end{aligned} \quad (4.43)$$

It is not hard to evaluate $f_\Delta^\pm(x)$

$$\begin{aligned} f_\Delta^+(x) &= (1-x)^{2\Delta_\psi} \frac{\Gamma(2\Delta)}{\Gamma(\Delta)^2} {}_2F_1(\Delta, 1-\Delta; 1; x) \\ f_\Delta^-(x) &= -(1-x)^{2\Delta_\psi} \frac{\sin[\pi(\Delta - 2\Delta_\psi)]}{\pi} x^{\Delta-2\Delta_\psi} {}_2F_1(\Delta, \Delta; 2\Delta; x). \end{aligned} \quad (4.44)$$

$f_\Delta^+(x)$ is coming from the logarithmic branch cut of the direct channel conformal block starting at $z = 1$. The crossed channel conformal block has a power-law singularity at $z = 1$, so that $f_\Delta^-(x)$ is essentially the original conformal block with a sine prefactor. We are going to study functionals of the form

$$\begin{aligned} \omega(F_\Delta) &= \frac{1}{\pi} \int_0^1 dx h(x) (1-x)^{-2\Delta_\psi} \text{Im} [F_\Delta(z(x) + i\epsilon)] \\ &= \int_0^1 dx h(x) (1-x)^{-2\Delta_\psi} [f_\Delta^+(x) - f_\Delta^-(x)] \end{aligned} \quad (4.45)$$

where $h(x)$ is a suitable integral kernel. We also explicitly eliminated the prefactor $(1-x)^{2\Delta_\psi}$ common to $f_\Delta^\pm(x)$. It is natural to expand $h(x)$ in the basis of solution of the

conformal Casimir equation which are regular at $x = 0, 1$. Note that this choice breaks the symmetry between the direct and crossed conformal block since the Casimir equation is not invariant under $z \leftrightarrow 1 - z$. However, we will see that the symmetry is partially restored by the full $h(x)$. The conformal Casimir equation in the direct channel written in the x -coordinate is just the Legendre differential equation

$$\frac{d}{dx} \left[x(1-x) \frac{dg(x)}{dx} \right] + \Delta(\Delta - 1)g(x) = 0. \quad (4.46)$$

The solutions regular at $x = 0, 1$ have $\Delta = n \in \mathbb{N}$ and read

$$p_n(x) = {}_2F_1(n, 1 - n; 1; x) = (-1)^{n-1} P_{n-1}(2x - 1), \quad (4.47)$$

where $P_m(y)$ are the Legendre polynomials. $p_n(x)$ form a complete set of functions on $x \in [0, 1]$ orthogonal with respect to the standard inner product with constant weight. We can expand $h(x)$ in this basis

$$h(x) = \sum_{n=1}^{\infty} a_n p_n(x). \quad (4.48)$$

In the following sections, we are going to present analytic formulas for a_n that make ω into extremal functionals. Substituting (4.48) into (4.45), the action of ω becomes (we use $\omega(F_\Delta)$ and $\omega(\Delta)$ interchangeably in this chapter)

$$\omega(\Delta) = \sum_{n=1}^{\infty} s(\Delta, n) a_n, \quad (4.49)$$

where

$$s(\Delta, n) = s^+(\Delta, n) - s^-(\Delta, n) \quad (4.50)$$

and we have defined overlaps of the imaginary part of F_Δ with our basis functionals

$$s^\pm(\Delta, n) = \int_0^1 dx (1-x)^{-2\Delta_\psi} f_\Delta^\pm(x) p_n(x). \quad (4.51)$$

The overlaps can be found in a closed form as follows. $(1-x)^{-2\Delta_\psi} f_\Delta^+(x)$ satisfies the differential equation (4.46), and so the overlap is particularly simple

$$s^+(\Delta, n) = \frac{\Gamma(2\Delta)}{\Gamma(\Delta)^2} \frac{\sin[\pi(\Delta - n)]}{\pi(\Delta - n)(\Delta + n - 1)}. \quad (4.52)$$

In particular, for $\Delta = m \in \mathbb{N}$, we find orthogonality

$$s^+(m, n) = \frac{\Gamma(2m)}{\Gamma(m)^2} \int_0^1 dx p_m(x) p_n(x) = \frac{\Gamma(2m-1)}{\Gamma(m)^2} \delta_{mn}. \quad (4.53)$$

The formula for $s^-(\Delta, n)$ is more complicated because the Casimir equations in the two channels do not coincide

$$s^-(\Delta, n) = (-1)^n \frac{\Gamma(2\Delta)}{\Gamma(\Delta)^2} \frac{\sin[\pi(\Delta - 2\Delta_\psi)]}{\pi} R_{\Delta_\psi}(\Delta, n), \quad (4.54)$$

where

$$R_{\Delta_\psi}(\Delta, n) \equiv \frac{\Gamma(\beta)^2 \Gamma(\gamma)^2}{\Gamma(\delta) \Gamma(\epsilon) \Gamma(\zeta)} {}_4F_3 \left(\begin{matrix} \beta & \beta & \gamma & \gamma \\ \delta & \epsilon & \zeta \end{matrix}; 1 \right) \quad (4.55)$$

with

$$\begin{aligned} \beta &= \Delta \\ \gamma &= \Delta - 2\Delta_\psi + 1 \\ \delta &= 2\Delta \\ \epsilon &= \Delta - 2\Delta_\psi - n + 2 \\ \zeta &= \Delta - 2\Delta_\psi + n + 1. \end{aligned} \quad (4.56)$$

A comment is in order concerning the regime of validity of (4.54). $f_\Delta^-(x) p_n(x) = O(x^{\Delta-2\Delta_\psi})$ as $x \rightarrow 0$, so we would expect $s^-(\Delta, n)$ to be defined only for $\Delta > 2\Delta_\psi - 1$. Indeed, $R_{\Delta_\psi}(\Delta, n)$ is an analytic function of Δ for $\Delta > 2\Delta_\psi - 1$ with a simple pole at $\Delta = 2\Delta_\psi - 1$. However, this pole is precisely cancelled by a zero of $\sin[\pi(\Delta - 2\Delta_\psi)]$ in the full expression for $s^-(\Delta, n)$. In fact, the formula (4.54) defines $s^-(\Delta, n)$ as a function analytic in Δ for any $\Delta \geq 0$. The reason is that the imaginary part of F_Δ^- on the branch cut is also the discontinuity of F_Δ^- across the branch cut. The integral (4.51) can then be thought of as a contour integral in the complex x -plane with the contour starting at $x = 1$, running under the branch cut, going around $x = 0$ and coming back to $x = 1$ above the branch cut. The contour can be deformed away from the real axis, and thus the singularity at $x = 0$ is avoided, as illustrated in Figure 4.4, leading to a finite answer for any $\Delta \geq 0$. The proper generalization of our functionals (4.45) to an arbitrary Δ is then

$$\omega(F_\Delta) = \frac{1}{2\pi i} \int_\Gamma dx h(x) (1-x)^{-2\Delta_\psi} F_\Delta(z(x)). \quad (4.57)$$

Note that when passing from derivatives at $y = 0$ to contour integrals as explained in the previous subsection, singularities of the integrand on the unit disc are avoided in the same

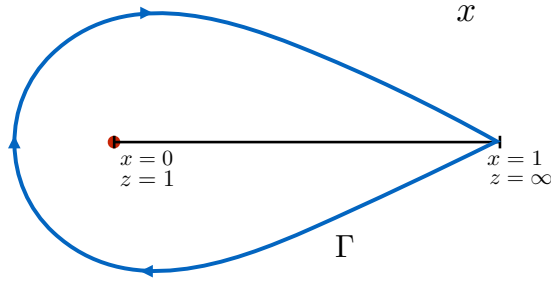


Figure 4.4: The choice of integration contour leading to a well-defined action of ω , equation (4.57).

manner. The bottom line is that the expression (4.54) can be trusted for any $\Delta \geq 0$. A further subtlety will later arise from the fact that $h(x)$, being an infinite linear combination of $p_n(x)$, develops a branch cut at $x \in (-\infty, 0)$. Some care will then be needed to give meaning to (4.57). However, no ambiguity is present when $h(x)$ is a single basis vector $p_n(x)$.

4.4 Constructing extremal functionals

4.4.1 General properties of the new basis

Let us first explain why the new basis is particularly suitable for the construction of extremal functionals for 1D bootstrap. We will assume that Δ_ψ is an integer or half-integer, so that the oscillating factors in (4.52) and (4.54) are in phase. The action of the general functional (4.45) can then be written as

$$\omega(\Delta) = \frac{\Gamma(2\Delta)}{\Gamma(\Delta)^2} \frac{\sin(\pi\Delta)}{\pi} \sum_{n=1}^{\infty} \hat{s}(\Delta, n) a_n, \quad (4.58)$$

where

$$\hat{s}(\Delta, n) = \frac{(-1)^n}{(\Delta - n)(\Delta + n - 1)} + (-1)^{2\Delta_\psi + n + 1} R_{\Delta_\psi}(\Delta, n). \quad (4.59)$$

In order to prove that the bootstrap bound is saturated by the generalized free fermion, we need to find coefficients a_n so that $\omega(\Delta)$ has the properties listed in (4.27). This means that $\Delta = 2\Delta_\psi + 1$ is a zero of odd order of $\omega(\Delta)$, while $\Delta = 2\Delta_\psi + 2j + 1$ is a zero of even order for any $j \in \mathbb{N}$. We will assume that in fact $\Delta = 2\Delta_\psi + 1$ is a simple zero and

the higher $\Delta = 2\Delta_\psi + 2j + 1$ are all double zeros. The first key property of our basis is that it is in a sense a basis dual to the set of functions F_Δ with $\Delta \in \mathbb{N}$ and $\Delta \geq 2\Delta_\psi$. Indeed, suppose $\Delta = m \in \mathbb{N}$. The sine prefactor in (4.58) guarantees that $\omega(m)$ can only be non-zero if the sum in (4.58) has a pole at $\Delta = m$. As explained in the previous section, $R_{\Delta_\psi}(\Delta, n)$ has no poles for $\Delta > 2\Delta_\psi - 1$, so that in this range of Δ the pole must come from the first term in (4.59) and the summand $n = m$. We conclude that

$$\omega(m) = \frac{\Gamma(2m-1)}{\Gamma(m)^2} a_m \quad \text{for } m \in \mathbb{N}, m \geq 2\Delta_\psi. \quad (4.60)$$

In other words, the coefficient a_m is proportional to the value of the functional at $\Delta = m$. It is also illuminating to consider the behaviour of the functionals at $\Delta = 0$. The prefactor in (4.58) has a double zero there, so any contribution must come from a double pole of $R_{\Delta_\psi}(\Delta, n)$. Indeed, there is such double pole, and its contribution can be written in a closed form

$$\omega(0) = -\frac{1}{\Gamma(2\Delta_\psi)^2} \sum_{n=2\Delta_\psi}^{\infty} (n-2\Delta_\psi+1)_{4\Delta_\psi-2} a_n, \quad (4.61)$$

where $(a)_b$ is the Pochhammer symbol. This formula also follows from applying ω to the solution of crossing corresponding to the massive scalar in AdS_2 and using (4.60). Note that the Pochhammer symbol is only non-vanishing for $n \geq 2\Delta_\psi$ and that it is positive in that range. It follows that if $\omega(0) = 0$, as is required from an extremal functional, the coefficients a_n for $n \geq 2\Delta_\psi$ must not all have the same sign. In particular, at least one of them, say a_{n^*} , is negative. Going back to (4.60), we conclude

$$\omega(n^*) < 0. \quad (4.62)$$

Hence the bootstrap bound following from the existence of ω must be strictly above $\Delta = n^*$. The lowest choice is $n^* = 2\Delta_\psi$, and we conclude that any bound following from the functionals at hand must lie strictly above $\Delta = 2\Delta_\psi$. Of course, we already knew this thanks to the existence of the generalized free fermion solution, but it is reassuring to see it follow so naturally in the present language. Assuming that ω is an extremal functional with the spectrum of the generalized free fermion, we can now conclude from (4.60) that

$$\begin{aligned} a_{2\Delta_\psi} &< 0 \\ a_{2\Delta_\psi+2j-1} &= 0 \quad \text{for } j \in \mathbb{N} \\ a_{2\Delta_\psi+2j} &> 0 \quad \text{for } j \in \mathbb{N}. \end{aligned} \quad (4.63)$$

Moreover, the condition $\omega(0) = 0$ determines $a_{2\Delta_\psi}$ in terms of the higher $a_{2\Delta_\psi+2j}$ through (4.61) as

$$a_{2\Delta_\psi} = - \sum_{j=1}^{\infty} \frac{(2j+1)_{4\Delta_\psi-2}}{(4\Delta_\psi-2)!} a_{2\Delta_\psi+2j}. \quad (4.64)$$

For the sum to be convergent, a_n must decay at least as fast as

$$a_n = O(n^{-\alpha}) \quad \text{as } n \rightarrow \infty \quad (4.65)$$

with

$$\alpha > 4\Delta_\psi - 1. \quad (4.66)$$

We will find out that in fact

$$\alpha = 4\Delta_\psi + 1. \quad (4.67)$$

In other words, the speed of convergence of the functionals to the optimal one improves with increasing Δ_ψ in the new basis. This is the exact opposite of what happens in the standard derivative basis, where high values of Δ_ψ require higher numbers of derivatives to achieve the same precision! This is one aspect of the particularly nice properties our functionals possess for $\Delta_\psi \gg 1$, elaborated on in section 4.6.

It remains to determine the values of a_n for $1 \leq n \leq 2\Delta_\psi - 1$ as well as $n = 2\Delta_\psi + 2j$ with $j \in \mathbb{Z}_{\geq 0}$. All these values of a_n are fixed by requiring that $\Delta = 2\Delta_\psi + 2j - 1$ are double zeros of the functional (4.58) for $j \geq 2$, while $\Delta = 2\Delta_\psi + 1$ is a simple zero. The sine prefactor has a simple zero at all these locations, so the existence of a double zero implies the sum in (4.58) must itself vanish there. Denote

$$\tilde{\omega}(\Delta) = \sum_{n=1}^{\infty} \hat{s}(\Delta, n) a_n. \quad (4.68)$$

The conditions of $\omega(\Delta)$ having a simple zero and positive derivative at $\Delta = 2\Delta_\psi + 1$ and double zeros at higher $\Delta = 2\Delta_\psi + 2j - 1$ read

$$\tilde{\omega}(2\Delta_\psi + 2j - 1) = (-1)^{2\Delta_\psi+1} \delta_{j1} \quad \text{for } j \in \mathbb{N}, \quad (4.69)$$

where the condition for $j = 1$ fixes the arbitrary normalization of ω . It is not hard to understand the mechanism of how these equations fix the values of non-zero a_n . We already know that $\tilde{\omega}(\Delta)$ has a simple pole at $\Delta = 2\Delta_\psi + 2j$ for $j \in \mathbb{N}$

$$\tilde{\omega}(2\Delta_\psi + 2j + \epsilon) \stackrel{\epsilon \rightarrow 0}{\sim} \frac{(-1)^{2\Delta_\psi}}{4\Delta_\psi + 4j - 1} \frac{a_{2\Delta_\psi+2j}}{\epsilon}. \quad (4.70)$$

Imagine changing Δ continuously from $\Delta = 2\Delta_\psi + 2j$ to $\Delta = 2\Delta_\psi + 2j + 2$. $\tilde{\omega}(\Delta)$ varies from plus to minus infinity, or vice versa, depending on the sign of $(-1)^{2\Delta_\psi}$. In any case, continuity implies

$$\tilde{\omega}(\Delta) = 0 \quad \text{for some } \Delta \in (2\Delta_\psi + 2j, 2\Delta_\psi + 2j + 2) \quad \text{for all } j \in \mathbb{N}. \quad (4.71)$$

It is only for a specific choice of values of a_n that all these zeroes of $\tilde{\omega}(\Delta)$ occur precisely at $\Delta = 2\Delta_\psi + 2j + 1$. In order to find those values, it is useful to think of (4.69) as an infinite matrix equation

$$\sum_{n=1}^{\infty} A_{jn} a_n = (-1)^{2\Delta_\psi+1} \delta_{j1} \quad \text{for } j \in \mathbb{N} \quad (4.72)$$

with

$$A_{jn} = \hat{s}(2\Delta_\psi + 2j - 1, n). \quad (4.73)$$

If the linear map defined by matrix A_{jn} were injective when acting on the subspace of a_n that is not fixed to zero by conditions (4.63), we could obtain a_n simply as the first column of the inverse of A_{jn}

$$a_n = (-1)^{2\Delta_\psi+1} A_{n1}^{-1}. \quad (4.74)$$

The injectivity is in general violated for $\Delta_\psi \geq 3/2$, and we will address this subtlety in section 4.5. Before we do that, let us first solve the case $\Delta_\psi = 1/2$, where a closed formula for $h(x)$ can be found more directly.

4.4.2 The extremal functional for $\Delta_\psi = 1/2$

Notice first that when $\Delta_\psi = 1/2$, orthogonality (4.60) is valid for all $m \in \mathbb{N}$. Since the extremal functional corresponding to the generalized free fermion should vanish for all $\Delta \in 2\mathbb{N}$, we conclude that only a_n with n odd can be nonzero

$$h(x) = \sum_{n \in 2\mathbb{N}-1} a_n p_n(x). \quad (4.75)$$

It follows from the symmetry property of the basis functions

$$p_n(x) = (-1)^{n-1} p_n(1-x) \quad (4.76)$$

that $h(x) = h(1-x)$. We would now like to impose the conditions on derivatives (4.69)

$$\begin{aligned} \omega'(2) &> 0 \\ \omega'(2j+2) &= 0 \quad \text{for } j \in \mathbb{N}, \end{aligned} \quad (4.77)$$

which take the explicit form

$$\sum_{n \in 2\mathbb{N}-1} \left[-\frac{1}{(\Delta-n)(\Delta+n-1)} - R_{\frac{1}{2}}(\Delta, n) \right] a_n = \begin{cases} 1 & \text{for } \Delta = 2 \\ 0 & \text{for } \Delta = 2j+2, j \in \mathbb{N}, \end{cases} \quad (4.78)$$

with $R_{\Delta_\psi}(\Delta, n)$ defined in (4.55). Rather than solving these equations directly for a_n , we will first express them in terms of scalar products of functions on the unit interval. Let us first define the following functions for $\Delta \in 2\mathbb{N}$

$$\begin{aligned} q_\Delta(x) &= Q_{\Delta-1}(2x-1) \\ r_\Delta(x) &= \frac{\Gamma(\Delta)^2}{2\Gamma(2\Delta)} [x^{\Delta-1} {}_2F_1(\Delta, \Delta; 2\Delta; x) + (1-x)^{\Delta-1} {}_2F_1(\Delta, \Delta; 2\Delta; 1-x)] \\ s_\Delta(x) &= q_\Delta(x) - r_\Delta(x), \end{aligned} \quad (4.79)$$

where $Q_m(y)$ is the Legendre function of the second kind. When $\Delta \in 2\mathbb{N}$ both $q_\Delta(x)$ and $r_\Delta(x)$ are symmetric under $x \leftrightarrow 1-x$ and hence

$$s_\Delta(1-x) = s_\Delta(x). \quad (4.80)$$

The leading logarithmic divergence and constant term of $q_\Delta(x)$ and $r_\Delta(x)$ at the boundary of the interval precisely cancel and we find $s_\Delta(0) = s_\Delta(1) = 0$. Define the usual scalar product on the space of function on the unit interval

$$\langle f, g \rangle = \int_0^1 dx f(x)g(x). \quad (4.81)$$

Unlike the Legendre polynomials, $q_\Delta(x)$ are not orthogonal with respect to this scalar product. However, the corrected functions $s_\Delta(x)$ are mutually orthogonal

$$\langle s_\Delta, s_{\Delta'} \rangle = \frac{\pi^2}{4(2\Delta-1)} \delta_{\Delta\Delta'} \quad \text{for } \Delta, \Delta' \in 2\mathbb{N}. \quad (4.82)$$

Indeed, $s_\Delta(x)$ form an orthogonal basis for functions on $x \in (0, 1)$ satisfying $f(x) = f(1-x)$. The crucial observation arises from computing the scalar product of $s_\Delta(x)$ and $p_n(x)$ with n odd

$$\langle s_\Delta, p_n \rangle = -\frac{1}{(\Delta-n)(\Delta+n-1)} - R_{\frac{1}{2}}(\Delta, n). \quad (4.83)$$

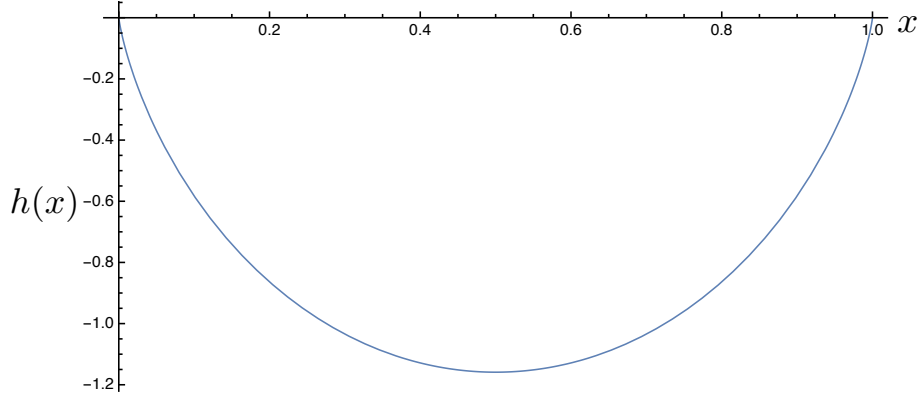


Figure 4.5: The integral kernel $h(x)$ for $\Delta_\psi = 1/2$, given by equation (4.86).

The first and second term come from the overlap with $q_\Delta(x)$ and $r_\Delta(x)$ respectively. We recognize that the scalar product is precisely the coefficient with which p_n contributes to the derivative of $\omega(\Delta)$! Equation (4.78) can thus be written simply as

$$\sum_{n=1}^{\infty} \langle s_{2j}, p_n \rangle a_n = \delta_{j1} \quad \text{for } j \in \mathbb{N}. \quad (4.84)$$

In other words

$$\langle s_{2j}, h \rangle = \delta_{j1} \quad \text{for } j \in \mathbb{N}, \quad (4.85)$$

where $h(x)$ is the sought integral kernel. Since $s_{2j}(x)$ are orthogonal, the last equation is telling us precisely that $h(x)$ must be proportional to $s_2(x)$. Hence, up to an overall irrelevant positive constant

$$h(x) = s_2(x) = \frac{1}{x(1-x)} - 1 + \left[\frac{x(2x^2 - 5x + 5)}{2(1-x)^2} \log(x) + (x \leftrightarrow 1-x) \right]. \quad (4.86)$$

Figure 4.5 shows the shape of $h(x)$. Note that $h(0) = h(1) = 0$, so that the integral in (4.45) is convergent on both ends. It is also possible to find a closed formula for the coefficients a_n . Define the function

$$\Omega_{\frac{1}{2}}(\Delta) = \frac{1}{(\Delta-2)(\Delta+1)} - \left[\Delta(\Delta-1) + \frac{1}{2} \right] \Psi' \left(\frac{\Delta}{2} \right) - 2, \quad (4.87)$$

where

$$\Psi(z) = \frac{d}{dz} \log \left[\frac{\Gamma(z + \frac{1}{2})}{\Gamma(z)} \right] = \psi(z + 1/2) - \psi(z), \quad (4.88)$$

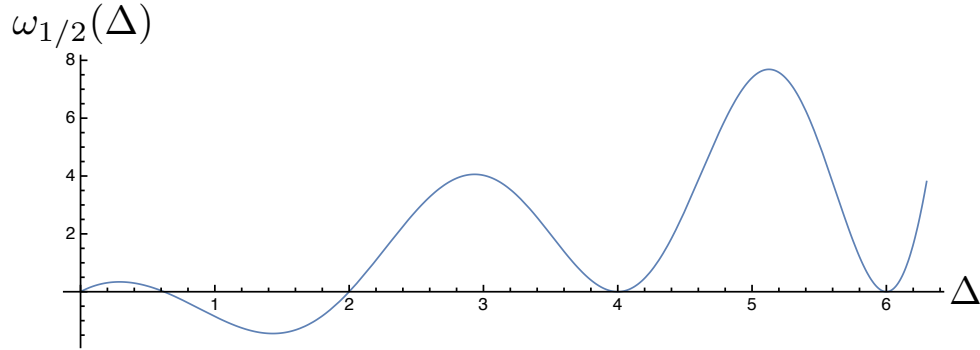


Figure 4.6: The action of the extremal functional for $\Delta_\psi = 1/2$, given by equation (4.91).

with $\psi(z)$ the digamma function. Coefficients a_n take the form

$$a_n = \begin{cases} (2n-1)\Omega_{\frac{1}{2}}(n) & \text{for } n \text{ odd} \\ 0 & \text{for } n \text{ even.} \end{cases} \quad (4.89)$$

The nonzero a_n decay like $a_n = O(n^{-3})$ as $n \rightarrow \infty$, a special case of the general formula $a_n = O(n^{-4\Delta_\psi-1})$. It is not hard to find a formula for the action of the extremal functional on F_Δ for any Δ . It follows from (4.60) that

$$\omega_{\frac{1}{2}}(\Delta) = \begin{cases} \frac{\Gamma(2\Delta)}{\Gamma(\Delta)^2} \Omega_{\frac{1}{2}}(\Delta) & \text{for } \Delta \in \mathbb{N} \text{ odd} \\ 0 & \text{for } \Delta \in \mathbb{N} \text{ even.} \end{cases} \quad (4.90)$$

The simplest meromorphic function of Δ interpolating between these values is

$$\omega_{\frac{1}{2}}(\Delta) = \frac{\Gamma(2\Delta)}{\Gamma(\Delta)^2} \sin^2\left(\frac{\pi\Delta}{2}\right) \Omega_{\frac{1}{2}}(\Delta), \quad (4.91)$$

which turns out to be the correct formula. The function $\omega_{\frac{1}{2}}(\Delta)$ is plotted in Figure 4.6. As expected, $\omega_{\frac{1}{2}}(\Delta)$ has double zeros at $\Delta = 2 + 2j$, $j \in \mathbb{N}$. The simple pole of $\Omega_{\frac{1}{2}}(\Delta)$ at $\Delta = 2$ makes this into a simple zero of $\omega_{\frac{1}{2}}(\Delta)$.

We can use the explicit formula for $h(x)$ to produce a closed formula for the coefficients b_j of the functional in the basis of y -derivatives evaluated at $y = 0$

$$\omega = \sum_{j=1}^{\infty} \frac{b_j}{(2j-1)!} \left. \frac{d^{2j-1}}{dy^{2j-1}} \right|_{y=0}, \quad (4.92)$$

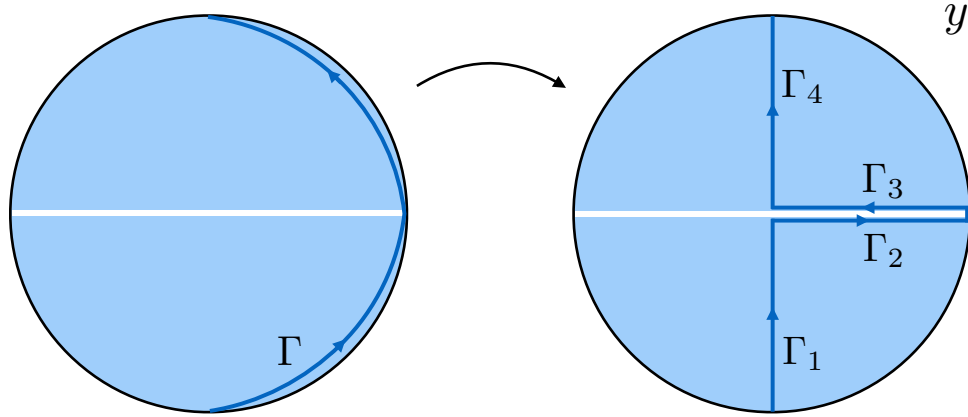


Figure 4.7: The contour deformation in the y -coordinate used to find a closed formula (4.100) for the coefficients b_j of the extremal functional in the y -derivative basis. The white stripe shows the branch cut of $h(x)$.

described in subsection 4.3.1. Recall from (4.57) that the action of the functional is⁵

$$\omega(\Delta) = \frac{1}{2\pi i} \int_{\Gamma} dx \frac{h(x)}{1-x} F_{\Delta}(x), \quad (4.93)$$

where the contour Γ is shown in Figure 4.4. However, formula (4.86) shows that $h(x)$ has a branch cut on $x \in (-\infty, 0)$ so the contour integral seems not well-defined since its value depends on where the contour Γ intersects the branch cut of $h(x)$. It is possible to see that the choice of Γ that reproduces the correct action (4.58) is the one intersecting the real axis arbitrarily close to $x = 0$. In other words, we recover the prescription (4.45). The advantage of the description using a contour integral passing arbitrarily close to $x = 0$ as opposed to (4.45) is that the former will be valid for any Δ_{ψ} . To pass to the derivative basis, let us start by transforming the integral (4.93) to the Zhukovsky coordinate y defined by (4.30), which is related to x via

$$x(y) = - \left(\frac{y-1}{y+1} \right)^2. \quad (4.94)$$

The contour Γ gets mapped to the blue curve in the left half of Figure 4.7. $F_{\Delta}(y)$ is holomorphic inside the unit circle of variable y . $h(x(y))$ has a branch cut along $y \in (-1, 1)$

⁵By a slight abuse of notation, we write $F_{\Delta}(x)$, $F_{\Delta}(y)$ instead of $F_{\Delta}(z(x))$, $F_{\Delta}(z(y))$ here and in the following.

coming from the $\log(x)$ term in (4.86). We can deform the contour as in Figure 4.7 to get a contour with four components as follows:

$$\begin{aligned}
\Gamma_1 : \quad y(t) &= -i + it & t \in [0, 1] \\
\Gamma_2 : \quad y(t) &= t - i\epsilon & t \in [0, 1] \\
\Gamma_3 : \quad y(t) &= 1 - t + i\epsilon & t \in [0, 1] \\
\Gamma_4 : \quad y(t) &= it & t \in [0, 1]
\end{aligned} \tag{4.95}$$

where $\epsilon \rightarrow 0^+$. The integrals along Γ_1 and Γ_4 combine to depend only on the imaginary part of $h(x(y))$ along the imaginary axis, the result being

$$\frac{1}{2\pi i} \int_{\Gamma_1 \cup \Gamma_4} dx \frac{h(x)}{1-x} F_\Delta(x) = - \int_{\Gamma_4} dy \frac{3y^4 + 26y^2 + 3}{(1-y^2)^3} F_\Delta(y). \tag{4.96}$$

The integrals along Γ_2 and Γ_3 combine to depend only on the discontinuity of $h(x(y))$ across the branch cut, the result being

$$\begin{aligned}
& \frac{1}{2\pi i} \int_{\Gamma_2 \cup \Gamma_3} dx \frac{h(x)}{1-x} F_\Delta(x) = \\
& = \int_0^1 dy \frac{(1-y)^3 (3y^4 + 3y^3 + 8y^2 + 3y + 3)}{(y+1)^3 (y^2+1)^3} F_\Delta(y).
\end{aligned} \tag{4.97}$$

The coefficients b_j can now be found by substituting the Taylor expansion of $F_\Delta(y)$ around $y = 0$ into (4.96) and (4.97). We find

$$\begin{aligned}
b_j^{(1)} &= - \int_{\Gamma_4} dy \frac{3y^4 + 26y^2 + 3}{(1-y^2)^3} y^{2j-1} = \\
&= \frac{(-1)^j}{4} \left[8(2j-1) - (4j-1)(4j-3) \Psi\left(\frac{j}{2}\right) \right],
\end{aligned} \tag{4.98}$$

with $\Psi(z)$ defined in (4.88). Similarly,

$$\begin{aligned}
b_j^{(2)} &= \int_0^1 dy \frac{(1-y)^3 (3y^4 + 3y^3 + 8y^2 + 3y + 3)}{(y+1)^3 (y^2+1)^3} y^{2j-1} = \\
&= \frac{(4j-3)(4j-1)}{2} \Psi(j) - \frac{(2j-3)(2j+1)}{16} \Psi\left(\frac{2j+1}{4}\right) - \frac{15j-11}{4}.
\end{aligned} \tag{4.99}$$

The derivative coefficients are simply the sum

$$b_j = b_j^{(1)} + b_j^{(2)}. \quad (4.100)$$

The first few values of b_j read

$$\begin{aligned} b_1 &= \frac{3}{4} - \frac{3}{16}\pi - \frac{3}{2}\log(2) \approx -0.878769 \\ b_2 &= \frac{55}{4} - \frac{5}{16}\pi - \frac{35}{2}\log(2) \approx 0.638177 \\ b_3 &= \frac{119}{4} + \frac{21}{16}\pi - \frac{99}{2}\log(2) \approx -0.437445 \\ b_4 &= \frac{307}{4} - \frac{45}{16}\pi - \frac{195}{2}\log(2) \approx 0.332421 \\ &\vdots \end{aligned} \quad (4.101)$$

Figure 4.8 shows a comparison between the exact values for b_j and those obtained by standard numerical bootstrap when derivatives are truncated to maximal degree N_{\max} . Only ratios of derivative coefficients can be compared since the overall normalization is arbitrary. The dashed lines are obtained from the exact values (4.100) while dots of the same color correspond to the appropriate numerical bootstrap results. The plot shows convincing evidence that the numerical bootstrap tends to the exact answer as $N_{\max} \rightarrow \infty$.

Finally, we would like to point out that although our choice of basis for the bootstrap functionals breaks the symmetry between direct and crossed channels $z \leftrightarrow 1 - z$, the full extremal functional enjoys a version of this symmetry. $z \leftrightarrow 1 - z$ corresponds to $x \leftrightarrow 1/x$, so such symmetry can only be a property of the full sum (4.75). The integral kernel can be rewritten

$$\frac{h(x)}{1-x} dx = \tilde{h}(z) dz, \quad (4.102)$$

with

$$\tilde{h}(z) = 1 - \frac{1}{z(1-z)} - \left[\frac{(1-z)(2z^2+z+2)}{2z^2} \log(z-1) + \frac{z(2z^2-5z+5)}{2(1-z)^2} \log(z) \right]. \quad (4.103)$$

The last expression is symmetric under $z \leftrightarrow 1 - z$ up to a minus sign picked up by the argument of the first logarithm. A similar property holds also for higher Δ_ψ , see Appendix 4.A. It would be interesting to see if the same symmetry is present for arbitrary Δ_ψ .

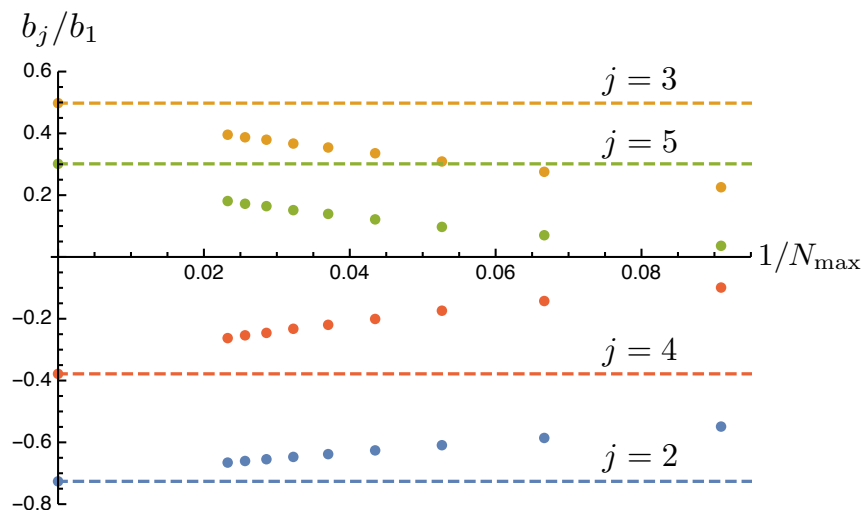


Figure 4.8: Comparison of the analytic extremal functional in the derivative basis (4.100) (dashed lines) and the numerical bootstrap extremal functionals (dots) for $\Delta_\psi = 1/2$. b_j is the coefficient of the y -derivative of order $2j - 1$ and N_{\max} is the order of the maximal z -derivative used in the numerics.

4.5 Higher values of Δ_ψ

4.5.1 Linear dependence of elementary functionals

Before we write down analytic formulas for the extremal functionals when Δ_ψ is an arbitrary positive integer or half-integer, we need to explain one subtlety. The functions $p_n(x)$, $n \in \mathbb{N}$ are linearly independent so we would expect that their overlaps with F_Δ given by

$$s(\Delta, n) = \frac{\Gamma(2\Delta)}{\Gamma(\Delta)^2} \frac{\sin(\pi\Delta)}{\pi} \left[\frac{(-1)^n}{(\Delta - n)(\Delta + n - 1)} + (-1)^{2\Delta_\psi + n + 1} R_{\Delta_\psi}(\Delta, n) \right] \quad (4.104)$$

are linearly independent as functions of Δ . This is easily seen to be true for $n \geq 2\Delta_\psi$ thanks to the orthogonality (4.60). However, it is generally not true for $1 \leq n \leq 2\Delta_\psi - 1$, in spite of the fact that all $s^+(\Delta, n)$ as well as all $s^-(\Delta, n)$ are linearly independent. In other words, the linear dependence arises thanks to precise cancellations between the contribution of the direct and crossed conformal blocks. A direct computation leads to the following examples

for small Δ_ψ

$$\begin{aligned}\Delta_\psi = 1 &: s(\Delta, 1) = 0 \\ \Delta_\psi = \frac{3}{2} &: s(\Delta, 1) = -s(\Delta, 2) \\ \Delta_\psi = 2 &: s(\Delta, 1) = s(\Delta, 2) = -\frac{1}{5}s(\Delta, 3)\end{aligned}\tag{4.105}$$

where the equalities hold for arbitrary $\Delta \in \mathbb{R}$. It is natural to ask what is the kernel of the map

$$\varphi : h(x) \mapsto \int_{\Gamma} dx h(x)(1-x)^{-2\Delta_\psi} F_\Delta(x).\tag{4.106}$$

Since $p_n(x)$ is a polynomial of degree $n-1$, the kernel lies within the space of polynomials of degree at most $2\Delta_\psi - 2$. In fact, it is possible to give a simple explicit description of $\ker \varphi$ as follows

$$\ker \varphi = \begin{cases} \langle x^a(x-1)^{2b}, a+b = \Delta_\psi - 1 \rangle & \text{for } \Delta_\psi \in \mathbb{N} \\ \langle x^a(x-1)^{2b+1}, a+b = \Delta_\psi - 3/2 \rangle & \text{for } \Delta_\psi \in \mathbb{N} - \frac{1}{2}, \end{cases}\tag{4.107}$$

where $\langle \alpha \rangle$ denotes the span of the set α and $a, b \in \mathbb{Z}_{\geq 0}$. We see that $s(\Delta, n)$ with $1 \leq n \leq 2\Delta_\psi - 1$ considered as functions of Δ generate a space of roughly half the full dimensionality, specifically

$$\dim(\langle s(\Delta, n), 1 \leq n \leq 2\Delta_\psi - 1 \rangle) = \begin{cases} \Delta_\psi - 1 & \text{for } \Delta_\psi \in \mathbb{N} \\ \Delta_\psi - \frac{1}{2} & \text{for } \Delta_\psi \in \mathbb{N} - \frac{1}{2}. \end{cases}\tag{4.108}$$

In fact, in both cases $\langle s(\Delta, n), 1 \leq n \leq 2\Delta_\psi - 1 \rangle$ is generated by the linearly independent set $\{s(\Delta, 2j), 1 \leq j \leq \lfloor \Delta_\psi - 1/2 \rfloor\}$.

The linear dependence implies that some columns of matrix A_{jn} appearing (4.72) are linearly dependent and we can not find a_n simply by inverting the full A_{jn} . However, A_{jn} can be inverted when n is restricted to a set corresponding to linearly independent functions $s(\Delta, n)$. Any two solutions of (4.72) differ by a vector δa_n corresponding to a function in $\ker \varphi$

$$\sum_{n=1}^{2\Delta_\psi-1} \delta a_n p_n(x) \in \ker \varphi.\tag{4.109}$$

We will see that this redundancy can be eventually fixed by requiring that the integral kernel has a Fourier expansion as in (4.38), in other words that $(1-x)^{-2\Delta_\psi} h(x)$ has at most a logarithmic singularity at $x = 1$.

4.5.2 Extremal functionals for $\Delta_\psi \in \mathbb{N}$

We are now ready to write down an explicit formula for a_n leading to the extremal functional ω_{Δ_ψ} corresponding to the optimal bootstrap bound $2\Delta_\psi + 1$ for $\Delta_\psi \in \mathbb{N}$. Recall from subsection 4.4.1 that $a_{2\Delta_\psi+2j-1} = 0$ for $j \in \mathbb{N}$ and from subsection 4.5.1 that it is sufficient to keep only even n from among $1 \leq n \leq 2\Delta_\psi - 1$. Therefore, $h(x)$ can be written as

$$h(x) = \sum_{n \in 2\mathbb{N}} a_n p_n(x). \quad (4.110)$$

Consequently, $h(1-x) = -h(x)$ since $p_n(1-x) = (-1)^{n-1} p_n(x)$. Note that the map $x \leftrightarrow 1-x$ corresponds to $z \leftrightarrow z/(z-1)$ and hence to swapping positions x_3 and x_4 in the four-point function. It would be interesting to see if there is a physical interpretation of this symmetry of $h(x)$.

a_{2k} satisfy the equation (4.72)

$$\sum_{k=1}^{\infty} \tilde{A}_{jk} a_{2k} = -c_{\Delta_\psi} \delta_{j1} \quad \text{for } j \in \mathbb{N}, \quad (4.111)$$

where

$$\tilde{A}_{jk} = \hat{s}(2\Delta_\psi + 2j - 1, 2k) \quad (4.112)$$

with $\hat{s}(\Delta, n)$ given by (4.59) and c_{Δ_ψ} is an arbitrary positive normalization. \tilde{A}_{jk} is now non-singular when the j, k indices are truncated to an arbitrary range $j, k \in \{1, \dots, J\}$. In spite of the rather complicated form of the entries of \tilde{A}_{jk} , the normalizable solution of equation (4.111) can be written in a closed form for arbitrary Δ_ψ as follows. Define

$$\begin{aligned} \alpha_{\Delta_\psi}(\Delta, m) &= [1 + 4m(\Delta_\psi - m)] \frac{\Gamma(4m+1)\Gamma(m-\frac{1}{2})^2 \Gamma(\frac{\Delta+1}{2})^2 \Gamma(\frac{\Delta+1}{2}-m)^2}{2^{8m}\pi(4m-1)\Gamma(m+1)^2\Gamma(\frac{\Delta}{2})^2 \Gamma(\frac{\Delta}{2}+m)^2} \\ \beta_{\Delta_\psi}(\Delta, m) &= [1 - 2(\Delta_\psi - m)] \frac{\Gamma(4m+1)\Gamma(m+\frac{1}{2})^2 \Gamma(\frac{\Delta+1}{2})^2 \Gamma(\frac{\Delta-1}{2}-m) \Gamma(\frac{\Delta+1}{2}-m)}{2^{8m+1}\pi\Gamma(m+1)^2\Gamma(\frac{\Delta}{2})^2 \Gamma(\frac{\Delta}{2}+m) \Gamma(\frac{\Delta}{2}+m+1)}. \end{aligned} \quad (4.113)$$

Use these to define $\Omega_{\Delta_\psi}(\Delta)$ for $\Delta_\psi \in \mathbb{N}$

$$\Omega_{\Delta_\psi}(\Delta) = \Delta(\Delta-1) + \Delta_\psi + \sum_{m=0}^{\Delta_\psi} [\alpha_{\Delta_\psi}(\Delta, m) + \beta_{\Delta_\psi}(\Delta, m)]. \quad (4.114)$$

The formula for a_n is then

$$a_n = \begin{cases} (2n-1)\Omega_{\Delta_\psi}(n) & \text{for } n \text{ even} \\ 0 & \text{for } n \text{ odd} \end{cases} \quad (4.115)$$

It can be checked that $a_{2\Delta_\psi} < 0$ and $a_{2\Delta_\psi+2j} > 0$ for $j \in \mathbb{N}$ as required from an extremal functional. It is interesting to study the behaviour of a_n for fixed Δ_ψ and $n \gg 1$. Note first that

$$\begin{aligned} \alpha_{\Delta_\psi}(n, m) &= O(n^{-4m+2}) \\ \beta_{\Delta_\psi}(n, m) &= O(n^{-4m}) \end{aligned} \quad (4.116)$$

as $n \rightarrow \infty$. However, due to delicate cancellations among all the terms in the sum in (4.114), a_n decays as

$$a_n = O(n^{-4\Delta_\psi-1}) \quad \text{as } n \rightarrow \infty. \quad (4.117)$$

In particular, this means that the sum (4.110) converges to a smooth integral kernel $h(x)$ for $x \in (0, 1)$ for any $\Delta_\psi \in \mathbb{N}$ and the convergence improves as Δ_ψ increases.

We can also find a closed formula for the action of ω_{Δ_ψ} on F_Δ for any $\Delta \geq 0$. Orthogonality (4.60) implies

$$\omega_{\Delta_\psi}(\Delta) = \begin{cases} \frac{\Gamma(2\Delta)}{\Gamma(\Delta)^2} \Omega_{\Delta_\psi}(\Delta) & \text{for } \Delta \in \mathbb{N} \text{ even, } \Delta \geq 2\Delta_\psi \\ 0 & \text{for } \Delta \in \mathbb{N} \text{ odd, } \Delta \geq 2\Delta_\psi + 1. \end{cases} \quad (4.118)$$

The simplest meromorphic function of Δ with no other zeros or poles for $\Delta \geq 2\Delta_\psi$ is

$$\omega_{\Delta_\psi}(\Delta) = \frac{\Gamma(2\Delta)}{\Gamma(\Delta)^2} \cos^2\left(\frac{\pi\Delta}{2}\right) \Omega_{\Delta_\psi}(\Delta), \quad (4.119)$$

which turns out to be the right answer. Figure 4.9 shows the action of the extremal functional for $\Delta_\psi = 2$. $\Omega_{\Delta_\psi}(\Delta)$ is positive with no zeros or poles for $\Delta > 2\Delta_\psi + 1$. The only zeros in this region are thus the double zeros coming from $\cos^2(\pi\Delta/2)$. $\Omega_{\Delta_\psi}(\Delta)$ has a simple pole at $\Delta = 2\Delta_\psi + 1$ coming from the $\beta_{\Delta_\psi}(\Delta, \Delta_\psi)$ summand in (4.114), leading to a simple zero at that location. All the double zeros of $\cos^2(\pi\Delta/2)$ in the region $0 < \Delta < 2\Delta_\psi$ are cancelled by double poles of $\Omega_{\Delta_\psi}(\Delta)$. The only zero of $\omega_{\Delta_\psi}(\Delta)$ in this region occurs at some non-integer value Δ_0 . We will see in section 4.6 that

$$\frac{\Delta_0}{\Delta_\psi} \rightarrow \sqrt{2} \quad \text{as } \Delta_\psi \rightarrow \infty, \quad (4.120)$$

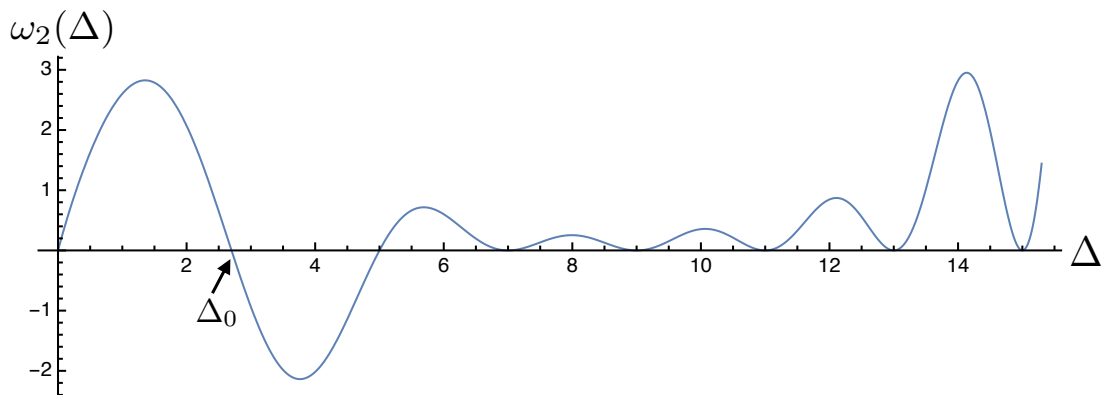


Figure 4.9: The action of the extremal functional for $\Delta_\psi = 2$, given by equation (4.119). The location Δ_0 of the only zero in $0 < \Delta < 2\Delta_\psi + 1$ will satisfy as $\Delta_0/\Delta_\psi \rightarrow \sqrt{2}$ as $\Delta_\psi \rightarrow \infty$.

which will be crucial to make contact with the flat-space limit. The functional ω_{Δ_ψ} satisfies all the properties (4.27), thus establishing rigorously that the 1D bootstrap bound on the gap is $2\Delta_\psi + 1$ for any $\Delta_\psi \in \mathbb{N}$.

We were not able to find a closed form for the kernel defined by the sum (4.110). The kernel is observed to have the following behaviour near $x = 0$

$$h(x) \sim h_1(x) + \log(x)h_2(x), \quad (4.121)$$

where $h_1(x)$ and $h_2(x)$ are analytic at $x = 0$ with the leading behaviour

$$\begin{aligned} h_1(x) &= a_0 + a_1x + \dots \\ h_2(x) &= b_0x^{2\Delta_\psi} + b_1x^{2\Delta_\psi+1} + \dots \end{aligned} \quad (4.122)$$

Recall that for general Δ , the action of ω must be defined via the contour integral (4.57). The branch cut of $h(x)$ along $x \in (-\infty, 0)$ arising from the infinite sum over $p_n(x)$ leads to a dependence on deformations of Γ . This dependence appears because the infinite sum over n and the analytic continuation in x do not commute. The correct choice reproducing the answer (4.119) is one where the contour intersects the negative real axis arbitrarily close to $x = 0$. We can not take the contour all the way to $x = 0$ because of the $x^{\Delta-2\Delta_\psi}$ singularity in $F_\Delta(x)$. The $x^{2\Delta_\psi}$ suppression of $h_2(x)$ seen in (4.122) guarantees that the value of the contour integral converges as the intercept approaches $x = 0$.

4.5.3 Fixing the remaining redundancy

As explained in Section 4.3, the extremal functional for any Δ_ψ can likely be expressed in the basis of derivatives with respect to the Zhukovsky variable y

$$\omega_{\Delta_\psi} = \sum_{j=1}^{\infty} \frac{b_j}{(2j-1)!} \frac{d^{2j-1}}{dy^{2j-1}} \Big|_{y=0}, \quad (4.123)$$

where $b_j \in \mathbb{R}$ depend on Δ_ψ . Requiring the existence of this representation will fix the redundancy in $h(x)$ described in subsection 4.5.1. Recall from section 4.3 that (ignoring the singularity at $\theta = 0$ present only for small Δ) (4.123) can be expressed as the integral

$$\omega_{\Delta_\psi}(\Delta) = \frac{4}{\pi} \int_0^{\pi/2} d\theta g_{\Delta_\psi}(\theta) \text{Im}[F_\Delta(e^{i\theta})], \quad (4.124)$$

where

$$g_{\Delta_\psi}(\theta) = \sum_{j=1}^{\infty} b_j \sin[(2j-1)\theta]. \quad (4.125)$$

In other words, b_j are simply the Fourier coefficients of the integral kernel constructed above. Coordinates x and θ are related through

$$x = \tan^2\left(\frac{\theta}{2}\right), \quad (4.126)$$

and the Fourier coefficients can be obtained from the integral kernel $h(x)(1-x)^{-2\Delta_\psi}$ via

$$b_j = \frac{1}{\pi} \int_0^1 dx \sin[(2j-1)\theta(x)] h(x)(1-x)^{-2\Delta_\psi}. \quad (4.127)$$

According to the results of the previous subsection, $h(x)$ remains nonzero as $x \rightarrow 1$. Therefore, the integral diverges at $x = 1$ for any $\Delta_\psi \in \mathbb{N}$ and the integral kernel seems not to have a Fourier expansion. Fortunately, this problem can be amended by recalling there is an ambiguity in $h(x)$, described in subsection 4.5.1. The behaviour of $h(x)$ defined by (4.110) and (4.115) near $x = 1$ is

$$h(x) \sim -h_1(1-x) - h_2(1-x) \log(1-x), \quad (4.128)$$

with $h_{1,2}(x)$ as in (4.122). Therefore, only $h_1(1-x)$ up to $O((x-1)^{2\Delta_\psi-1})$ contributes to the singularity of (4.127), while the logarithmic term does not contribute to the singularity since it is sufficiently suppressed. We must now ask whether there exists a polynomial $c(x) \in \ker \varphi$ such that

$$-h_1(1-x) + c(x) = O((x-1)^{2\Delta_\psi}) \quad (4.129)$$

as $x \rightarrow 1$. This is a priori an overconstrained problem since we need to cancel $2\Delta_\psi$ independent coefficients of h_1 using a polynomial taken from the space $\ker \varphi$ of dimension Δ_ψ . However, we found that it was possible for all $1 \leq \Delta_\psi \leq 5$ and therefore it is likely possible in general. We were not able to find a closed formula for $c(x)$ for general $\Delta_\psi \in \mathbb{N}$. Listed below are some low-lying examples of $c(x)$

$$\begin{aligned} \Delta_\psi = 1: \quad c(x) &= -\frac{3}{8} \\ \Delta_\psi = 2: \quad c(x) &= \frac{15}{16}x - \frac{2505}{1024}(x-1)^2 \\ \Delta_\psi = 3: \quad c(x) &= \frac{35}{8}x^2 - \frac{6055}{1024}x(x-1)^2 - \frac{418985}{65536}(x-1)^4. \end{aligned} \quad (4.130)$$

Clearly $c(x) \in \ker \varphi$ with $\ker \varphi$ given by (4.107) in all these examples. The Fourier coefficients can now be derived as

$$b_j = \frac{1}{\pi} \int_0^1 dx \sin[(2j-1)\theta(x)] [h(x) + c(x)] (1-x)^{-2\Delta_\psi}. \quad (4.131)$$

The extremal functionals coming from numerical bootstrap in the derivative basis were checked to tend to these analytic predictions for $\Delta_\psi = 1$ as N_{\max} was increased although the convergence rate was slower compared to $\Delta_\psi = 1/2$ presented in Figure 4.8.

4.5.4 Extremal functionals for $\Delta_\psi \in \mathbb{N} - \frac{1}{2}$

Let us move on to describe the extremal functionals in the case $\Delta_\psi \in \mathbb{N} - 1/2$. It follows from the result of subsection 4.4.1 that only a_n with n odd are nonvanishing for $n \geq 2\Delta_\psi$. Analogously to (4.110), we might hope that $h(x)$ can be expanded using only $p_n(x)$ with n odd. However, the space of functions $s(\Delta, n)$ with $1 \leq n \leq 2\Delta_\psi - 1$ is spanned by the same functions with n restricted to be even, but not n restricted to be odd. Indeed, it turns out that in order for the functional to have double zeros at the right locations, i.e.

for (4.72) to hold, some a_n with $1 \leq n \leq 2\Delta_\psi - 1$ and n even must be nonvanishing. We can write

$$h(x) = \tilde{h}(x) + c(x), \quad (4.132)$$

where

$$\tilde{h}(x) = \sum_{n \in 2\mathbb{N}-1} \tilde{a}_n p_n(x), \quad (4.133)$$

and $c(x)$ is a polynomial of degree at most $2\Delta_\psi - 2$. We expect the extremal functional can still be represented by a derivative series (4.123), meaning

$$h(x)(1-x)^{-2\Delta_\psi} \quad (4.134)$$

has at most a logarithmic singularity at $x = 1$. This requirement fixes $c(x)$ for any choice of the sequence \tilde{a}_{2j-1} . We will now present a formula for \tilde{a}_n such that the corresponding $h(x)$ with $c(x)$ fixed by this requirement satisfies (4.72). First, define

$$\begin{aligned} \tilde{\alpha}_{\Delta_\psi}(\Delta, m) &= -[2m(\Delta_\psi - m - 1) + \Delta_\psi] \frac{\pi \Gamma(4m+1) \Gamma(m)^2 \Gamma(\frac{\Delta+1}{2})^2 \Gamma(\frac{\Delta}{2} - m)^2}{2^{8m+1} \Gamma(m + \frac{1}{2}) \Gamma(m + \frac{3}{2}) \Gamma(\frac{\Delta}{2})^2 \Gamma(\frac{\Delta+1}{2} + m)^2} \\ \tilde{\beta}_{\Delta_\psi}(\Delta, m) &= (\Delta_\psi - m - 1) \frac{\pi \Gamma(4m+2) \Gamma(m+1)^2 \Gamma(\frac{\Delta+1}{2})^2 \Gamma(\frac{\Delta}{2} - m) \Gamma(\frac{\Delta}{2} - m - 1)}{2^{8m+2} \Gamma(m + \frac{1}{2}) \Gamma(m + \frac{3}{2}) \Gamma(\frac{\Delta}{2})^2 \Gamma(\frac{\Delta+1}{2} + m) \Gamma(\frac{\Delta+3}{2} + m)}. \end{aligned} \quad (4.135)$$

Use these to define $\Omega_{\Delta_\psi}(\Delta)$ for $\Delta_\psi \in \mathbb{N} - 1/2$

$$\Omega_{\Delta_\psi}(\Delta) = -[\Delta(\Delta - 1) + \Delta_\psi] \Psi' \left(\frac{\Delta}{2} \right) - 2 - \sum_{m=1}^{\Delta_\psi - \frac{1}{2}} \tilde{\alpha}_{\Delta_\psi}(\Delta, m) - \sum_{m=0}^{\Delta_\psi - \frac{1}{2}} \tilde{\beta}_{\Delta_\psi}(\Delta, m) \quad (4.136)$$

with $\Psi(z)$ defined in (4.88).

The formula for \tilde{a}_n is

$$\tilde{a}_n = \begin{cases} (2n-1)\Omega_{\Delta_\psi}(n) & \text{for } n \text{ odd} \\ 0 & \text{for } n \text{ even} \end{cases} \quad (4.137)$$

We were not able to find a closed formula for $c(x)$ completing $\tilde{h}(x)$ to the full integral kernel for any Δ_ψ , but checked that $c(x)$ consistent with the constraints existed for all

$1/2 \leq \Delta_\psi \leq 9/2$. Several low-lying examples follow

$$\begin{aligned} \Delta_\psi = \frac{1}{2} : c(x) &= 0 \\ \Delta_\psi = \frac{3}{2} : c(x) &= \frac{35}{12}(x-2) \\ \Delta_\psi = \frac{5}{2} : c(x) &= (x-2) \left[\frac{1001}{120}(x^2-x+1) + \frac{\pi^2}{10}(2x^2+x-1) \right]. \end{aligned} \tag{4.138}$$

Analogously to the case with $\Delta_\psi \in \mathbb{N}$, the action of the extremal functionals on F_Δ with any $\Delta > 0$ reads

$$\omega_{\Delta_\psi}(\Delta) = \frac{\Gamma(2\Delta)}{\Gamma(\Delta)^2} \sin^2\left(\frac{\pi\Delta}{2}\right) \Omega_{\Delta_\psi}(\Delta). \tag{4.139}$$

Discussion following (4.119) concerning zeros $\omega_{\Delta_\psi}(\Delta)$ applies in this case too with obvious modifications. **In summary, we have constructed functionals which prove that the optimal bootstrap bound is $2\Delta_\psi + 1$ for $\Delta_\psi \in \mathbb{N}/2$.**

The resummation of (4.133) is simpler than in the case of integer Δ_ψ . It appears $h(x)$ for $\Delta_\psi \in \mathbb{N} - 1/2$ can always be written in terms of rational, log and Li_2 functions. We present some closed formulas for $\tilde{h}(x)$ in Appendix 4.A.

4.6 Emergence of AdS physics at large Δ_ψ

4.6.1 A review of massive scattering in large AdS_2

It turns out that the extremal functional constructed in the previous section has a clear physical meaning for large Δ_ψ in terms scattering of massive particles in large AdS_2 . As a first hint, we can notice that the location of the only zero Δ_0 of $\omega_{\Delta_\psi}(\Delta)$ in the region $0 < \Delta < 2\Delta_\psi$ tends to

$$\lim_{\Delta_\psi \rightarrow \infty} \frac{\Delta_0}{\Delta_\psi} \rightarrow \sqrt{2}, \tag{4.140}$$

which corresponds to the point fixed by the crossing symmetry of the flat-space S-matrix. We begin by reviewing aspects of two-dimensional scattering and its holographic dictionary. More details and derivations can be found in [118]. Consider a $2 \rightarrow 2$ scattering amplitude of identical particles of mass m_ψ in (1+1)D flat spacetime. The amplitude is fully described by the S-matrix $S(\sigma)$, where

$$\sigma = \frac{(p_1 + p_2)^2}{m_\psi^2} \tag{4.141}$$

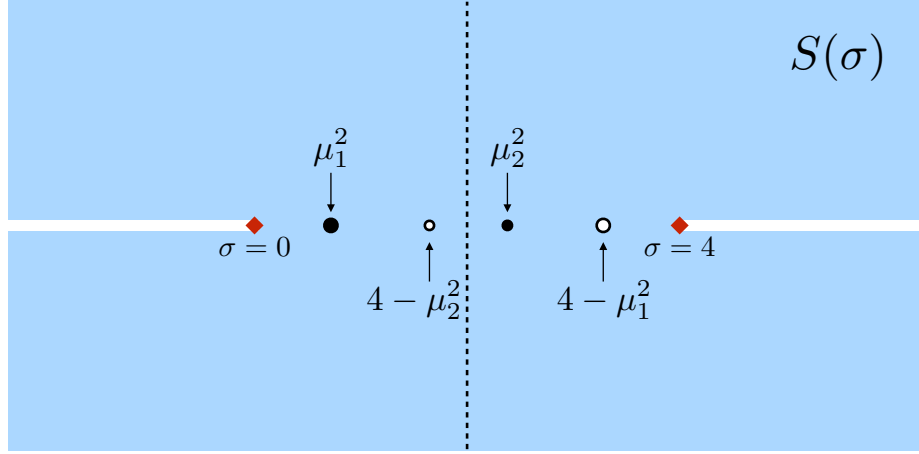


Figure 4.10: The analytic structure of the S-matrix on the first sheet. There is a branch cut for real $\sigma > 4$ corresponding to two-particle final states. Crossing symmetry implies $S(4 - \sigma) = S(\sigma)$. The region $0 < \sigma < 4$ contains poles coming from bound states. Full and empty dots denote s- and t-channel poles respectively.

is a dimensionless version of the usual Mandelstam variable s . The analytic structure of the S-matrix is illustrated in Figure 4.10. Physical scattering regime corresponds to $\sigma \geq 4$, and $S(\sigma)$ has a branch cut there. The branch cut is of the square root type. In the extreme non-relativistic regime $\sigma \rightarrow 4$ the particles become free, and thus the leading behaviour is

$$S(\sigma) = \pm 1 + \alpha\sqrt{4 - \sigma} + O(4 - \sigma), \quad (4.142)$$

where the upper, lower sign corresponds to bosons, fermions respectively and $\alpha \in \mathbb{R}$. Unitarity implies

$$|S(\sigma)| \leq 1 \quad \text{for } \sigma \geq 4, \sigma \in \mathbb{R}. \quad (4.143)$$

The S-matrix also satisfies crossing symmetry

$$S(4 - \sigma) = S(\sigma). \quad (4.144)$$

Let us assume the scattered particle is the lightest particle of the theory. In that case, the only other singularities of $S(\sigma)$ on the first sheet are simple poles on the real axis in $0 < \sigma < 4$, coming from bound states and located at $\sigma_j = \mu_j^2$, as well as the corresponding t -channel poles located at $\sigma_j = 4 - \mu_j^2$, where

$$\mu_j = \frac{m_j}{m_\psi} \quad (4.145)$$

and m_j is the bound state mass. The two kinds of poles can be distinguished by the sign of their residue

$$S(\sigma) \sim \begin{cases} -\mathcal{J}_j \frac{g_j^2}{\sigma - \mu_j^2} & \text{near } \sigma = \mu_j^2 \\ \mathcal{J}_j \frac{g_j^2}{\sigma - (4 - \mu_j^2)} & \text{near } \sigma = 4 - \mu_j^2, \end{cases} \quad (4.146)$$

where $g_j \in \mathbb{R}$ is the effective three-point coupling between the external particles and the bound state, and \mathcal{J}_j is the positive prefactor

$$\mathcal{J}_j = \frac{1}{2\mu_j \sqrt{4 - \mu_j^2}}. \quad (4.147)$$

Placing the theory in AdS₂ of radius R defines a family of 1D CFTs parametrized by R . Bulk masses and boundary scaling dimensions of primary operators are related by

$$(m_{\mathcal{O}}R)^2 = \Delta_{\mathcal{O}}(\Delta_{\mathcal{O}} - 1), \quad (4.148)$$

When we send $R \rightarrow \infty$, all scaling dimensions of a theory whose bulk dual is a massive QFT tend to infinity. Their ratios tend to the ratios of the corresponding masses

$$\lim_{\Delta_{\psi} \rightarrow \infty} \frac{\Delta_j}{\Delta_{\psi}} = \mu_j. \quad (4.149)$$

The $2 \rightarrow 2$ scattering corresponds to a four-point function of primary operators $\psi(x)$ sourcing the external particle. Primary operators appearing in the $\psi \times \psi$ OPE correspond to intermediate states of the scattering process. Those with $\Delta_{\mathcal{O}} \lesssim 2\Delta_{\psi}$ play the role of bound states, while those with $\Delta_{\mathcal{O}} \gtrsim 2\Delta_{\psi}$ correspond to two-particle states. The flat-space physics governs the leading behaviour of the CFT data as $\Delta_{\psi} \rightarrow \infty$. The flat-space scattering amplitude can be recovered as a specific limit of the boundary Mellin amplitude [118, 121]. For example, the leading behaviour of the OPE coefficient $c_{\psi\psi\mathcal{O}_j}$ corresponding to a bound state of mass $m_j = \mu_j m_{\psi}$ takes the form

$$(c_{\psi\psi\mathcal{O}_j})^2 \sim \frac{2\sqrt{\pi}g_j^2}{\mu_j^{3/2}(4 - \mu_j^2)(\mu_j + 2)} \sqrt{\Delta_{\psi}} [v(\mu_j)]^{-\Delta_{\psi}} \quad \text{as } \Delta_{\psi} \rightarrow \infty, \quad (4.150)$$

where

$$v(\mu) = \frac{4^{2+\mu}}{|\mu - 2|^{2-\mu}(\mu + 2)^{2+\mu}}, \quad (4.151)$$

and g_j is defined in (4.146). We inserted the absolute value around $\mu - 2$ for future convenience. In the bound state region $0 < \mu < 2$, we have $v(\mu) > 1$, and thus $c_{\psi\psi\mathcal{O}_j}$ is exponentially suppressed in the large Δ_ψ limit. This suppression is coming from the amplitude for the massive particles to propagate across an increasingly large distance in AdS, as explained in [119, 120]. We will be able to recover the exponential suppression including the precise dependence of the exponent on μ from conformal bootstrap.

Consider now the primary operators in the $\psi \times \psi$ OPE coming from the two-particle states. When the bulk theory is that of free real bosons or fermions, there is an exact formula for the OPE coefficients

$$(c_{\psi\psi\mathcal{O}}^{\text{free}})^2 = \frac{2\Gamma(\Delta_{\mathcal{O}})^2\Gamma(\Delta_{\mathcal{O}} + 2\Delta_\psi - 1)}{\Gamma(2\Delta_{\mathcal{O}} - 1)\Gamma(2\Delta_\psi)^2\Gamma(\Delta_{\mathcal{O}} - 2\Delta_\psi + 1)}, \quad (4.152)$$

and the scaling dimensions are $\Delta_{\mathcal{O}} = 2\Delta_\psi + n$, where n is an even, odd non-negative integer for bosons, fermions respectively. For a general theory in AdS₂, define the spectral density

$$\rho_{\Delta_\psi}(\mu) = \sum_{\mathcal{O} \in \psi \times \psi} (c_{\psi\psi\mathcal{O}})^2 \delta\left(\mu - \frac{\Delta_{\mathcal{O}}}{\Delta_\psi}\right). \quad (4.153)$$

It can be shown [118] that $\rho_{\Delta_\psi}(\mu)$ is universal in the flat-space limit in the sense that it tends to the asymptotic spectral density of free fields, namely

$$\rho_{\Delta_\psi}(\mu) \sim \tilde{\rho}_{\Delta_\psi}(\mu) = \frac{4\sqrt{\mu}}{\sqrt{\pi}\sqrt{\mu-2}(\mu+2)^{\frac{3}{2}}} \sqrt{\Delta_\psi} [v(\mu)]^{-\Delta_\psi} \quad \text{as } \Delta_\psi \rightarrow \infty, \quad (4.154)$$

with $v(\mu)$ again given by (4.151). Equation (4.154) is valid in the sense of distributions when acting on smooth functions of μ .

Finally, it is also possible to recover the S-matrix from the shifts of scaling dimension of two-particle states compared to their free-field positions. To this end, define the following smeared average of an arbitrary function $f(\mu, \Delta_\psi)$

$$\langle f(\mu, \Delta_\psi) \rangle_\epsilon = \frac{\int_{\mu-\epsilon}^{\mu+\epsilon} d\nu \rho_{\Delta_\psi}(\nu) [v(\nu)]^{\Delta_\psi} f(\nu, \Delta_\psi)}{\int_{\mu-\epsilon}^{\mu+\epsilon} d\nu \rho_{\Delta_\psi}(\nu) [v(\nu)]^{\Delta_\psi}}, \quad (4.155)$$

where $\rho_{\Delta_\psi}(\nu)$ is the exact spectral density at finite Δ_ψ . The factor $[v(\nu)]^{\Delta_\psi}$ cancels the fast variation of $\rho_{\Delta_\psi}(\nu)$ with ν when $\Delta_\psi \rightarrow \infty$. The S-matrix for $\sigma \geq 4$ can now be recovered through the formula

$$S(\mu^2) = \lim_{\epsilon \rightarrow 0} \lim_{\Delta_\psi \rightarrow \infty} \langle e^{-i\pi(\mu-2)\Delta_\psi} \rangle_\epsilon, \quad (4.156)$$

where the order of limits is important. In other words, $S(\mu^2)$ is simply the large Δ_ψ limit of the average value of $e^{-i\pi(\Delta_{\mathcal{O}}-2\Delta_\psi)}$ over all primaries with $\Delta_{\mathcal{O}} \sim \mu\Delta_\psi$, weighted by $(c_{\psi\psi\mathcal{O}}/c_{\psi\psi\mathcal{O}}^{\text{free}})^2$.

4.6.2 AdS₂ physics from crossing in a 1D CFT

We will now show how some of the features pertaining to the scattering of massive particles in large AdS₂ presented in the previous subsection follow from crossing in the 1D CFT living at the boundary. We will also derive a simple sum rule for OPE coefficients of primary operators corresponding to two-particle states produced at rest.

Consider a unitary solution to the bootstrap equation in 1D

$$\sum_{\mathcal{O} \in \psi \times \psi} (c_{\psi\psi\mathcal{O}})^2 F_{\Delta_{\mathcal{O}}}(z) = 0, \quad (4.157)$$

with $(c_{\psi\psi\mathcal{O}})^2 > 0$. We can apply the extremal functional constructed in section 4.5 to get a single equation

$$\sum_{\mathcal{O} \in \psi \times \psi} (c_{\psi\psi\mathcal{O}})^2 \omega_{\Delta_\psi}(\Delta_{\mathcal{O}}) = 0. \quad (4.158)$$

When the solution to crossing corresponds to the free massive real fermion in AdS₂, the last equation is automatically satisfied since $\omega_{\Delta_\psi}(\Delta_{\mathcal{O}}) = 0$ for any $\mathcal{O} \in \psi \times \psi$. However, in general it represents a universal constraint valid on any solution of crossing. In order to make contact with massive QFT in AdS₂, let us assume we have a family of solutions where all dimensions scale linearly with Δ_ψ , i.e. that $\Delta_{\mathcal{O}} \sim \mu_{\mathcal{O}}\Delta_\psi$ with $\mu_{\mathcal{O}}$ fixed as $\Delta_\psi \rightarrow \infty$. We would like to understand the leading behaviour of (4.158) as $\Delta_\psi \rightarrow \infty$. The functional $\omega_{\Delta_\psi}(\mu\Delta_\psi)$ with large Δ_ψ exhibits very different behaviour for $0 < \mu < 2$ and $\mu > 2$, as illustrated in Figure 4.11.

Let us focus first on the region $0 < \mu < 2$. It is possible to show directly from (4.119) that

$$\omega_{\Delta_\psi}(\mu\Delta_\psi) \sim \frac{\sqrt{2}(\mu^2 - 2)}{\pi\mu^{\frac{5}{2}}(\mu - 2)} [v(\mu)]^{\Delta_\psi} \quad \text{for } 0 < \mu < 2 \quad (4.159)$$

as $\Delta_\psi \rightarrow \infty$ where $v(\mu)$ was defined in (4.151). Crucially, the functional grows exponentially with Δ_ψ with the exponent governed by $v(\mu)$. It follows that any two operators $\mathcal{O}_j, \mathcal{O}_k$ with $0 < \mu_{j,k} < 2$ that both contribute to (4.158) at the leading order as $\Delta_\psi \rightarrow \infty$ must have OPE coefficients related by

$$\frac{(c_{\psi\psi\mathcal{O}_j})^2}{(c_{\psi\psi\mathcal{O}_k})^2} \sim \left[\frac{v(\mu_j)}{v(\mu_k)} \right]^{-\Delta_\psi} \quad (4.160)$$

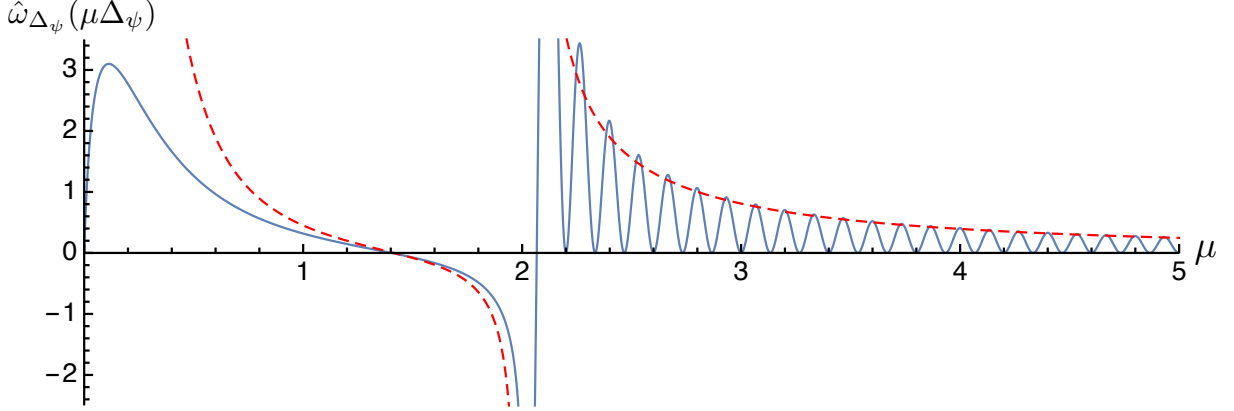


Figure 4.11: The analytic extremal functional for $\Delta_\psi = 15$. The blue curve represents $\hat{\omega}_{\Delta_\psi}(\mu\Delta_\psi) = [v(\mu)]^{-\Delta_\psi} \omega_{\Delta_\psi}(\mu\Delta_\psi)$ with $v(\mu)$ given by (4.151) and $\omega_{\Delta_\psi}(\Delta)$ given by (4.119). $\hat{\omega}_{\Delta_\psi}(\mu\Delta_\psi)$ in the region $0 < \mu < 2$ converges to the red dashed curve given by $\sqrt{2}\pi^{-1}\mu^{-5/2}(\mu-2)^{-1}(\mu^2-2)$ as $\Delta_\psi \rightarrow \infty$. The functional is oscillatory in the region $\mu > 2$ with evenly spaced double zeros that condense as $\Delta_\psi \rightarrow \infty$. The height of peaks converges to the red dashed curve given by $4\sqrt{2}\pi^{-1}\mu^{-5/2}(\mu-2)^{-1}(\mu^2-2)$.

up to a prefactor independent of Δ_ψ . This is consistent with the exponential suppression of $c_{\psi\psi\mathcal{O}}$ when \mathcal{O} corresponds to a bound state of two ψ particles in the flat space limit, seen in (4.150). **The extremal functional thus provides a universal CFT justification of the exponential decay of bound state OPE coefficients.** Assuming the full expression (4.150), we can evaluate the contribution of a single bound state to (4.158)

$$(c_{\psi\psi\mathcal{O}_j})^2 \omega_{\Delta_\psi}(\Delta_{\mathcal{O}_j}) = 2\sqrt{\frac{8\Delta_\psi}{\pi}} \text{Res}_{\sigma=\mu_j^2} \left[\frac{(\sigma-2)}{\sigma^{\frac{3}{2}}(4-\sigma)^{\frac{3}{2}}} S(\sigma) \right] + O(1), \quad (4.161)$$

i.e. the bound states contribute at $O(\sqrt{\Delta_\psi})$. Since the function in square brackets is odd under $\sigma \leftrightarrow 4-\sigma$, and remembering that every s-channel pole has its t-channel counterpart, we can rewrite the contribution of all bound states to (4.158) at $O(\sqrt{\Delta_\psi})$ as a contour integral in the σ plane along a contour Γ_1 surrounding all the poles on the real axis, as illustrated in Figure 4.12

$$\sum_{\mathcal{O}: \mu_{\mathcal{O}} < 2} (c_{\psi\psi\mathcal{O}})^2 \omega_{\Delta_\psi}(\Delta_{\mathcal{O}}) = \frac{1}{2\pi i} \sqrt{\frac{8\Delta_\psi}{\pi}} \oint_{\Gamma_1} \frac{(\sigma-2)}{\sigma^{\frac{3}{2}}(4-\sigma)^{\frac{3}{2}}} [S(\sigma) + 1] d\sigma + O(1), \quad (4.162)$$

where we added 1 to the S-matrix for future convenience without affecting the result. We

will assume that the scattered particles are fermions, so that $S(0) = S(4) = -1$. The bosonic cases $S(0) = S(4) = 1$ can presumably be treated analogously.

Let us now study the asymptotic behaviour of the functional for $\mu > 2$. As illustrated in Figure 4.11, it is oscillatory with frequency proportional to Δ_ψ . The asymptotics can be found in a closed form

$$\omega_{\Delta_\psi}(\mu\Delta_\psi) \sim 4 \cos^2 \left(\frac{\pi\mu\Delta_\psi}{2} \right) \frac{\sqrt{2}(\mu^2 - 2)}{\pi\mu^{\frac{5}{2}}(\mu - 2)} [v(\mu)]^{\Delta_\psi} \quad \text{for } \mu > 2, \quad (4.163)$$

where we can see the same exponential behaviour once again. Let us describe the spectrum of our solution to crossing for $\mu > 2$ using the spectral density $\rho_{\Delta_\psi}(\mu)$, defined in (4.153). The contribution of the $\mu > 2$ operators to (4.158) can be written as an integral

$$\sum_{\mathcal{O}: \mu_{\mathcal{O}} > 2} (c_{\psi\psi\mathcal{O}})^2 \omega_{\Delta_\psi}(\Delta_{\mathcal{O}}) = \int_2^\infty \rho_{\Delta_\psi}(\mu) \omega_{\Delta_\psi}(\mu\Delta_\psi) d\mu. \quad (4.164)$$

Assuming that states with any μ contribute to (4.158) at the leading order as $\Delta_\psi \rightarrow \infty$, we arrive at the same exponential dependence of ρ_{Δ_ψ} on Δ_ψ as the one corresponding to two-particle states in AdS₂, see formula (4.154). Let us now evaluate (4.164) using the asymptotics (4.163) and assuming the formula (4.154). Note that the oscillating prefactor in (4.163) can be rewritten using

$$2 \cos^2 \left(\frac{\pi\mu\Delta_\psi}{2} \right) = \text{Re} \left[e^{-i\pi(\mu-2)\Delta_\psi} + 1 \right], \quad (4.165)$$

where we used $\Delta_\psi \in \mathbb{N}$. The oscillating prefactor is clearly related to the S-matrix on the branch cut as computed by (4.156). Indeed, it is not too hard to show from (4.156) that

$$\sum_{\mathcal{O}: \mu_{\mathcal{O}} > 2} (c_{\psi\psi\mathcal{O}})^2 \omega_{\Delta_\psi}(\Delta_{\mathcal{O}}) = \frac{1}{\pi} \sqrt{\frac{8\Delta_\psi}{\pi}} \int_4^\infty \frac{(\sigma - 2)}{\sigma^{\frac{3}{2}}(\sigma - 4)^{\frac{3}{2}}} 2\text{Re} [S(\sigma) + 1] d\sigma + O(1). \quad (4.166)$$

It is now useful to notice that for real $\sigma > 4$

$$2 \frac{\text{Re} [S(\sigma) + 1]}{(\sigma - 4)^{\frac{3}{2}}} = i \left[\frac{S(\sigma) + 1}{(4 - \sigma)^{\frac{3}{2}}} \right]_{\sigma - i\epsilon}^{\sigma + i\epsilon}, \quad (4.167)$$

and therefore the last integral can be written as the contour integral

$$\sum_{\mathcal{O}: \mu_{\mathcal{O}} > 2} (c_{\psi\psi\mathcal{O}})^2 \omega_{\Delta_\psi}(\Delta_{\mathcal{O}}) = \frac{1}{2\pi i} \sqrt{\frac{8\Delta_\psi}{\pi}} \oint_{\Gamma_2} \frac{(\sigma - 2)}{\sigma^{\frac{3}{2}}(4 - \sigma)^{\frac{3}{2}}} [S(\sigma) + 1] d\sigma + O(1), \quad (4.168)$$

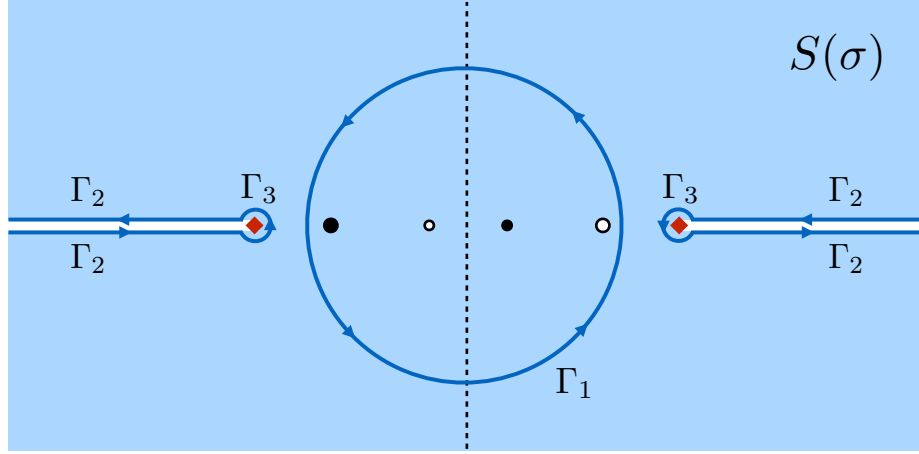


Figure 4.12: Contour integrals describing the contributions of various states to the crossing equation (4.158) at the leading order as $\Delta_\psi \rightarrow \infty$. Γ_1 , Γ_2 and Γ_3 give the contribution of bound states, two-particle states and $\mu = 2$ states respectively. The integrand takes the form $(\sigma - 2)\sigma^{-3/2}(4 - \sigma)^{-3/2}[S(\sigma) + 1]$. Conformal bootstrap at the leading order in $1/\Delta_\psi$ is equivalent to the total contour integral being zero, in other words to the analyticity of the S-matrix away from the real axis.

where Γ_2 consists of four half-lines lying on the branch cuts, as depicted in Figure 4.12, and we used $S(4 - \sigma) = S(\sigma)$ to duplicate the contour from $\sigma > 4$ to $\sigma < 0$.

We arrived at a contour integral of exactly the same function as in the case of bound states (4.162), only the contour is different now. The integrand decays as σ^{-2} so it would be tempting to deduce the validity of (4.158) at the leading order in Δ_ψ from analyticity of $S(\sigma)$ away from the real axis by deforming $\Gamma_1 \cup \Gamma_2$ to the empty contour. However, this is not a legal operation because the integrand has poles at $\sigma = 0, 4$ and thus the contour integral picks up a non-zero contribution from the infinitesimal contour Γ_3 depicted in Figure 4.12. On the CFT side, this contribution is coming from operators with $\mu = 2$. The conformal bootstrap equation will thus be satisfied at the leading order if and only if

$$\sum_{\mathcal{O}: \mu_{\mathcal{O}}=2} (c_{\psi\psi\mathcal{O}})^2 \omega_{\Delta_\psi}(\Delta_{\mathcal{O}}) = \frac{1}{2\pi i} \sqrt{\frac{8\Delta_\psi}{\pi}} \oint_{\Gamma_3} \frac{(\sigma - 2)}{\sigma^{\frac{3}{2}}(4 - \sigma)^{\frac{3}{2}}} [S(\sigma) + 1] ds + O(1). \quad (4.169)$$

Our asymptotic formulas (4.159), (4.163) for $\omega_{\Delta_\psi}(\mu\Delta_\psi)$ break down when $\mu = 2$ and need to be modified. Primary operators \mathcal{O} with $\mu = 2$ are precisely those for which $\Delta_{\mathcal{O}} - 2\Delta_\psi$

remains finite as $\Delta_\psi \rightarrow \infty$. Denote

$$\delta_{\mathcal{O}} = \lim_{\Delta_\psi \rightarrow \infty} (\Delta_{\mathcal{O}} - 2\Delta_\psi). \quad (4.170)$$

The asymptotics of ω_{Δ_ψ} is modified to become a power-law

$$\omega_{\Delta_\psi}(2\Delta_\psi + \delta_{\mathcal{O}}) \sim -\frac{1}{\Gamma\left(\frac{1-\delta}{2}\right)\Gamma\left(\frac{3-\delta}{2}\right)} \left(\frac{\Delta_\psi}{2}\right)^{-\delta_{\mathcal{O}}+1} \quad (4.171)$$

as $\Delta_\psi \rightarrow \infty$. The contour integral on the right-hand side of (4.169) can be evaluated using expansion (4.142)

$$\frac{1}{2\pi i} \sqrt{\frac{8\Delta_\psi}{\pi}} \oint_{\Gamma_3} \frac{(\sigma-2)}{\sigma^{\frac{3}{2}}(4-\sigma)^{\frac{3}{2}}} [S(\sigma)+1] ds = -\sqrt{\frac{2\Delta_\psi}{\pi}} \alpha, \quad (4.172)$$

where α is the coefficient of the square-root term in (4.142). Equation (4.169) now implies the following sum rule for the OPE coefficients of the $\mu=2$ states

$$\sum_{\mathcal{O}: \mu_{\mathcal{O}}=2} \frac{1}{\Gamma\left(\frac{1-\delta_{\mathcal{O}}}{2}\right)\Gamma\left(\frac{3-\delta_{\mathcal{O}}}{2}\right)} \left(\frac{\Delta_\psi}{2}\right)^{-\delta_{\mathcal{O}}+\frac{1}{2}} (c_{\psi\psi\mathcal{O}})^2 = \frac{2\alpha}{\sqrt{\pi}} + O\left(\Delta_\psi^{-1/2}\right), \quad (4.173)$$

In particular, the OPE coefficients should scale as

$$(c_{\psi\psi\mathcal{O}})^2 \sim a_{\mathcal{O}} \Delta_\psi^{\delta_{\mathcal{O}}-1/2} \quad (4.174)$$

as $\Delta_\psi \rightarrow \infty$ for these operators. We have shown that provided (4.173) holds, **the validity of the conformal bootstrap equation (4.158) at the leading order at large Δ_ψ follows from analyticity of the flat-space S-matrix away from the real axis.**

It would be interesting to derive the behaviour (4.174) and the sum rule (4.173) directly from quantum field theory in AdS₂. Note that the sum rule is trivially satisfied by the free fermion since then $\alpha=0$, and $1/[\Gamma\left(\frac{1-\delta}{2}\right)\Gamma\left(\frac{3-\delta}{2}\right)]$ vanishes for δ positive odd integer.

4.7 An analytic bound in 2D

4.7.1 The new basis in 2D

We will now discuss a generalization of the new class of bootstrap functionals to two dimensions and how it can be used to produce an analytic constraint on the low-lying

spectrum. The conformal blocks with four identical external scalar primaries $\phi(x)$ read

$$G_{h,\bar{h}}^{2D}(z, \bar{z}) = G_h(z)G_{\bar{h}}(\bar{z}) + (h \leftrightarrow \bar{h}), \quad (4.175)$$

where $G_h(z)$ is the 1D conformal block (4.19) and

$$h = \frac{\Delta + l}{2}, \quad \bar{h} = \frac{\Delta - l}{2}, \quad (4.176)$$

where Δ, l are the dimension and spin of the propagating primary. The bootstrap equation now reads

$$\sum_{\mathcal{O} \in \phi \times \phi} (c_{\phi\phi\mathcal{O}})^2 F_{h,\bar{h}}(z, \bar{z}) = 0, \quad (4.177)$$

where

$$F_{h,\bar{h}}(z, \bar{z}) = [g_h(z)g_{\bar{h}}(\bar{z}) - g_h(1-z)g_{\bar{h}}(1-\bar{z})] + (h \leftrightarrow \bar{h}), \quad (4.178)$$

where

$$g_h(z) = z^{h-\Delta_\phi} {}_2F_1(h, h; 2h; z). \quad (4.179)$$

z, \bar{z} should be thought of as independent complex variables. For any value of \bar{z} , functions $F_{h,\bar{h}}(z, \bar{z})$ have a pair of branch cuts in z located at $z \in (-\infty, 0)$ and $z \in (1, \infty)$, and vice versa with z and \bar{z} interchanged. Let us then define a basis of linear functionals α_n acting on functions $g_h(z)$ as in subsection 4.3.2

$$\begin{aligned} \alpha_n [g_h(z)] &= s^+(h, n) \\ \alpha_n [g_h(1-z)] &= s^-(h, n), \end{aligned} \quad (4.180)$$

where $s^\pm(h, n)$ appear in (4.52) and (4.54). It is also convenient to define basis functionals β_n acting in the opposite way, i.e. by scalar products of Legendres against the discontinuity on the branch cut $z \in (-\infty, 0)$

$$\begin{aligned} \beta_n [g_h(z)] &= s^-(h, n) \\ \beta_n [g_h(1-z)] &= s^+(h, n). \end{aligned} \quad (4.181)$$

These functionals are not independent from α_n in 1D, but are needed in 2D. The basis for our class of functionals acting on the 2D crossing equation consists of the following tensor products

$$\begin{aligned} (\alpha_m \otimes \bar{\alpha}_n) [F_{h,\bar{h}}(z, \bar{z})] &= [s^+(h, m)s^+(\bar{h}, n) - s^-(h, m)s^-(\bar{h}, n)] + (h \leftrightarrow \bar{h}) \\ (\alpha_m \otimes \bar{\beta}_n) [F_{h,\bar{h}}(z, \bar{z})] &= [s^+(h, m)s^-(\bar{h}, n) - s^-(h, m)s^+(\bar{h}, n)] + (h \leftrightarrow \bar{h}), \end{aligned} \quad (4.182)$$

where α, β acts on the z variable, while $\bar{\alpha}, \bar{\beta}$ acts on the \bar{z} variable. The other combinations are not independent since

$$\begin{aligned}\beta_m \otimes \bar{\beta}_n &= -\alpha_m \otimes \bar{\alpha}_n \\ \beta_m \otimes \bar{\alpha}_n &= -\alpha_m \otimes \bar{\beta}_n\end{aligned}\tag{4.183}$$

when acting on $F_{h,\bar{h}}(z, \bar{z})$. The symmetrization under $h \leftrightarrow \bar{h}$ in $F_{h,\bar{h}}(z, \bar{z})$ guarantees that the functionals appearing in (4.182) satisfy symmetry properties

$$\begin{aligned}\alpha_n \otimes \bar{\alpha}_m &= \alpha_m \otimes \bar{\alpha}_n \\ \alpha_n \otimes \bar{\beta}_m &= -\alpha_m \otimes \bar{\beta}_n.\end{aligned}\tag{4.184}$$

It is therefore natural to use the following as an independent basis of functionals with $m, n \in \mathbb{N}$

$$\gamma_{mn} = \alpha_m \otimes \bar{\alpha}_n + \alpha_m \otimes \bar{\beta}_n,\tag{4.185}$$

so that the first, second line of (4.182) are respectively the symmetric and antisymmetric part of the matrix γ_{mn} . The action of γ_{mn} becomes

$$\gamma_{mn} [F_{h,\bar{h}}(z, \bar{z})] = s(h, m)\tilde{s}(\bar{h}, n) + (h \leftrightarrow \bar{h}),\tag{4.186}$$

where

$$\begin{aligned}s(h, m) &= s^+(h, m) - s^-(h, m) \\ \tilde{s}(h, m) &= s^+(h, m) + s^-(h, m).\end{aligned}\tag{4.187}$$

In other words, $s(h, m)$ is precisely the function (4.50) giving the action of α_n on the vectors $F_h(z)$ entering the crossing equation in 1D. On the other hand, $\tilde{s}(h, m)$ is the action of α_n on the vectors $\tilde{F}_\Delta(z)$ for the 1D crossing equation with the wrong sign

$$\begin{aligned}\sum_{\mathcal{O} \in \psi \times \psi} (c_{\psi\psi\mathcal{O}})^2 \tilde{F}_{\Delta\mathcal{O}}(z) &= 0 \\ \tilde{F}_\Delta(z) &= z^{-2\Delta_\psi} G_\Delta(z) + (1-z)^{-2\Delta_\psi} G_\Delta(1-z).\end{aligned}\tag{4.188}$$

It is easy to see this equation has no nontrivial solution, as witnessed by any functional in the form of a positive linear combination of even derivatives of $[z(1-z)]^{2\Delta_\psi} \tilde{F}_\Delta(z)$ evaluated at $z = 1/2$.

4.7.2 Analytic bounds from factorized functionals

Having defined a natural basis for conformal bootstrap functionals in 2D, the remaining task is to find coefficients $a_{mn} \in \mathbb{R}$ so that

$$\omega = \sum_{m,n \in \mathbb{N}} a_{mn} \gamma_{mn}\tag{4.189}$$

is an extremal functional. Since the action of γ_{mn} essentially factorizes into a holomorphic and antiholomorphic part, it is natural to consider a restricted class of functionals where a_{mn} factorizes into a pair of sequences

$$a_{mn} = a_m \tilde{a}_n. \quad (4.190)$$

The action of ω then becomes

$$\omega(F_{h,\bar{h}}) = u(h)\tilde{u}(\bar{h}) + u(\bar{h})\tilde{u}(h), \quad (4.191)$$

where

$$\begin{aligned} u(h) &= \sum_{m \in \mathbb{N}} a_m s(h, m) \\ \tilde{u}(h) &= \sum_{n \in \mathbb{N}} \tilde{a}_n \tilde{s}(h, n). \end{aligned} \quad (4.192)$$

We will take a_n to be the coefficients in the 1D extremal functional for the gap $2\Delta_\psi + 1 = \Delta_\phi + 1$, assuming it exists for any Δ_ϕ . Hence

$$\begin{aligned} u(0) &= 0 \\ u(h) &\text{ has a first-order zero and a positive slope at } h = \Delta_\phi + 1 \\ u(h) &\geq 0 \text{ for } h \geq \Delta_\phi + 1 \\ u(h) &\text{ has second-order zeros at } h = \Delta_\phi + 2j + 1, j \in \mathbb{N}. \end{aligned} \quad (4.193)$$

Since the 1D crossing with the wrong sign has no nontrivial solutions, it is easy to find \tilde{a}_n such that

$$\tilde{u}(h) > 0 \quad (4.194)$$

for all $h \geq 0$. We can take for example \tilde{a}_n corresponding to the functional in the form of the second derivative of $[z(1-z)]^{2\Delta_\psi} \tilde{F}_\Delta(z)$ at $z = 1/2$. Consider now (4.191) as a function of Δ for fixed l , denoting $\omega(\Delta, l) = \omega(F_{h,\bar{h}})$. We find the following properties

$$\begin{aligned} \omega(0, 0) &= 0 \\ \omega(\Delta, l) &\text{ has a first-order zero and a positive slope at } \Delta = 2\Delta_\phi + 2 + l, l \in 2\mathbb{N} \\ \omega(\Delta, l) &\geq 0 \text{ for } \Delta \geq 2\Delta_\phi + 2 + l, l \in 2\mathbb{N} \end{aligned} \quad (4.195)$$

It follows that unless all primary operators of a unitary solution to (4.177) coincide with the zeros of $\omega(\Delta, l)$, the solution must contain at least one primary in the negative region of $\omega(\Delta, l)$. In other words, there must be a primary distinct from identity with twist

$$\tau_{\text{gap}} \leq 2\Delta_\phi + 2. \quad (4.196)$$

An analogous result holds in $d > 2$, where there must exist an operator with τ arbitrarily close to $2\Delta_\phi$ [66, 67]. This upper bound on the minimal twist does not rely on Virasoro symmetry, and therefore holds for arbitrary 2D conformal defects. In fact, Virasoro symmetry implies the existence of operators with $\tau = 0$ and $l \geq 2$, so the bound is automatically satisfied. However, the functional ω carries useful information in this case too. Note that when $0 \leq \Delta_\phi \leq 1$

$$\omega(l, l) = u(l)\tilde{u}(0) \geq 0 \quad \text{for } l \in 2\mathbb{N}, \quad (4.197)$$

so the Virasoro descendants of identity do not help and the bound (4.196) must be satisfied by an operator of non-zero twist. Assuming the operator of minimal non-zero twist is a scalar (such as in all theories with Virasoro symmetry where all Virasoro primaries are scalar), numerical bootstrap shows our analytic bound is strictly above the optimal upper bound on the scalar gap for $0 < \Delta_\phi < 1$, but it becomes optimal at $\Delta_\phi = 1$, where the extremal solution corresponds to the correlator $\langle \epsilon\epsilon\epsilon\epsilon \rangle$ in the 2D Ising model, the twist-four primary being $\mathcal{L}_{-2}\tilde{\mathcal{L}}_{-2}\mathbb{1}$.

4.8 Future directions

We expect that the class of functionals introduced in this work will be useful for extracting analytic predictions from the conformal bootstrap equations in a wider variety of contexts. Work is currently in progress to generalize the results to more spacetime dimensions, where the bootstrap bounds exhibit interesting features at locations corresponding to interacting CFTs.

An especially promising property of our functionals is their well-controlled behaviour when the external scaling dimensions are large. This is in sharp contrast with the derivative functionals normally used for the numerical bootstrap, whose constraining power deteriorates with increasing external dimensions [118]. For this reason, the functionals from this chapter are useful for extracting the consequences of boundary crossing symmetry on AdS physics, as demonstrated in section 4.6. In this context, it would also be interesting to test the sum rule (4.173), for example by constructing exact solutions to crossing corresponding to scattering in integrable theories in large AdS₂.

It would also be very interesting to identify the extremal functionals for bounds on OPE coefficients analytically in our basis. In 1D with large external scaling dimension, the numerical upper bound on the OPE coefficients of bound states coming from CFT crossing was observed to coincide with the corresponding analytical bound coming from S-matrix bootstrap in flat space [118, 122]. It is conceivable that similar methods to those presented

in this chapter can be used to prove this upper bound analytically on the CFT side. The main challenge seems to be able to place the double zeros of the extremal functionals to more general locations than the equally spaced points occurring in the present work.

Crossing symmetry of mixed correlators dramatically improves the bootstrap bounds [6, 37]. Similar improvements are observed to occur in 1D [123]. Our basis for functionals is expected to generalize to this context too, hopefully paving the way towards an analytic understanding of bootstrap islands in more spacetime dimensions. Related functionals might also be useful for modular bootstrap, where suggestions concerning the analytic nature of extremal functionals recently appeared in [124].

It could be fruitful to explore the utility of our basis for standard numerical bootstrap. Truncating the space of integral kernels to the span of Legendre polynomials of a bounded order, it is impossible to impose positivity for arbitrarily large scaling dimension since the functionals eventually become oscillating. However, one could try imposing positivity only up to the maximum order of a Legendre used.

Finally, one should look for an interpretation of what the presented functionals are trying to do physically. The partial restoration of the $z \leftrightarrow 1 - z$ symmetry, described in the last paragraph of section 4.4 is a hint that our basis, which breaks this symmetry explicitly, might not be the optimal choice.

4.A Closed formulas for the integral kernel

The goal of this appendix is to explain how one can obtain closed formulas for the integral kernel $\tilde{h}(x)$ corresponding to $\Delta_\psi \in \mathbb{N} - 1/2$, specified by the formulas (4.133) and (4.137). Define

$$\langle f, g \rangle = \int_0^1 dx f(x)g(x) \quad (4.198)$$

the usual scalar product of real functions on the unit interval. The basis functions are orthogonal

$$\langle p_m, p_n \rangle = \frac{\delta_{mn}}{2m - 1} \quad \text{for } m, n \in \mathbb{N}, \quad (4.199)$$

so that $\tilde{h}(x)$ is the unique function satisfying

$$\tilde{a}_n = (2n - 1) \langle \tilde{h}, p_n \rangle. \quad (4.200)$$

Our strategy for finding $\tilde{h}(x)$ will be to write $\tilde{a}_n/(2n-1)$ as a linear combination of overlaps between p_n and some relatively simple functions. It is useful to define the following functions

$$\begin{aligned} q_\Delta(x) &= Q_{\Delta-1}(2x-1) \\ r_\Delta(x) &= \frac{\Gamma(\Delta)^2}{2\Gamma(2\Delta)} \left[x^{\Delta-1} {}_2F_1(\Delta, \Delta; 2\Delta; x) + (1-x)^{\Delta-1} {}_2F_1(\Delta, \Delta; 2\Delta; 1-x) \right], \end{aligned} \quad (4.201)$$

where $Q_n(y)$ is the Legendre function of the second kind. When Δ is even, we have $q_\Delta(1-x) = q_\Delta(x)$, and therefore $\langle q_\Delta, p_n \rangle$ is nonzero only for n odd. In that case, we find the following overlaps

$$\langle q_\Delta, p_n \rangle = \frac{1}{\lambda - \Delta(\Delta-1)}, \quad (4.202)$$

where $\lambda = n(n-1)$. Clearly, the overlaps $\langle r_\Delta, p_n \rangle$ are nonvanishing again only for n odd. For $\Delta = 1, 2$ we find

$$\begin{aligned} \langle r_1, p_n \rangle &= -\frac{1}{2} \Psi' \left(\frac{n}{2} \right) \\ \langle r_2, p_n \rangle &= \left[n(n-1) + \frac{1}{2} \right] \Psi' \left(\frac{n}{2} \right) + 2, \end{aligned} \quad (4.203)$$

with $\Psi(z) = \psi(z+1/2) - \psi(z)$, $\psi(z) = \Gamma'(z)/\Gamma(z)$. It is now possible to see that

$$\frac{\tilde{a}_n}{2n-1} = -\langle r_2, p_n \rangle + (2\Delta_\psi - 1) \langle r_1, p_n \rangle + H_{\Delta_\psi}(\lambda), \quad (4.204)$$

where $H_{\Delta_\psi}(\lambda)$ is a rational function of λ with simple and double poles at $\lambda = \Delta(\Delta-1)$ where $\Delta \in \{2, 4, \dots, 2\Delta_\psi + 1\}$. $H_{\Delta_\psi}(\lambda) \rightarrow 0$ as $\lambda \rightarrow \infty$ and therefore $H_{\Delta_\psi}(\lambda)$ can be written as a linear combination of

$$\frac{1}{[\lambda - \Delta(\Delta-1)]^a} \quad (4.205)$$

with $a = 1, 2$ and $\Delta \in \{2, 4, \dots, 2\Delta_\psi + 1\}$. Any summand with $a = 1$ can be written as the overlap $\langle q_\Delta, p_n \rangle$ thanks to (4.202). It remains to find functions $\tilde{q}_\Delta(x)$ such that

$$\langle \tilde{q}_\Delta, p_n \rangle = \frac{1}{[\lambda - \Delta(\Delta-1)]^2}. \quad (4.206)$$

We could not find a closed formula for $\tilde{q}_\Delta(x)$ but worked out a few low-lying examples. It was useful to notice that $\tilde{q}_\Delta(x)$ is the solution of the Legendre equation with resonant forcing

$$[x(1-x)\tilde{q}'_\Delta(x)]' + \Delta(\Delta-1)\tilde{q}_\Delta(x) = -q_\Delta(x) \quad (4.207)$$

and boundary conditions

$$\tilde{q}_\Delta(0) = \tilde{q}_\Delta(1) = \frac{\psi' \left(\frac{1-\Delta}{2} \right) - \psi' \left(\frac{\Delta}{2} \right)}{4(2\Delta - 1)}. \quad (4.208)$$

The bottom line is that $\tilde{h}(x)$ can be written as a linear combination of $r_1(x)$, $r_2(x)$, $q_\Delta(x)$ and $\tilde{q}_\Delta(x)$ with $\Delta \in \{2, 4, \dots, 2\Delta_\psi + 1\}$. In this way, one can obtain the following explicit formulas for small Δ_ψ . The kernel for $\Delta_\psi = 1/2$ takes the form

$$\tilde{h}(x) = \left[\frac{1-y}{2y} - \frac{(2x^2+x+2)(x-1)}{2x^2} \log(1-x) \right] + (x \leftrightarrow 1-x), \quad (4.209)$$

where we use the shorthand notation $y = x(1-x)$. The kernel for $\Delta_\psi = 3/2$ takes the form

$$\tilde{h}(x) = \left[\frac{12y^2 + 11y + 12}{24y} - \frac{(2x^2 + 3x + 2)(x-1)^3}{2x^2} \log(1-x) \right] + (x \leftrightarrow 1-x). \quad (4.210)$$

Beginning from $\Delta_\psi = 5/2$, we get contributions from $\tilde{q}_\Delta(x)$ which contain the dilogarithm. The kernel for $\Delta_\psi = 5/2$ takes the form

$$\begin{aligned} \tilde{h}(x) = & \left[\frac{-120y^3 + 154y^2 + 641y + 120}{240y} + \frac{3}{5}(2x-1)(y+2)\text{Li}_2(x) + \right. \\ & \left. + \frac{(x-1)(y-1)(10x^4 - 5x^3 - 22x^2 - 5x + 10)}{10x^2} \log(1-x) \right] + (x \leftrightarrow 1-x). \end{aligned} \quad (4.211)$$

Note that the full kernel is given by $h(x) = \tilde{h}(x) + c(x)$ with $c(x)$ given by (4.138). It turns out that the kernel has simple transformation properties under $z \leftrightarrow 1-z$. We leave further exploration of these for a future study.

References

- [1] D. Gaiotto, D. Mazac, and M. F. Paulos, “Bootstrapping the 3d Ising twist defect,” *JHEP* **03** (2014) 100, [arXiv:1310.5078 \[hep-th\]](#).
- [2] N. Bobev, S. El-Showk, D. Mazac, and M. F. Paulos, “Bootstrapping SCFTs with Four Supercharges,” *JHEP* **08** (2015) 142, [arXiv:1503.02081 \[hep-th\]](#).
- [3] N. Bobev, S. El-Showk, D. Mazac, and M. F. Paulos, “Bootstrapping the Three-Dimensional Supersymmetric Ising Model,” *Phys. Rev. Lett.* **115** no. 5, (2015) 051601, [arXiv:1502.04124 \[hep-th\]](#).
- [4] S. El-Showk, M. F. Paulos, D. Poland, S. Rychkov, D. Simmons-Duffin, and A. Vichi, “Solving the 3D Ising Model with the Conformal Bootstrap,” *Phys. Rev.* **D86** (2012) 025022, [arXiv:1203.6064 \[hep-th\]](#).
- [5] S. El-Showk, M. F. Paulos, D. Poland, S. Rychkov, D. Simmons-Duffin, and A. Vichi, “Solving the 3d Ising Model with the Conformal Bootstrap II. c-Minimization and Precise Critical Exponents,” *J. Stat. Phys.* **157** (2014) 869, [arXiv:1403.4545 \[hep-th\]](#).
- [6] F. Kos, D. Poland, and D. Simmons-Duffin, “Bootstrapping Mixed Correlators in the 3D Ising Model,” *JHEP* **11** (2014) 109, [arXiv:1406.4858 \[hep-th\]](#).
- [7] D. Simmons-Duffin, “A Semidefinite Program Solver for the Conformal Bootstrap,” *JHEP* **06** (2015) 174, [arXiv:1502.02033 \[hep-th\]](#).
- [8] F. Kos, D. Poland, D. Simmons-Duffin, and A. Vichi, “Precision islands in the Ising and $O(N)$ models,” *JHEP* **08** (2016) 036, [arXiv:1603.04436 \[hep-th\]](#).
- [9] D. Mazac, “Analytic Bounds and Emergence of AdS_2 Physics from the Conformal Bootstrap,” *JHEP* **04** (2017) 146, [arXiv:1611.10060 \[hep-th\]](#).

- [10] A. Pelissetto and E. Vicari, “Critical phenomena and renormalization group theory,” *Phys. Rept.* **368** (2002) 549–727, [arXiv:cond-mat/0012164 \[cond-mat\]](#).
- [11] S. Ferrara, A. F. Grillo, and R. Gatto, “Tensor representations of conformal algebra and conformally covariant operator product expansion,” *Annals Phys.* **76** (1973) 161–188.
- [12] A. M. Polyakov, “Nonhamiltonian approach to conformal quantum field theory,” *Zh. Eksp. Teor. Fiz.* **66** (1974) 23–42.
- [13] R. Rattazzi, V. S. Rychkov, E. Tonni, and A. Vichi, “Bounding scalar operator dimensions in 4D CFT,” *JHEP* **12** (2008) 031, [arXiv:0807.0004 \[hep-th\]](#).
- [14] V. S. Rychkov and A. Vichi, “Universal Constraints on Conformal Operator Dimensions,” *Phys. Rev.* **D80** (2009) 045006, [arXiv:0905.2211 \[hep-th\]](#).
- [15] F. Caracciolo and V. S. Rychkov, “Rigorous Limits on the Interaction Strength in Quantum Field Theory,” *Phys. Rev.* **D81** (2010) 085037, [arXiv:0912.2726 \[hep-th\]](#).
- [16] R. Rattazzi, S. Rychkov, and A. Vichi, “Central Charge Bounds in 4D Conformal Field Theory,” *Phys. Rev.* **D83** (2011) 046011, [arXiv:1009.2725 \[hep-th\]](#).
- [17] D. Poland and D. Simmons-Duffin, “Bounds on 4D Conformal and Superconformal Field Theories,” *JHEP* **05** (2011) 017, [arXiv:1009.2087 \[hep-th\]](#).
- [18] R. Rattazzi, S. Rychkov, and A. Vichi, “Bounds in 4D Conformal Field Theories with Global Symmetry,” *J. Phys.* **A44** (2011) 035402, [arXiv:1009.5985 \[hep-th\]](#).
- [19] A. Vichi, “Improved bounds for CFT’s with global symmetries,” *JHEP* **01** (2012) 162, [arXiv:1106.4037 \[hep-th\]](#).
- [20] D. Poland, D. Simmons-Duffin, and A. Vichi, “Carving Out the Space of 4D CFTs,” *JHEP* **05** (2012) 110, [arXiv:1109.5176 \[hep-th\]](#).
- [21] S. Rychkov, “Conformal Bootstrap in Three Dimensions?,” [arXiv:1111.2115 \[hep-th\]](#).
- [22] P. Liendo, L. Rastelli, and B. C. van Rees, “The Bootstrap Program for Boundary CFT_d,” *JHEP* **07** (2013) 113, [arXiv:1210.4258 \[hep-th\]](#).

- [23] S. El-Showk and M. F. Paulos, “Bootstrapping Conformal Field Theories with the Extremal Functional Method,” *Phys. Rev. Lett.* **111** no. 24, (2013) 241601, [arXiv:1211.2810 \[hep-th\]](#).
- [24] F. Gliozzi, “More constraining conformal bootstrap,” *Phys. Rev. Lett.* **111** (2013) 161602, [arXiv:1307.3111 \[hep-th\]](#).
- [25] F. Kos, D. Poland, and D. Simmons-Duffin, “Bootstrapping the $O(N)$ vector models,” *JHEP* **06** (2014) 091, [arXiv:1307.6856 \[hep-th\]](#).
- [26] L. F. Alday and A. Bissi, “The superconformal bootstrap for structure constants,” *JHEP* **09** (2014) 144, [arXiv:1310.3757 \[hep-th\]](#).
- [27] M. Berkooz, R. Yacoby, and A. Zait, “Bounds on $\mathcal{N} = 1$ superconformal theories with global symmetries,” *JHEP* **08** (2014) 008, [arXiv:1402.6068 \[hep-th\]](#). [Erratum: JHEP01,132(2015)].
- [28] Y. Nakayama and T. Ohtsuki, “Approaching the conformal window of $O(n) \times O(m)$ symmetric Landau-Ginzburg models using the conformal bootstrap,” *Phys. Rev.* **D89** no. 12, (2014) 126009, [arXiv:1404.0489 \[hep-th\]](#).
- [29] Y. Nakayama and T. Ohtsuki, “Five dimensional $O(N)$ -symmetric CFTs from conformal bootstrap,” *Phys. Lett.* **B734** (2014) 193–197, [arXiv:1404.5201 \[hep-th\]](#).
- [30] S. M. Chester, J. Lee, S. S. Pufu, and R. Yacoby, “The $\mathcal{N} = 8$ superconformal bootstrap in three dimensions,” *JHEP* **09** (2014) 143, [arXiv:1406.4814 \[hep-th\]](#).
- [31] F. Caracciolo, A. Castedo Echeverri, B. von Harling, and M. Serone, “Bounds on OPE Coefficients in 4D Conformal Field Theories,” *JHEP* **10** (2014) 020, [arXiv:1406.7845 \[hep-th\]](#).
- [32] Y. Nakayama and T. Ohtsuki, “Bootstrapping phase transitions in QCD and frustrated spin systems,” *Phys. Rev.* **D91** no. 2, (2015) 021901, [arXiv:1407.6195 \[hep-th\]](#).
- [33] M. F. Paulos, “JuliBootS: a hands-on guide to the conformal bootstrap,” [arXiv:1412.4127 \[hep-th\]](#).
- [34] J.-B. Bae and S.-J. Rey, “Conformal Bootstrap Approach to $O(N)$ Fixed Points in Five Dimensions,” [arXiv:1412.6549 \[hep-th\]](#).

- [35] C. Beem, M. Lemos, P. Liendo, L. Rastelli, and B. C. van Rees, “The $\mathcal{N} = 2$ superconformal bootstrap,” *JHEP* **03** (2016) 183, [arXiv:1412.7541 \[hep-th\]](#).
- [36] S. M. Chester, S. S. Pufu, and R. Yacoby, “Bootstrapping $O(N)$ vector models in $4 < d < 6$,” *Phys. Rev.* **D91** no. 8, (2015) 086014, [arXiv:1412.7746 \[hep-th\]](#).
- [37] F. Kos, D. Poland, D. Simmons-Duffin, and A. Vichi, “Bootstrapping the $O(N)$ Archipelago,” *JHEP* **11** (2015) 106, [arXiv:1504.07997 \[hep-th\]](#).
- [38] S. M. Chester, S. Giombi, L. V. Iliesiu, I. R. Klebanov, S. S. Pufu, and R. Yacoby, “Accidental Symmetries and the Conformal Bootstrap,” *JHEP* **01** (2016) 110, [arXiv:1507.04424 \[hep-th\]](#).
- [39] C. Beem, M. Lemos, L. Rastelli, and B. C. van Rees, “The $(2, 0)$ superconformal bootstrap,” *Phys. Rev.* **D93** no. 2, (2016) 025016, [arXiv:1507.05637 \[hep-th\]](#).
- [40] L. Iliesiu, F. Kos, D. Poland, S. S. Pufu, D. Simmons-Duffin, and R. Yacoby, “Bootstrapping 3D Fermions,” *JHEP* **03** (2016) 120, [arXiv:1508.00012 \[hep-th\]](#).
- [41] F. Rejon-Barrera and D. Robbins, “Scalar-Vector Bootstrap,” *JHEP* **01** (2016) 139, [arXiv:1508.02676 \[hep-th\]](#).
- [42] D. Poland and A. Stergiou, “Exploring the Minimal 4D $\mathcal{N} = 1$ SCFT,” *JHEP* **12** (2015) 121, [arXiv:1509.06368 \[hep-th\]](#).
- [43] M. Lemos and P. Liendo, “Bootstrapping $\mathcal{N} = 2$ chiral correlators,” *JHEP* **01** (2016) 025, [arXiv:1510.03866 \[hep-th\]](#).
- [44] H. Kim, P. Kravchuk, and H. Ooguri, “Reflections on Conformal Spectra,” *JHEP* **04** (2016) 184, [arXiv:1510.08772 \[hep-th\]](#).
- [45] Y.-H. Lin, S.-H. Shao, D. Simmons-Duffin, Y. Wang, and X. Yin, “ $\mathcal{N}=4$ Superconformal Bootstrap of the K3 CFT,” [arXiv:1511.04065 \[hep-th\]](#).
- [46] S. M. Chester, L. V. Iliesiu, S. S. Pufu, and R. Yacoby, “Bootstrapping $O(N)$ Vector Models with Four Supercharges in $3 \leq d \leq 4$,” *JHEP* **05** (2016) 103, [arXiv:1511.07552 \[hep-th\]](#).
- [47] S. M. Chester and S. S. Pufu, “Towards bootstrapping QED_3 ,” *JHEP* **08** (2016) 019, [arXiv:1601.03476 \[hep-th\]](#).

- [48] C. Behan, “PyCFTBoot: A flexible interface for the conformal bootstrap,” [arXiv:1602.02810 \[hep-th\]](#).
- [49] P. Dey, A. Kaviraj, and K. Sen, “More on analytic bootstrap for $O(N)$ models,” *JHEP* **06** (2016) 136, [arXiv:1602.04928 \[hep-th\]](#).
- [50] Y. Nakayama, “Bootstrap bound for conformal multi-flavor QCD on lattice,” *JHEP* **07** (2016) 038, [arXiv:1605.04052 \[hep-th\]](#).
- [51] S. El-Showk and M. F. Paulos, “Extremal bootstrapping: go with the flow,” [arXiv:1605.08087 \[hep-th\]](#).
- [52] Z. Li and N. Su, “Bootstrapping Mixed Correlators in the Five Dimensional Critical $O(N)$ Models,” *JHEP* **04** (2017) 098, [arXiv:1607.07077 \[hep-th\]](#).
- [53] Y. Pang, J. Rong, and N. Su, “ ϕ^3 theory with F_4 flavor symmetry in $6 + 2\epsilon$ dimensions: 3-loop renormalization and conformal bootstrap,” *JHEP* **12** (2016) 057, [arXiv:1609.03007 \[hep-th\]](#).
- [54] Y.-H. Lin, S.-H. Shao, Y. Wang, and X. Yin, “(2,2) Superconformal Bootstrap in Two Dimensions,” [arXiv:1610.05371 \[hep-th\]](#).
- [55] M. Lemos, P. Liendo, C. Meneghelli, and V. Mitev, “Bootstrapping $\mathcal{N} = 3$ superconformal theories,” *JHEP* **04** (2017) 032, [arXiv:1612.01536 \[hep-th\]](#).
- [56] C. Beem, L. Rastelli, and B. C. van Rees, “More $\mathcal{N} = 4$ superconformal bootstrap,” [arXiv:1612.02363 \[hep-th\]](#).
- [57] H. Diehl and S. Dietrich, “Field-theoretical approach to multicritical behavior near free surfaces,” *Physical Review B* **24** no. 5, (1981) 2878. http://prb.aps.org/abstract/PRB/v24/i5/p2878_1.
- [58] D. McAvity and H. Osborn, “Conformal field theories near a boundary in general dimensions,” *Nucl.Phys.* **B455** (1995) 522–576, [arXiv:cond-mat/9505127 \[cond-mat\]](#).
- [59] K. Binder and D. Landau, “Critical phenomena at surfaces,” *Physica A: Statistical Mechanics and its Applications* **163** no. 1, (1990) 17 – 30. <http://www.sciencedirect.com/science/article/pii/037843719090311F>.
- [60] M. Bill, M. Caselle, D. Gaiotto, F. Gliozzi, M. Meineri, and R. Pellegrini, “Line defects in the 3d Ising model,” *JHEP* **07** (2013) 055, [arXiv:1304.4110 \[hep-th\]](#).

- [61] K. G. Wilson and M. E. Fisher, “Critical exponents in 3.99 dimensions,” *Phys.Rev.Lett.* **28** (1972) 240–243.
- [62] J. Le Guillou and J. Zinn-Justin, “Accurate critical exponents from the ε -expansion,” *Journal de Physique Lettres* **46** no. 4, (1985) 137–141.
http://jphyslet.journaldephysique.org/articles/jphyslet/abs/1985/04/jphyslet_1985__46_4_137_0/jphyslet_1985__46_4_137_0.html.
- [63] S. El-Showk, M. Paulos, D. Poland, S. Rychkov, D. Simmons-Duffin, and A. Vichi, “Conformal Field Theories in Fractional Dimensions,” *Phys. Rev. Lett.* **112** (2014) 141601, [arXiv:1309.5089](https://arxiv.org/abs/1309.5089) [hep-th].
- [64] A. Kolezhuk, S. Sachdev, R. R. Biswas, and P. Chen, “Theory of quantum impurities in spin liquids,” *Physical Review B* **74** no. 16, (2006) 165114.
- [65] J. L. Cardy, “Boundary conditions in conformal field theory,” in *In *Jimbo, M. (ed.) et al.: Integrable systems in quantum field theory and statistical mechanics* 127-148 (QC174.45:S78:1988). (see Book Index)*. 1990.
- [66] A. L. Fitzpatrick, J. Kaplan, D. Poland, and D. Simmons-Duffin, “The Analytic Bootstrap and AdS Superhorizon Locality,” *JHEP* **12** (2013) 004, [arXiv:1212.3616](https://arxiv.org/abs/1212.3616) [hep-th].
- [67] Z. Komargodski and A. Zhiboedov, “Convexity and Liberation at Large Spin,” *JHEP* **11** (2013) 140, [arXiv:1212.4103](https://arxiv.org/abs/1212.4103) [hep-th].
- [68] F. A. Dolan and H. Osborn, “Conformal Partial Waves: Further Mathematical Results,” [arXiv:1108.6194](https://arxiv.org/abs/1108.6194) [hep-th].
- [69] C. Beem, L. Rastelli, and B. C. van Rees, “The $\mathcal{N} = 4$ Superconformal Bootstrap,” *Phys. Rev. Lett.* **111** (2013) 071601, [arXiv:1304.1803](https://arxiv.org/abs/1304.1803) [hep-th].
- [70] L. F. Alday and A. Bissi, “Generalized bootstrap equations for $\mathcal{N} = 4$ SCFT,” *JHEP* **02** (2015) 101, [arXiv:1404.5864](https://arxiv.org/abs/1404.5864) [hep-th].
- [71] L. F. Alday, A. Bissi, and T. Lukowski, “Lessons from crossing symmetry at large N ,” [arXiv:1410.4717](https://arxiv.org/abs/1410.4717) [hep-th].
- [72] C. Beem, M. Lemos, P. Liendo, W. Peelaers, L. Rastelli, and B. C. van Rees, “Infinite Chiral Symmetry in Four Dimensions,” *Commun. Math. Phys.* **336** no. 3, (2015) 1359–1433, [arXiv:1312.5344](https://arxiv.org/abs/1312.5344) [hep-th].

- [73] C. Beem, L. Rastelli, and B. C. van Rees, “ \mathcal{W} symmetry in six dimensions,” *JHEP* **05** (2015) 017, [arXiv:1404.1079 \[hep-th\]](#).
- [74] C. Beem, W. Peelaers, L. Rastelli, and B. C. van Rees, “Chiral algebras of class S,” *JHEP* **05** (2015) 020, [arXiv:1408.6522 \[hep-th\]](#).
- [75] M. Lemos and W. Peelaers, “Chiral Algebras for Trinion Theories,” *JHEP* **02** (2015) 113, [arXiv:1411.3252 \[hep-th\]](#).
- [76] S. M. Chester, J. Lee, S. S. Pufu, and R. Yacoby, “Exact Correlators of BPS Operators from the 3d Superconformal Bootstrap,” *JHEP* **03** (2015) 130, [arXiv:1412.0334 \[hep-th\]](#).
- [77] D. Bashkirov, “Bootstrapping the $\mathcal{N} = 1$ SCFT in three dimensions,” [arXiv:1310.8255 \[hep-th\]](#).
- [78] T. Nishioka and K. Yonekura, “On RG Flow of τ_{RR} for Supersymmetric Field Theories in Three-Dimensions,” *JHEP* **05** (2013) 165, [arXiv:1303.1522 \[hep-th\]](#).
- [79] S. Thomas, “Emergent supersymmetry.” Kitp talk, 2005. <http://online.kitp.ucsb.edu/online/qpt-c05/thomas/>.
- [80] S.-S. Lee, “Emergence of supersymmetry at a critical point of a lattice model,” *Phys. Rev.* **B76** (2007) 075103, [arXiv:cond-mat/0611658 \[cond-mat\]](#).
- [81] Y. Yu and K. Yang, “Simulating Wess-Zumino Supersymmetry Model in Optical Lattices,” *Phys. Rev. Lett.* **105** (2010) 150605, [arXiv:1005.1399 \[cond-mat.quant-gas\]](#).
- [82] P. Ponte and S.-S. Lee, “Emergence of supersymmetry on the surface of three dimensional topological insulators,” *New J. Phys.* **16** no. 1, (2014) 013044, [arXiv:1206.2340 \[cond-mat.str-el\]](#).
- [83] T. Grover, D. N. Sheng, and A. Vishwanath, “Emergent Space-Time Supersymmetry at the Boundary of a Topological Phase,” *Science* **344** no. 6181, (2014) 280–283, [arXiv:1301.7449 \[cond-mat.str-el\]](#).
- [84] F. A. Dolan and H. Osborn, “Conformal partial waves and the operator product expansion,” *Nucl. Phys.* **B678** (2004) 491–507, [arXiv:hep-th/0309180 \[hep-th\]](#).

- [85] Z. U. Khandker, D. Li, D. Poland, and D. Simmons-Duffin, “ $\mathcal{N} = 1$ superconformal blocks for general scalar operators,” *JHEP* **08** (2014) 049, [arXiv:1404.5300 \[hep-th\]](#).
- [86] A. L. Fitzpatrick, J. Kaplan, Z. U. Khandker, D. Li, D. Poland, and D. Simmons-Duffin, “Covariant Approaches to Superconformal Blocks,” *JHEP* **1408** (2014) 129, [arXiv:1402.1167 \[hep-th\]](#).
- [87] W. Nahm, “Supersymmetries and their Representations,” *Nucl. Phys.* **B135** (1978) 149.
- [88] F. A. Dolan and H. Osborn, “Conformal four point functions and the operator product expansion,” *Nucl. Phys.* **B599** (2001) 459–496, [arXiv:hep-th/0011040 \[hep-th\]](#).
- [89] V. K. Dobrev and V. B. Petkova, “All Positive Energy Unitary Irreducible Representations of Extended Conformal Supersymmetry,” *Phys. Lett.* **B162** (1985) 127–132.
- [90] S. Minwalla, “Restrictions imposed by superconformal invariance on quantum field theories,” *Adv. Theor. Math. Phys.* **2** (1998) 781–846, [arXiv:hep-th/9712074 \[hep-th\]](#).
- [91] M. Hogervorst, S. Rychkov, and B. C. van Rees, “Truncated conformal space approach in d dimensions: A cheap alternative to lattice field theory?,” *Phys. Rev.* **D91** (2015) 025005, [arXiv:1409.1581 \[hep-th\]](#).
- [92] V. K. Dobrev and V. B. Petkova, “ON THE GROUP THEORETICAL APPROACH TO EXTENDED CONFORMAL SUPERSYMMETRY: CLASSIFICATION OF MULTIPLETS,” *Lett. Math. Phys.* **9** (1985) 287–298.
- [93] V. K. Dobrev and V. B. Petkova, “Group Theoretical Approach to Extended Conformal Supersymmetry: Function Space Realizations and Invariant Differential Operators,” *Fortsch. Phys.* **35** (1987) 537.
- [94] V. Dobrev and V. Petkova, “Reducible representations of the extended conformal superalgebra and invariant differential operators,” in *Conformal Groups and Related Symmetries Physical Results and Mathematical Background*, A. Barut and H.-D. Doebner, eds., vol. 261 of *Lecture Notes in Physics*, pp. 291–299. Springer Berlin Heidelberg, 1986. http://dx.doi.org/10.1007/3540171630_89.

- [95] G. Mack, “All Unitary Ray Representations of the Conformal Group $SU(2,2)$ with Positive Energy,” *Commun. Math. Phys.* **55** (1977) 1.
- [96] A. Vichi, *A New Method to Explore Conformal Field Theories in Any Dimension*. PhD thesis, EPFL, Lausanne, LPPC, 2011-08-12.
http://infoscience.epfl.ch/record/167898/files/EPFL_TH5116.pdf.
- [97] J. Wess and B. Zumino, “Supergauge transformations in four dimensions,” *Nuclear Physics B* **70** no. 1, (1974) 39 – 50.
<http://www.sciencedirect.com/science/article/pii/0550321374903551>.
- [98] M. J. Strassler, “An Unorthodox introduction to supersymmetric gauge theory,” in *Strings, Branes and Extra Dimensions: TASI 2001: Proceedings*, pp. 561–638. 2003. [arXiv:hep-th/0309149](https://arxiv.org/abs/hep-th/0309149) [hep-th].
- [99] C. Closset, T. T. Dumitrescu, G. Festuccia, and Z. Komargodski, “Supersymmetric Field Theories on Three-Manifolds,” *JHEP* **05** (2013) 017, [arXiv:1212.3388](https://arxiv.org/abs/1212.3388) [hep-th].
- [100] Y. Imamura and D. Yokoyama, “N=2 supersymmetric theories on squashed three-sphere,” *Phys. Rev.* **D85** (2012) 025015, [arXiv:1109.4734](https://arxiv.org/abs/1109.4734) [hep-th].
- [101] C. Vafa and N. P. Warner, “Catastrophes and the Classification of Conformal Theories,” *Phys. Lett.* **B218** (1989) 51–58.
- [102] W. Lerche, C. Vafa, and N. P. Warner, “Chiral Rings in N=2 Superconformal Theories,” *Nucl. Phys.* **B324** (1989) 427–474.
- [103] D. L. Jafferis, “The Exact Superconformal R-Symmetry Extremizes Z,” *JHEP* **05** (2012) 159, [arXiv:1012.3210](https://arxiv.org/abs/1012.3210) [hep-th].
- [104] S. Giombi and I. R. Klebanov, “Interpolating between a and F ,” *JHEP* **03** (2015) 117, [arXiv:1409.1937](https://arxiv.org/abs/1409.1937) [hep-th].
- [105] J. Golden and M. F. Paulos, “No unitary bootstrap for the fractal Ising model,” *JHEP* **03** (2015) 167, [arXiv:1411.7932](https://arxiv.org/abs/1411.7932) [hep-th].
- [106] J.-H. Park, “Superconformal symmetry in three-dimensions,” *J. Math. Phys.* **41** (2000) 7129–7161, [arXiv:hep-th/9910199](https://arxiv.org/abs/hep-th/9910199) [hep-th].
- [107] A. L. Fitzpatrick and J. Kaplan, “Unitarity and the Holographic S-Matrix,” *JHEP* **10** (2012) 032, [arXiv:1112.4845](https://arxiv.org/abs/1112.4845) [hep-th].

- [108] W. Boucher, D. Friedan, and A. Kent, “Determinant Formulae and Unitarity for the $N=2$ Superconformal Algebras in Two-Dimensions or Exact Results on String Compactification,” *Phys. Lett.* **B172** (1986) 316.
- [109] D. Friedan, Z.-a. Qiu, and S. H. Shenker, “Superconformal Invariance in Two-Dimensions and the Tricritical Ising Model,” *Phys. Lett.* **B151** (1985) 37–43.
- [110] G. Mussardo, G. Sotkov, and M. Stanishkov, “ $N=2$ SUPERCONFORMAL MINIMAL MODELS,” *Int. J. Mod. Phys.* **A4** (1989) 1135.
- [111] G. Mussardo, G. Sotkov, and M. Stanishkov, “Fusion Rules, Four Point Functions and Discrete Symmetries of $N = 2$ Superconformal Models,” *Phys. Lett.* **B218** (1989) 191–199.
- [112] E. B. Kiritsis, “The Structure of $N = 2$ Superconformally Invariant ‘Minimal’ Theories: Operator Algebra and Correlation Functions,” *Phys. Rev.* **D36** (1987) 3048.
- [113] J. M. Maldacena and A. Strominger, “AdS(3) black holes and a stringy exclusion principle,” *JHEP* **12** (1998) 005, [arXiv:hep-th/9804085 \[hep-th\]](#).
- [114] G. Waterson, “Bosonic Construction of an $N = 2$ Extended Superconformal Theory in Two-dimensions,” *Phys. Lett.* **B171** (1986) 77–80.
- [115] I. Heemskerck, J. Penedones, J. Polchinski, and J. Sully, “Holography from Conformal Field Theory,” *JHEP* **10** (2009) 079, [arXiv:0907.0151 \[hep-th\]](#).
- [116] D. M. Hofman, D. Li, D. Meltzer, D. Poland, and F. Rejon-Barrera, “A Proof of the Conformal Collider Bounds,” *JHEP* **06** (2016) 111, [arXiv:1603.03771 \[hep-th\]](#).
- [117] T. Hartman, S. Jain, and S. Kundu, “Causality Constraints in Conformal Field Theory,” *JHEP* **05** (2016) 099, [arXiv:1509.00014 \[hep-th\]](#).
- [118] M. F. Paulos, J. Penedones, J. Toledo, B. C. van Rees, and P. Vieira, “The S-matrix Bootstrap I: QFT in AdS,” [arXiv:1607.06109 \[hep-th\]](#).
- [119] T. Bargheer, J. A. Minahan, and R. Pereira, “Computing Three-Point Functions for Short Operators,” *JHEP* **03** (2014) 096, [arXiv:1311.7461 \[hep-th\]](#).
- [120] J. A. Minahan and R. Pereira, “Three-point correlators from string amplitudes: Mixing and Regge spins,” *JHEP* **04** (2015) 134, [arXiv:1410.4746 \[hep-th\]](#).

- [121] J. Penedones, “Writing CFT correlation functions as AdS scattering amplitudes,” *JHEP* **03** (2011) 025, [arXiv:1011.1485 \[hep-th\]](#).
- [122] M. F. Paulos, J. Penedones, J. Toledo, B. C. van Rees, and P. Vieira, “The S-matrix Bootstrap II: Two Dimensional Amplitudes,” [arXiv:1607.06110 \[hep-th\]](#).
- [123] D. Mazáč and E. Trevisani, “Mixed-Correlator Bootstrap of Conformal Line Defects,”. work in progress.
- [124] S. Collier, Y.-H. Lin, and X. Yin, “Modular Bootstrap Revisited,” [arXiv:1608.06241 \[hep-th\]](#).